ANALYSIS OF
CHOPPER CONTROLLED D.C. MOTOR DRIVES
INCLUDING THE EFFECTS OF SOME MECHANICAL FACTORS

A THESIS

submitted in fulfilment of the
requirements for the award of the degree
of
DOCTOR OF PHILOSOPHY
in
ELECTRICAL ENGINEERING

By

SHAMSUDDIN AHMAD

DEPARTMENT OF ELECTRICAL ENGINEERING
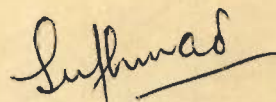UNIVERSITY OF ROORKEE
ROORKEE-247667 (INDIA)

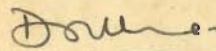December, 1982

To
My Parents

CANDIDATE'S DECLARATION

I hereby certify that the work which is being presented in the thesis entitled ANALYSIS OF CHOPPER CONTROLLED D.C. MOTOR DRIVES INCLUDING THE EFFECTS OF SOME MECHANICAL FACTORS in fulfilment of the requirement for the award of the Degree of Doctor of Philosophy, submitted in the Department of Electrical Engineering of the University is an authentic record of my own work carried out during a period from January 1980 to November 1982 under the supervision of Dr. D.R. Kohli, Professor of Electrical Engineering, University of Roorkee.

The matter embodied in the thesis has not been submitted by me for the award of any other degree.

(SHAMSUDDIN AHMAD)

This is to certify that the above statement made by the candidate is correct to the best of my knowledge.

Dated: December 6 ,1982

(D.R. KOHLI)
Professor and Head
Department of Electrical Engg.
University of Roorkee
Roorkee (India)

ABSTRACT

The d.c. motor is a widely used type of motor in industry. The bulk of d.c. drives find their application in variable speed drives. The use of thyristors has further increased the scope of d.c. motors as it has led to the development of a variety of efficient techniques of speed control. One such frequently used technique is chopper control which converts a constant d.c. voltage to a pulsed type of voltage. Considerable interest has been shown in the last few years to upgrade the methods of analysis to predict the performance of chopper controlled drives more accurately, and to incorporate improvements in design based on such accurate analyses. The work presented in this thesis is an effort in this direction.

The performance of an electric drive not only depends upon its electrical components but is also significantly affected by its mechanical features such as elasticity of shaft, misalignment, backlash, etc. Extensive work is available in literature on the performance analysis of electrical drives but without including the effect of these mechanical factors. The development of high performance d.c. drive systems requires a precise analysis of such systems, in which case these factors can no longer be ignored.

The basic aims of this work are (i) to develop better techniques of analysis for chopper controlled drives, (ii) to determine the effects of mechanical factors and to establish the importance of including such factors in the analysis, and

(iii) to suggest changes required in design in order to improve the drive performance.

The work presented deals mainly with the analysis of separately excited d.c. motor drives, fed by a chopper as well as ordinary d.c. supply. The analysis includes the effects of mechanical factors associated with drives, such as elasticity of coupling and periodic variation of load torque. The effects of these mechanical features on the performance of d.c. series motor drives are also investigated and compared with those in separately excited d.c. motor drives.

The work presented in this thesis is summarized below:

The performance of an electro-mechanical system consisting of a d.c. motor fed by a constant d.c. voltage and coupled through an elastic shaft to a load with periodic torque variation is analysed (Chapter-2). A mathematical model of the system is given and equations are solved using State Space techniques. Closed-form solution is obtained to give the system performance under transient as well as steady state conditions. The analysis is illustrated by an example and inferences drawn. It is observed that the performance is significantly affected by elasticity of shaft, specially when the load torque is pulsating in nature. Some suggestions are given to improve the performance.

A new technique for the analysis of chopper fed d.c. motor drives using pulse width control is presented (Chapter-3). The methods of analysis of such drives given by earlier authors involve a progressive step-by-step solution of system differential equations. Closed-form solutions using such techniques are

not available and the computation efforts are large. The proposed
analytical technique which overcomes these limitations is superior
because of the following advantages:

  (i) A single set of equations is needed to describe the system
       in duty as well as freewheeling intervals.

  (ii) The performance in terms of current and speed at any
       instant, in transient as well as steady state conditions,
       can be directly obtained without using step by step methods
       starting from switching-in condition. The computational
       efforts are therefore, greatly reduced.

 (iii) The solutions are in closed-form, and therefore provide
       an insight into the transient and steady state performance
       of the drive.

  (iv) The solutions are more accurate, as speed over a chopper
       cycle is not assumed constant.

The frequent use of chopper controlled d.c. drives makes
it imperative to investigate the effects of mechanical factors on
performance of such drives. An analysis of chopper fed d.c. motor
drives with elastic coupling and pulsating load torque is presen-
ted in Chapter-4. The equations governing the performance of
such a system are expressed in State model form. The analytical
technique of Chapter-3 is used to obtain closed-form solutions
for system performance. The effects of mechanical factors is
observed to be more severe when the motor is fed through a chopper.
The conditions leading to resonance are investigated and sugges-
tions are made to avoid such situations. Results are illustrated
by an example and inferences drawn therefrom.

PWM control is commonly used in closed-loop d.c. drives for obtaining the desired control of speed. The influence of mechanical features on performance of such drives has not been attemped so far. A system consisting of a d.c. separately excited motor with load coupled through an elastic shaft, and fed through a PWM supply obtained from a controller having a speed feed-back is analysed (Chapter-5). A mathematical model of the system for constant as well as pulsating load torque conditions is presented and the transfer function obtained. The effects of some of the system parameters on the dynamic stability of drive are studied using 'parameter-plane technique'. A set of values of system parameters to give stable operation and minimum settling time is determined, and performance of the system obtained using numerical techniques. The value of amplifier gain required to give minimum settling time is observed to be affected by elasticity of shaft. The effects of variation of system parameters on pulsations of current and speed are studied and conditions of resonance investigated.

The work discussed above (Chapters 2,4,5) deals with the analysis of linearised systems assuming the frequency of load torque equal to average steady state motor speed. For certain types of driven mechanisms, this frequency is proportional to instantaneous value of motor speed and leads to non-linear system equations. Such non-linearity is accounted for in the analysis (Chapter-6) and the system performance is determined using numerical techniques. The assumptions made in ignoring such non-linearity are shown to be valid.

D.C. series motors are also used in a variety of industrial drives and, therefore, it is worthwhile to analyse the effects of mechanical factors on performance of such drives. The influence of elasticity of coupling and periodic variation of load torque, on the performance of d.c. series motor drive fed by a chopper as well as constant d.c. voltage, is investigated (Chapter-7). The performance of this type of drive is compared with that of a similar motor when excited separately in order to identify the differences in the behaviour of these two types of drives.

The important results are summarized in Chapter-8.

ACKNOWLEDGMENT

TABLE OF CONTENTS

NOMENCLATURE

$A_1, \ldots, A_5$ coefficients of characteristic equation of open-loop d.c. drive electromechanical system

$Adj[X]$ adjoint of matrix $[X]$

B combined damping coefficient of motor and load, Nm/rad/s

B_1, B_2 damping coefficients for motor and load respectively, Nm/rad/s

C torsional stiffness of shaft, Nm/rad

d diameter of shaft, m

E_a amplitude of ramp signal, V

E_t threshold signal voltage, V

G modulus of rigidity of shaft material, Kg/m^2

I_{fl} motor full load current, A

i instantaneous value of armature current, A

i_t transient component of i, A

J combined moment of inertia of motor and load, $Kg\ m^2$

J_1, J_2 moment of inertia of motor and load respectively, $Kg\ m^2$

K_a gain of amplifier

K_c gain of controller

K_e electromagnetic torque constant, Nm/A

K_m motor back emf constant, V/rad/s

K_t tachometer constant, V/rad/s

L armature circuit inductance, H

L_f field winding inductance, H

l length of shaft, m

n	number of chopper voltage cycle
Q	shear stress in shaft, Kg/m^2
R	armature circuit resistance, ohm
R_f	field winding resistance, ohm
T	time period of chopper voltage cycle, s
T_1	time period of load torque pulsation ($= 2\pi/\omega_1$), s
T_e	electromagnetic torque developed by motor, Nm
T_{fl}	motor full load torque, Nm
T_L	load torque, Nm
T_{Lo}	constant component of T_L, Nm
T_{L1}	pulsating component of T_L, Nm
$[X]^T$	transpose of a matrix $[X]$
t	time, s
t_f	freewheeling period of chopper cycle, s
t_n	($t-nT$)
t_o	duty period of chopper cycle, s
V	d.c. supply voltage, V
v_r	voltage of reference signal, V
v_o	voltage of feedback signal, V
α	duty factor of chopper voltage ($= t_o/T$)
$\alpha_1, \alpha_2, \alpha_3$	real parts of roots of characteristic equation, rad/s
$\beta_1, \beta_2, \beta_3$	imaginary parts of roots of characteristic equation, rad/s
θ_1, θ_2	angular positions at motor and load ends respectively, rad
$\dot{\theta}_1, \dot{\theta}_2$	angular speeds at motor and load ends respectively, rad/s

$\dot{\theta}_{1t}$ transient component of speed $\dot{\theta}_1$, rad/s

$\emptyset$ angle defining phase of pulsating component of load torque, rad

τ_a armature time constant (= L/R), s

τ_m mechanical time constant (= J/B), s

τ_{m1} mechanical time constant (= J_1/B_1), s

τ_{m2} mechanical time constant (= J_2/B_2), s

ω angular frequency, rad/s

ω_d desired speed, rad/s

ω_n natural frequency of torsional oscillation, rad/s

ω_s average value of steady state speed, rad/s

ω_1 angular frequency of load torque pulsation, rad/s

ξ_1, ξ_2 damping ratios

$\mathcal{L}^{-1}$ Laplace inverse transform

INTRODUCTION AND LITERATURE REVIEW

1.1 INTRODUCTION

Improvements in manufacturing technology and growing complexity of methods of process control, have increased the demand for better performance and versatility of control of electric drives. One of the most remarkable developments in the field of electric drives is the application of solid state devices, specially the thyristors, to the control of motors. Thyristor control has been used to widen the scope of control and to upgrade the performance of such drives. Necessitated by these developements, there has been parallel effort towards better and more precise evaluation of the drive performance and to develop methods of analysis which need less effort. Such analytical inputs have contributed to improvements in methods of control and better designs. The work presented in this thesis is an effort in this direction.

Some features which govern the performance of an electric drive are; the type of drive motor used, the form of control system adopted, the nature of load contributed by the driven equipment, and the mechanical factors associated with the drives. These aspects are briefly discussed below:

(a) Type of Drive Motor:

Basically, the electric drives can be classified as a.c. and d.c. electric drives depending upon the type of electric motor employed to run the electromechanical (E M) system. Although the majority of industrial drives use a.c. motors as main driving motor, the d.c. motors find application in many areas because of certain inherent characteristics like flexibility for speed control, overload capability and nature of speed torque characteristics. The use of thyristors for their control has further increased the scope of d.c. motors in modern electric drives.

(b) Control System:

In a great variety of industrial applications of d.c. motors, a major consideration is its speed control, which can be obtained either by controlling the field flux or the average voltage across the armature. The field flux control method is normally used where speeds above the base speed are required, and variation over a small range is needed. Armature voltage control is adopted for obtaining speeds below the base speed and is capable of giving speeds down to very low values. A variation in voltage applied to armature can be accomplished either by changing the supply voltage impressed across the armature terminals or by adding an external resistance in series with the armature. The rheostatic control is not preferred as it gives rise to excessive power loss in armature circuit.

The use of thyristors for armature voltage control of d.c. motors has replaced the conventional methods of such controls, like the Ward-Leonard system and the use of thyratrons and mercury arc rectifiers. This is because the use of thyristors affords considerable advantage in comparison with the other systems in terms of economy, efficiency, speed of response, reversing and braking facilities and their compatibility for closed loop systems of control.

A variable d.c. voltage can be obtained by using a thyristor either from a.c. supply using converter control or from d.c. supply using chopper control. In converter control, the variation in output voltage is obtained by controlling the firing angle delay, whereas in chopper control this is affected by controlling the on/off time ratio of the output pulse. In both these methods of control, the armature current has a higher ripple content than that obtained with d.c. generator in the conventional Ward-Leonard system. Major problems with phase controlled converter are that they generate large amount of harmonics and reduce power factor, particularly at low speeds. The use of an uncontrolled rectifier followed by a d.c. chopper permits improved power factor and waveforms on the a.c. side, and the use of a relatively high chopper frequency permits reduced harmonics and losses in motor. Moreover, with a suitable choice of chopper circuit, speed of the motor can be controlled in a much wider range than is possible with phase control.

The chopper output voltage can be controlled either by 'Pulse Width Control' (Time Ratio Control) or by 'Current Limit Control'. In pulse-width control, the on/off time ratio of chopper is controlled. In the current limit control, the current is controlled between specified upper and lower limits. Therefore, the current will never be zero and there is no possibility of discontinuous conduction. The drive characteristics obtained by time ratio control are suitable for steady state operation in many applications including traction. In time ratio control (TRC), the output voltage can be varied in two different ways: either by constant frequency TRC, or by variable frequency TRC. In general, the constant frequency TRC method is preferable because it permits a choice of frequency suitable to the commutation circuit and the load, and also to get a complete range of variation of output voltage. Moreover, in a constant frequency scheme, harmonics of only definite frequencies will occur which may be filtered out.

(c) Nature of Load

From the consideration of their load torque, the driven mechanisms can be broadly classified under three catagories [13] described below:

Class A: This includes the mechanisms whose torque does not vary with speed. These may be such units as conveyers, crane hoists, shapers, etc.

Class B: These are the mechanisms whose torques vary with speed. Examples of such loads are centrifugal compressors, fans, induced draught fans and ship propellers. Under this class are also

included loads whose torque is a function of path travelled by the mechanism. These include piston pumps, crank presses, mechanisms with crank drives, metal cutting shears, etc.

Class C: These are the mechanisms whose load torque varies in a random manner, mainly because of the inconsistent properties of materials being processed. Typical machines of this class are rock crushers, clay mills, ball grinding mills, etc.

The variation of load torque in many applications, particularly those which come under class B, is cyclic in nature. Another cause for a cyclic variation in load torque is the presence of some of the mechanical factors discussed below.

(d) Mechanical Factors Associated With Drives:

The performance of an electric drive depends not only on the electrical components of the drive and the nature of load torque, but also on certain mechanical features. The mechanical factors which affect the drive performance include the effects of non-rigidity of shaft, backlash, misalignment, bending of shaft, etc. These factors may produce the following significant effects [10] in the characteristics of the electromechanical systems:

(i) Torsional Vibrations:

These are very lightly damped, relatively high frequency oscillations in speed, position, or torque, occurring because of the non-rigidity of shaft and couplings interacting with the inertia of rotating parts of system.

(ii) Cyclic rotational disturbances:

These may be caused by bent shafts, seams in felts or wires, or by eccentric mechanical misalignment or unbalanced rolls. Their principal effect is to impose a periodic load change on the drive.

(iii) Back-lash:

This is caused by loose tolerances in gear meshes, chain drives, and some types of couplings, resulting in play in the mechanical drive train.

It has been observed that these mechanical factors significantly affect the drive performance. The effects of these factors become all the more complex when more than one of these factors are prominent in the system in which case they may tend to amplify each other.

1.2 SCOPE OF WORK PRESENTED

A complete representation of an electromechanical drive system is shown in Fig.1.1 [3]. The system has been shown to be composed of four sub-systems, interconnected by different interface variables. The factors, occurring in the different subsystems, which influence the system performance are also shown. An important aspect related to system analysis is the non-linearities arising in the various elements of the system. These non-linearities are shown in Fig.1.1 against the sub-systems in which they arise.

DRIVE   SYSTEM   COMPONENTS

| ELECTRICAL SUPPLY SYSTEM | DRIVE MOTORS | MECHANICAL COUPLING | LOAD |

INTERFACE VARIABLES →   VOLTAGE CURRENT   TORQUE SPEED   TORQUE SPEED
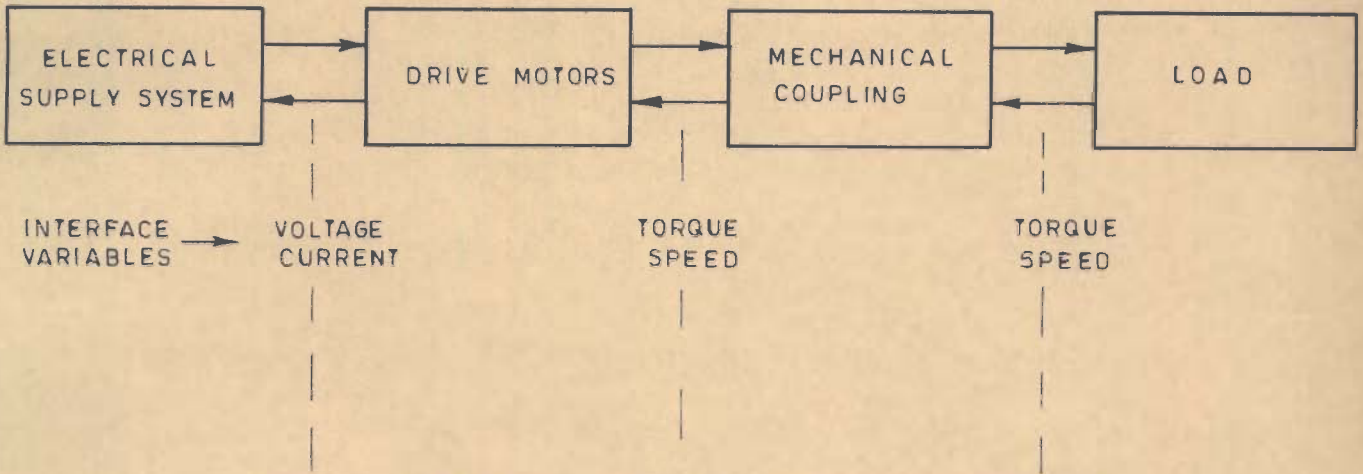
FACTORS AFFECTING DRIVE PERFORMANCE

1_ FAULTS

2_WAVE SHAPES

1_PULSATING TORQUES

2 _ IMBALANCES

3 _SWITCHING TRANSIENTS

1_ MISALIGNMENT

2 _ BENDING OF SHAFT

3 _ELASTICITY OF SHAFT

1_ IMPACTS

2 _ CYCLIC EFFECTS

3 _ IMBALANCES

4 _ PROCESS EFFECTS

DRIVE SYSTEM NON- LINEARITIES

1_ RECTIFIERS

2_ INVERTERS

3 _ CYCLO-CONVERTERS

1_ NON-LINEAR ELECTRICAL DYNAMICS

2_ SATURATION EFFECTS

1_ GEARING BACKLASH

2_ NON-LINEAR COUPLINGS

1_ LOAD V/S SPEED

2 _ PROCESS DYNAMICS

FIG. 1. 1_COMPONENTS OF AN ELECTROMECHANICAL DRIVE SYSTEM

For a precise determination of performance of such a system, the analysis should take into account all the factors which affect the drive performance, as also the non-linearities. Such an analysis will need a model of the system which will be far too complicated to be of much practical significance.

In this thesis, the analysis and various aspects of the performance evaluation of a d.c. motor driven electromechanical system, fed by a chopper as well as ordinary d.c. supply, are presented. Out of the various mechanical factors affecting system performance, only two more important factors, viz., the elasticity of the shaft coupling the motor to the load, and the periodic variation of load torque have been accounted for. Elasticity is an inherent feature of any mechanical coupling, and periodic variation in load torque may be a characteristic feature in many applications. These variations in load torque may be present due to mechanical factors like bent shafts, misalignment, eccentric or unbalanced rolls as also due to the nature of the driven mechanism.

Out of the non-linearities, those arising in the supply system, because of the device characteristics (eg. chopper) have been accounted for. The remaining non-linearities have not been considered in the present analysis, in order to ensure that the model of the system can be managed. Non-linearities of system equations have either been accounted for, or it has been shown that it is valid to ignore them.

The aim of this study is to give an analysis of a d.c. drive electromechanical system and to study the effects of some of the more important mechanical factors associated with drives. This will lead to a more accurate predetermination of performance, and will provide essential information for proper system design.

The work presented covers the following aspects:

(a) Analysis of a separately excited d.c. motor drive fed by a constant d.c. voltage taking into account the effects of elasticity of coupling and periodic variation of load torque [Chapter-2].

(b) Development of a new technique for the analysis of chopper fed d.c. motor drives which is superior to existing techniques in that it is more accurate, needs lesser computation efforts and gives closed-form solutions for system variables determining its performance [Chapter-3].

(c) Analysis of a chopper fed d.c. separately excited motor drive with an elastic coupling and pulsating load torque using the analytical technique of Chapter-3 [Chapter-4]

(d) Analysis of a closed loop pulsewidth modulated separately excited d.c. motor drive having an elastic coupling, for a constant as well as periodically varying load torques, and design of system parameters for a stable operation and minimum settling time [Chapper-5].

(e) Non-linear analysis of separately excited d.c. motor drive including some system non-linearities [Chapter-6].

(f) Analysis of d.c. series motor driven electromechanical system, fed by a chopper as well as a constant d.c. voltage, taking into account the effects of elasticity of coupling and periodic variation of load torque [Chapter-7].

1.3 LITERATURE REVIEW

The objective of the present work is to investigate the effects of some of the mechanical factors on the performance of d.c. motor drives fed by a chopper as well as a constant d.c. voltage supply. While some work dealing with the effects of mechanical factors on the performance of d.c. drives fed by a constant d.c. voltage has been reported in literature, no work seems to have been done on the analysis of chopper controlled d.c. drives taking into account these mechanical considerations.

The published work related to the area of this disser-tation can be catagorised as below:

(i) Work dealing with the analysis of chopper controlled d.c. drives but without considering the mechanical factors.

(ii) Work dealing with the effects of mechanical factors on the performance of d.c. drives fed by a constant d.c. voltage.

The following review summarises the published work under the above two categories:

1.3.1 Work Dealing With Analysis of Chopper Controlled D.C. Drives

In respect of chopper controlled d.c. drives, the publish-ed literature consists of various methods of analysis for obtain-ing the performance of such drives and some suggestions for

improving the performance. The effect of any of the mechanical factors which may influence the drive performance has not been taken into account by any author.

(a) Work dealing with analysis of chopper fed d.c. separately excited motor drives includes the following aspects:

Van Eck [60] has discussed the superiority of separately excited d.c. motors over d.c. series motors and cited a number of traction applications where separately excited motors are being used. The characteristics of separately excited d.c. motors fed either by a dc-dc converter or by ac-dc converter have been reported.

The current in armature circuit of chopper fed d.c. motors, specially for low values of load torque and armature inductance, may become discontinuous. A method for ensuring the continuity of armature current has been presented by Zabar and Alexandrovitz [65], in which the chopper turn off time is kept constant and average load voltage is regulated by varying the chopper time period.

In practical drives, the supply voltage and the load torque may have small variations. Taking these variations into account, Nitta et. al. [43] have determined the dynamic response of a d.c. drive driven by a pulsating power supply and derived its transfer function. The analysis is extended by Matsui and Miyari [37] and a critical condition under which the electrical time constant can be neglected, is obtained. Moreover, the analysis covers both, the continuous conduction as well as discontinuous modes of conduction.

Chopper fed d.c. drives suffer from a high value of ripple contents in armature current. Verma et.al. [61] have presented two analytical techniques for predicting the performance of such drives, and have obtained a relationship of pulse width with current ripple factor as well as variations in speed.

Various methods have been suggested by different authors to solve the differential equations describing the performance of chopper fed d.c. drives. One approach to solve these differential equations is using computer simulation techniques. Williams [62] has used state model technique to simulate the system on a digital computer. The simulation enables the prediction of performance in transient as well as steady state for any load conditions.This enables system characteristics and stability to be judged and modified theoretically. Damley and Dubey [18] have also presented a digital computer programme, employing numerical techniques, for the analysis of chopper fed d.c. motor drives. The method does not need prior knowledge of mode of operation of chopper circuit and the derivation of the relevant equations. The method is also applicable to d.c. series motor drives.

The second approach to obtain the performance of chopper fed d.c. drives involves separate sets of equations applicable to different modes of chopper operation. Closed-form solutions for each set of equations are obtained and the performance is deter-mined using these solutions by recursive step-by-step techniques. To facilitate the simplification of the analysis, different assump-tions and approximations have been suggested. However, rigorous closed-form solutions of system performance variables are not

available. Based on this approach, different methods of analysis [23,25,26,44] have been proposed.

Perimelalagan and Rajgopalan [44] have analysed the performance for the case of continuous conduction of armature current by four different methods. These methods are based on one of the following assumptions: negligible commutation interval, negligible ripple in armature current, constant current during commutation and direct solution of governing differential equations. A method has been suggested to calculate additional losses due to pulsations in motor current.

A comparative study of the two commonly used chopper control techniques, viz., time ratio control (TRC) and current limit control (CLC), has been presented by Dubey and Shephered[23]. The performance equations using these control techniques are given for continuous as well as discontinuous conduction of armature current. The analysis is based on the assumptions that the chopper output wave is a perfect square wave and the speed during a chopper cycle remains unchanged. Comparing the different techniques of chopper control, the authors suggest that TRC technique with variable on time and constant chopper frequency is superior.

For transient analysis of d.c. drives using TRC technique, the above authors have proposed three different methods [26], which are based on different assumptions. While the first two methods are applicable to the case of continuous conduction only, the third method considers the possibility of discontinuous conduction as well. These methods are approximate but need lesser computation time compared to other methods. The use of filters

has been proposed [22] so as to limit the range of discontinuous conduction. The same authors have also suggested three different methods [25] for transient analysis using CLC technique. The first method is exact and is taken as reference to compare the other two methods. The second method assumes the speed over a chopper cycle to be constant, while the third considers linear variation of current in a chopper cycle. The last method can be used to derive the transfer function and needs lesser computation time with an accuracy comparable to the other two methods.

Apart from the above two approaches of analysis of chopper fed d.c. drives, a third approach has also been reported by Singh and Kohli [52], which is based on the methods of Fourier analysis of the chopper output voltage wave. They have used this approach to analyse the performance under continuous mode of operation. The limitation of analysis is that the expressions for performance variables are interdependent. This limitation of the analysis has been overcome in their subsequent paper [51] which deals with the case of discontinuous conduction as well and in addition gives independent expressions for variables giving system performance. The analysis shows that the commutation interval significantly affects the drive performance.

Barton [1] has investigated an important feature of chopper controlled drives which was not considered by earlier workers. He studied the static transfer characteristics of a chopper feeding an active load and pointed out a marked difference in behaviour in the form of a very substantial reduction in incremental gain when transition from continuous to discontinuous

conduction takes place. This phenomenon results in sluggish res-
ponse of feed back systems employing choppers as power amplifiers.

(b) Work dealing with analysis of chopper fed d.c. series motor
drives includes the following aspects:

The analysis of chopper fed d.c. series motor drives is
relatively more complicated due to the non-linearity of the magne-
tisation characteristic of motor. For such drives, the problem
of calculation of motor induced voltage constant is not simple as
it depends on the value of armature current which itself varies
with time in transient as well as steady state conditions. This
problem has been tackled by various researches and methods based
on different approximations are suggested [17,20,27,28].

Franklin [28] has given a mathematical model of chopper
fed d.c. series motor and its performance is predicted in terms
of average and instantaneous values of torque and speed. The non-
linearity of magnetic circuit is considered by a suitable approxi-
mation.

Dubey and Shepherd [27] have proposed a method of analysis
of chopper fed d.c. series motor drives based on the assumption
that the motor induced voltage constant is a function of the
average value of armature current rather than its instantaneous
value. Based on the same assumptions, in another paper, Dubey[24]
has given two analytical methods which can take into account the
effect of commutation interval. In the first method, the current
during commutation interval is assumed constant, while in the
second, the ripples in armature current are neglected. The effect
of commutation interval is also considered in the analysis

presented by Ranade and Dubey [46]. The methods presented in references [27,24] are approximate but need less computation time. A numerical technique for representing the non-linear magnetisation characteristics of series motor has also been suggested [17], but the analysis using this technique requires large computation time.

For the transient analysis of chopper fed d.c. series motor, different methods have been suggested using time ratio control [20] as well as current limit control [21]. Some of these methods can be used for deriving the transfer function of motor for small signal perturbations about a steady state operating point. Using the block diagram approach, Bhadra [2] has analysed the transient performance of such drives for small sudden variations in load torque and the on-period of the thyristor. The linearized perturbation equations are solved to calculate the instantaneous values of performance variables.

The papers discussed above deal mainly with the analytical techniques applicable for determining the performance of open loop chopper controlled d.c. drives. There are a few more papers dealing with chopper control but for closed loop d.c. drive systems using the pulse-width modulation. These are discussed below:

Jacob Tal [54] has suggested the use of switching amplifiers for d.c. servo systems in order to reduce the high power dissipation inherent with linear amplifiers. One method of operating the switching amplifiers with constant frequency and variable on time, called PWM has been discussed. A general

scheme of voltage regulator feed back control using PWM control is given by Maisel [36]. The regulator uses a ramp signal to modulate a d.c. signal into a square wave pulse signal. The duty factor of the modulated pulse is a function of error signal. A departure of output from the desired value changes the pulse duty factor and hence the average value of input maintaining the output at desired level. Taft et.al. [53] have described two methods, the dither method and the limit cycle method, for obtaining pulse width modulated signals. It has been pointed out that the inductance added in series with armature to reduce the current ripples, adversely affects the transient response of the motor. The advantages of closing a current loop around the amplifier, which include the improvement in stability at high value of gains and short circuit protection, are discussed.

The analysis given by Burger [6] deals with the basic characteristics of a PWM d.c. converter. These include operational characteristics like efficiency, ripple, regulation, settling time and physical characteristics like weight, size, cost and reliability. The system is simulated on an analog computer to study its small signal stability. Unnikrishnan [58,59] has suggested a method for maintaining the average voltage of a dc-dc converter. This is achieved by introducing a gain in feed back path. The stability of the system is also studied.

1.3.2 Work Dealing With Effects of Mechanical Factors

The work available in literature dealing with the effects of mechanical factors pertains only to drives fed by constant d.c. voltage. No attempt so far has been made to analyse the effects

of mechanical factors on the performance of d.c. motor drives fed through a chopper controlled supply. The work reported on the mechanical considerations of d.c. drive EM systems is summarised below:

A comprehensive description of various mechanical factors affecting the performance of electric drives is given by Carter[10]. The factors discussed include elasticity of shaft, backlash, misalignment, bending of shaft, unbalance of rolls, etc. The effect of these factors is mainly to produce torsional oscillations in the system and to impose cyclic rotational disturbance in the form of either impact loads or periodic changes in load torques. The system instability at resonance is discussed and possible methods of stabilisation suggested. Although complete analysis of the drive is not given, yet the paper gives a general overview of the problems arising due to such effects.

Bishop and Mayer [3] have emphasized the need of accurate modelling of the total system including the system non-linearities and component interactions. The drive system has been divided into four functional system components. The interface variables which connect these components and the dynamic interactions have been shown [Fig.1.1]. Drive system disturbance sources such as pulsating torques, imbalances and switching transients of the drive motor, impacts and cyclic effects of the load and mechanical inaccuracies are discussed. Various types of drive system non-linearities such as, non-linear electrical dynamics, saturation effects, gear backlash, non-linear coupling, etc. are identified. The paper gives a good description of the problem and the sources

of complexity are defined. The effect of model fidelity on the
predicted dynamic torques in different drive systems are discussed.
In another paper Mayer [39] has discussed the various sources of
excitation of torsional oscillations for cement industry drives.
The importance of torsional mechanical system with the electric
drive system and its control have been emphasized.

Out of the various mechanical factors mentioned above,
only one such factor, the elasticity of coupling, seems to have
attracted the attention of researchers, because of its greater
effect on performance. The work reported, mainly in Russian,
deals with the analysis of d.c. motor drives coupled to load
through an elastic shaft [7-9,30-32,39,45,57]. The transient
analysis of such a system with constant load torque and neglecting
the damping, has been presented by Tsekhovitch [57]. The system
equations are solved using classical methods to find the ampli-
tudes of oscillations of the motor torque and that of the shaft
elastic torque. The ratio of these amplitudes, termed as degree
of influence, is obtained to plot the dimensionless amplitude-
frequency characteristics (AFC) of the system.

The interaction of the two mechanical factors, the elasti-
city of shaft and periodic variation of load torque, produces
resonance in the system. Kaminskaya [30] has studied the vibra-
tions of an EM system under resonance condition. The mechanism
is represented by a two mass system connected through a single
elastic coupling. System aperiodic stability is also determined.
Kluchev [32] has analysed the performance of a d.c. motor drive
supplied through a controller and having an elastic coupling.

The AFC of the system is obtained for normal operation as well as for resonance condition. Depending upon the AFC, the elastic coupling has been catagorised as weak, effective or rigid. The interaction of mechanical oscillations with armature current for weak and rigid couplings is observed to be negligible, whereas this interaction is significant for effective couplings. This sets a limit for a proper value of elasticity of coupling. For an electric drive system with an elastic coupling, Burgin [9] has analysed the effects of variation of drive parameters on the AFC of the system. This helps in selection of proper values of system parameters. For a small change in the frequency of harmonic load torque disturbance, the corresponding change in electric torque is obtained and the effect of resonance on AFC studied.

The non-linear analysis of a d.c. drive EM system with elastic coupling has also been presented by Burgin [7]. The non-linearity considered in the system is due to the backlash in the transmission system. The stability of such a system is studied using Lyapunov method. In another paper [8], the same author has given the transient analysis of a linearised double mass EM system with an elastic coupling using a d.c. series motor. Kluchev et.al. [31] have analysed a closed-loop d.c. drive EM system, having linear and non-linear electrical and mechanical couplings. The effects of backlash in the coupling and gear teeth have also been considered. The system is linearized and modelled on a computer to analyse its performance. The performance studies include, working out criteria for neglecting the influence of coupling, dynamic properties and stability of non-linear EM

system, and the conditions for minimum amplitude at resonance for forced vibrations. These studies enable a suitable design of electrical and mechanical parameters of the system.

The work discussed above deals with the effects of mechanical factors on performance of d.c. drive EM systems fed by a constant voltage. For a d.c. drive fed by a thyristor bridge converter with elastic coupling, Polyakov et.al. [45] have identified the conditions leading to resonance. It is pointed out that any alignment between the resonance frequencies of AFC of the system and the frequency spectrum of thyristor control voltage should be avoided in order to avoid resonance.

CHAPTER-2

ANALYSIS OF OPEN-LOOP D.C. MOTOR DRIVE WITH ELASTIC COUPLING AND PULSATING LOAD TORQUE

2.1 INTRODUCTION

An electric drive invariably contains a mechanical link in the form of the shaft coupling the motor to the load. In practical systems, this link is always elastic, and not rigid as is generally assumed for simplifying the analysis. For precise determination of performance, specially under dynamic conditions, the elasticity of shaft must be taken into account. In a large number of practical applications, due to the inherent nature of the driven mechanism, the load torque is not constant but is pulsating in nature. Examples of such loads are compressors, crank-piston mechanisms, machine tools, etc. [55,63]. Factors such as eccentric or unbalanced rolls, bent shafts or mechanical misalignment [10] may also introduce periodic variations in load torque.

The problem of torsional oscillations in the d.c. motor drives caused by the elasticity of shaft, has been analysed in the past [30,32,39,45,57]. The work available includes the transient analysis and the study of amplitude-frequency characteristics of a d.c. drive with elastic coupling and constant load torque neglecting the effect of damping [57]. The amplitudes of oscillation of the motor torque and that of the elastic torque in the shaft, are compared [9,32,57] to assess the extent of influence of

elasticity of shaft. The amplitudes of these torques at resonance are also studied [9,31]. However, a complete analysis of a d.c. drive, fed by a constant d.c. voltage source, with an elastic coupling and pulsating load torque, which gives a closed form solution of system performance variables for transient as well as steady state conditions is not available. The effects of variation of drive parameters on the performance has also not been studied.

2.2 WORK PRESENTED

In this chapter, analysis of a d.c. separately excited motor with a pulsating load torque and taking into account the elasticity of coupling and damping, is presented. The effects of system parameters, like moment of inertia, elasticity of shaft, damping and the frequency of load torque pulsation, on the drive performance are studied. Conditions leading to resonance are investigated. Some suggestions are given to improve the design of the system.

The system analysed consists of a d.c. separately excited motor supplied with a constant d.c. voltage and connected to the load through an elastic shaft as shown in Fig. 2.1. The system is represented by a two rotor system and the moments of inertia and damping for the motor and the load are considered separately as shown in Fig. 2.2(a). This type of system is referred to as 'Two rotor, semi-definite, two degree of freedom system' [14,56]. The load torque is considered to consist of a non-varying component T_{Lo} superposed by a sinusoidally varying component T_{L1} as shown in Fig. 2.2(b). A mathematical model of the system is given and the equations are expressed in State model form. The system equations are solved to obtain closed-form solutions for armature
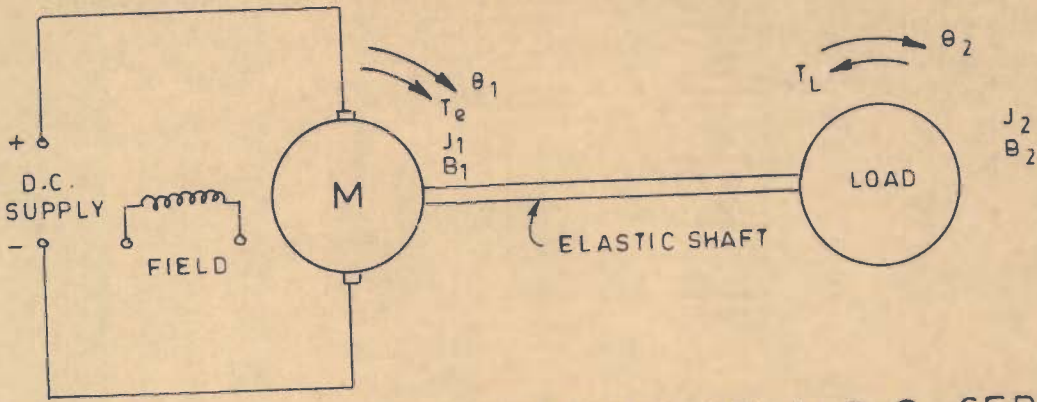
FIG. 2.1 _ SCHEMATIC DIAGRAM OF A D.C. SEPARATELY EXCITED MOTOR WITH ELASTIC COUPLING AND PULSATING LOAD TORQUE
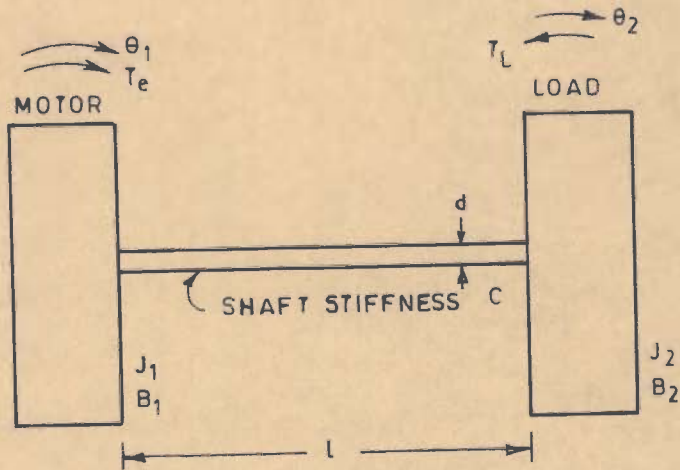
(a)_ TWO ROTOR SEMI-DEFINITE SYSTEM REPRESENTING D.C. MOTOR COUPLED TO LOAD THROUGH AN ELASTIC SHAFT
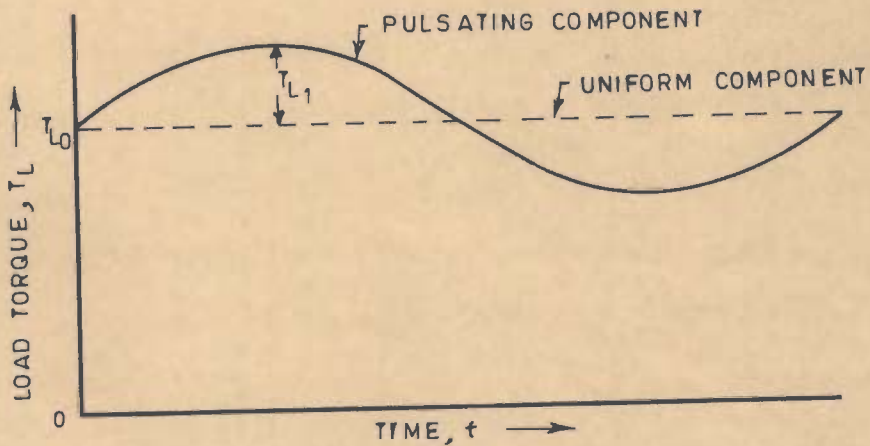
(b)_ PERIODIC VARIATION OF LOAD TORQUE

FIG. 2.2

current and motor speed under transient as well as steady state conditions.

2.3 PERFORMANCE EQUATIONS

The system shown in Fig.2.1 can be described by the following equations:

$$V = L \frac{di}{dt} + R i + K_m \dot{\theta}_1 \tag{2.1}$$

$$T_e = J_1 \ddot{\theta}_1 + B_1 \dot{\theta}_1 + C(\theta_1 - \theta_2) \tag{2.2}$$

$$-T_L = J_2 \ddot{\theta}_2 + B_2 \dot{\theta}_2 + C(\theta_2 - \theta_1) \tag{2.3}$$

where $T_e = K_e i$

The motor field current in the above equations has been assumed to be constant. A periodically varying load torque T_L, can be considered to be consisting of a constant component and a number of sinusoidally varying components, and can in general be expressed as:

$$T_L = T_{Lo} + T_{L1} \sin(\omega_1 t - \emptyset) + T_{L2} \sin(2\omega_1 t - \emptyset') + \ldots \tag{2.4}$$

For the sake of simplicity, in the analysis that follows, only the constant component and the first alternating component are taken into account. However, the method of analysis is general and can take into account any number of harmonic components, and is therefore applicable for any type of periodic load torque. The load torque as shown in Fig.2.2(b) can, therefore, be represented as:

$$T_L = T_{Lo} + T_{L1} \sin(\omega_1 t - \emptyset) \tag{2.5}$$

The frequency of the load torque for certain applications depends upon the angular speed of the shaft. This leads to non-linear system equations. However, the pulsations in speed being very small compared to the average value (as will be observed from the results of this analysis) can be neglected, and the frequency of pulsating component of load torque ω_1 can be justifiably assumed to be proportional to the average value of shaft speed. This makes the system equations linear and simplifies the analysis without causing an appreciable error in the results (A non-linear analysis of the system taking ω_1 equal to shaft speed $\dot{\theta}_2$ is presented in Chapter-6). Thus ω_1 can be written as $\omega_1 = k\omega_s$, where ω_s is the average steady state speed and k is a constant which depends on the type of mechanical load coupled to motor shaft. In this analysis, the value of k is taken as unity, implying that the load torque completes one cycle in one revolution of the machine shaft. Systems for other values of k can be analysed in a similar fashion.

2.4. SYSTEM CHARACTERISTIC-EQUATION

Eqns. (2.1-2.5) can be expressed in the State-model form as[*]

$$\dot{x} = Ax + Du \qquad (2.6)$$

where

---

[*] In state equation (2.6) symbol D is used, in place of usually used symbol B, as B denotes damping in this text.

$$A = \begin{bmatrix} 0 & 1 & 0 & 0 & 0 \\ -C/J_1 & -B_1/J_1 & C/J_1 & 0 & K_e/J_1 \\ 0 & 0 & 0 & 1 & 0 \\ C/J_2 & 0 & -C/J_2 & -B_2/J_2 & 0 \\ 0 & -K_m/L & 0 & 0 & -1/\tau_a \end{bmatrix} \qquad (2.7)$$

$$D = \begin{bmatrix} 0 & 0 & 0 & 0 & 1/L \\ 0 & 0 & 0 & -1/J_2 & 0 \end{bmatrix}^T, \qquad (2.8)$$

forcing function vector $u = \begin{bmatrix} V \\ T_L \end{bmatrix}$ (2.9)

and, state variable vector $x = [\theta_1 \quad \dot{\theta}_1 \quad \theta_2 \quad \dot{\theta}_2 \quad i]^T$ (2.10)

Taking Laplace transform of eqn.(2.6):

$$X(s) = [sI-A]^{-1} DU(s) + [sI-A]^{-1} x(0) \qquad (2.11)$$

where I is a unit matrix of the same order as matrix A. The motor is assumed to start from quiescent state, i.e. the initial values of state variables are zero,

$$x(0) = [0 \quad 0 \quad 0 \quad 0 \quad 0]^T$$

For steady state performance, the results so obtained will be independent of initial values x(0). For transient studies other than those beginning with quiescent initial conditions, appropriate initial conditions may be used and results obtained in a similar fashion.

From eqn.(2.11), $X(s)$ can be written as:

$$X(s) = \frac{1}{\Delta} [\emptyset_{ij}]DU(s) \qquad (2.12)$$

where $[\emptyset_{ij}] = \text{Adj } [sI-A]$

and Δ is the determinant of $[sI-A]$ matrix.

The characteristic equation of the system, $\Delta = 0$, can be written as:

$$A_1 s^5 + A_2 s^4 + A_3 s^3 + A_4 s^2 + A_5 s = 0 \qquad (2.13)$$

The characteristic equation (2.13) for the drive with an elastic shaft is of order five. However, if the elasticity of shaft is not taken into account, the order of the characteristic equation reduces to two. The coefficients of the characteristic equation (2.13) are:

$$\left.\begin{aligned}
A_1 &= \tau_a J_1 J_2 \\
A_2 &= \tau_a (B_1 J_2 + B_2 J_1) + J_1 J_2 \\
A_3 &= B_1 J_2 + B_2 J_1 + \tau_a B_1 B_2 + C \tau_a (J_1 + J_2) + K_e K_m J_2 / R \\
A_4 &= B_1 B_2 + B_2 K_e K_m / R + C \tau_a (B_1 + B_2) + C(J_1 + J_2) \\
A_5 &= C(B_1 + B_2 + K_e K_m / R)
\end{aligned}\right\} \qquad (2.14)$$

In the case of separately excited d.c. motors, the armature circuit inductance is generally low and the roots of the characteristic equation (2.13) can be represented as:

$$s_1 = 0 \ , \ s_2 = -\alpha_1 \ , \ s_3 = -\alpha_2 \ , \ s_{4,5} = -\alpha_3 \pm j\beta_3$$

where α_1, α_2 and α_3 are real positive values and determine the rate of decay of transient component of system response. However,

for large values of armature inductance, roots s_2 and s_3 may become complex. The imaginary part β_3 of the complex roots $s_{4,5}$ gives the damped natural frequency of oscillation of the system [14]. The values of α_3 and β_3 depend upon the values of undamped natural frequency of torsional oscillation ω_n and the damping ratio as:

$$\alpha_3 = \xi\,\omega_n \quad \text{and} \quad \beta_3 = \omega_n(1-\xi^2)^{1/2} \tag{2.15}$$

where ξ is damping ratio. The value of ω_n is related to elasticity of shaft and moment of inertia of the system as:

$$\omega_n = \left[\,C\left(\frac{1}{J_1} + \frac{1}{J_2}\right)\right]^{1/2} \tag{2.16}$$

Thus Δ can be represented as:

$$\Delta = s(s+\alpha_1)(s+\alpha_2)(s+\alpha_3-j\beta_3)(s+\alpha_3+j\beta_3) \tag{2.17}$$

2.5 DETERMINATION OF SYSTEM RESPONSE

The closed form solutions for performance variables i.e. armature current and motor angular speed, can be determined by taking the inverse Laplace transform of eqn.(2.12). Thus

$$\begin{bmatrix} \theta_1(t) \\ \dot{\theta}_1(t) \\ \theta_2(t) \\ \dot{\theta}_2(t) \\ i(t) \end{bmatrix} = \mathcal{L}^{-1}\frac{1}{\Delta}\begin{bmatrix} \emptyset_{11}(s)\ldots\emptyset_{51}(s) \\ \emptyset_{12}(s)\ldots\emptyset_{52}(s) \\ \emptyset_{13}(s)\ldots\emptyset_{53}(s) \\ \emptyset_{14}(s)\ldots\emptyset_{54}(s) \\ \emptyset_{15}(s)\ldots\emptyset_{55}(s) \end{bmatrix}\begin{bmatrix} 0 \\ 0 \\ 0 \\ -\frac{1}{J_2}\left\{\frac{T_{Lo}}{s}+\frac{T_{L1}(\omega_1\cos\emptyset-s\sin\emptyset)}{(s^2+\omega_1^2)}\right\} \\ \frac{V}{sL} \end{bmatrix} \tag{2.18}$$

2.5.1   Solution For Armature Current

From eqn.(2.18), armature current $i(t)$ can be written as:

$$i(t) = \mathcal{L}^{-1} \frac{1}{\Delta}\left[-\frac{\emptyset_{45}(s)}{J_2}\left\{\frac{T_{Lo}}{s} + \frac{T_{L1}(\omega_1 \cos\emptyset - s \sin\emptyset)}{(s^2 + \omega_1^2)}\right\} + \emptyset_{55}\frac{V}{sL}\right] \quad (2.19)$$

From eqn.(2.19), the expression for armature current can be obtained as:

$$i(t) = i_1 + i_2 + i_3 \exp(-\alpha_1 t) + i_4 \exp(-\alpha_2 t) + i_5 \exp(-\alpha_3 t) \quad (2.20)$$

where $i_1 = K_{28}\dfrac{V}{L} + K_{17}\dfrac{T_{Lo}}{J_2}$

$$i_2 = K_{27}\frac{T_{L1}}{J_2}\sin(\omega_1 t - \psi_2)$$

$$i_3 = K_{18}\frac{T_{Lo}}{J_2} + K_{22}\frac{T_{L1}}{J_2} + K_{29}\frac{V}{L}$$

$$i_4 = K_{19}\frac{T_{Lo}}{J_2} + K_{23}\frac{T_{L1}}{J_2} + K_{30}\frac{V}{L}$$

$$i_5 = K_{21}\frac{T_{Lo}}{J_2}\sin(\beta_3 t - \emptyset_4) + K_{26}\frac{T_{L1}}{J_2}\sin(\beta_3 t - \emptyset_5)$$

$$+ K_{32}\frac{V}{L}\sin(\beta_3 t - \emptyset_6)$$

[Expressions for different symbols are given in appendix A-1]

2.5.1.1   Steady State Armature Current

The solution for steady state armature current, $i_s(t)$, can be written from eqn.(2.20) as:

$$i_s(t) = i_1 + i_2 \quad (2.21)$$

2.5.2 Solution For Motor Speed

From eqn.(2.18), motor speed $\dot{\theta}_1(t)$ can written as:

$$\dot{\theta}_1(t) = \mathcal{L}^{-1} \frac{1}{\Delta}\left[-\frac{\emptyset_{42}(s)}{J_2}\left\{\frac{T_{Lo}}{s} + \frac{T_{L1}(\omega_1 \cos\emptyset - s\sin\emptyset)}{(s^2 + \omega_1^2)}\right\} + \frac{\emptyset_{52}V}{sL}\right] \quad (2.22)$$

From eqn.(2.22), the solution for speed can be obtained as:

$$\dot{\theta}_1(t) = n_1 + n_2 + n_3 \exp(-\alpha_1 t) + n_4 \exp(-\alpha_2 t) + n_5 \exp(-\alpha_3 t) \quad (2.23)$$

where, $n_1 = K_{12}\dfrac{V}{L} - K_1 \dfrac{T_{Lo}}{J_2}$

$$n_2 = -K_{10}\frac{T_{L1}}{J_2}\sin(\omega_1 t - \psi_1)$$

$$n_3 = -K_2\frac{T_{Lo}}{J_2} - K_6\frac{T_{L1}}{J_2} + K_{13}\frac{V}{L}$$

$$n_4 = -K_3\frac{T_{Lo}}{J_2} - K_7\frac{T_{L1}}{J_2} + K_{14}\frac{V}{L}$$

$$n_5 = -K_5\frac{T_{Lo}}{J_2}\sin(\beta_3 t - \emptyset_1) - K_{11}\frac{T_{L1}}{J_2}\sin(\beta_3 t - \emptyset_2)$$

$$+ K_{16}\frac{V}{L}\sin(\beta_3 t - \emptyset_3)$$

[Expressions for the various symbols used above are

given in appendix A-1]

2.5.2.1 Steady State Speed

The solution for steady state speed, $\dot{\theta}_{1s}(t)$, can be
written from eqn.(2.23) as:

$$\dot{\theta}_{1s}(t) = n_1 + n_2 \quad (2.24)$$

2.6 NATURE OF ARMATURE CURRENT AND MOTOR SPEED

2.6.1 Steady State Performance

The armature current and motor speed in steady state consist of two components [eqns. (2.21 , 2.24)]. One is a non-varying component (i_1 , n_1) while the other is a pulsating component (i_2 , n_2) varying sinusoidally at the frequency of the pulsating component of the load torque, ω_1.

2.6.1.1 Frequency of Load Torque Pulsation for Maximum and Minimum Pulsations of Current and Speed

The steady state pulsating components of current and speed (i_2 and n_2) depend upon the values of M_2 and N_2 [appendix A-1]. The frequency of load torque pulsation for maximum and minimum values of i_2 and n_2 can be obtained from the condition given below:

$$\frac{d}{d\,\omega_1} \left[(\frac{M_2}{\omega_1})^2 + (\frac{N_2}{\omega_1})^2 \right] = 0$$

This leads to the following conclusions:

(i) The amplitude of the pulsating component of current or speed is maximum when the frequency of load torque is equal to β_3. This frequency may be termed as resonance frequency 'ω_r' and its value depends upon the natural frequency ω_n and damping ratio ξ [eqn. (2.15)]. For practical electric drive systems damping ratio is very small and β_3 is nearly equal to ω_n. The peak value of current and speed under resonance condition depends upon the damping ratio.

(ii) The minimum value of these components occurs at a frequency of load torque which is equal to $1/\sqrt{2}$ times the value of resonance frequency. This frequency may be termed as critical frequency $'\omega_c'$.

2.6.2 Transient State Performance

In addition to the two components of steady state condition, the armature current and speed each have three components exponentially decaying with time (i_3, i_4, i_5 and n_3, n_4, n_5 respectively)[eqns.(2.20 , 2.23)]. The components i_5 and n_5 of current and speed respectively are sinusoidal components of frequency β_3 and exponentially decaying amplitudes. For an undamped system ($\alpha_3 = 0, \beta_3 = \omega_n$), these components persist and vary sinusoidally for indefinite time. In the case of a rigid shaft, these components are absent.

2.7 TYPICAL PERFORMANCE STUDIES

To illustrate the analysis presented in sections 2.3-2.6 , the performance of a d.c. drive system with the following specifications is analysed:

Motor:

Separately excited d.c. motor:

Supply voltage, V = 200 V

Armature circuit resistance, R = 4 ohm

Armature circuit inductance, L = 0.06 H

Full load current, I_{fl} = 6.3 A (1 pu)

Rated speed = 1000 rpm (1 pu)

Moment of inertia of rotating parts, J_1 = 0.05 Kg m^2

Damping coefficient, B_1 = 0.008 Nm/rad/s

Electromagnetic torque constant, Ke = 1.86 Nm/A

Motor back emf constant, Km = 1.86 V/rad/s

Mechanical System:

Torsional stiffness of shaft, C = 6750 Nm/rad

Moment of inertia of load, J_2 = 0.05 Kg m^2

Damping coefficient of load, B_2 = 0.008 Nm/rad/s

Constant component of load torque, T_{Lo} = 0.75 full load torque

Pulsating component of load torque, T_{L1} = 0.25 full load torque

Shaft length, l = 1 m

Shaft diameter, d = 0.03 m

Modulus of rigidity of shaft material, G = 0.85 x 10^{10} Kg/m^2

Phase angle of load torque, $\emptyset$ = 0

The performance as computed using this analysis is depicted in Figs. 2.4-2.13 . For a load torque varying as shown in Fig.2.3., the variations in armature current and motor speed under steady state condition are shown in Figs. 2.4 and 2.5 respectively. It is observed that both the armature current and motor speed have a pulsating component superposed on a nonvarying component. The frequency of these pulsating components is same as the frequency of pulsation of the load torque.

It may be inferred that if the load torque is periodic in nature, such that it can be resolved into a constant component and a number of sinusoidally varying harmonic components, then the armature current and speed will also have a similar nature under steady state conditions.
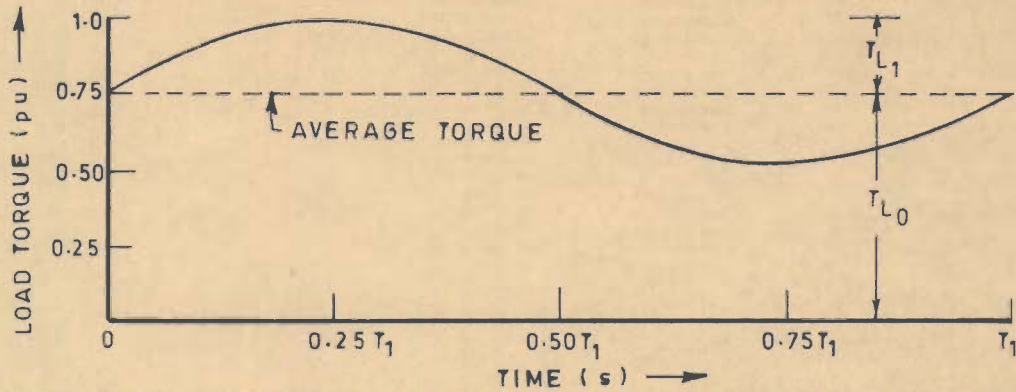
FIG. 2.3 _ VARIATION OF LOAD TORQUE, ω_1 =95.33 rad/s
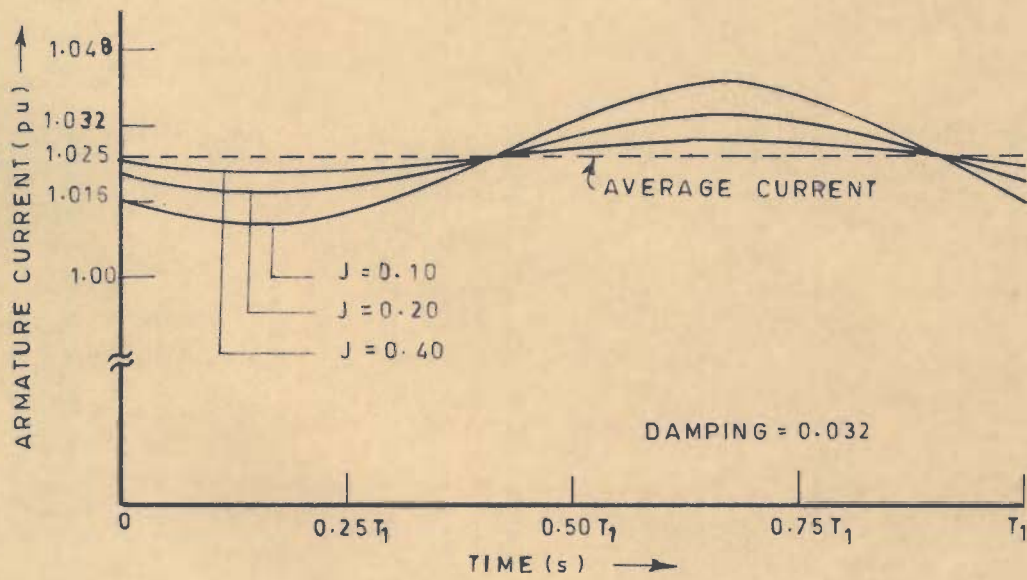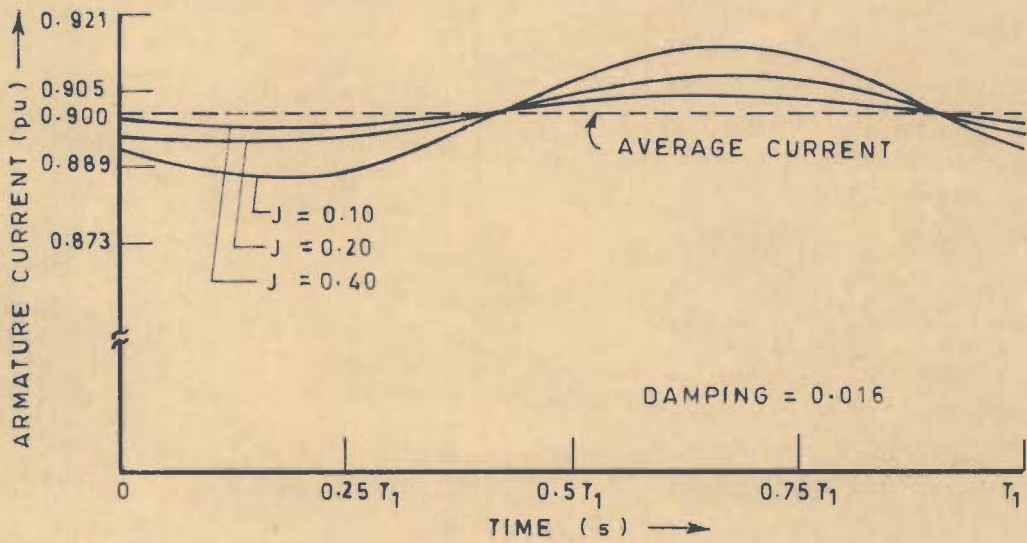
FIG. 2.4 _ EFFECT OF MOMENT OF INERTIA AND DAMPING ON STEADY STATE ARMATURE CURRENT FOR A PULSATING LOAD TORQUE
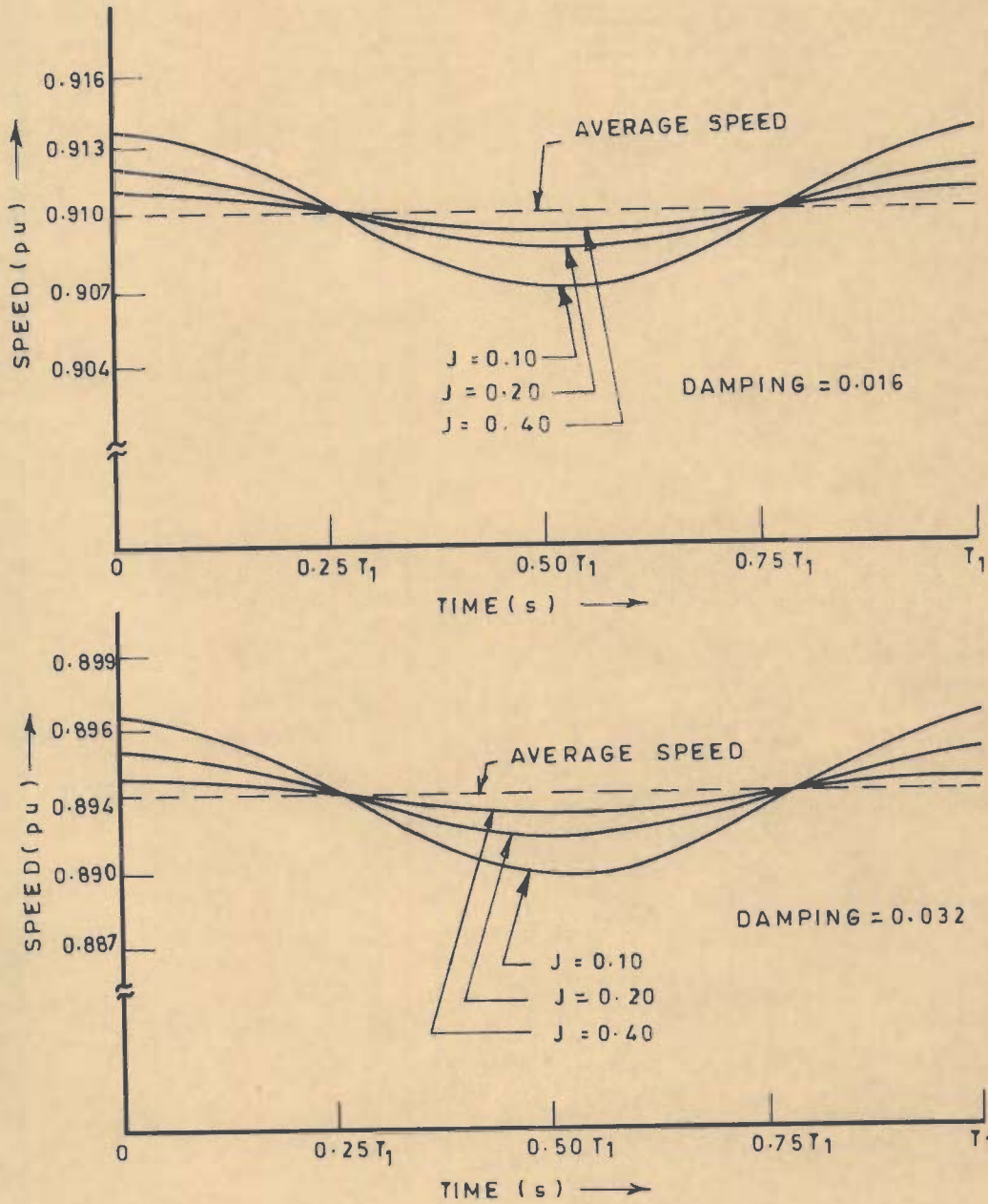
FIG. 2.5 _ EFFECT OF MOMENT OF INERTIA AND
DAMPING ON STEADY STATE MOTOR SPEED
FOR A PULSATING LOAD TORQUE

The amplitudes of pulsations of armature current and motor speed depend on the moment of inertia and the amplitude of pulsating component of load torque. As the moment of inertia is increased, the amplitude of current and speed pulsations reduces [Figs. 2.4 , 2.5]. The pulsations of steady state current and speed become very large when the frequency of load torque pulsation becomes equal to the natural frequency of oscillation of system as shown in Figs. 2.6 , 2.7 , 2.8 ,2.9 . The amplitudes of armature current and speed at resonance also depend on the damping and moment of inertia of the system as shown in Figs. 2.10 and 2.11 . The instantaneous values of armature current and motor speed in transient condition are shown in Figs. 2.12 and 2.13 respectively.

2.8 EFFECTS OF SYSTEM PARAMETERS ON PERFORMANCE

The effects of operating conditions like nature of load torque and some of the design parameters like elasticity of shaft, moment of inertia and damping, on the performance of the drive are discussed below:

2.8.1 Effect of Nature of Load Torque

(a) Steady State Performance:

With a pulsating load torque, the armature current and speed also pulsate at a frequency equal to that of the pulsating component of load torque. The amplitude of pulsations of current and speed is proportional to the amplitude of pulsating component of load torque. These pulsating components of current and speed

may have phase lags with the pulsating component of load torque as shown in Figs. 2.3 , 2.4 and 2.5 .

The effect of variation of frequency of pulsating component of load torque on pulsations of current and speed is shown in Figs. 2.6 and 2.7 respectively. It is observed that as the frequency of load torque pulsations is increased, the amplitudes of pulsating components of current and speed decrease and become a minimum at a particular value, say ω_c [Table 2.1]. When the frequency of load torque pulsations becomes equal to natural frequency of torsional oscillation of system ω_n, the amplitudes of pulsation of current and speed attain large values. This phenomenon is termed as 'resonance'. A comparison of the pulsations of current and speed under normal operating conditions and the resonance condition is shown in Figs. 2.8 and 2.9 respectively.

TABLE 2.1 : Effect Of Frequency Of Pulsation Of Load Torque:

S. No.	ω_1 rad/sec	amplitude of pulsating component	
		current %	speed %
1	1.0	25.063	3.240
2	10.0	17.777	2.133
3	50.0	3.809	0.621
4	100.0	1.269	0.305
5	366.7 (ω_c)	0.222	0.156
6	510.0	1.476	1.480
7	520.162 (ω_n)	93.921	95.626
8	530.0	1.349	1.385
9	560.0	0.397	0.535
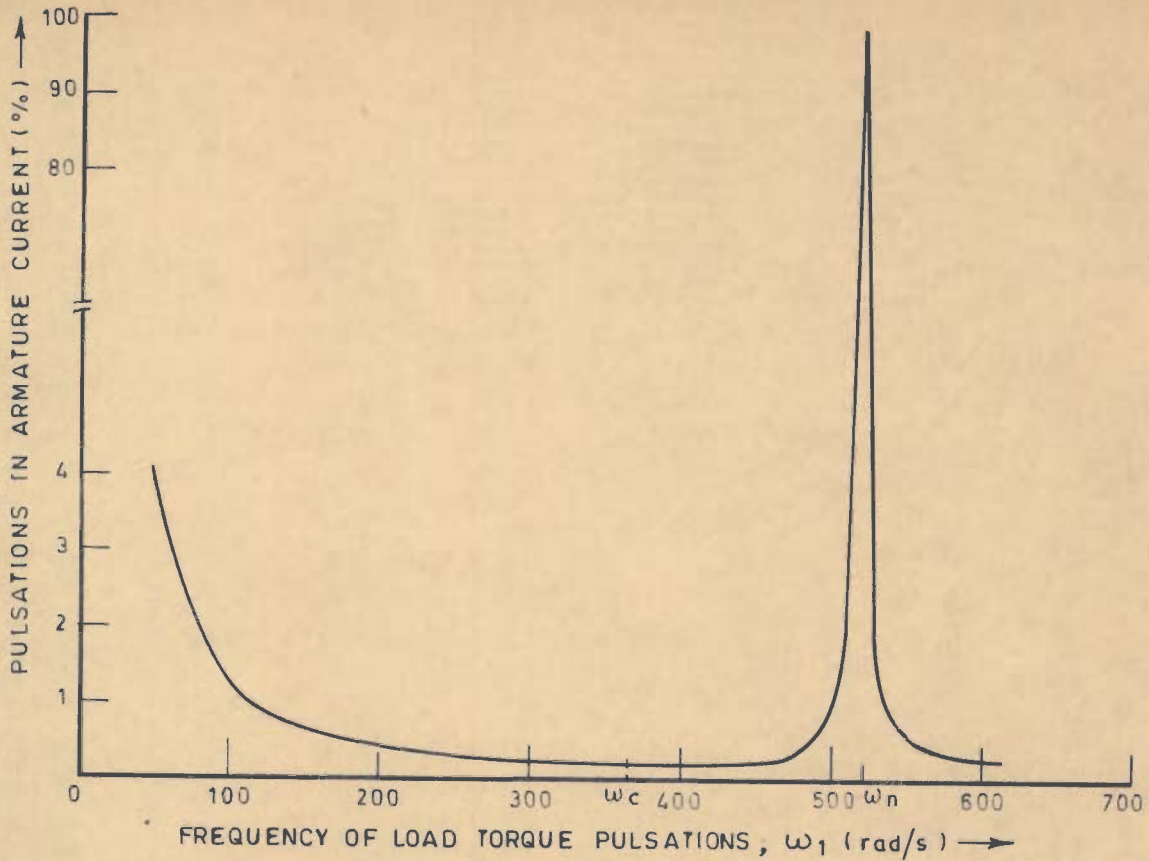
FIG. 2.6 _ EFFECT OF FREQUENCY OF LOAD TORQUE
ON PULSATIONS OF ARMATURE CURRENT
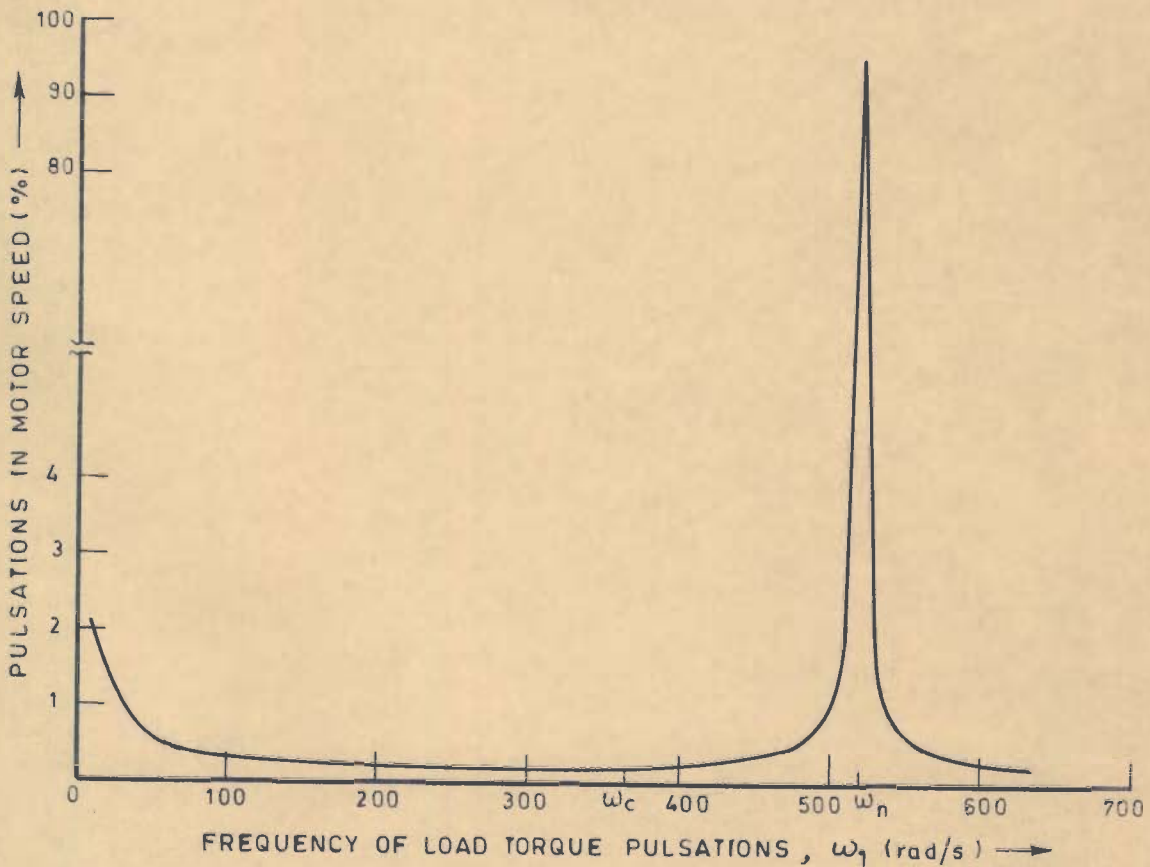
FIG. 2.7 _ EFFECT OF FREQUENCY OF LOAD TORQUE
ON PULSATIONS OF MOTOR SPEED
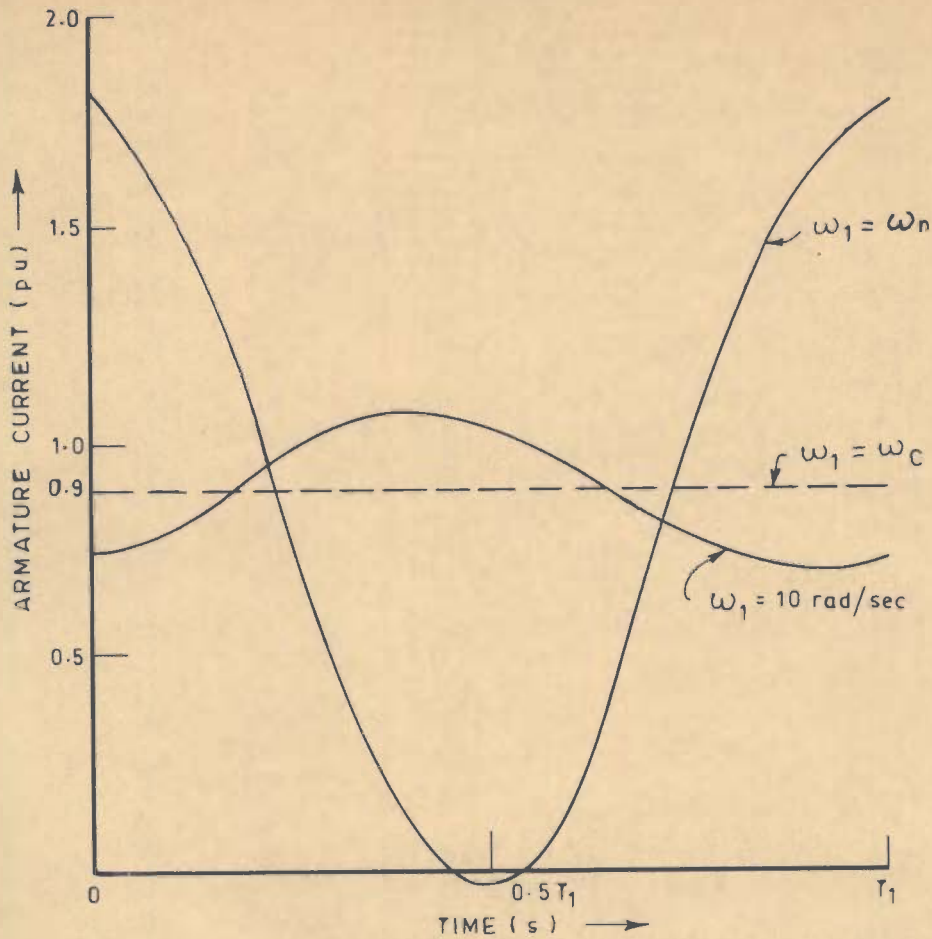
FIG. 2.8 – EFFECT OF FREQUENCY OF LOAD
TORQUE ON STEADY STATE ARMATURE
CURRENT
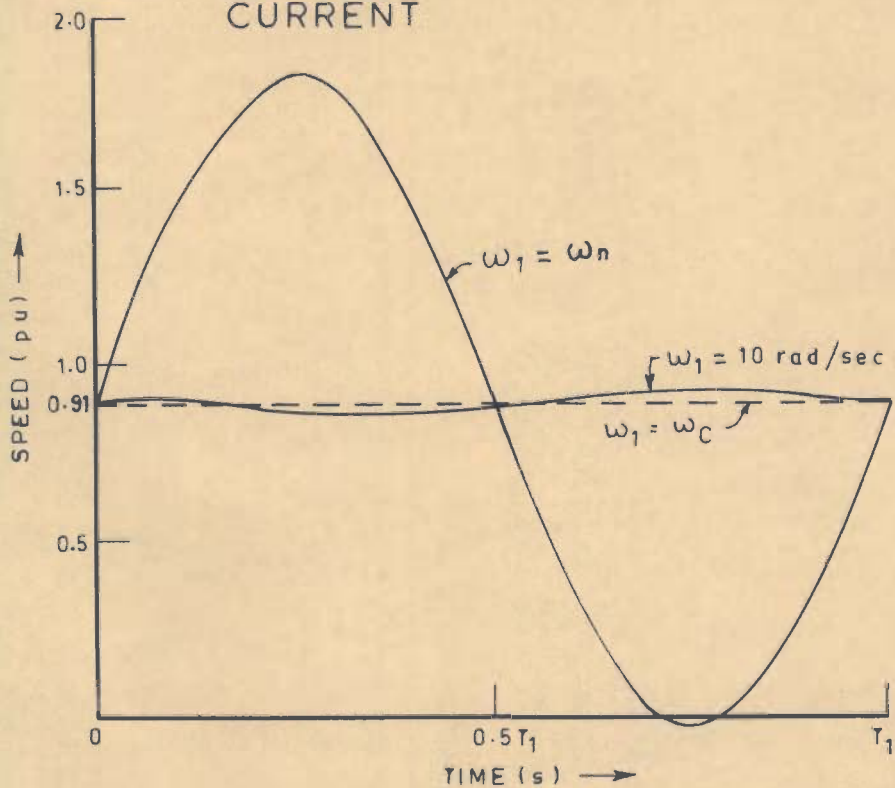
FIG. 2.9 – EFFECT OF FREQUENCY OF LOAD
TORQUE ON STEADY STATE SPEED

(b) Transient State Performance:

The frequency of the pulsating component of load torque does not seem to affect the three transient components of current and speed.

2.8.2 Effect of Elasticity of Shaft

(a) Steady State Performance:

The steady state armature current and speed are not significantly affected by the value of torsional stiffness of the shaft. Stiffness determines only the natural frequency of the system and hence the frequency at which resonance will occur.

(b) Transient State Performance:

The armature current and speed have exponentially decaying component (i_5, n_5), which vary sinusoidally at frequency β_3. In the case of a rigid shaft this component will not be present. Assumption of a rigid shaft thus results in ignoring this component of armature current and speed.

An increase in the value of torsional stiffness increases the natural frequency of the system and decreases the amplitude of this component of current and speed.

2.8.3 Effect of Moment of Inertia:

(a) Steady State Performance:

For the same value of load torque and damping, an increase in moment of inertia decreases the amplitudes of pulsation in current and speed. However, moment of inertia has no effect on

average values of current and speed as shown in Figs. 2.4,2.5
and Table 2.2. Under resonance condition,an increase in moment
of inertia decreases the peak value of pulsations in speed. The
effect of moment of inertia on peak value of current in resonance
condition is not much appreciable as this value mainly depends on
damping of the system [Figs. 2.10,2.11 and Table 2.3].

TABLE 2.2 : Effect Of Moment Of Inertia And Damping On Steady
State Performance

| S.N. | damping Nm/rad/s | moment of inertia Kg m^2 | average value | | amplitude of pulsation | |
			current pu	speed pu	current %	speed %
1	0.008	0.05			1.428	0.325
		0.10	0.900	0.910	0.730	0.164
		0.20			0.381	0.088
2	0.016	0.05			1.476	0.330
		0.10	1.026	0.894	0.746	0.167
		0.20			0.397	0.089
3	0.032	0.05			1.571	0.342
		0.10	1.264	0.863	0.794	0.173
		0.20			0.413	0.091

TABLE 2.3 : Effect Of Moment Of Inertia And Damping On
Performance Under Resonance Condition

S.N.	moment of inertia Kg m^2	damping Nm/rad/s	amplitude of pulsation		resonance frequency rad/s
			current %	speed %	
1	0.05	0.008	95.238	95.632	520.162
		0.016	61.047	62.395	
		0.032	36.000	36.809	
2	0.10	0.008	90.016	66.798	367.804
		0.016	65.857	48.175	
		0.032	42.857	31.350	
3	0.20	0.008	77.952	41.303	260.068
		0.016	63.365	33.579	
		0.032	46.111	24.437	

TABLE 2.4 : Current And Speed Pulsations For Loads Of
Large Damping And Inertia

B_2/B_1	J_2/J_1	average current pu	current pulsation %	average speed pu	speed pulsation %
1	1	0.900	1.428	0.910	0.325
10	10	1.432	0.153	0.841	0.067
10	1	1.432	1.028	0.841	0.379

CURVES	DAMPING $B_1=B_2$ (Nm/rad/s)	M. INERTIA $J_1=J_2$ kg-m^2	$\omega_1=\omega_n$ rad/s
1	0.008	0.05	520.16
2	0.016	0.05	520.16
3	0.032	0.05	520.16
4	0.032	0.10	367.8
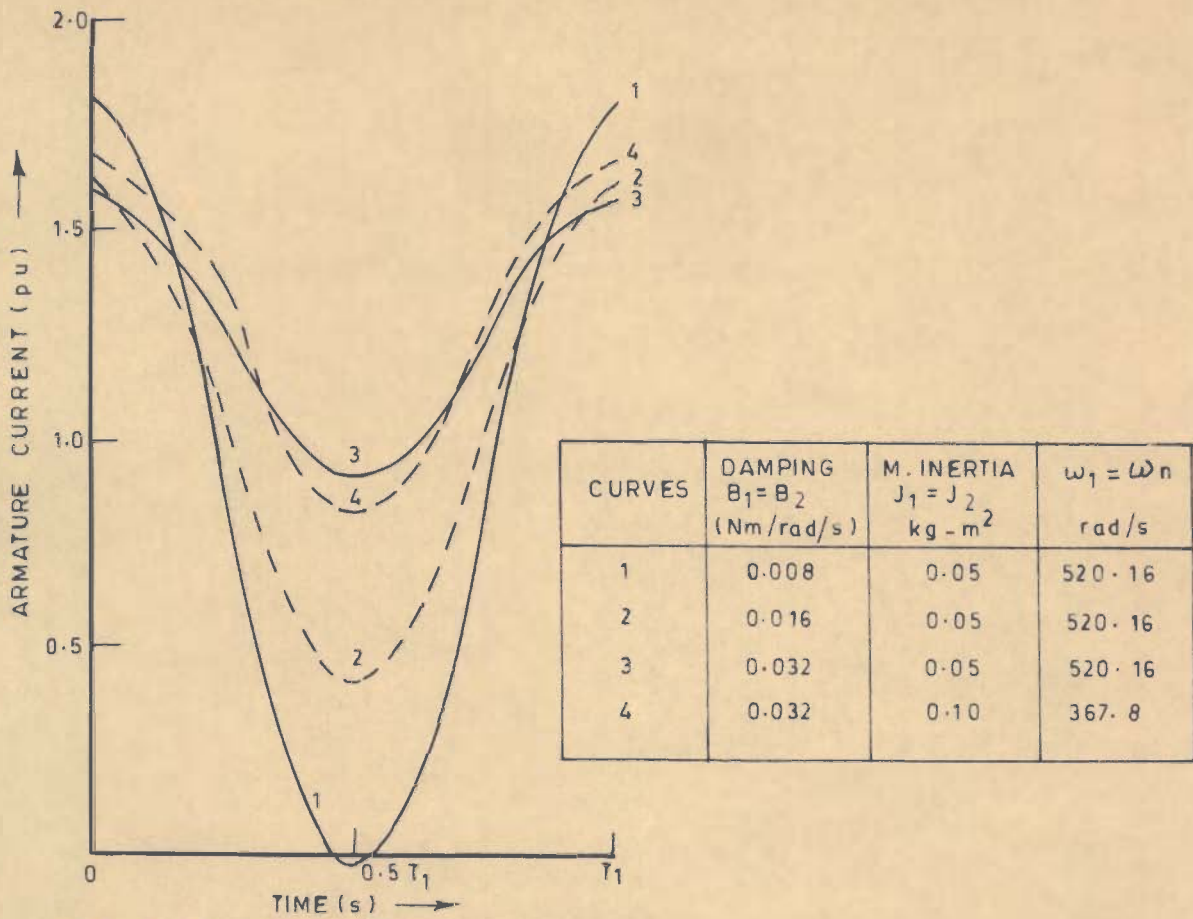
FIG. 2.10 _ EFFECT OF DAMPING AND MOMENT OF INERTIA ON STEADY STATE ARMATURE CURRENT AT RESONANCE
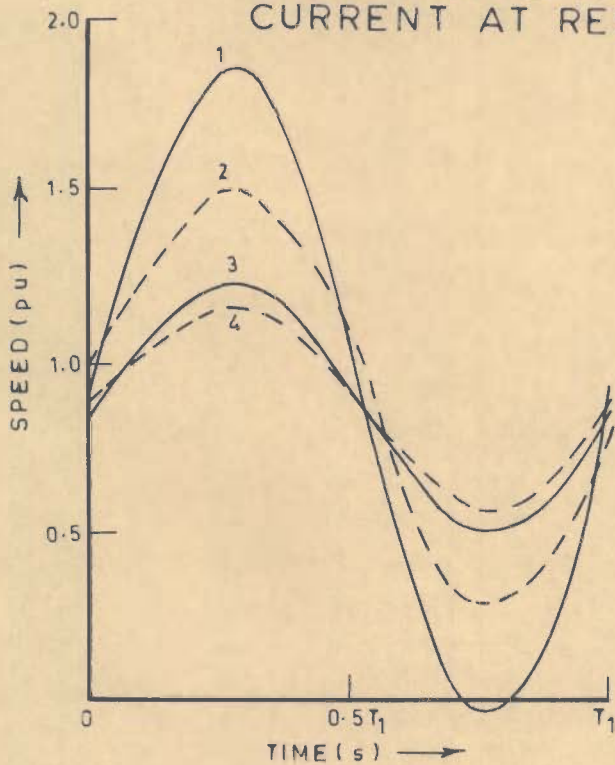
FIG. 2.11 _ EFFECT OF DAMPING AND MOMENT OF INERTIA ON STEADY STATE SPEED AT RESONANCE

(b) Transient State Performance:

A large value of moment of inertia reduces the value of natural frequency of oscillation and increases the amplitude of sinusoidally decaying components (i_5 , n_5) of current and speed. A large value of moment of inertia also increases slightly the peak value of armature current and the system requires more time to reach the steady state condition as shown in Figs. 2.12 and 2.13.

2.8.4 Effect of Damping

An increase in the value of damping does not affect much the amplitudes of steady state pulsations of current and speed. However, it increases the average value of current and decreases the average value of speed [Table 2.2] as shown in Figs. 2.4,2.5 . Under resonance condition, an increase in damping decreases appreciably the peak values of current and speed [Table 2.3] as shown in Fig. 2.10 and 2.11.

For loads like compressors or ship propellers, damping coefficients and moment of inertia of load are much larger than those of the motor ($J_2 \gg J_1$ and $B_2 \gg B_1$). In such systems the pulsation in current and speed are significantly reduced. The major contribution to this reduction is due to the increased moment of inertia. An increase in damping only reduces the pulsation in current but increases the pulsation in speed. Table 2.4 shows comparative figures for different combinations of moment of inertia and damping.

2.8.5 Effect of Armature Reaction

In the analysis presented, linearity of magnetic circuit is assumed, and brushes are in the geometrical neutral axis. With these assumptions, the total flux per pole remains unchanged when the field is distorted by armature reaction. However, if saturation is present, the net flux per pole will reduce. This can be accounted for by decreasing the value of motor back emf constant. For the example considered, a 5 percent reduction in K_m (which corresponds to 5 percent reduction in flux per pole due to armature reaction) decreases the pulsation in current and speed by 0.269 and 0.03 percent respectively. This shows that the armature reaction effect on pulsations in current and speed is not significant.

2.9 CONCLUSIONS

In this chapter, the performance analysis of a d.c. electric drive with a pulsating load torque and elastic mechanical link between motor and the load has been presented. Closed-form expressions for armature current and motor speed, for transient and steady state conditions have been obtained. The analysis reveals that the drive performance is significantly affected by the pulsations in the load torque particularly when the shaft is not rigid. Under steady state condition the current and speed have pulsating components of frequency equal to the frequency of the pulsating component of load torque. The amplitude of these components decreases with:
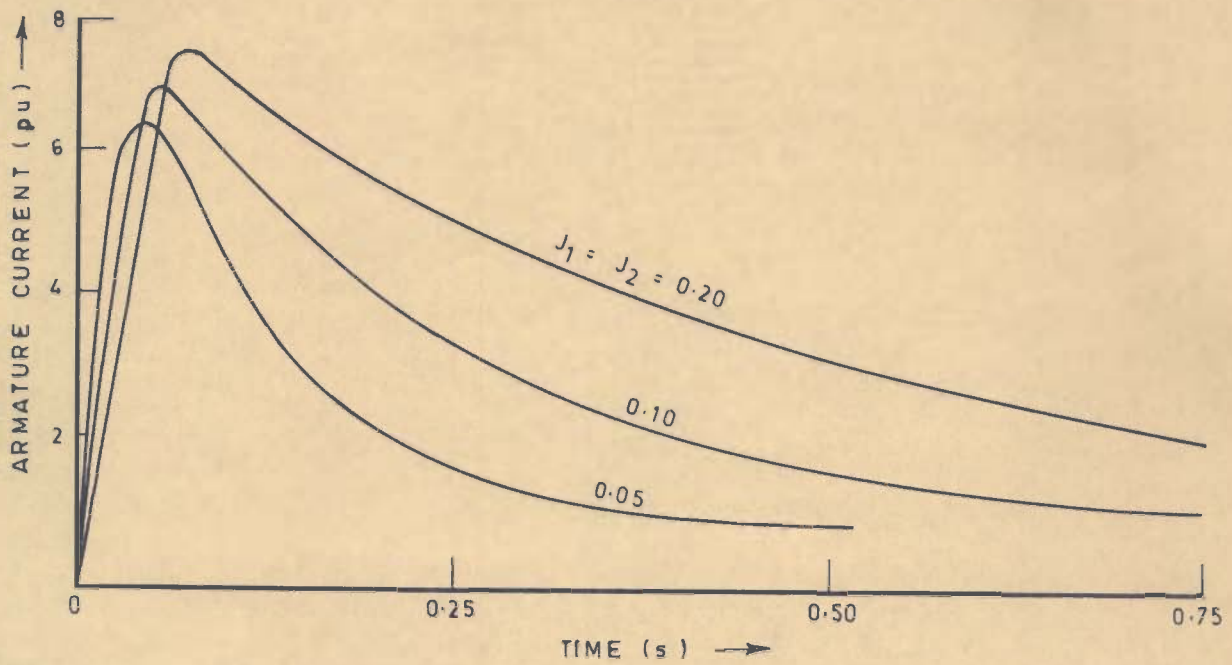
FIG. 2.12 _ EFFECT OF MOMENT OF INERTIA ON SWITCHING-
IN TRANSIENT ARMATURE CURRENT
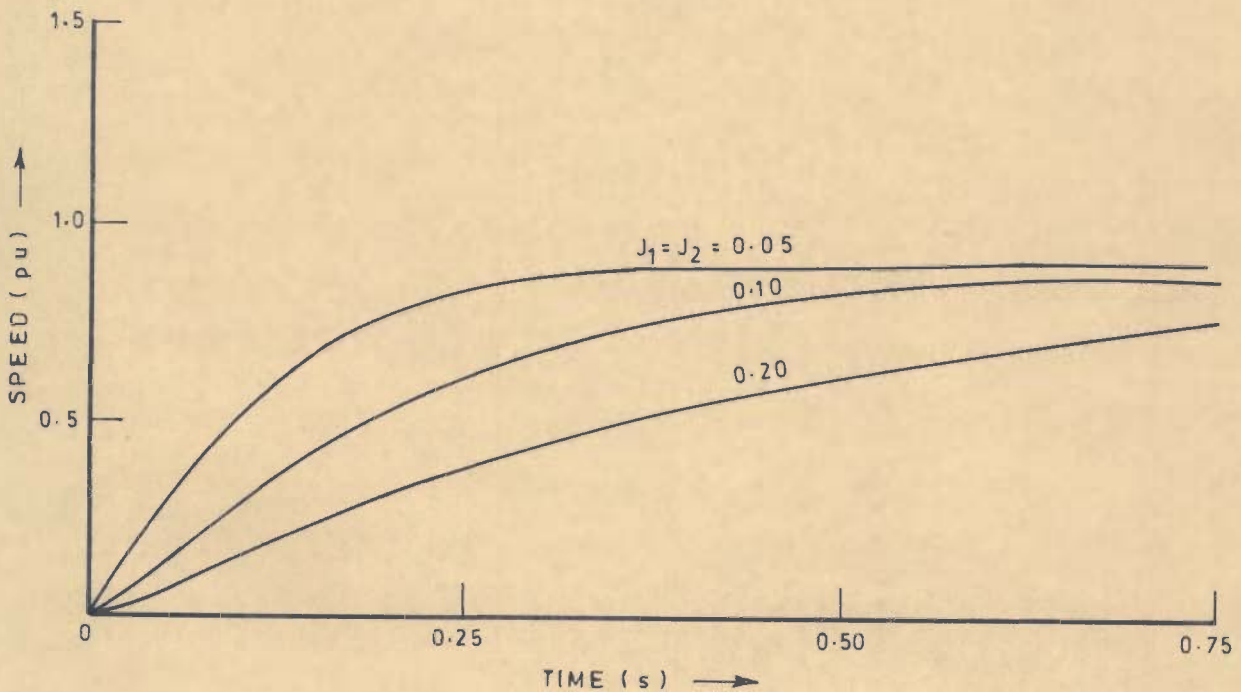
FIG. 2.13 _ EFFECT OF MOMENT OF INERTIA ON
MOTOR SPEED IN TRANSIENT CONDITION

(i) decrease in amplitude of pulsating component of load torque.

(ii) increase in value of moment of inertia.

(iii) increase in frequency of load torque pulsation.

The following suggestions are made to improve the performance of such drives:

(a) The load torque should be analysed and it must be ensured that the natural frequency of the system does not match with the frequency of any of the components of the load torque. Otherwise, there is a possibility of resonance, resulting in very high instantaneous current and speed. If the natural frequency of the system happens to be near the frequency of any of the components of the load torque, the natural frequency of the system must be changed by changing the stiffness of the shaft (changing the ratio of diameter/length) or the moment of inertia.

(b) It is shown that the amplitudes of steady state pulsations of armature current and speed are minimum when the frequency of load torque pulsation is equal to $1/\sqrt{2}$ times the resonance frequency. This provides a criterion for design of the system for minimum pulsations in current and speed . As such, in order to minimize these pulsations, it is suggested that for a given value of frequency of load torque pulsation ω_1, a combination of values of moment of inertia and torsional stiffness of the system may be selected such that the natural frequency of oscillation ω_n is $\sqrt{2}$ time ω_1.

(c)   The amplitudes of steady state pulsations of current and speed can be reduced by increasing the value of load moment of inertia. However, the choice of increase in moment of inertia is restricted due to mechanical design considerations. Damping does not affect much the steady state pulsations in current and speed.

(d)   The amplitudes of steady state pulsations of current and speed under resonance conditions can be reduced by increasing the damping of the system. However, this will increase the average value of current and decrease the average speed.

(e)   The amplitude of alternating components (i_5 , n_5) of current and speed in transient condition can be reduced by increasing the value of torsional stiffness of the shaft.

CHAPTER-3

A NEW ANALYTICAL TECHNIQUE FOR PERFORMANCE DETERMINATION OF CHOPPER CONTROLLED D.C. MOTOR DRIVES

3.1 INTRODUCTION

A commonly used type of thyristor control of d.c. motors is the 'chopper control' which converts a constant d.c. voltage to a pulsed type voltage. Chopper control offers many advantages over the other competitive method of d.c. motor control known as 'phase control'. These advantages include improved power factor and wave forms on a.c. side, and reduced harmonics and associated losses due to the use of relatively high values of chopper frequency. Also, with such a control, the speed of motor can be controlled over much wider range than is possible with phase control. Due to these features, chopper control finds application for the control of d.c. motors in a variety of industrial drives. As a consequence, there have been parallel advances in developing better analytical techniques to predict the performance of such drives.

Extensive work dealing with the methods of analysis of chopper controlled d.c. motor drives using time ratio control is available. The chopper alternately operates in two different modes, known as the conducting (duty) mode and the freewheeling mode corresponding to 'on' and 'off' periods respectively, of the chopper cycle. In the existing methods [23,25,26,44] of analysis, two separate sets of differential equations applicable to duty and

freewheeling modes of operation respectively are required. Each set of equations comprises the voltage-current equation for armature circuit and the dynamic equation of motion. If the commutation interval of the chopper is also taken into account, an additional third set of equations is needed.

To determine the system performance, the above sets of equations are solved. The approach followed so far has been to solve the above sets of equations either by using a numerical technique or by step-by-step methods.

To obtain the steady state solution using a numerical technique [18], the solutions can be started from any point in time with known or assumed initial conditions. The calculations are repeated till near steady state conditions are obtained. Theoretically the steady state will occur after infinite time. As such the calculations have to be repeated for a large interval of time. Such methods of analysis suffer from two inherent drawbacks. Firstly, the computation time required is large, specially when the solutions with a high accuracy are required. Secondly, such methods do not yield closed-form solutions.

The second approach followed for the analysis of such systems is to solve the above sets of differential equations using step-by-step method. This type of analysis involves obtaining a closed-form solution of these equations for duty period of first chopper cycle using the known initial conditions (which are generally all zeros for switching-in from rest). The values of performance variables at the end of the first duty period are calculated using this closed-form solution and are used as the initial

conditions for freewheeling interval of first chopper cycle. The equations for the free-wheeling mode are then analytically solved. For both these analytical solutions (for conducting mode, and the free-wheeling mode) the speed over a chopper cycle is assumed constant [23,25]. This process is repeated for the subsequent cycles with only initial conditions changed till the steady state or the desired time interval is reached [25,26]. This necessitates step-by-step solutions of two sets of differential equations; one for duty mode and the other for freewheeling mode of operation with the initial conditions changing at each stage. This approach has three main disadvantages. Firstly, the analysis has to be started right from the first chopper cycle, and hence computer time needed is large. Secondly, a general closed-form solution is not obtainable. Lastly, the analysis is less accurate as it assumes the speed over a chopper cycle as constant.

A chopper fed d.c. drive with a rigid shaft is a system of second order. However for a precise analysis, the elasticity of coupling should be taken into account in which case the order of the system increases to five. Handling the analysis of such complex systems (analysis in Chapter-4) and solving the two sets of equations, one for duty and the other for freewheeling modes, by existing techniques is highly involved and needs exceptionally large computational efforts. There is, therefore, a pressing need for a new technique which is more accurate, needs lesser computation time and can be used for more complex systems.

3.2 WORK PRESENTED

In this chapter, a new analytical technique for analysis of a chopper fed separately excited d.c. motor using 'time ratio control' at constant chopper frequency is presented. The system is modelled in such a manner that only one set of equations is applicable to both duty as well as freewheeling modes of chopper operation. Closed-form solutions for armature current and motor speed are obtained for transient as well as steady state conditions corresponding to any set of operating conditions. The solutions at any point in time, under transient as well as steady state conditions, can be directly obtained without starting from the switching-in instant. The computational efforts and time needed are, therefore, extremely small as compared to other methods.

The proposed technique is applied to the analysis of chopper fed d.c. motor drive with elastic coupling and pulsating load torque discussed in Chapter-4.

The system analysed consists of a chopper fed separately excited d.c. motor delivering a constant load torque as shown in Fig.3.1. A thyristor chopper CH converts a constant d.c. voltage V to a pulsed voltage v(t) as shown in Fig.3.2. A freewheeling diode FWD in parallel with the armature is provided which allows the flow of current in armature during freewheeling interval.

3.3 SALIENT FEATURES OF THE PROPOSED TECHNIQUE

The proposed technique of analysis overcomes the draw-backs of existing methods. In this method, the chopper output

M = D.C. MOTOR
CH = CHOPPER
FWD = FREE-WHEELING DIODE
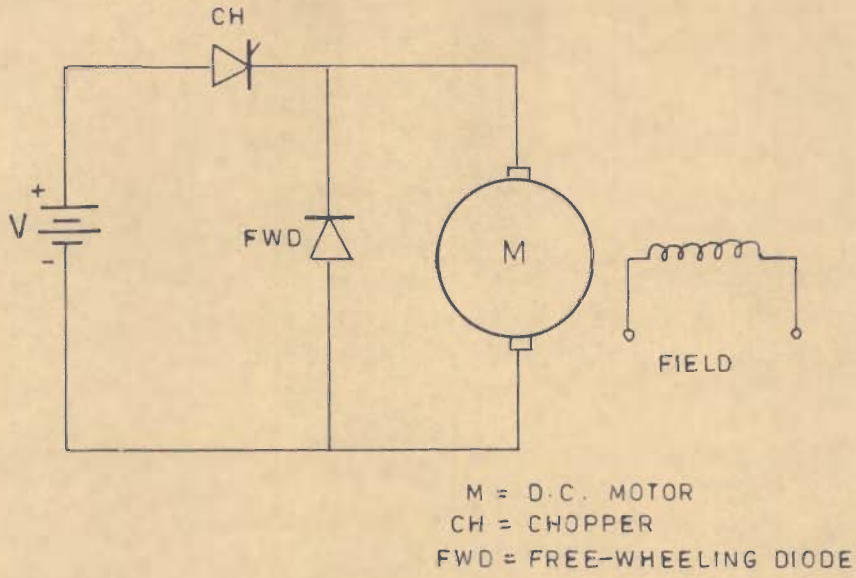
FIG. 3.1 – CHOPPER CONTROLLED SEPARATELY
EXCITED D.C. MOTOR
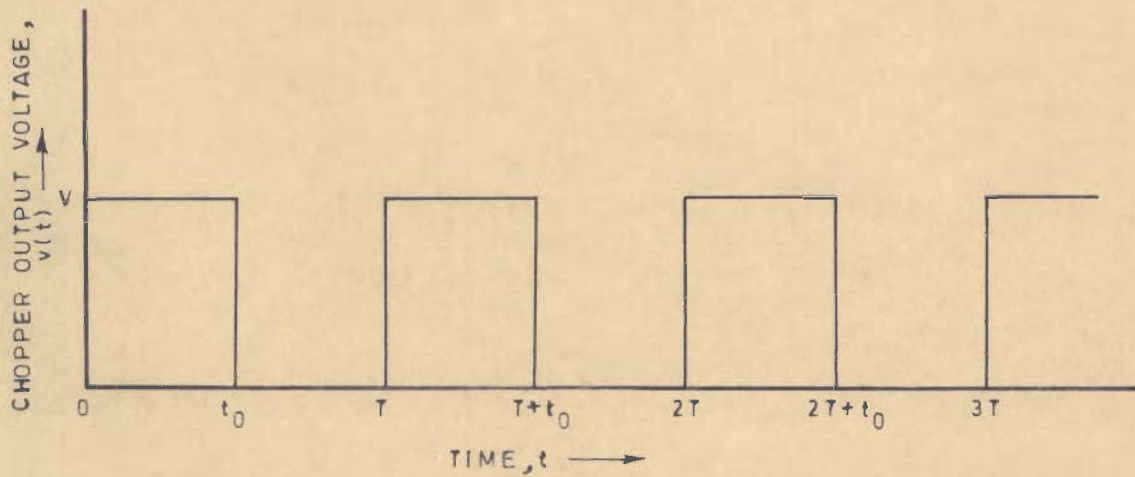
FIG. 3.2 – CHOPPER OUTPUT VOLTAGE

voltage is expressed as a sum of series of step voltages, and Laplace transform of this type of voltage is obtained. A single set of equations consisting of the voltage-current equation for armature and the dynamic equation of motion is thus applicable to duty as well as freewheeling modes of chopper operation. The equations are expressed in State model form. In order to obtain the closed-form solutions for system variables in time domain, the inverse Laplace transform of the solution in s domain is required. For obtaining the inverse Laplace transform of a particular form of function occurring in this analysis, a theorem has been developed. The philosophy of expressing the chopper output voltage as a sum of series of step voltages and the procedure for obtaining the response in duty as well as freewheeling intervals of a chopper cycle, say nth cycle, is explained below:

Fig. 3.3 shows the component unit step voltages with time phase difference, applied alternatingly in positive and negative directions at the end of freewheeling and duty intervals respectively. These step voltages added together at different intervals of time are shown in Fig. 3.4. This shows that a sum of step voltages applied with proper time phase difference is equivalent to the waveform obtained from the output of the chopper. The response in duty and freewheeling intervals of nth chopper cycle can be determined in the following manner:

(a) duty interval:

The voltage applied and the corresponding limits of time interval for different chopper cycles is given below:
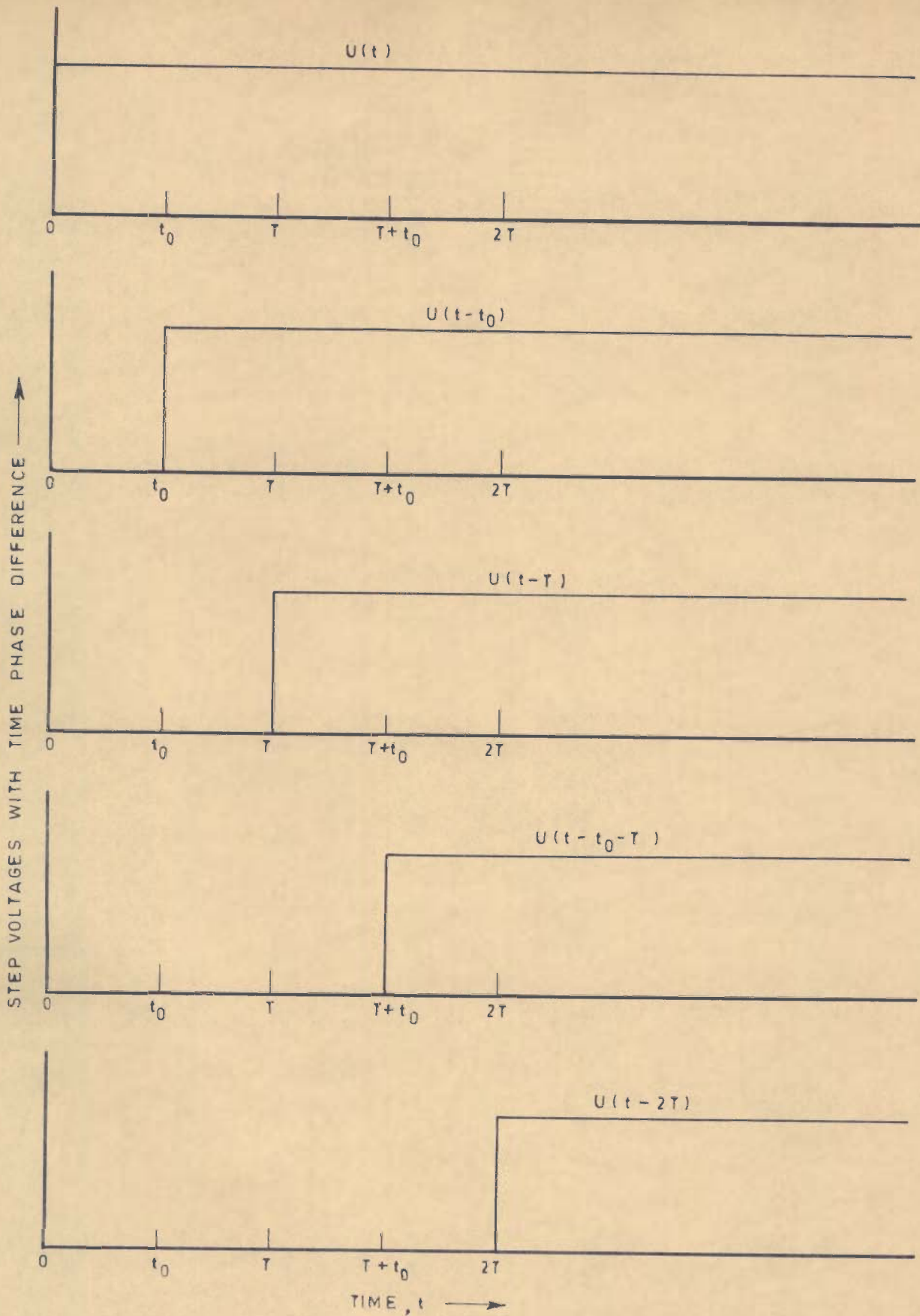
FIG. 3.3 _ COMPONENT STEP VOLTAGES WITH TIME PHASE
DIFFERENCE FOR OBTAINING PULSED TYPE OF
VOLTAGE OF FIG. 3.2

$U(t) - U(t - t_0)$

$U(t) - U(t - t_0) + U(t - T)$

$U(t) - U(t - t_0) + U(t - T) - U(t - t_0 - T)$

$U(t) - U(t - t_0) + U(t - T) - U(t - t_0 - T) + U(t - 2T)$

SUM OF STEP VOLTAGES WITH TIME PHASE DIFFERENCE ⟶

TIME, t ⟶
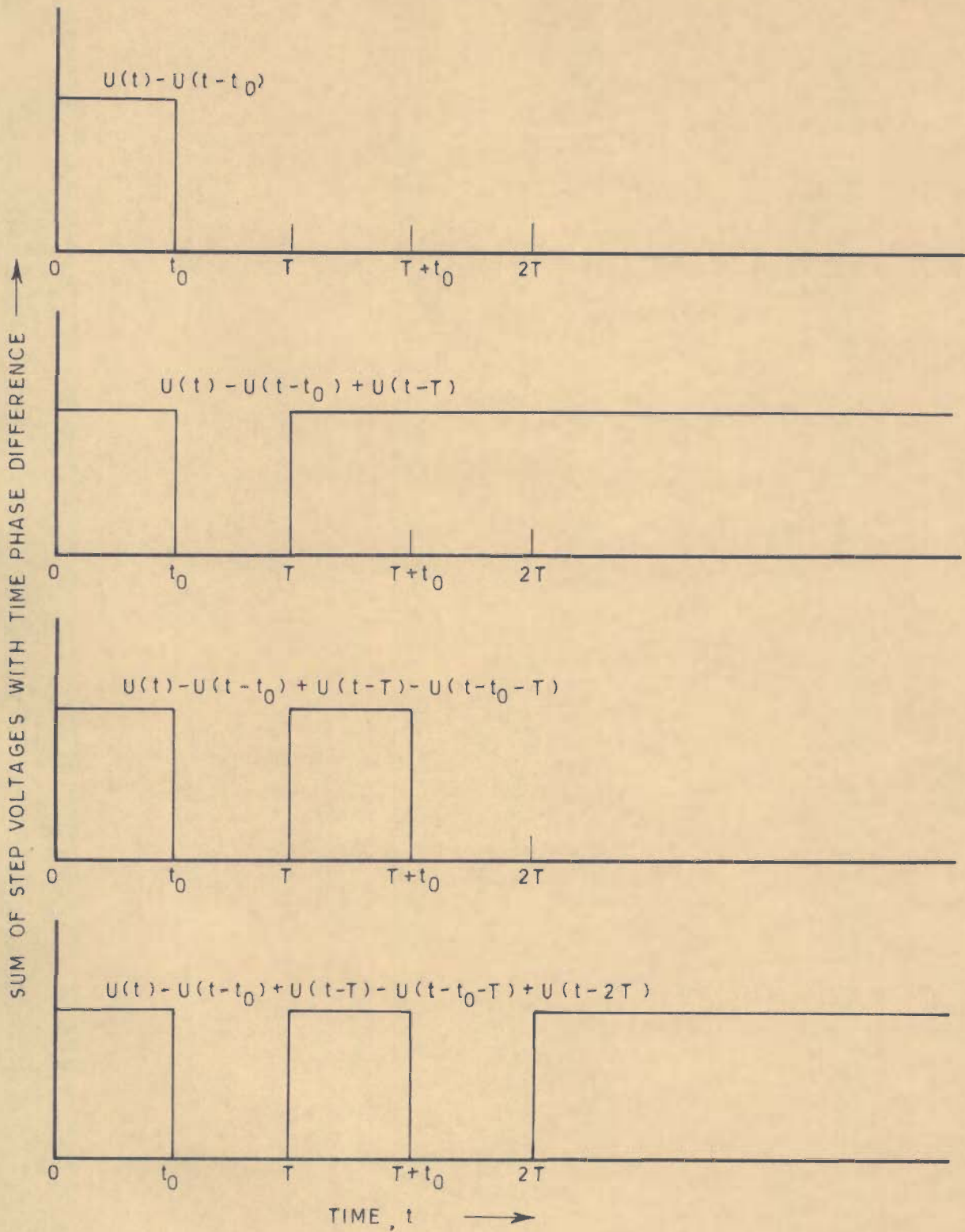
FIG. 3.4 _ SUCCESSIVE ADDITION OF STEP VOLTAGES
WITH TIME PHASE DIFFERENCE TO OBTAIN
A PULSED VOLTAGE EQUIVALENT TO CHOPPER
OUTPUT VOLTAGE

chopper cycle	time interval	step voltage applied
1	$0 \le t \le t_0$	$U(t)$
2	$T \le t \le (T+t_0)$	$U(t)-U(t-t_0)+U(t-T)$
3	$2T \le t \le (2T+t_0)$	$U(t)-U(t-t_0)+U(t-T)$ $-U(t-t_0-T)+U(t-2T)$
⋮		
n	$(n-1)T \le t \le (\overline{n-1}T+t_0)$	$U(t)-U(t-t_0)+U(t-T)-U(t-t_0-T)$ $+U(t-2T) \ldots\ldots -U(t-t_0-\overline{n-2}T)$ $+U(t-\overline{n-1}T)$

The response in duty interval of nth chopper cycle is that due to the sum of step voltages given above which can be written as:

$$\sum_{r=1}^{n} U(t-\overline{r-1}T) - \sum_{r=1}^{n-1} U(t-t_0-\overline{r-1}T)$$

(b) freewheeling interval:

The voltage applied and the corresponding limits of time interval for different chopper cycle is given below:

chopper cycle	time interval	step voltage applied
1	$t_0 \le t \le T$	$U(t)-U(t-t_0)$
2	$(T+t_0) \le t \le 2T$	$U(t)-U(t-t_0)+U(t-T)-U(t-t_0-T)$
3	$(2T+t_0) \le t \le 3T$	$U(t)-U(t-t_0)+U(t-T)-U(t-t_0-T)+U(t-2T)$ $-U(t-t_0-2T)$
⋮		
n	$(\overline{n-1}T+t_0) \le t \le nT$	$U(t)-U(t-t_0)+U(t-T)-U(t-t_0-T)+U(t-2T)$ $-U(t-t_0-2T)\ldots\ldots+U(t-\overline{n-1}T)-U(t-t_0-\overline{n-1}T)$

The response in freewheeling interval of nth chopper cycle is that due to the sum of step voltages given above which can be written as:

$$\sum_{r=1}^{n} U(t-\overline{r-1}T) - \sum_{r=1}^{n} U(t-t_o-\overline{r-1}T)$$

3.3.1 Assumptions

Following assumptions are made in the analysis:

(a) armature inductance is sufficiently large to allow a continuous flow of current in armature circuit, i.e. the chopper operates in duty and freewheeling modes only and there is no zero current interval of operation,

(b) chopper output voltage is a perfect square wave, i.e. the commutation interval is neglected,

(c) field current remains unchanged during motor operation,

(d) resistance and inductance of motor armature are constant.

3.4 PERFORMANCE EQUATIONS

The system shown in Fig.3.1 can be described by the following equations:

$$v(t) = L \frac{di}{dt} + R i + K_m \dot{\theta} \qquad (3.1)$$

$$T_e = J \ddot{\theta} + B \dot{\theta} + T_L \qquad (3.2)$$

where $\quad T_e = K_e i$

In above equations, $v(t)$ is the chopper output voltage, and i and $\dot{\theta}$ are the instantaneous values of armature current and motor angular speed, respectively. The above equations are

applicable to both duty as well as freewheeling modes of chopper operation. These equations are to be solved in order to determine the system performance in terms of armature current and motor speed.

3.5 SYSTEM CHARACTERISTIC EQUATION

Equations (3.1) and (3.2) can be expressed in State model form as:

$$\dot{x} = Ax + Du \tag{3.3}$$

where

$$A = \begin{bmatrix} -1/\tau_a & -K_m/L \\ \\ K_e/J & -1/\tau_m \end{bmatrix}, \quad D = \begin{bmatrix} 1/L & 0 \\ \\ 0 & -1/J \end{bmatrix} \tag{3.4}$$

forcing function vector $u = \begin{bmatrix} v(t) \\ T_L \end{bmatrix}$

and, state variable vector $x = \begin{bmatrix} i \\ \dot{\theta} \end{bmatrix}$

Taking Laplace transform of eqn. (3.3):

$$X(s) = [sI-A]^{-1} DU(s) + [sI-A]^{-1} x(0) \tag{3.5}$$

where I is a unit matrix of the same order as that of matrix A. For the system starting from quiescent state,

$$x(0) = \begin{bmatrix} 0 \\ 0 \end{bmatrix}$$

Taking the Laplace transform of the chopper output voltage v(t) and that of the constant forcing function T_L,

U(s) is given by:

$$U(s) = \begin{bmatrix} \frac{V}{s}\{\frac{1 - \exp(-st_o)}{1 - \exp(-sT)}\} \\ \\ \frac{T_L}{s} \end{bmatrix}$$

From eqn.(3.5), X(s) can be written as:

$$X(s) = \begin{bmatrix} I(s) \\ \\ \dot{\theta}(s) \end{bmatrix} = \frac{1}{\Delta} \begin{bmatrix} \frac{V}{sL}(s + \frac{1}{\tau_m})\{\frac{1 - \exp(-st_o)}{1 - \exp(-sT)}\} + \frac{K_m T_L}{sJL} \\ \\ \frac{VK_e}{sJL}\{\frac{1 - \exp(-st_o)}{1 - \exp(-sT)}\} - \frac{T_L}{sJ}(s + \frac{1}{\tau_a}) \end{bmatrix} \quad (3.6)$$

where Δ is the determinant of $[sI-A]$ matrix.

The characteristic equation of the system, $\Delta = 0$, is given by

$$s^2 + (\frac{1}{\tau_a} + \frac{1}{\tau_m})s + \frac{K_e K_m + BR}{JL} = 0 \quad (3.7)$$

It is observed that the characteristic equation (3.7) is a quadratic in s, the two roots of which may be expressed as:

$$s_1 = -\alpha_1 \quad \text{and} \quad s_2 = -\alpha_2$$

where α_1 and α_2 are real positive values. Thus Δ can be written as:

$$\Delta = (s + \alpha_1)(s + \alpha_2) \quad (3.8)$$

The roots of the characteristic equation may also be complex for certain combination of values of electrical and mechanical parameters. However, the procedure of analysis presented remains the same.

3.6 DETERMINATION OF SYSTEM RESPONSE

The closed-form solutions for system variables i.e. armature current $i(t)$ and motor angular speed $\dot{\theta}(t)$ can be obtained by taking inverse Laplace transform of eqn.(3.6) as:

$$x(t)=\begin{bmatrix} i(t) \\ \\ \dot{\theta}(t) \end{bmatrix}=\mathcal{L}^{-1}\left\{\frac{1}{(s+\alpha_1)(s+\alpha_2)}\begin{bmatrix} \frac{V}{sL}(s+\frac{1}{\tau_m})\{\frac{1-\exp(-st_o)}{1-\exp(-sT)}\}+\frac{K_mT_L}{sJL} \\ \\ \frac{VK_e}{sJL}\{\frac{1-\exp(-st_o)}{1-\exp(-sT)}\}-\frac{T_L}{sJ}(s+\frac{1}{\tau_a}) \end{bmatrix}\right\} \qquad (3.9)$$

For obtaining the performance variables $i(t)$ and $\dot{\theta}(t)$, in duty and freewheeling intervals, the inverse Laplace transform of terms containing $\{1-\exp(-st_o)\}/\{1-\exp(-sT)\}$ in eqn.(3.9) is required. The inverse Laplace transform of such a function can not be obtained by usual available methods. For this purpose the following theorem is proposed. The proof of this theorem is given in appendix A-2.1.

THEOREM

If $\emptyset(s)$ is the Laplace transform of $\emptyset(t)$, then for:

(i) duty interval: $(n-1)T \leq t \leq \{(n-1)T+t_o\}$:

$$\mathcal{L}^{-1}\left[\emptyset(s)\{\frac{1-\exp(-st_o)}{1-\exp(-sT)}\}\right]=\sum_{r=1}^{n}\emptyset(t-\overline{r-1}\,T)-\sum_{r=1}^{n-1}\emptyset(t-t_o-\overline{r-1}\,T) \quad (3.10)$$

(ii) freewheeling interval: $\{(n-1)T+t_o\} \leq t \leq nT$:

$$\mathcal{L}^{-1}\left[\emptyset(s)\{\frac{1-\exp(-st_o)}{1-\exp(-sT)}\}\right]=\sum_{r=1}^{r}\left[\emptyset(t-\overline{r-1}\,T)-\emptyset(t-t_o-\overline{r-1}\,T)\right] \quad (3.11)$$

3.6.1 Expression For Armature Current

The armature current $i(t)$ for duty and freewheeling intervals can be obtained [appendix A-2.2] as:

(a) Armature current in duty interval:

From eqns.(3.9) and (3.10), armature current in duty interval for nth chopper cycle, $i_{d_n}(t)$, can be obtained as:

$$
\begin{aligned}
i_{d_n}(t) = {} & \frac{K_m T_L}{J\,L}\{K_1 + K_2\,\exp(-\alpha_1 t) + K_3\,\exp(-\alpha_2 t)\} \\
& + \frac{V}{R\,\tau_a}\Big[K_4 + K_5\,\exp(-\alpha_1 t)\{\frac{\exp(nT\alpha_1)-1}{\exp(T\alpha_1)-1}\} \\
& + K_6\,\exp(-\alpha_2 t)\{\frac{\exp(nT\alpha_2)-1}{\exp(T\alpha_2)-1}\} - K_5\,\exp(-\overline{t-t_o}\,\alpha_1)\{\frac{\exp(\overline{n-1}\,T\alpha_1)-1}{\exp(T\alpha_1)-1}\} \\
& - K_6\,\exp(-\overline{t-t_o}\,\alpha_2)\{\frac{\exp(\overline{n-1}\,T\alpha_2)-1}{\exp(T\alpha_2)-1}\}\Big]
\end{aligned}
\tag{3.12}
$$

(b) Armature current in freewheeling interval:

From eqns.(3.9) and (3.11), armature current in freewheeling interval for nth chopper cycle, $i_{f_n}(t)$, can be obtained as:

$$
\begin{aligned}
i_{f_n}(t) = {} & \frac{K_m T_L}{JL}\{K_1 + K_2\,\exp(-\alpha_1 t) + K_3\,\exp(-\alpha_2 t)\} \\
& + \frac{V}{R\,\tau_a}\Big[K_5\,\exp(-\alpha_1 t)\{\frac{\exp(nT\alpha_1)-1}{\exp(T\alpha_1)-1}\}\{1 - \exp(\alpha_1 t_o)\} \\
& + K_6\,\exp(-\alpha_2 t)\{\frac{\exp(nT\alpha_2)-1}{\exp(T\alpha_2)-1}\}\{1 - \exp(\alpha_2 t_o)\}\Big]
\end{aligned}
\tag{3.13}
$$

3.6.1.1 Steady State Armature Current

The constant terms plus the terms containing (t-nT) in eqns. (3.12) and (3.13) constitute the steady state armature current which is independent of number of chopper cycle n (or time t), since as t becomes very large, n also becomes very large and the difference (t-nT) remains finite and independent of n. The steady state values of armature current are obtained as below:

(a) Steady State Armature Current in duty interval:

From eqn. (3.12), steady state armature current in duty interval $i_{ds}(t)$ can be written as:

$$i_{ds}(t) = \frac{K_m T_L}{JL} K_1 + \frac{V}{R\,\tau_a}\left[K_4 + K_5 \exp(-\alpha_1 \overline{t-nT})\{\frac{1-\exp(-\alpha_1 \overline{T-t_o})}{\exp(\alpha_1 T) - 1}\}\right.$$
$$\left. + K_6 \exp(-\alpha_2 \overline{t-nT})\{\frac{1-\exp(-\alpha_2 \overline{T-t_o})}{\exp(\alpha_2 T) - 1}\}\right] \quad (3.14)$$

(b) Steady State Armature Current in freewheeling interval:

From eqn. (3.13), steady state armature current in freewheeling interval $i_{fs}(t)$ can be written as:

$$i_{fs}(t) = \frac{K_m T_L}{JL} K_1 + \frac{V}{R\,\tau_a}\left[K_5 \exp(-\alpha_1 \overline{t-nT})\{\frac{1-\exp(\alpha_1 t_o)}{\exp(\alpha_1 T)-1}\}\right.$$
$$\left. + K_6 \exp(-\alpha_2 \overline{t-nT})\{\frac{1-\exp(\alpha_2 t_o)}{\exp(\alpha_2 T) - 1}\}\right] \quad (3.15)$$

The expressions for steady state current given in eqns. (3.14) and (3.15), contain the terms t and n which are not known for steady state conditions. To obtain the variation of current with time for steady state, instead of substituting

t, the term (t-nT) is treated as a single variable and the response
is calculated by varying value of (t-nT). The same procedure is
followed for obtaining the steady state speed response. The
limit between which the value of (t-nT) varies for duty and free-
wheeling intervals (explained in section 4.5.2.1) is given as:

duty interval   : $-T \leq (t-nT) \leq (-T+t_o)$

freewheeling interval: $(-T+t_o) \leq (t-nT) \leq 0$

3.6.2 Expression For Motor Speed

The motor angular speed $\dot{\theta}(t)$ for duty and freewheeling
intervals can be obtained [appendix A-2.3] as:

(a) Speed in duty interval:

From eqns. (3.9) and (3.10), angular speed in duty interval
for nth chopper cycle, $\dot{\theta}_{d_n}(t)$, can be obtained as:

$$\dot{\theta}_{d_n}(t) = -\frac{T_L}{J}\{K_7 + K_8 \exp(-\alpha_1 t) + K_9 \exp(-\alpha_2 t)\}$$

$$+ \frac{VK_e}{JL}\left[K_1 + K_2 \exp(-\alpha_1 t)\{\frac{\exp(nT\alpha_1)-1}{\exp(T\alpha_1)-1}\}\right.$$

$$+ K_3 \exp(-\alpha_2 t)\{\frac{\exp(nT\alpha_2)-1}{\exp(T\alpha_2)-1}\} - K_2 \exp(\overline{-t-t_o}\alpha_1)\{\frac{\exp(\overline{n-1}\ T\alpha_1)-1}{\exp(T\alpha_1)-1}\}$$

$$\left. - K_3 \exp(-\overline{t-t_o}\alpha_2)\{-\frac{\exp(\overline{n-1}\ T\alpha_2)-1}{\exp(T\alpha_2)-1}\}\right] \tag{3.16}$$

(b) Speed in freewheeling interval:

From eqns. (3.9) and (3.11), angular speed in freewheeling
interval for nth chopper cycle, $\dot{\theta}_{f_n}(t)$, can be obtained as:

$$\dot{\Theta}_{f_n}(t) = - \frac{T_L}{J}\{K_7 + K_8 \exp(-\alpha_1 t) + K_9 \exp(-\alpha_2 t)\}$$

$$+ \frac{VK_e}{JL}\left[K_2 \exp(-\alpha_1 t)\{\frac{\exp(nT\alpha_1)-1}{\exp(T\alpha_1)-1}\}\{1-\exp(\alpha_1 t_o)\}\right.$$

$$\left. + K_3 \exp(-\alpha_2 t)\{\frac{\exp(nT\alpha_2)-1}{\exp(T\alpha_2)-1}\}\{1-\exp(\alpha_2 t_o)\}\right] \qquad (3.17)$$

3.6.2.1 Steady State Motor Speed

From eqns. (3.16) and (3.17), the steady state angular speed for duty and freewheeling intervals can be obtained (as discussed in section 3.6.1.1) as below:

(a) Steady state speed in duty interval:

From eqn. (3.16), steady state speed in duty interval for nth chopper cycle, $\dot{\Theta}_{ds}(t)$, can be written as:

$$\dot{\Theta}_{ds}(t) = - \frac{T_L}{J}K_7 + \frac{VK_e}{JL}\left[K_1 + K_2 \exp(-\alpha_1 \overline{t-nT})\{\frac{1-\exp(-\alpha_1 \overline{T-t_o})}{\exp(\alpha_1 T)-1}\}\right.$$

$$\left. + K_3 \exp(-\alpha_2 \overline{t-nT})\{\frac{1-\exp(-\alpha_2 \overline{T-t_o})}{\exp(\alpha_2 T)-1}\}\right] \qquad (3.18)$$

(b) Steady state speed in freewheeling interval:

From eqn. (3.17), steady state speed in freewheeling interval for nth chopper cycle, $\dot{\Theta}_{fs}(t)$, can be written as:

$$\dot{\Theta}_{fs}(t) = - \frac{T_L}{J} K_7 + \frac{VK_e}{JL}\left[K_2 \exp(-\alpha_1 \overline{t-nT})\{\frac{1-\exp(\alpha_1 t_o)}{\exp(\alpha_1 T)-1}\}\right.$$

$$\left. + K_3 \exp(-\alpha_2 \overline{t-nT})\{\frac{1-\exp(\alpha_2 t_o)}{\exp(\alpha_2 T)-1}\}\right] \qquad (3.19)$$

3.7 TYPICAL PERFORMANCE STUDIES

The proposed analytical technique is illustrated by obtaining the performance of a chopper fed separately excited d.c. motor drive system with the following data:

Motor data:

supply voltage, V = 200 V

full load current, I_{fl} = 6.3 A (1 pu)

rated speed = 1000 rpm (1 pu)

armature resistance, R = 4 ohr

armature inductance, L = 0.06 H

motor constant, K_e (or K_m) = 1.86

coefficient of damping, B = 0.0162 N-m/rad/s

moment of inertia, J = 0.1 Kg m^2

load torque, T_L = 0.5 full load torque

Chopper data:

frequency = 200 Hz

duty factor, α = 0.6

duty interval, t_o = 0.0015 s

freewheeling interval, t_f = 0.0010 s

The performance of drive computed using the proposed technique is discussed below.

3.7.1 Transient State Performance

For a motor switched-in from rest against a constant load torque, the variation of armature current for the first few cycles of chopper voltage immediately after switching-in is
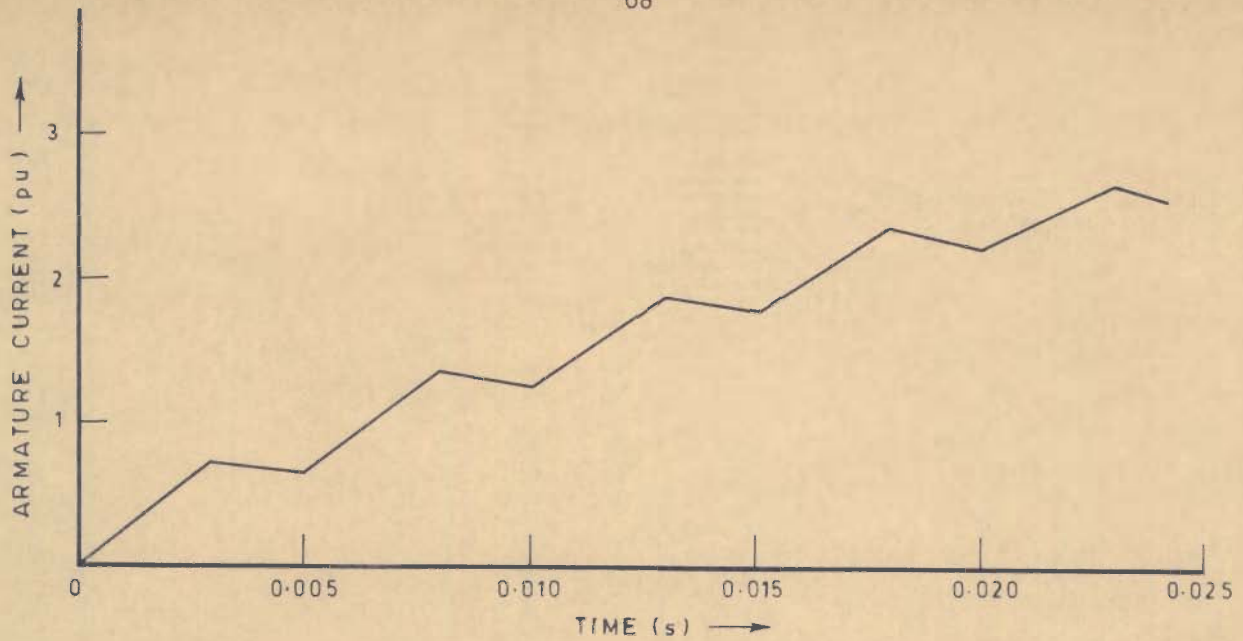
FIG. 3.5(a) _ VARIATION OF ARMATURE CURRENT FOR
FIRST FEW CHOPPER CYCLES

(a) MAX. CURRENT IN A CYCLE
(b) MINI. CURRENT IN A CYCLE
(c) AVERAGE CURRENT IN A CYCLE
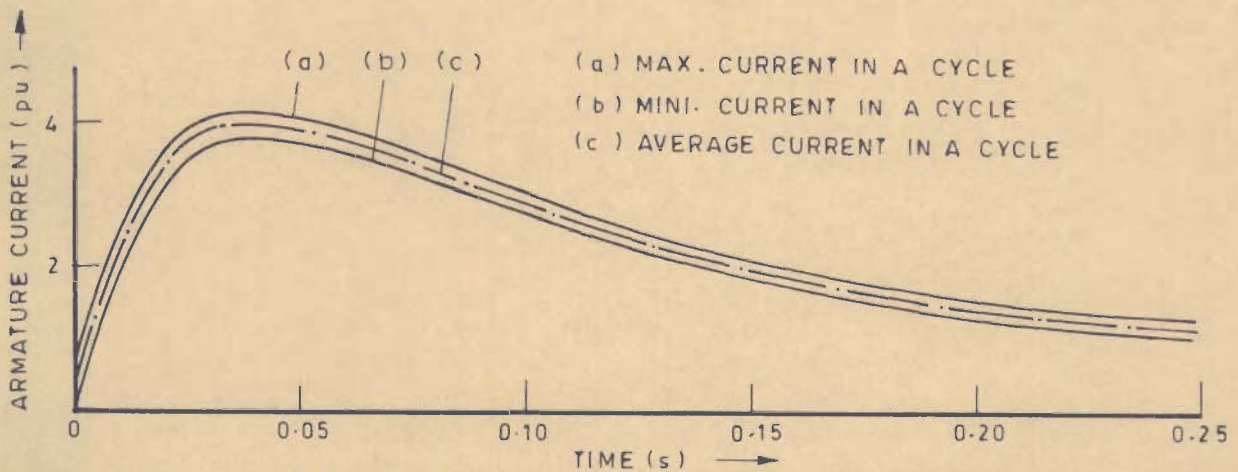
FIG. 3.5(b)-VARIATION OF ARMATURE CURRENT IN TRANSIENT
CONDITION
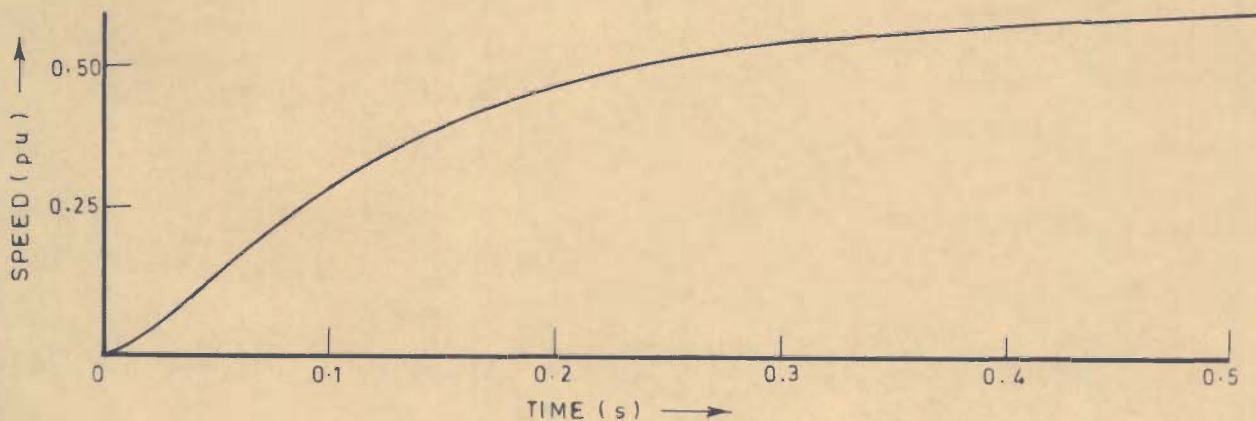
FIG. 3.6 _ MOTOR SPEED AVERAGED OVER A CHOPPER
CYCLE IN TRANSIENT CONDITION
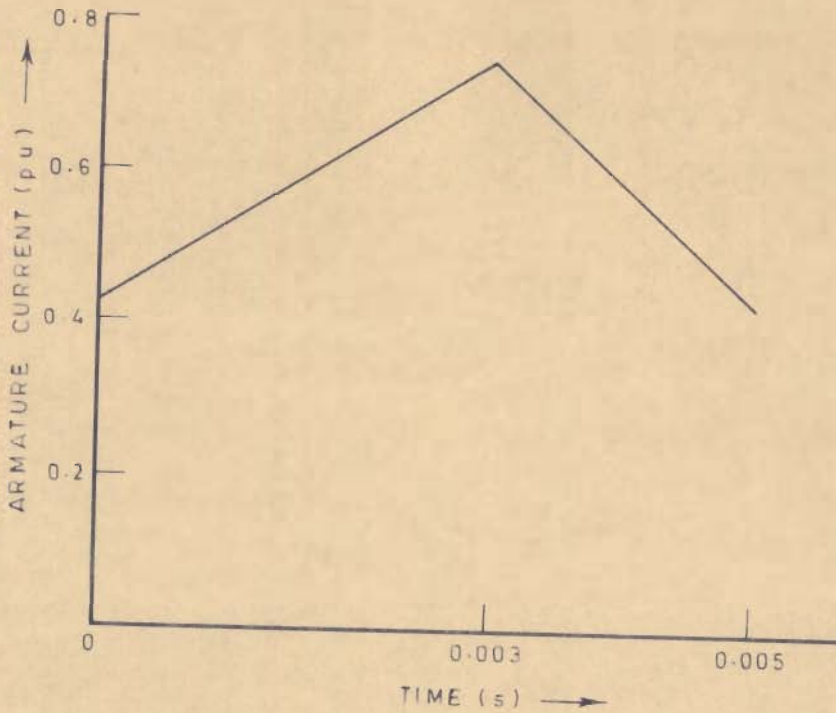
FIG. 3.7 _ VARIATION OF STEADY STATE ARMATURE
CURRENT OVER A CHOPPER CYCLE
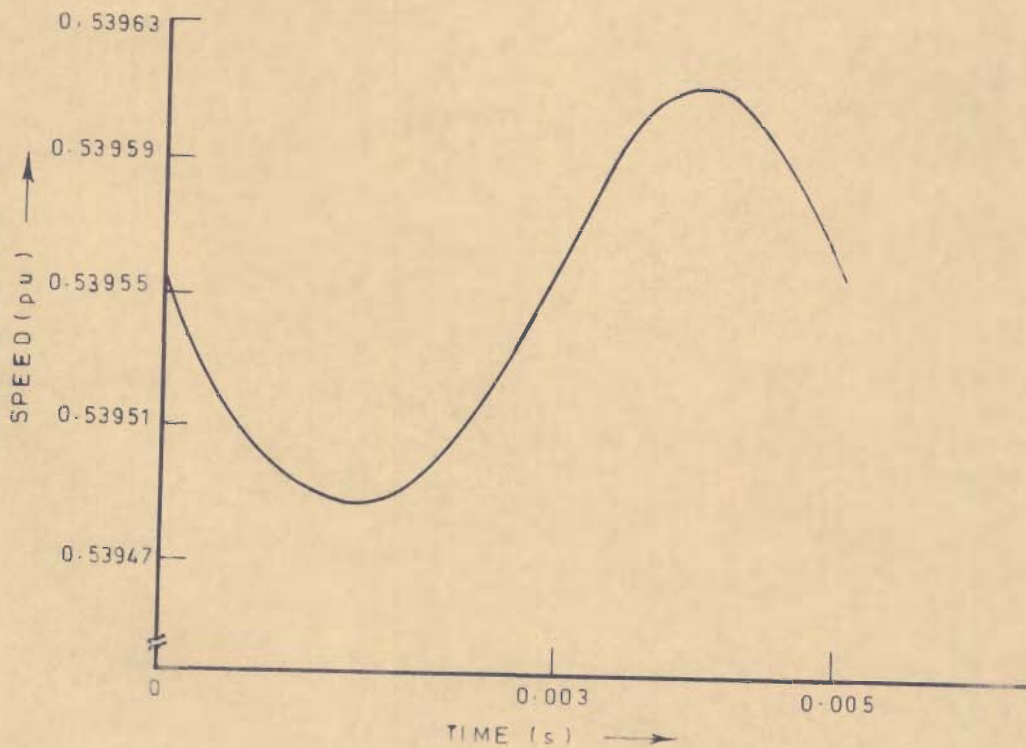
FIG. 3.8 _ VARIATION OF STEADY STATE SPEED OVER
A CHOPPER CYCLE

shown in Fig. 3.5(a). The envelope of the armature current during acceleration process under the condition of switching-in is as shown in Fig. 3.5(b). It may be seen that the range of variation of current per cycle, during the acceleration process remains nearly constant. The mid-line of this envelope gives the average armature current during acceleration process.

The acceleration characteristics of motor i.e. variation of average speed per chopper cycle against time is plotted as shown in Fig. 3.6.

3.7.2 Steady State Performance

Under steady state conditions, the armature current varies between two fixed values (0.432 and 0.749 pu) determined by operating conditions. This variation is shown in Fig. 3.7. The variation of current within an on-period or off-period follows exponential law, but appear linear in Figs. 3.5(a),3.7 because chopper frequency is large.

Under steady state condition, the speed fluctuates between a minimum and a maximum value (0.53956 and 0.53962 pu) depending upon the operating conditions as shown in Fig. 3.8. During duty interval the speed decreases till it attains a minimum value, and then it increases. The reverse holds for freewheeling interval.

3.8 CONCLUSIONS

In this chapter, a new analytical technique for the analysis of chopper fed d.c. motors, using time ratio control with constant chopper frequency, is presented. The system

equations are expressed in State model form, and solved analyti-
cally to obtain closed-form solutions for armature current and
motor speed, for transient as well as steady state conditions.
The analysis presented is illustrated by an example.

The proposed analytical technique is superior to existing
methods of analysis in following respects:

(a) The system equations [eqns. (3.1, 3.2)] can describe the
system in duty as well as freewheeling modes of chopper
operation. Separate equations for the two modes are not
required.

(b) The steady state performance for any operating conditions,
i.e. load torque, duty factor, can be directly obtained
using the solutions presented in eqns. (3.14, 3.15, 3.18,
3.19). Unlike the existing methods, the solution does
not have to be started from the instant of switching and
continued till steady state conditions are obtained. The
computational efforts are, therefore, greatly reduced.

(c) The transient state solutions are also directly obtained
using eqns. (3.12, 3.13, 3.16, 3.17). For studying transients
at any point in time, the solution for that interval of
time is directly obtained, and one does not have to reach
this interval starting from the instant of switching.
Unlike the existing methods, this technique is not a
numerical technique and hence computation time needed is
greatly reduced.

(d) The solutions are in closed-form, and therefore provide an insight into the transient and steady state performance of the drive.

(e) The solutions are more accurate, as speed over a chopper cycle need not be assumed constant.

CHAPTER-4

PERFORMANCE OF CHOPPER CONTROLLED D.C. MOTOR DRIVE AS AFFECTED
BY ELASTICITY OF COUPLING AND PERIODIC VARIATION OF LOAD TORQUE

4.1 INTRODUCTION

For a d.c. drive fed by a constant voltage d.c. source,
the analysis given in Chapter-2 reveals that the mechanical
factors, like elasticity of coupling and periodic variation of
load torque, significantly affect the drive performance. Majority
of d.c. drives in present day industry find their use in variable
speed applications. In such cases, the drives may be fed through
either a chopper or a phase controlled convertor. Chopper control
offers many advantages (discussed in Chapter-3) and is, therefore,
being increasingly used for controlling the speed of d.c. drives.

The frequent use of chopper controlled d.c. drives makes
it imperative to precisely analyse the performance of such drives
and to investigate as to how a drive with an elastic coupling and
periodically varying load torque, behaves when operated from a
chopper voltage supply, and how these mechanical factors influence
the performance. The work available in literature deals mainly
with the analysis of chopper fed d.c. drives with constant load
torque without considering the effect of elasticity of shaft. The
analysis of effects of mechanical factors on the performance of
chopper fed d.c. drives has not been attempted so far.

4.2 WORK PRESENTED

In this chapter, analysis of chopper fed d.c. motor drive with a periodic load torque is presented. The effect of elasticity of the shaft connecting the motor to load is included in the analysis. Closed-form solutions for system performance in terms of motor armature current, angular positions and speed are obtained for transient as well as steady state conditions. The nature of variation of motor current and speed, and twist in the shaft are studied for the cases of constant as well as periodically varying load torques. The situations leading to system resonance are investigated. The possibilities of mechanical failure of shaft, due to excessive shear stress and fatigue, are predicted. The effects of variation of chopper duty factor and chopper frequency on the drive performance are discussed. Results are illustrated by an example and useful inferences are drawn. Suggestions are given to improve the design as well as performance of the drive.

The system analysed, as shown in Fig.4.1, represents a separately excited d.c. motor coupled to the load through an elastic shaft. The moment of inertia as well as damping of motor and load are considered independently, while the shaft inertia is neglected. This type of electromechanical system is referred to as 'Two rotor, semi-definite, two degree of freedom' system [section 2.2]. The input to the motor is through a chopper which converts a constant d.c. source voltage into a pulsed voltage. The chopper output voltage is shown in Fig.4.2. A free-wheeling diode in parallel with armature allows the flow of current during
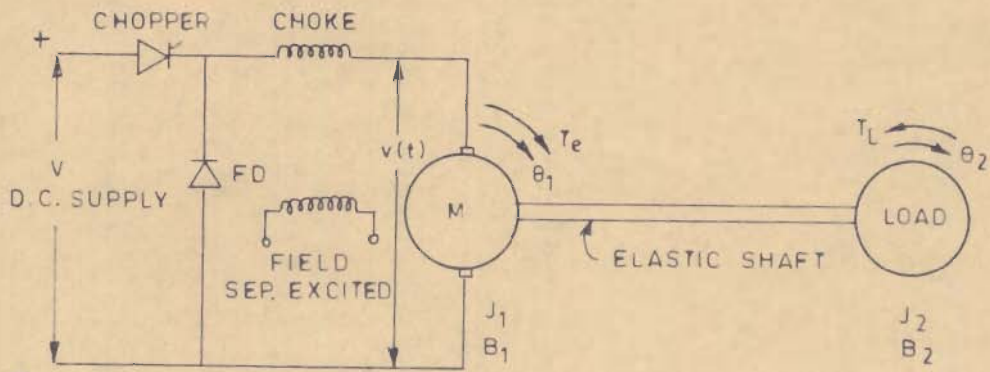
FIG. 4·1 _ SCHEMATIC DIAGRAM OF CHOPPER
FED D.C. ELECTRIC DRIVE WITH
ELASTIC COUPLING
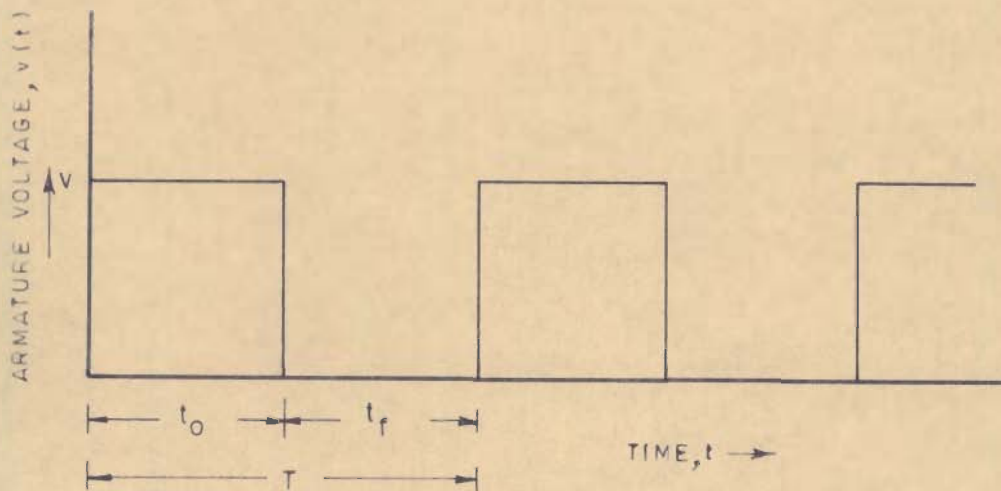
FIG. 4·2 _ CHOPPER OUTPUT VOLTAGE

pulse-off (freewheeling) periods of chopper voltage. A choke is connected in series with armature to reduce the ripples in armature current. The 'Time Ratio Control' technique, with constant chopper frequency is employed to control the average voltage applied to armature, which in turn controls the motor speed.

Any periodic load torque can be considered to be composed of a uniform component and several sinusoidally varying alternating components. For the sake of simplicity of the analysis, the torque is considered to be composed of a non-varying component and only one sinusoidally varying component, neglecting other harmonic components [Fig.2.2(b)]. However, the method of analysis holds in the presence of more than one alternating components as well.

A mathematical model of the system is given. The motor torque developed drives the system inertia, friction, load torque and the elastic torque. The system equations are expressed in State model form. The technique of analysis of chopper controlled d.c. drives developed in Chapter-3 is used to determine. the performance, as this technique is superior and offers many advantages over other existing techniques (discussed in section 3.8).

The analysis is based on the same assumptions as stated in section 3.3.1.

4.3 PERFORMANCE EQUATIONS

The equations governing the system performance can be written as below:

$$v(t) = L \frac{di}{dt} + R i + K_m \dot{\theta}_1 \tag{4.1}$$

$$T_e = J_1 \ddot{\theta}_1 + B_1 \dot{\theta}_1 + C(\theta_1 - \theta_2) \tag{4.2}$$

$$-T_L = J_2 \ddot{\theta}_2 + B_2 \dot{\theta}_2 + C(\theta_2 - \theta_1) \tag{4.3}$$

where $\quad T_e = K_e \, i \tag{4.4}$

and $\quad T_L = T_{Lo} + T_{L1} \sin(\omega_1 t - \emptyset) \tag{4.5}$

Equations (4.2)-(4.5) are same as eqns.(2.2)-(2.5), and are rewritten here to maintain the continuity in the text. These equations can be expressed in State model form as:

$$\dot{x} = A x + D u \tag{4.6}$$

where [A] and [D] are given by eqns.(2.7) and (2.8) respectively, and the

forcing function vector $U = \begin{bmatrix} v(t) \\ T_L \end{bmatrix}$

and state variable vector $x = [\theta_1 \quad \dot{\theta}_1 \quad \theta_2 \quad \dot{\theta}_2 \quad i]^T$

4.3.1 System Characteristic Equation

From eqn.(4.6):

$$X(s) = [sI-A]^{-1} DU(s) + [sI-A]^{-1} x(0) \tag{4.7}$$

For the system starting from quiescent state, all variables have a value zero at t= 0,

$$x(0) = [0 \quad 0 \quad 0 \quad 0 \quad 0]^T$$

From eqn.(4.7), X(s) can be written as:

$$X(s) = \frac{1}{\Delta} [f_{ij}] DU(s) \tag{4.8}$$

where $[f_{ij}] = Adj[sI-A]$

The system characteristic equation is given as:

$$|sI-A| = A_1 s^5 + A_2 s^4 + A_3 s^3 + A_4 s^2 + A_5 s = 0 \qquad (4.9)$$

This is same as obtained for drive with constant voltage input [eqn.(2.13)]. The coefficients, A_1 - A_5, depend upon values of electrical and mechanical parameters of the system as given in eqn.(2.14). The characteristic equation has one root at origin and two pairs of complex conjugate roots with real parts as α_1 and α_2 and imaginary parts as β_1 and β_2 respectively. Thus Δ can be written as:

$$\Delta = s(s + \alpha_1 \pm j \beta_1)(s + \alpha_2 \pm j \beta_2)$$

The value of β_1 is a function of circuit inductance and moment of inertia of the system. For low values of inductance, β_1 may even be zero. The value of β_2 depends upon the torsional stiffness of the shaft, moment of inertia, and damping of the system. β_1 and β_2 are termed as the damped natural frequencies of oscillation of the system. The undamped natural frequencies ω_{n1} and ω_{n2} are given as:

$$\omega_{n1} = (\alpha_1^2 + \beta_1^2)^{1/2} \qquad ; \qquad \omega_{n2} = (\alpha_2^2 + \beta_2^2)^{1/2}$$

The values of α_1, α_2 and β_1, β_2 depend upon damping ratio and are:

$$\alpha_1 = \xi_1 \omega_{n1} , \quad \alpha_2 = \xi_2 \omega_{n2}$$

$$\beta_1 = (1 - \xi_1^2)^{1/2} \omega_{n1} \qquad , \qquad \beta_2 = (1 - \xi_2^2)^{1/2} \omega_{n2}$$

4.4 DETERMINATION OF SYSTEM RESPONSE

The solution in time domain for state variables which describe the system response, can be obtained by taking Laplace inverse transform of eqn. (4.8) as:

$$
\begin{bmatrix} \theta_1(t) \\ \dot{\theta}_1(t) \\ \theta_2(t) \\ \dot{\theta}_2(t) \\ i(t) \end{bmatrix} = \mathcal{L}^{-1} \frac{1}{\Delta} \begin{bmatrix} f_{11}(s)\ldots f_{51}(s) \\ f_{12}(s)\ldots f_{52}(s) \\ f_{13}(s)\ldots f_{53}(s) \\ f_{14}(s)\ldots f_{54}(s) \\ f_{15}(s)\ldots f_{55}(s) \end{bmatrix} \begin{bmatrix} 0 \\ 0 \\ 0 \\ -\frac{1}{J_2}\{\frac{T_{Lo}}{s}+\frac{T_{L1}(\omega_1 \cos \emptyset - s \sin \emptyset)}{(s^2 + \omega_1^2)}\} \\ \frac{V}{sL}\{\frac{1-\exp(-st_o)}{1-\exp(-sT)}\} \end{bmatrix} \quad (4.10)
$$

where $\frac{V}{sL}\{\frac{1-\exp(-st_o)}{1-\exp(-sT)}\}$ is the Laplace transform of chopper output voltage shown in Fig. 4.2 .

From eqn. (4.10);

$$
i(t) = \mathcal{L}^{-1} \left[\frac{-f_{45}(s)}{\Delta J_2}\{\frac{T_{Lo}}{s}+\frac{T_{L1}(\omega_1 \cos \emptyset - s \sin \emptyset)}{(s^2 + \omega_1^2)}\} + \frac{f_{55}(s)V}{\Delta sL}\{\frac{1-\exp(-st_o)}{1-\exp(-sT)}\} \right]
$$
$$\ldots (4.11)$$

$$
\theta_1(t) = \mathcal{L}^{-1} \left[\frac{-f_{41}(s)}{\Delta J_2}\{\frac{T_{Lo}}{s}+\frac{T_{L1}(\omega_1 \cos \emptyset - s \sin \emptyset)}{(s^2 + \omega_1^2)}\} + \frac{f_{51}(s)V}{\Delta sL}\{\frac{1-\exp(-st_o)}{1-\exp(-sT)}\} \right]
$$
$$\ldots (4.12)$$

$$
\theta_2(t) = \mathcal{L}^{-1} \left[\frac{-f_{43}(s)}{\Delta J_2}\{\frac{T_{Lo}}{s}+\frac{T_{L1}(\omega_1 \cos \emptyset - s \sin \emptyset)}{(s^2 + \omega_1^2)}\} + \frac{f_{53}(s)V}{\Delta sL}\{\frac{1-\exp(-st_o)}{1-\exp(-sT)}\} \right]
$$
$$\ldots (4.13)$$

where values of $f_{41}(s)\ldots f_{55}(s)$ are given in appendix A-3.1.

The system response can be obtained by solving eqns. (4.11)-(4.13) which involves determination of Laplace inverse

transforms of the three terms containing T_{Lo}, T_{L1}, and V. The Laplace inverse of the first two terms involving T_{Lo} and T_{L1} is simple and can be obtained by usual methods. However, the Laplace inverse of terms containing $[\{1-\exp(-st_o)\}/\{1-\exp(-sT)\}]$ cannot be obtained by usual methods and for this purpose the following theorem derived in appendix A-2.1 is used:

(a) For duty interval:

$$\mathcal{L}^{-1}\left[f(s)\{\frac{1-\exp(-st_o)}{1-\exp(-sT)}\}\right] = \sum_{r=1}^{n} f(t-\overline{r-1}T) - \sum_{r=1}^{n-1} f(t-t_o-\overline{r-1}T) \quad (4.14)$$

(b) For freewheeling interval:

$$\mathcal{L}^{-1}\left[f(s)\{\frac{1-\exp(-st_o)}{1-\exp(-sT)}\}\right] = \sum_{r=1}^{n} [f(t-\overline{r-1}T) - f(t-t_o-\overline{r-1}T)] \quad (4.15)$$

In the above, the value of t for nth chopper cycle lies in the range:

duty interval: $(n-1)T \leq t \leq \{(n-1)T + t_o\}$

freewheeling interval: $\{(n-1)T + t_o\} \leq t \leq nT$

A sample procedure of determining the current response $i_{d_n}(t)$ and $i_{f_n}(t)$ from eqn.(4.11) is given in appendix A-3.2. The expressions for $\theta_1(t)$ and $\theta_2(t)$ can be obtained in a similar fashion from eqns.(4.12) and (4.13) respectively.

4.5 SOLUTION FOR ARMATURE CURRENT

4.5.1 General Solution

(a) Duty interval:

The armature current in duty interval of nth chopper cycle, $i_{d_n}(t)$, can be obtained by solving eqn.(4.11) and using the theorem of eqn.(4.14). Thus

$$i_{d_n}(t) = \sum_{m=1}^{2}\left[i_{ds_m} + i_{t_m} + i_{t_{m+2}}\right] + i_{ds_3} + i_{ds_4} \tag{4.16}$$

where

$$i_{ds_m} = V\,K_2^m\exp(-\alpha_m t_n)[\{\exp(\alpha_m T)\sin(\beta_m t_{n1}-\emptyset_2^m)-\sin(\beta_m t_n-\emptyset_2^m)\}$$
$$- \exp(-\alpha_m t_f)\{\exp(\alpha_m T)\sin(\beta_m t_{n3}-\emptyset_2^m)-\sin(\beta_m t_{n2}-\emptyset_2^m)\}]/(L\,D_m)$$

$$i_{t_m} = V\,K_2^m\exp(-\alpha_m t)[\{\sin(\beta_m t-\emptyset_2^m)-\exp(\alpha_m T)\sin(\beta_m t_1-\emptyset_2^m)\}$$
$$- \exp(\alpha_m t_o)\{\sin(\beta_m t_2-\emptyset_2^m)-\exp(\alpha_m T)\sin(\beta_m t_3-\emptyset_2^m)\}]/(L\,D_m)$$

$$i_{t_{m+2}} = \exp(-\alpha_m t)[T_{Lo}\,K_1^m\sin(\beta_m t-\emptyset_1^m)+T_{L1}\,K_1^{m+2}\sin(\beta_m t-\emptyset_1^{m+2})]/J_2$$

$$i_{ds_3} = V\,K_5^2/L + T_{Lo}\,K_5^1/J_2$$

$$i_{ds_4} = T_{L1}\,K_1^5\sin(\omega_1 t - \emptyset_1^5)/J_2$$

The expressions of different constants used in above equations are given in appendix A-3.1 and some symbols are defined as:

$$t_n = t-nT\ ,\quad t_{n1} = t-nT+T\ ,\quad t_{n2} = t-nT+T-t_o\ ,\quad t_{n3} = t-nT+2T-t_o$$

$$t_{n4} = t-nT-t_o\ ,\quad t_f = T-t_o\ ,\quad t_1 = t+T\ ,\quad t_2 = t-t_o\ ,\quad t_3 = t+T-t_o$$

$$D_1 = 1 + \exp(\alpha_1 T)\{\exp(\alpha_1 T) - 2\cos\beta_1 T\}$$

$$D_2 = 1 + \exp(\alpha_2 T)\{\exp(\alpha_2 T) - 2\cos\beta_2 T\}$$

(b) Freewheeling interval:

The armature current in freewheeling interval for nth chopper cycle, $i_{f_n}(t)$, can be obtained by solving eqn.(4.11) and using the theorem of eqn.(4.15) as below:

$$i_{f_n}(t) = \sum_{m=1}^{2} \left[i_{fs_m} + i_{t_m} + i_{t_{m+2}} \right] + i_{fs_3} + i_{fs_4} \qquad (4.17)$$

where

$$i_{fs_m} = V\, K_2^m\, \exp(-\alpha_m\, t_n)[\{\exp(\alpha_m\, T)\sin(\beta_m\, t_{n1} - \emptyset_2^m) - \sin(\beta_m\, t_n - \emptyset_2^m)\}$$
$$- \exp(\alpha_m\, t_o)\{\exp(\alpha_m\, T)\sin(\beta_m\, t_{n2} - \emptyset_2^m) - \sin(\beta_m\, t_{n4} - \emptyset_2^m)\}]/(L\, D_m)$$
$$i_{fs_3} = T_{Lo}\, K_5^1/J_2 \quad , \quad i_{fs_4} = i_{ds_4}$$

4.5.2 Steady State Armature Current

The steady state armature current in duty and freewheeling intervals can be obtained from eqns.(4.16) and (4.17) by taking only those terms which do not decay with time. It is to be noted that the terms containing t_n also give steady state response, since as t becomes very large, n also becomes very large and the difference t_n remains finite and independent of n.

It is further noted that the terms t_{n1}, t_{n2}, t_{n3} and t_{n4} depend on (t-n T) and therefore, the terms in the expression of current (as well as speed) containing $t_{n1} \cdots t_{n4}$ are also independent of n and give steady state response. The steady state current in duty and freewheeling intervals can be written as:

(a) Duty interval:

From eqn.(4.16), the steady state armature current in duty interval of nth chopper cycle, $i_{ds}(t)$, is given by:

$$i_{ds}(t) = i_{ds_1} + i_{ds_2} + i_{ds_3} + i_{ds_4} \tag{4.18}$$

(b) Freewheeling interval:

From eqn.(4.17), the steady state armature current in freewheeling interval of nth chopper cycle, $i_{fs}(t)$, is given by:

$$i_{fs}(t) = i_{fs_1} + i_{fs_2} + i_{fs_3} + i_{fs_4} \tag{4.19}$$

4.5.2.1 Value of (t-nT) in Steady State

Although, two variables t (time) and n (number of chopper cycle) appear in the expressions of steady state current given by equations (4.18) and (4.19), it is not necessary to substitute t and n as separate variables. For this purpose the term (t-nT) can be viewed as another variable, t_n. The solution for steady state current (as well as speed) can, therefore, be obtained even if the values of t and n after which steady state is achieved are not known (as is generally the case). As such, the computations do not have to be performed starting from switching-in instant. The other time variables t_{n1}, t_{n2}, t_{n3} and t_{n4} are functions of t_n.

Fig.4.3 shows the range over which the time variables t_n, $t_{n1}, \ldots, t_{n4}$ vary in different chopper cycles. The point in time at which these time variables attain zero values are also marked. For nth chopper cycle, the range of these time variables vary as
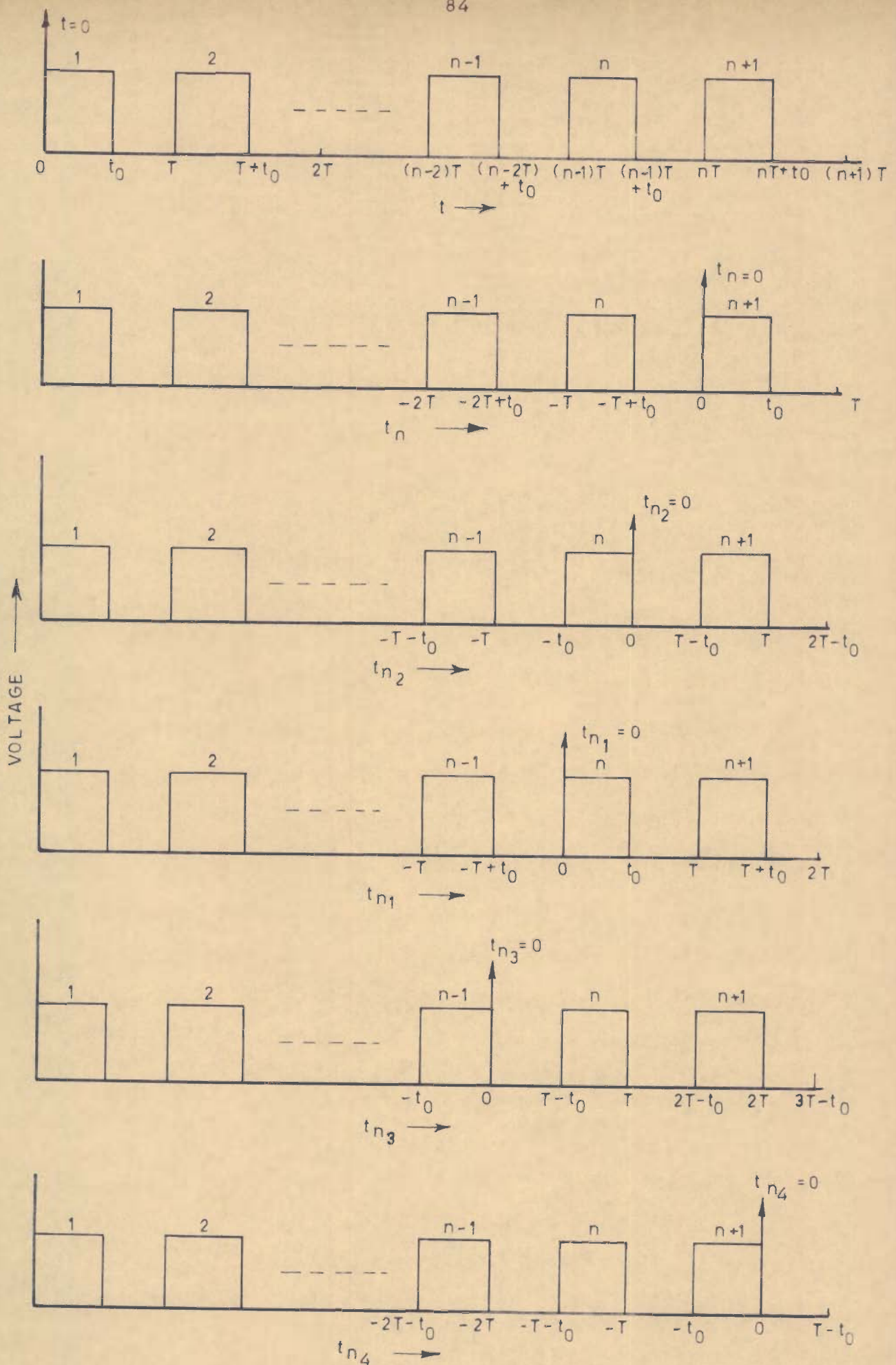
FIG. 4.3 _ VARIATION OF TIME VARIABLES $t_n, t_{n1}, \ldots t_{n4}$

below:

time variable	variation in duty interval	variation in free-wheeling interval
t_n	$-T \le t_n \le (-T+t_o)$	$(-T+t_o) \le t_n \le 0$
t_{n1}	$0 \le t_{n1} \le t_o$	$t_o \le t_{n1} \le T$
t_{n2}	$-t_o \le t_{n2} \le 0$	$0 \le t_{n2} \le (T-t_o)$
t_{n3}	$(T-t_o) \le t_{n3} \le T$	$T \le t_{n3} \le (2T-t_o)$
t_{n4}	$(-T-t_o) \le t_{n4} \le -T$	$-T \le t_{n4} \le -t_o$

For obtaining the steady state response, in duty as well as freewheeling intervals, any one time variable amongst t_n, t_{n1},...,t_{n4} can be selected and varied between the range given above. The values of remaining time variables can be substituted in terms of the selected time variable. For example, for obtaining the steady state current response in duty interval from eqn.(4.18), the time interval t_n may be selected and varied from $-T$ to $(-T+t_o)$. Similarly the steady state current in free-wheeling interval can be obtained from eqn.(4.19) varying the value of t_n from $(-T+t_o)$ to zero. The values of other time intervals appearing in eqns.(4.18) and (4.19) can be substituted in terms of t_n as below:

$$t_{n1} = t_n + T \qquad , \qquad t_{n2} = t_n + T - t_o$$

$$t_{n3} = t_n + 2T - t_o \qquad , \qquad t_{n4} = t_n - t_o$$

The steady state response, thus can be obtained following the procedure discussed above.

4.6 SOLUTION FOR ANGULAR POSITION $\theta_1(t)$

(a) Duty interval:

From eqns. (4.12) and (4.14), angular position in duty interval for nth chopper cycle, $\theta_{1d_n}(t)$, is obtained as:

$$\theta_{1d_n}(t) = \sum_{m=1}^{2}\left[\theta_{1ds_m} + \theta_{1t_m} + \theta_{1t_{m+2}}\right] + \theta_{1ds_3} + \theta_{1ds_4} + \theta_{1t_5} \qquad (4.20)$$

where

$$\theta_{1ds_m} = V\,K_2^{5+m}\exp(-\alpha_m\,t_n)[\{\exp(\alpha_m\,T)\sin(\beta_m\,t_{n1} - \emptyset_2^{5+m})$$

$$- \sin(\beta_m\,t_n - \emptyset_2^{5+m})\} - \exp(-\alpha_m\,t_f)\{\exp(\alpha_m\,T)\sin(\beta_m\,t_{n3} - \emptyset_2^{5+m})$$

$$- \sin(\beta_m\,t_{n2} - \emptyset_2^{5+m})\}]/(L\,D_m)$$

$$\theta_{1t_m} = V\,K_2^{5+m}\exp(-\alpha_m\,t)[\{\sin(\beta_m\,t - \emptyset_2^{5+m}) - \exp(\alpha_m\,T)\sin(\beta_m\,t_1 - \emptyset_2^{5+m})\}$$

$$- \exp(\alpha_m\,t_o)\{\sin(\beta_m\,t_2 - \emptyset_2^{5+m}) - \exp(\alpha_m\,T)\sin(\beta_m\,t_3 - \emptyset_2^{5+m})\}]/$$

$$(L\,D_m)$$

$$\theta_{1t_{m+2}} = -\exp(-\alpha_m\,t)[T_{Lo}\,K_1^{5+m}\sin(\beta_m\,t - \emptyset_1^{5+m}) + T_{L1}K_1^{7+m}\sin(\beta_m\,t$$

$$- \emptyset_1^{7+m})]/J_2$$

$$\theta_{1ds_3} = V\,K_5^7/L - (T_{Lo}\,K_5^4 + T_{L1}\,K_5^5)/J_2$$

$$\theta_{1ds_4} = T_{L1}\,K_1^{10}\sin(\omega_1\,t - \emptyset_1^{10})/J_2$$

$$\theta_{1t_5} = -T_{Lo}\,K_5^3\,t/J_2 + [V\,K_5^6\{t - (n-1)t_f\}]/L$$

(b) Freewheeling interval:

From eqns. (4.12) and (4.15), angular position in free-wheeling interval for nth chopper cycle, $\theta_{1f_n}(t)$, is given by:

$$\theta_{1f_n}(t) = \sum_{m=1}^{2} \left[\theta_{1fs_m} + \theta_{1t_m} + \theta_{1t_{m+2}} \right] + \theta_{1fs_3} + \theta_{1fs_4} + \theta_{1t_6} \qquad (4.21)$$

where

$$\theta_{1fs_m} = V K_2^{5+m} \exp(-\alpha_m t_n)[\{\exp(\alpha_m T)\sin(\beta_m t_{n1} - \emptyset_2^{5+m})$$

$$- \sin(\beta_m t_n - \emptyset_2^{5+m})\} - \exp(\alpha_m t_o)\{\sin(\beta_m t_{n2} - \emptyset_2^{5+m})\exp(\alpha_m T)$$

$$- \sin(\beta_m t_{n4} - \emptyset_2^{5+m})\}]/(L D_m)$$

$$\theta_{1fs_3} = -(T_{Lo} K_5^4 + T_{L1} K_5^5)/J_2$$

$$\theta_{1fs_4} = \theta_{1ds_4}$$

$$\theta_{1t_6} = -T_{Lo} K_5^3 t/J_2 + V K_5^6 n t_o/L$$

4.7 SOLUTION FOR ANGULAR POSITION $\theta_2(t)$

(a) Duty interval:

From eqns. (4.13) and (4.14), angular position in duty interval for nth chopper cycle, $\theta_{2d_n}(t)$, is obtained as:

$$\theta_{2d_n}(t) = \sum_{m=1}^{2} \left[\theta_{2ds_m} + \theta_{2t_m} + \theta_{2t_{m+2}} \right] + \theta_{2ds_3} + \theta_{2ds_4} + \theta_{2t_5}$$

$$(4.22)$$

where

$$\theta_{2ds_m} = V K_4^{5+m} \exp(-\alpha_m t_n)[\{\exp(\alpha_m T)\sin(\beta_m t_{n1} - \emptyset_4^{5+m})$$

$$- \sin(\beta_m t_n - \emptyset_4^{5+m})\} - \exp(-\alpha_m t_f)\{\exp(\alpha_m T)\sin(\beta_m t_{n3} - \emptyset_4^{5+m})$$

$$- \sin(\beta_m t_{n2} - \emptyset_4^{5+m})\}]/(L D_m)$$

$$\theta_{2t_m} = V\, K_4^{5+m}\, \exp(-\alpha_m\, t)[\{\sin(\beta_m\, t - \emptyset_4^{5+m}) - \exp(\alpha_m\, T)\sin(\beta_m\, t_1$$

$$- \emptyset_4^{5+m})\} - \exp(\alpha_m\, t_o)\{\sin(\beta_m\, t_2 - \emptyset_4^{5+m}) - \exp(\alpha_m\, T)\sin(\beta_m\, t_3$$

$$- \emptyset_4^{5+m})\}]/(L\, D_m)$$

$$\theta_{2t_{m+2}} = -\exp(-\alpha_m\, t)[T_{Lo}\, K_3^{5+m}\, \sin(\beta_m\, t - \emptyset_3^{5+m})$$

$$+ T_{L1}\, K_2^{7+m}\, \sin(\beta_m\, t - \emptyset_2^{7+m})]/J_2$$

$$\theta_{2ds_3} = V\, K_6^2/L - (T_{Lo}\, K_5^9 + T_{L1}\, K_6^0)/J_2$$

$$\theta_{2ds_4} = -T_{L1}\, K_2^{10}\, \sin(\omega_1\, t - \emptyset_2^{10})/J_2$$

$$\theta_{2t_5} = -T_{Lo}\, K_5^8\, t/J_2 + V\, K_6^1\{t - (n-1)t_f\}/L$$

(b) Freewheeling interval:

From eqns. (4.13) and (4.15), angular position in free-wheeling interval for nth chopper cycle, θ_{2f_n} (t), is given by:

$$\theta_{2f_n}(t) = \sum_{m=1}^{2}\left[\theta_{2fs_m} + \theta_{2t_m} + \theta_{2t_{m+2}}\right] + \theta_{2fs_3} + \theta_{2fs_4} + \theta_{2t_6} \qquad (4.23)$$

where

$$\theta_{2fs_m} = V\, K_4^{5+m}\, \exp(-\alpha_m\, t_n)[\{\exp(\alpha_m\, T)\sin(\beta_m\, t_{n1} - \emptyset_4^{5+m})$$

$$- \sin(\beta_m\, t_n - \emptyset_4^{5+m})\} - \exp(\alpha_m\, t_o)\{\sin(\beta_m\, t_{n2} - \emptyset_4^{5+m})\exp(\alpha_m\, T)$$

$$- \sin(\beta_m\, t_{n4} - \emptyset_4^{5+m})\}]/(L\, D_m)$$

$$\theta_{2fs_3} = -(T_{Lo}\, K_5^9 + T_{L1}\, K_6^0)/J_2 \quad , \quad \theta_{2fs_4} = \theta_{2ds_4}$$

$$\theta_{2t_6} = -T_{Lo}\, K_5^8\, t/J_2 + V\, K_6^1\, n\, t_o/L$$

4.8 SOLUTION FOR MOTOR SPEED $\dot{\theta}_1(t)$

4.8.1 General Solution

(a) Duty interval:

Differentiating eqn.(4.20) w.r.to t, angular speed in duty interval for nth chopper cycle, $\dot{\theta}_{1d_n}(t)$, is obtained as:

$$\dot{\theta}_{1d_n}(t) = \sum_{m=1}^{2} \left[\dot{\theta}_{1ds_m} + \dot{\theta}_{1t_m} + \dot{\theta}_{1t_{m+2}} \right] + \dot{\theta}_{1ds_3} + \dot{\theta}_{1ds_4} \qquad (4.24)$$

where

$$\dot{\theta}_{1ds_m} = V \, K_3^m \, \exp(-\alpha_m t_n)[\{\exp(\alpha_m T)\sin(\beta_m t_{n1} - \emptyset_3^m) - \sin(\beta_m t_n - \emptyset_3^m)\}$$

$$- \exp(-\alpha_m t_f)\{\exp(\alpha_m T)\sin(\beta_m t_{n3} - \emptyset_3^m)$$

$$- \sin(\beta_m t_{n2} - \emptyset_3^m)\}]/(L \, D_m)$$

$$\dot{\theta}_{1t_m} = V \, K_3^m \, \exp(-\alpha_m t)[\{\sin(\beta_m t - \emptyset_3^m) - \exp(\alpha_m T)\sin(\beta_m t_1 - \emptyset_3^m)\}$$

$$- \exp(\alpha_m t_o)\{\sin(\beta_m t_2 - \emptyset_3^m) - \exp(\alpha_m T)\sin(\beta_m t_3 - \emptyset_3^m)\}]/(L \, D_m)$$

$$\dot{\theta}_{1t_{m+2}} = -\exp(-\alpha_m t)[T_{Lo} \, K_4 \, \sin(\beta_m t - \emptyset_4^m)$$

$$+ T_{L1} \, K_4^{m+2} \, \sin(\beta_m t - \emptyset_4^{m+2})]/J_2$$

$$\dot{\theta}_{1ds_3} = V \, K_5^6/L - T_{Lo} \, K_5^3/J_2$$

$$\dot{\theta}_{1ds_4} = -T_{L1} \, K_1^{10} \, \omega_1 \, \sin(\omega_1 t - \emptyset_1^{10} + \pi/2)$$

(b) Freewheeling interval:

Differentiating eqn.(4.21) with respect to t, angular speed in freewheeling interval for nth chopper cycle, $\dot{\theta}_{1f_n}(t)$, is obtained as:

$$\dot{\theta}_{1f_n}(t) = \sum_{m=1}^{2} \left[\dot{\theta}_{1fs_m} + \dot{\theta}_{1t_m} + \dot{\theta}_{1t_{m+2}} \right] + \dot{\theta}_{1fs_3} + \dot{\theta}_{1fs_4} \qquad (4.25)$$

where

$$\dot{\theta}_{1fs_m} = V K_3^m \exp(-\alpha_m t_n)[\{\exp(\alpha_m T)\sin(\beta_m t_{n1} - \emptyset_3^m) - \sin(\beta_m t_n - \emptyset_3^m)\}$$

$$- \exp(\alpha_m t_o)\{\exp(\alpha_m T)\sin(\beta_m t_{n2} - \emptyset_3^m) - \sin(\beta_m t_{n4} - \emptyset_3^m)\}]/(L D_m)$$

$$\dot{\theta}_{1fs_3} = -T_{Lo} K_5^3/J_2 \quad , \quad \dot{\theta}_{1fs_4} = \dot{\theta}_{1ds_4}$$

4.8.2 Steady State Motor Speed

(a) Duty interval:

From eqn.(4.24), steady state component of speed in duty interval for nth chopper cycle, $\dot{\theta}_{1ds}(t)$, is given by:

$$\dot{\theta}_{1ds}(t) = \dot{\theta}_{1ds_1} + \dot{\theta}_{1ds_2} + \dot{\theta}_{1ds_3} + \dot{\theta}_{1ds_4} \tag{4.26}$$

(b) Freewheeling interval:

From eqn.(4.25) steady state component of speed in free-wheeling interval for nth chopper cycle, $\dot{\theta}_{1fs}(t)$, is given by:

$$\dot{\theta}_{1fs}(t) = \dot{\theta}_{1fs_1} + \dot{\theta}_{1fs_2} + \dot{\theta}_{1fs_3} + \dot{\theta}_{1fs_4} \tag{4.27}$$

4.9 NATURE OF ARMATURE CURRENT AND MOTOR SPEED

The steady state armature current in duty (as also in freewheeling interval) consists of four components [eqns.(4.18), (4.19)] which are as below:

(i) i_{ds_1} , i_{ds_2} (also i_{fs_1} , i_{fs_2}): These components of current, having frequencies β_1 and β_2 respectively are exponentially varying sinusoidal components whose amplitude depends upon the input voltage and duty factor.

The pattern of variation of these sinusoidal components in duty as well as freewheeling intervals repeats itself in each chopper cycle, and therefore, has a frequency of repetition equal to the chopper frequency.

(ii) i_{ds_3} (also i_{fs_3}): This is a non-varying component, which depends upon the magnitudes of input voltage and uniform component of load torque T_{Lo}.

(iii) i_{ds_4} (also i_{fs_4}): This represents a sinusoidally varying alternating component of current varying at the frequency of load torque pulsations ω_1. Its magnitude depends upon T_{L1}.

The steady state speed during duty and freewheeling intervals [eqns.(4.26,4.27)] also has four components ($\dot{\theta}_{1ds_1}$, $\dot{\theta}_{1ds_2}$, $\dot{\theta}_{1ds_3}$ and $\dot{\theta}_{1ds_4}$) similar to those of current discussed above.

The resultant armature current and speed is the sum of the above four components and comprise of a uniform component superposed by the sinusoidally varying components. The frequency of one of these components is ω_1 while that of the other is same as that of the chopper [Figs.4.4,4.5]. These oscillations are, hereafter, referred to as low frequency and high frequency oscillations respectively.

4.10 TYPICAL PERFORMANCE STUDIES

The performance of a typical system is computed using the method given in section 4.5-4.8, and the results are used to draw inferences regarding the performance features of such drives.
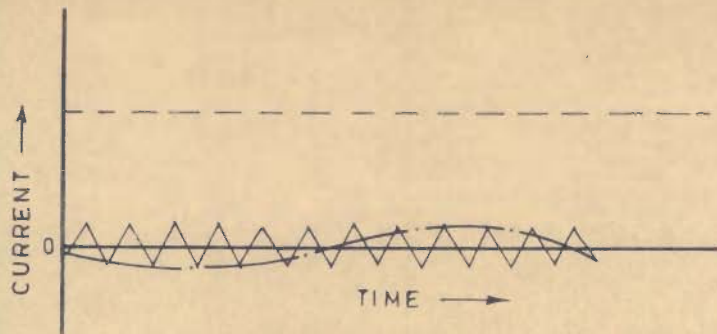
(a)_ COMPONENTS OF STEADY STATE
ARMATURE CURRENT

----- UNIFORM COMPONENT

—·— SINUSOIDAL COMPONENT
OF FREQUENCY ω_1

——— COMPONENT OF CHOPPER
FREQUENCY (CONSISTS OF
TWO SUB-COMPONENTS OF
FREQUENCIES β_1, β_2; NOT
SHOWN SEPARATELY)
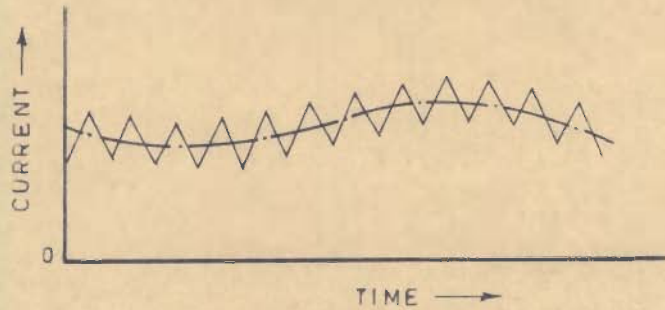
(b)_ RESULTANT STEADY STATE
ARMATURE CURRENT

FIG. 4.4
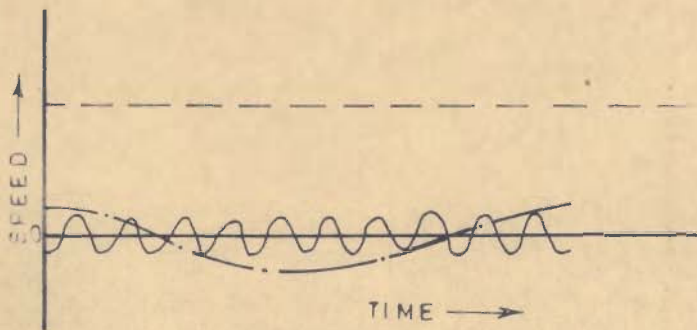
(a)_ COMPONENTS OF STEADY STATE
SPEED
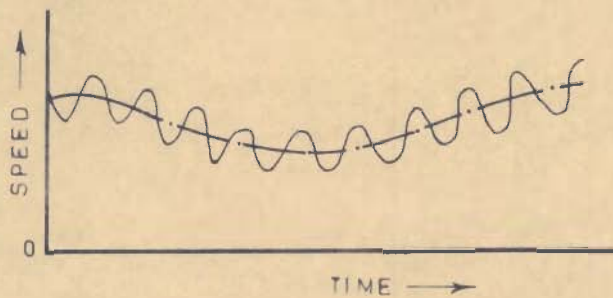
(b)_ RESULTANT STEADY STATE SPEED

FIG. 4.5

The drive represented by Fig.4.1, with the following data is analysed:

System Data:

Motor and the Mechanical System:

armature inductance including choke = 0.16 H

other data are same as given in section 2.7.

Chopper:

> frequency   = 200 Hz
>
> duty factor = 0.6

The dependence of performance on various factors is graphically depicted in Figs. 4.6-4.18 . In these studies the load torque is taken to comprise of a sinusoidally varying component T_{L1} superposed on a non-varying component T_{Lo} as shown in Fig.4.8. The frequency of load torque pulsation ω_1 is taken equal to the average value of steady state speed ω_s (as discussed in section 2.3). The value of ω_s is equal to $\dot{\theta}_{1ds_3}$ (as given in section 4.8). This value of load torque frequency implies that the load torque completes one cycle in one revolution of the machine shaft.

4.11   STEADY STATE PERFORMANCE

The steady state performance under normal operating conditions is shown in Figs.4.6-4.12. Under certain specific conditions, the system experiences resonance characterized by large pulsations in current and speed [Figs.4.13-4.16]. The switching-in transients of armature current and drive angular speed are

shown in Figs.4.17,4.18. The results and inferences therefrom
are discussed in the ensuing paragraphs.

Figs.4.6 and 4.7 show the instantaneous variations of
steady state armature current and speed for two chopper cycles on
an expanded scale. For the case of constant load torque, the
pattern of variation of speed, current and twist in steady state
condition repeats for each chopper cycle as shown in Fig.4.6. It
is observed that the instantaneous armature current rises in duty
interval, while it decays in freewheeling interval. These varia-
tions are exponential but appear to be linear in the diagram due
to the fact that the value of chopper frequency is quite high.
The speed first falls and then rises during a duty interval and
vice-versa for freewheeling interval.

For a pulsating load torque, the values of armature
current, speed and twist in the shaft for subsequent chopper cycles
under steady state are different as shown in Fig.4.7. This is
due to the fact that magnitude of load torque in the subsequent
chopper cycles does not remain same. The load torque in Fig.4.7
varies sinusoidally but this variation appears linear as it is
drawn for a very short interval of time. For a pulsating load
torque the current rises in duty interval and decays in free-
wheeling interval as for the case of constant load torque. Similar-
ly the speed decreases for part of duty interval and then rises
for remaining part of duty interval and vice-versa for free-
wheeling period.
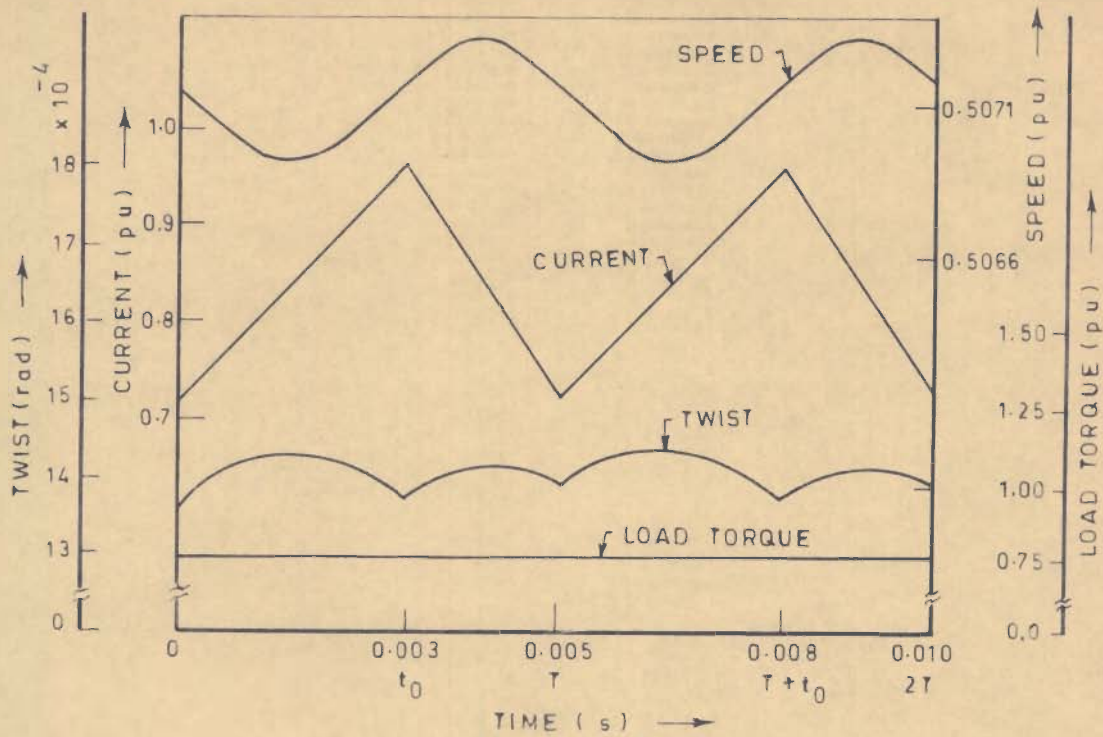
FIG. 4.6 _ VARIATION OF CURRENT, SPEED AND TWIST
UNDER STEADY STATE CONDITIONS FOR
CONSTANT LOAD TORQUE
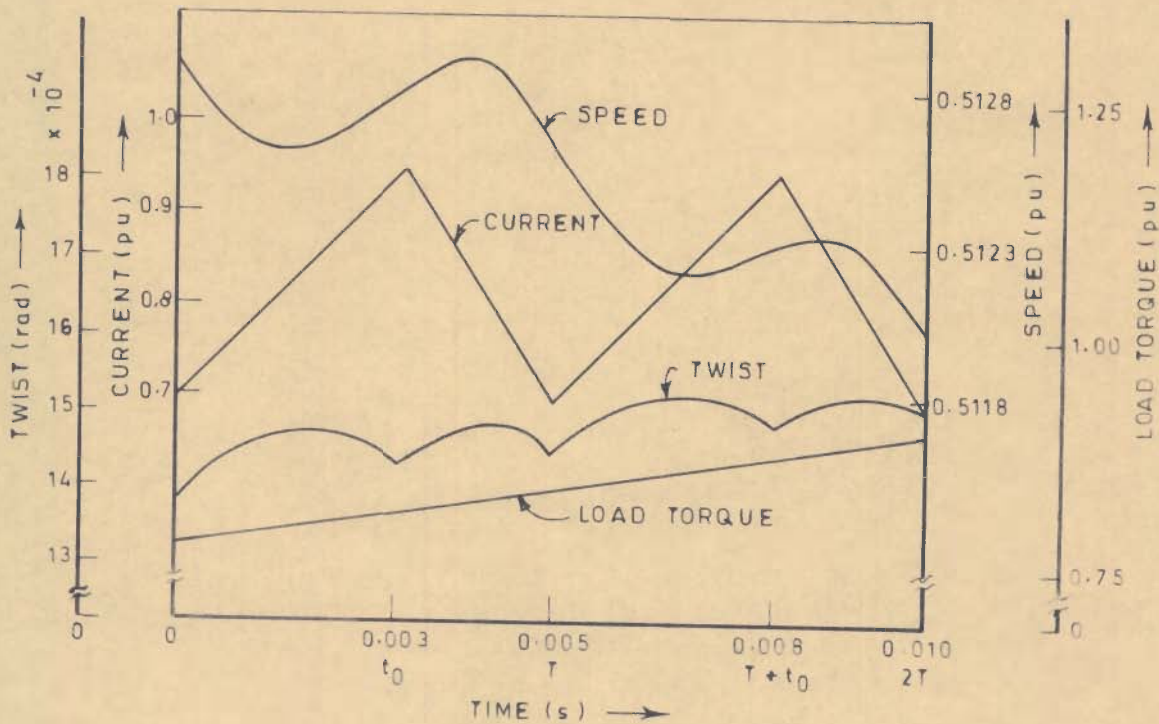
FIG. 4.7 _ VARIATION OF CURRENT, SPEED AND TWIST
UNDER STEADY STATE CONDITIONS FOR
PULSATING LOAD TORQUE

The magnitudes of variation of current and speed change in each successive chopper cycle and the whole pattern repeats after a lapse of time equal to the time period of load torque pulsation $(2\pi/\omega_1)$. In other words, one set of values of current and speed repeat after n' chopper cycles, where n' is the ratio of chopper frequency to load torque frequency. This is due to the fact that the load torque variation completes one cycle after n' chopper cycles. The variation of armature current for one cycle of load torque pulsation is shown in Fig.4.9.

For a load torque as in Fig.4.8, the variations of average values of armature current and speed (average over a cycle of chopper) are shown in Figs. 4.10,4.11 . It is observed that if the load torque is pulsating in nature, the armature current and speed averaged over a chopper cycle also pulsate at a frequency which is same as that of the frequency of load torque pulsation. However, they have a phase difference with respect to the load torque. The amplitude of these pulsations should be minimized in order to improve the performance. This can be achieved by increasing the system moment of inertia as discussed in section 2.8.3 . It can, therefore, be inferred that if the load torque is periodic in nature such that it can be resolved into a constant component, and a number of alternating components, then the armature current and speed averaged over a chopper cycle will have a similar nature.
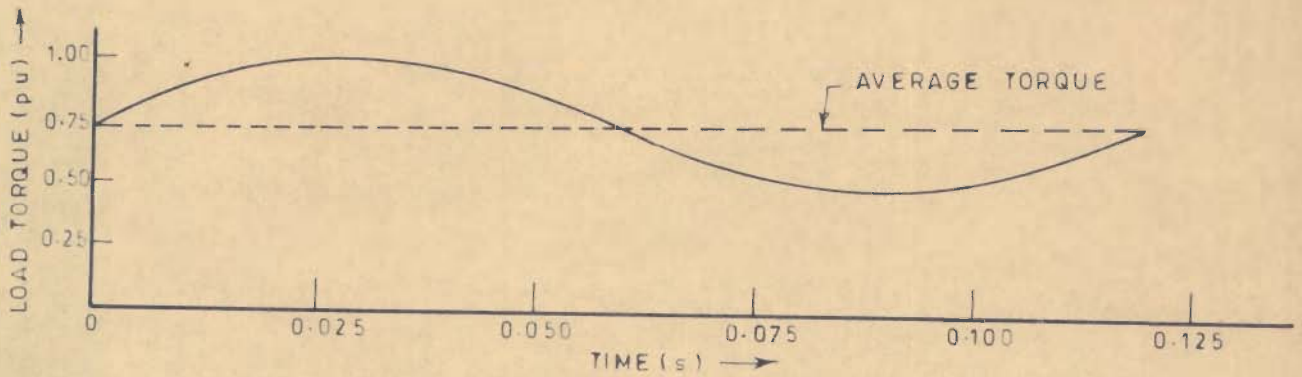
FIG. 4.8 _ VARIATION OF LOAD TORQUE

FIG. 4.9 _ VARIATION OF STEADY STATE ARMATURE
CURRENT

CURVE a : DUTY FACTOR = 0.6
CURVE b : DUTY FACTOR = 0.8
UNIFORM COMPONENT OF CURVE a
UNIFORM COMPONENT OF CURVE b
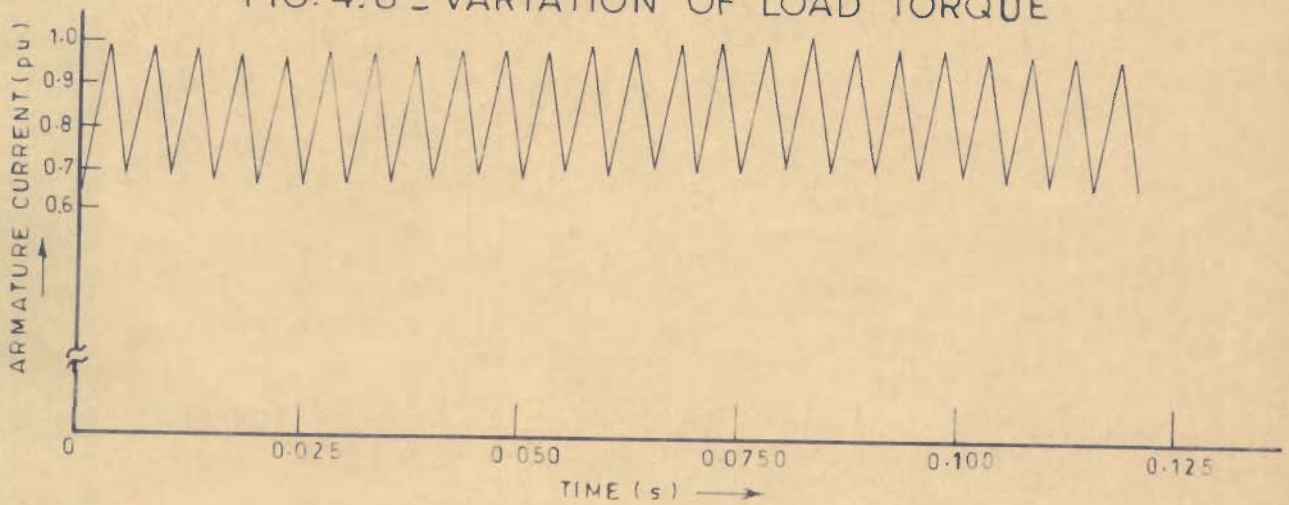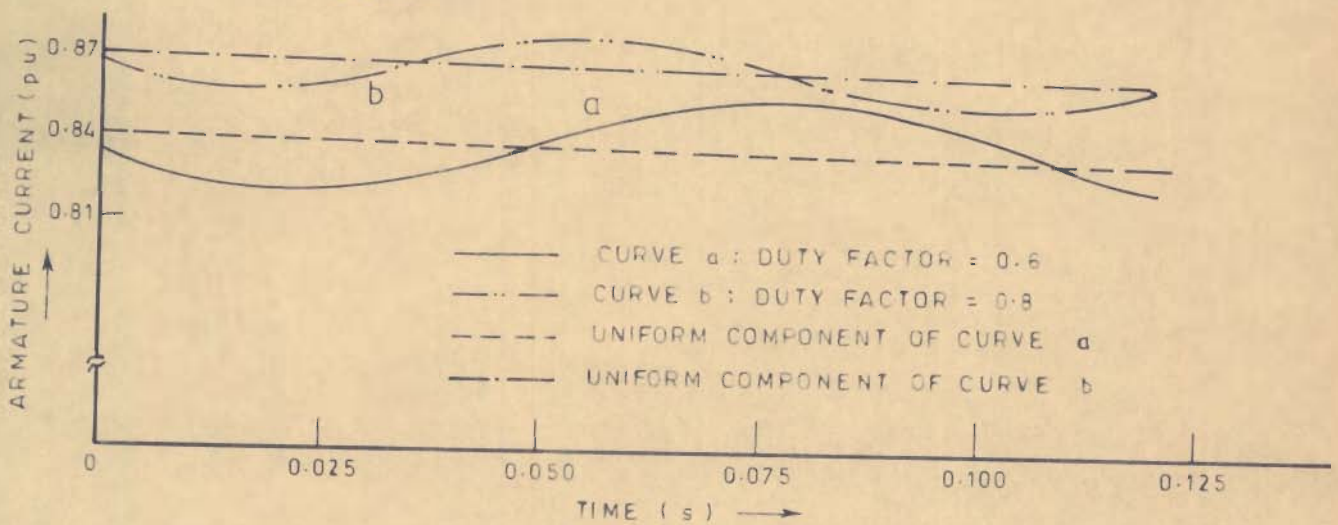
FIG. 4.10 _ VARIATION OF STEADY STATE ARMATURE CURRENT
AVERAGED OVER A CHOPPER CYCLE FOR DIFFERENT
DUTY FACTORS
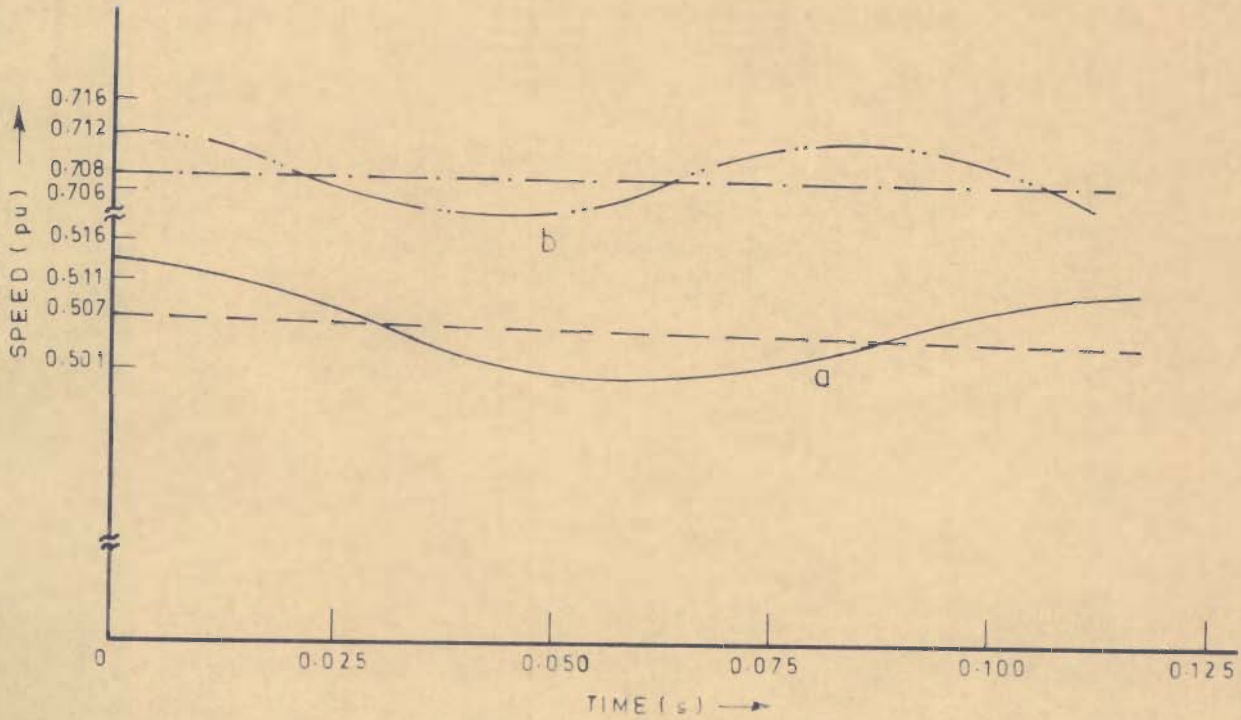
FIG. 4.11 _ VARIATION OF STEADY STATE SPEED AVERAGED
OVER A CHOPPER CYCLE FOR DIFFERENT DUTY
FACTORS
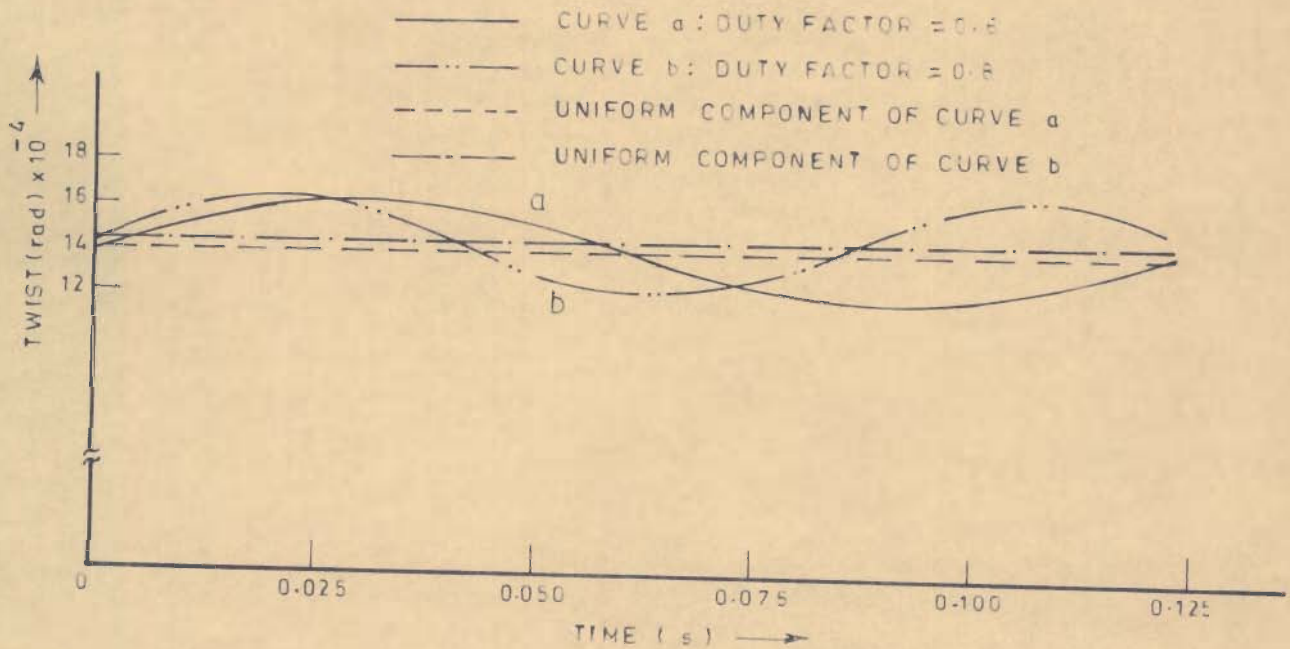
FIG. 4.12 _ VARIATION OF STEADY STATE TWIST
AVERAGED OVER A CHOPPER CYCLE FOR
DIFFERENT DUTY FACTORS

4.11.1 Effect of Chopper Duty Factor and Frequency

The effects of change of chopper duty factor and frequency on the performance have been studied and following observations made:

(a) As expected, an increase in the value of chopper duty factor increases the average values of armature current and speed as shown in Figs. 4.10, 4.11 .

(b) The amplitudes of pulsation in armature current and speed decrease appreciably with the increase in chopper duty factor as shown in Figs. 4.10, 4.11 .

(c) The amplitudes of pulsation of shaft twist as well as its average value are not much affected by change in chopper duty factor [Fig. 4.12].

(d) The average values of armature current and speed as well as their amplitudes of pulsation are not affected by change in chopper frequency.

TABLE 4.1 : Effect of Chopper Duty Factor on Steady State Performance

S. No.	duty factor	current		speed		twist	
		average value pu	pulsation %	average value pu	pulsation %	average value rad	pulsation %
1	0.6	0.842	2.24	0.507	1.15	14.07×10^{-2}	14.9
2	0.8	0.867	1.20	0.708	0.60	14.28×10^{-2}	15.1

The values of α_1 , α_2 , β_1 , β_2 , ω_{n1} , ω_{n2} (in rad/sec) and damping ratios ξ_1 , ξ_2 are as below:

$\alpha_1 = 12.57$, $\beta_1 = 7.87$, $\omega_{n1} = 14.83$, $\xi_1 = 0.847$

$\alpha_2 = 0.089$, $\beta_2 = 519.8$, $\omega_{n2} = 519.8$, $\xi_2 = 0.173 \times 10^{-3}$

The value of load torque pulsation frequency $= \omega_s = 53.1$ rad/sec.

4.12 PERFORMANCE UNDER RESONANCE CONDITION

The system, under certain specific operating conditions, exhibit peculiar performance as large peaks in armature current and speed are observed. Such a situation arises when the frequency of, at least, one of the two forcing functions of the system (applied voltage and the load torque) approaches the natural frequency of oscillation ω_{n2}. This phenomenon may be referred to as 'resonance'. The system performance under resonance condition has been studied and various curves are plotted to illustrate this situation.

The variation of armature current and speed at three different frequencies of load torque (viz., ω_s , ω_{n1} , ω_{n2}) have been plotted for two different chopper frequencies (200 Hz and ω_{n2}) as shown in Figs. 4.13-4.16 . As the value of ω_{n1}, for practical systems, is very small [Table 4.1], the performance at chopper frequency equal to ω_{n1} has not been studied. The variation of armature current and speed for above three frequencies of load torque are plotted for three subsequent chopper cycles keeping the value of chopper cycle fixed at 200 Hz as shown in Figs. 4.13,4.14 . It is observed that if the load torque frequency approaches ω_{n2}, large pulsations in armature current and speed are noticeable. These pulsations are comparatively small for $\omega_1 = \omega_s$ and $\omega_1 = \omega_{n1}$. Thus if the load torque frequency is equal to the natural frequency
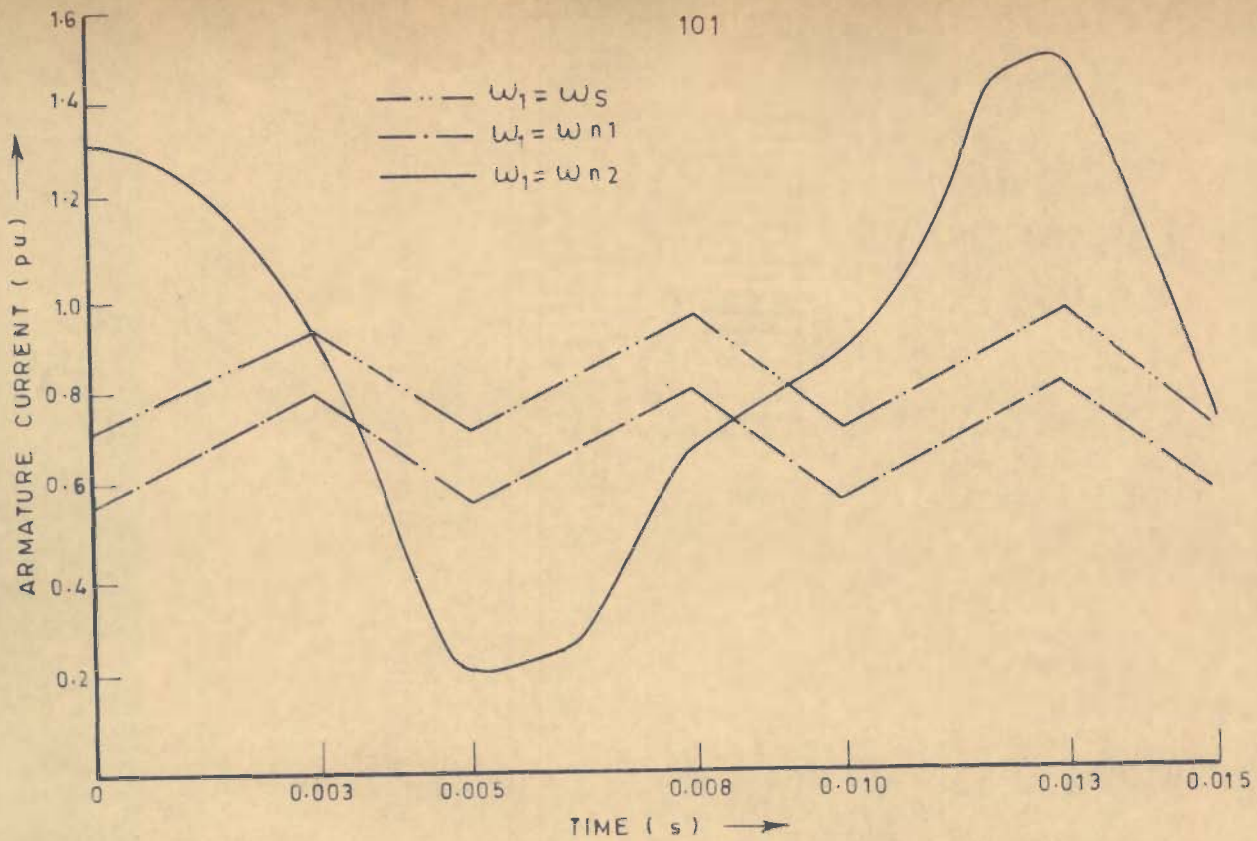
FIG. 4·13 _ VARIATION OF ARMATURE CURRENT AT
RESONANCE (CHOPPER FREQUENCY = 200 Hz)
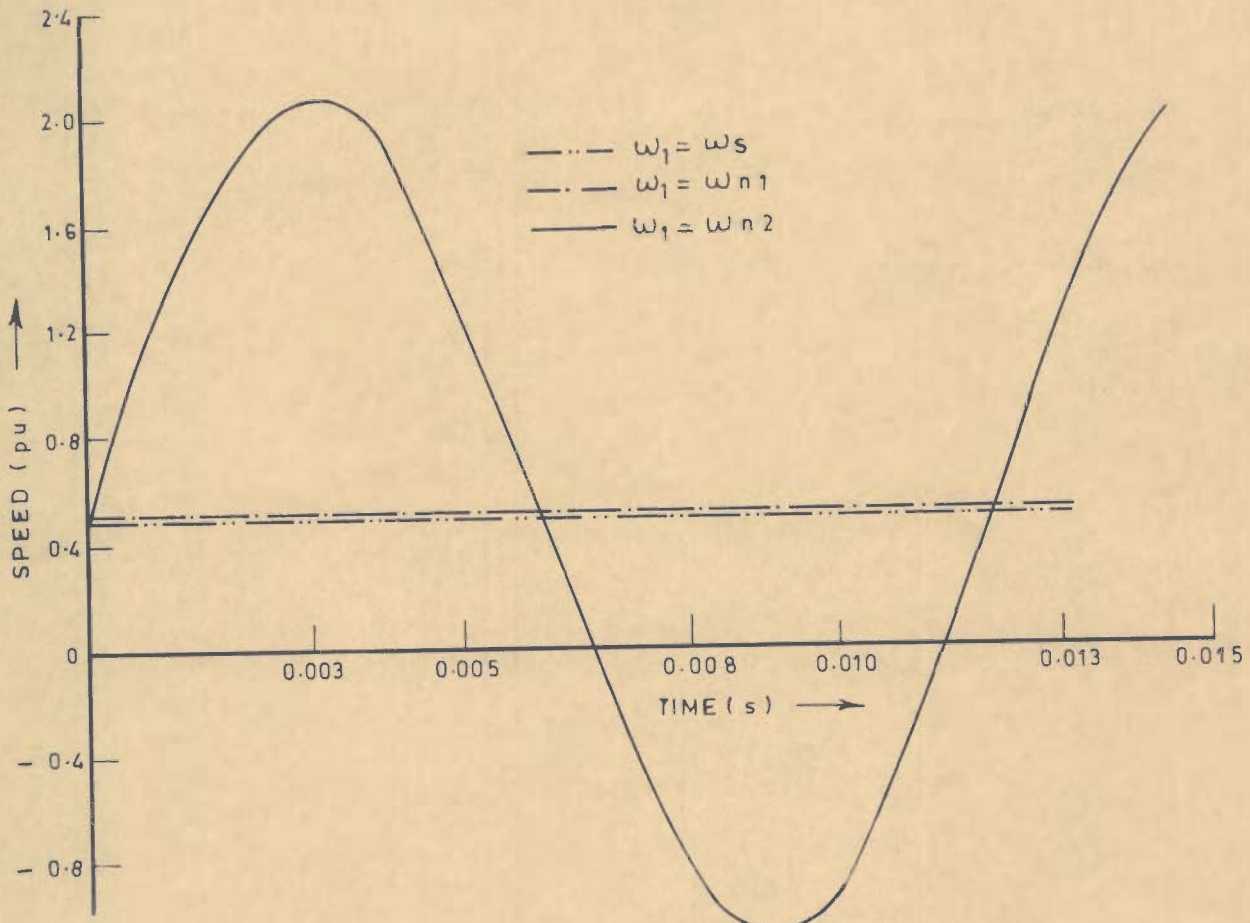
FIG. 4·14 _ VARIATION OF MOTOR SPEED AT RESONANCE
(CHOPPER FREQUENCY = 200 Hz)
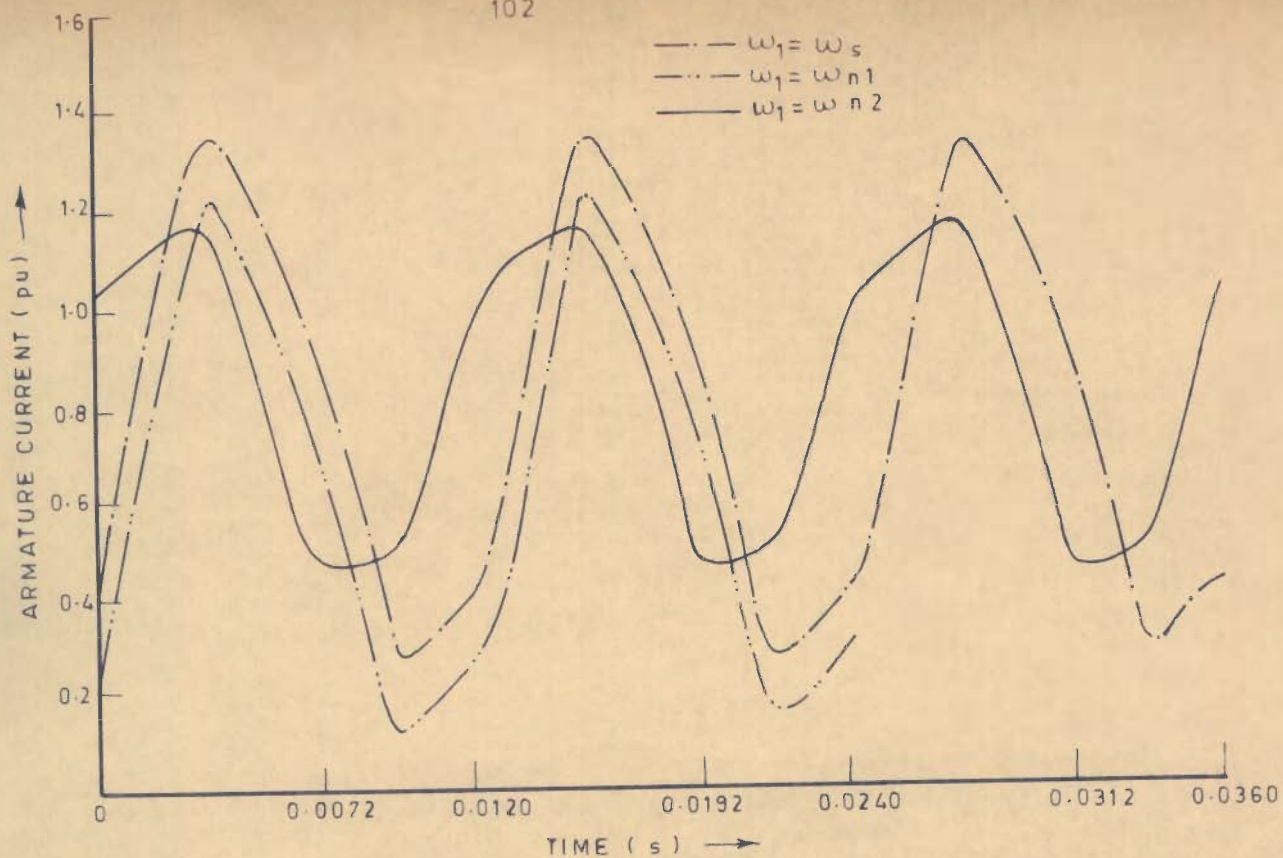
FIG. 4·15 _ VARIATION OF ARMATURE CURRENT AT RESONANCE
(CHOPPER FREQUENCY = ω_{n2} = 82.8 Hz)
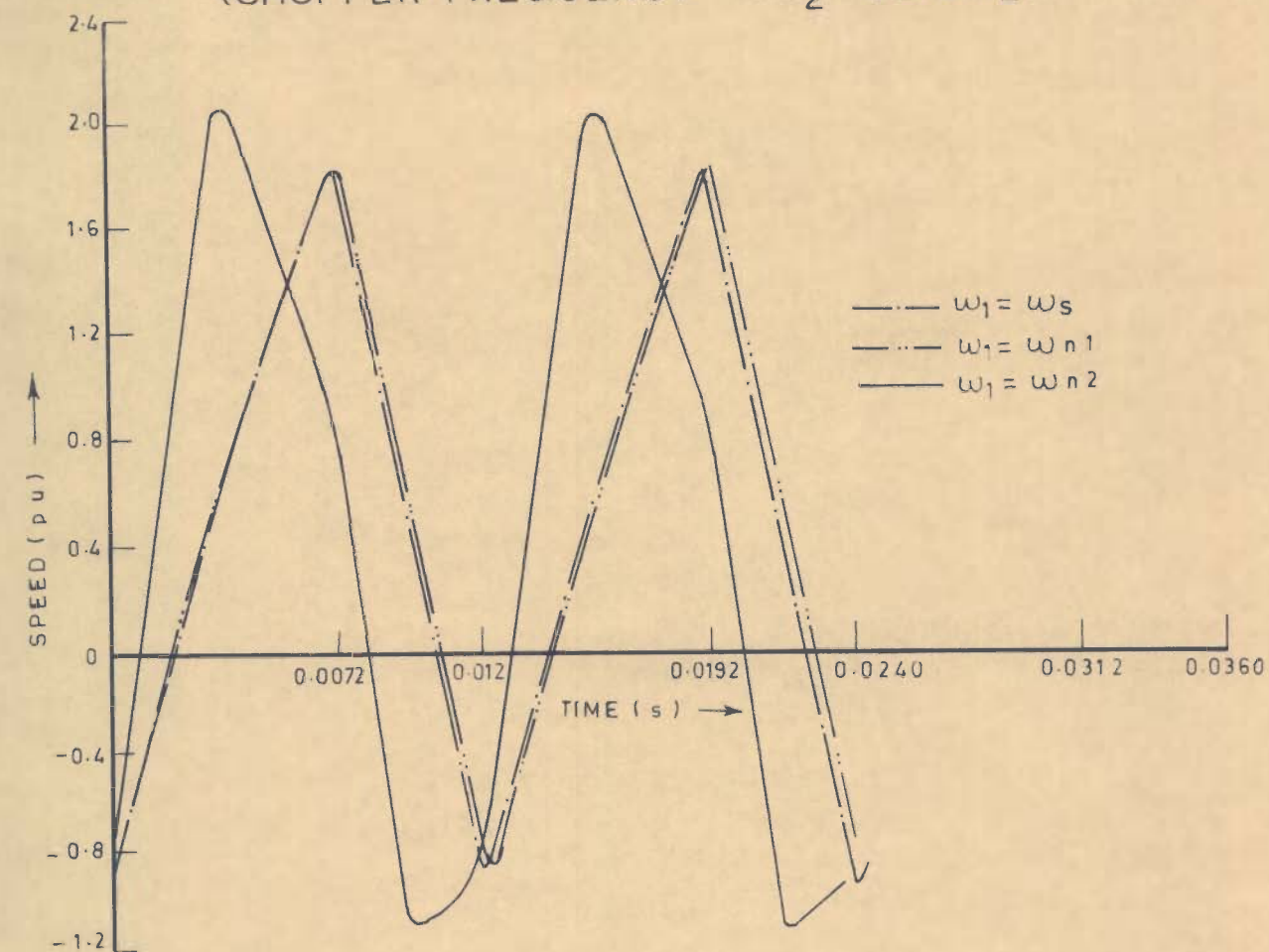
FIG. 4·16 _ VARIATION OF MOTOR SPEED AT RESONANCE
(CHOPPER FREQUENCY = ω_{n2} = 82.8 Hz)

of oscillation ω_{n2} , the system experiences resonance.

Figs. 4.15,4.16 show a plot of the variations of armature current and speed, for a different chopper frequency (equal to ω_{n2}) for above three frequencies of load torque. It is observed that large pulsations in current and speed are obtained for all these three values of frequency of load torque pulsation. This clearly shows that the resonance occurs when either the frequency of load torque pulsations or that of chopper becomes equal to ω_{n2}.

The following inferences can, therefore, be drawn:

(i)   The armature current and speed show very large pulsations, and large peak values when either the chopper frequency, or the load torque frequency; or both, approach the natural frequency of oscillation ω_{n2}. For practical d.c. drive system with an elastic shaft, under normal operating conditions, these oscillations, which are known as torsional oscillations and are due to non rigidity of shaft, are of high frequency and low amplitude. As such these oscillations are not noticeable. However, these oscillations attain large amplitudes at resonance resulting in abnormally large values of current and speed. It must be noted that resonance phenomenon is caused by a combination of factors. These factors are:

(a) an elastic mechanical link

(b) periodic forcing functions and

(c) the frequency of at least one of the forcing functions approaches the natural frequency of the system ω_{n2}.

The value of ω_{n2}, specially for low values of moment of inertia and high values of torsional stiffness, may be quite high and may be close to the normal operating frequency range of choppers. As such there is a strong possibility of resonance, even in systems with choppers operating in their usually normal frequency ranges.

(ii) Resonance can be avoided by suitably choosing the values of torsional stiffness (which itself depends upon length and diameter of shaft) and system moment of inertia such that the value of ω_{n2} is far away from the range of frequency at which the chopper is to be operated.

(iii) Care has also to be taken that ω_{n2} does not match the frequency of load torque pulsations ω_1. As the frequency of load torque is a system requirement, and not always the designer's choice, once again the only way to avoid resonance is a suitable selection of system parameters to avoid such values of ω_{n2}.

(iv) The value of β_1 depends mainly on the moment of inertia and armature circuit inductance. For practical systems β_1 is observed to be low and may even vanish for low values of inductance. It is observed that for the case under consideration, the value of α_1 is much greater than α_2 and β_1 is much lesser than β_2 [Table 4.1]. A high value of α_1 is measure of large damping ratio ξ_1 and, possibly, because of this reason resonance is not observed at $\omega_1 = \omega_{n1}$.

4.13 TRANSIENT STATE PERFORMANCE

The armature current, during transient period, consists of four time decaying components i_{t1} , i_{t2} , i_{t3} and i_{t4} ; in addition to those which appear under steady state, as given by eqn.(4.16). These components depend upon the input voltage and the load torque. The angular speed also has similar components [eqn.(4.24)].

The nature of switching-in transients of armature current, for the initial few chopper cycles, is shown in Fig.4.17(a). It is observed that the current rises rapidly and decays slowly during the duty and freewheeling intervals respectively. These variations are exponential in nature. The variation of armature current, averaged over a chopper cycle, is shown in Fig.4.17(b). As expected, the average current rises for first few chopper cycles and attains a peak value, which depends on the system parameters. Thereafter, it decays slowly till steady state is reached, when the average current becomes constant.

The rating of the main SCR of the chopper is determined by its peak instantaneous current, and the maximum average current passing through it. This maximum average current can be obtained from a plot of the current taken from supply in a chopper cycle [Fig.4.17(a)], the cycle in this case being chosen near the peak of the current variation shown in Fig.4.17(b).

The variation of average angular speed (average over a chopper cycle) is shown in Fig.4.18. In the analysis presented, as the motor is switched-in with considerable load on the shaft, the characteristic shows negative speed (dotted curve) for the
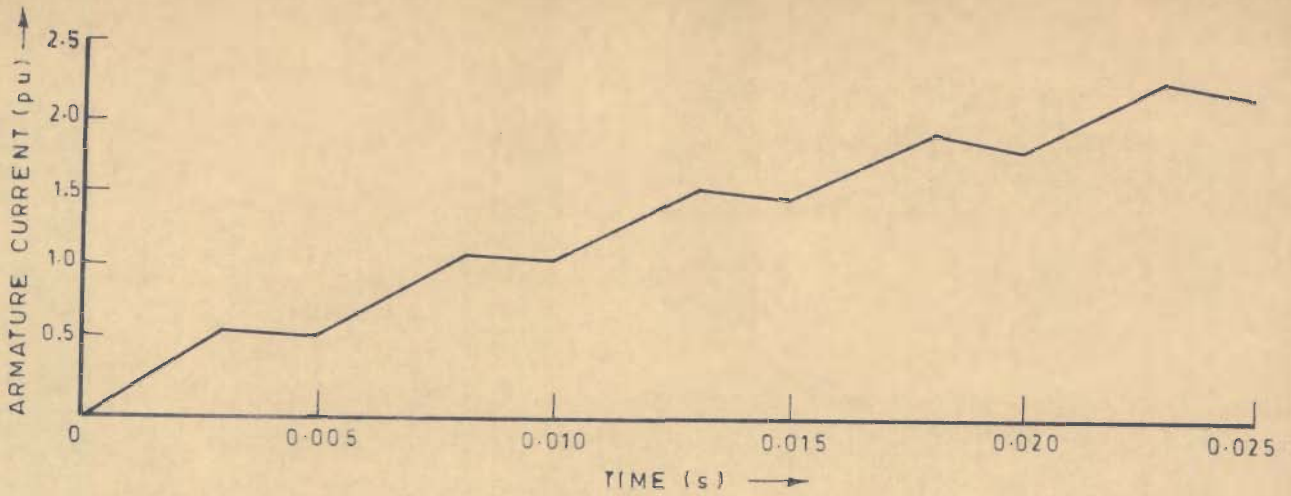
(a)_ SWITCHING-IN TRANSIENT ARMATURE CURRENT
FOR FIRST FEW CHOPPER CYCLES
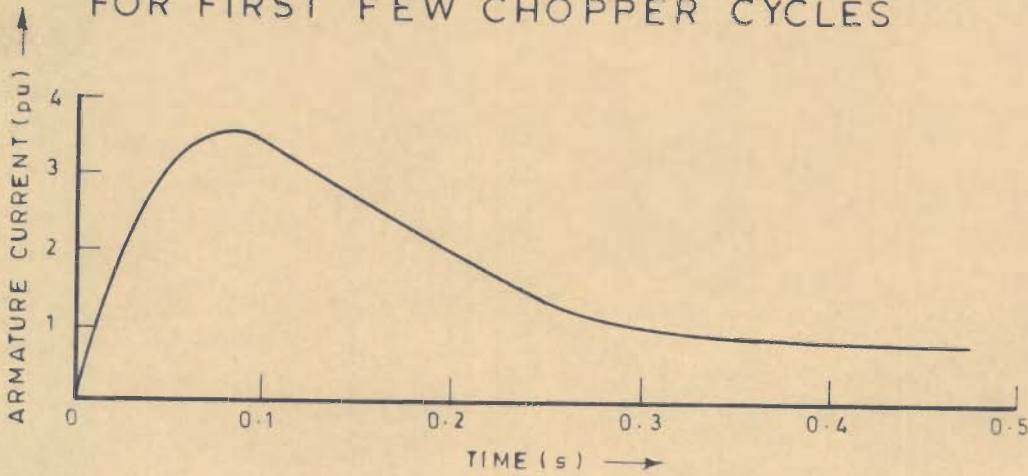
(b)_ VARIATION OF SWITCHING-IN ARMATURE CURRENT
AVERAGED OVER A CHOPPER CYCLE
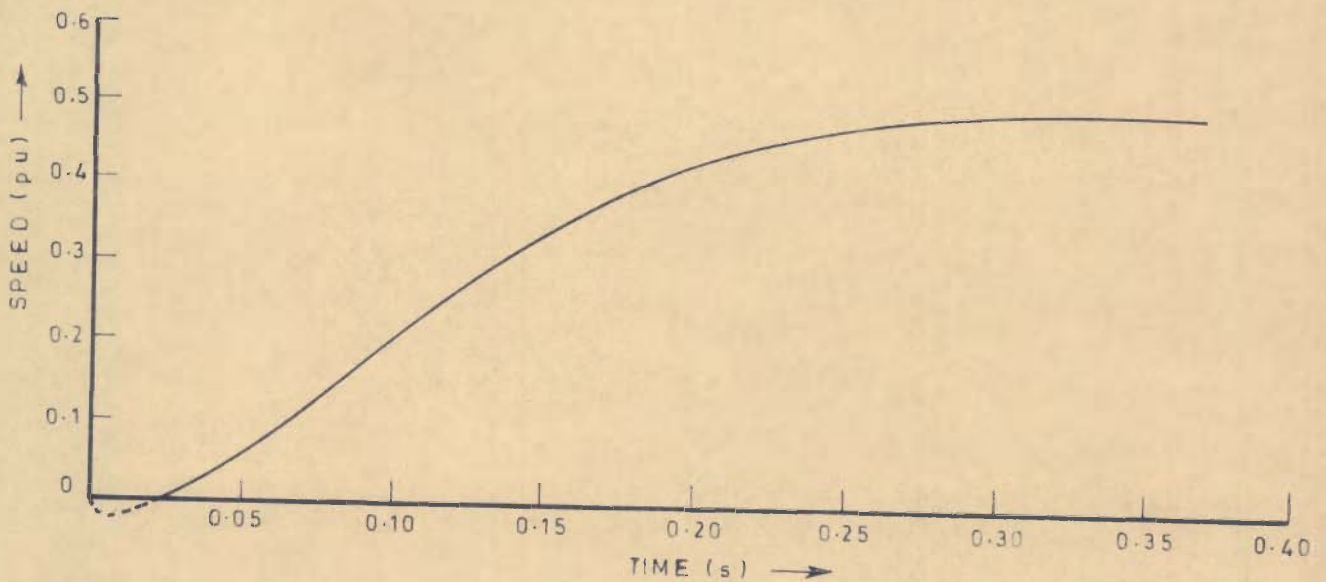
FIG. 4.17

FIG. 4.18 _ VARIATION OF TRANSIENT SPEED AVERAGED
OVER A CHOPPER CYCLE

initial few chopper cycles. The motor actually starts as soon as the motor developed torque overcomes the load torque. Thereafter the motor accelerates and finally the speed becomes constant as steady state is attained.

4.14   MECHANICAL CONSIDERATIONS

The non-rigidity of shaft produces angular twist, $(\theta_1 - \theta_2)$. The value of twist determines the shear stress in the shaft in accordance with the relation:

$$Q = G(\theta_1 - \theta_2)d/2l$$

The mechanical failure of the shaft may occur in the following ways:

(i) Failure of shaft due to excessive shear stress produced by large values of average twist under normal operating conditions. It may also fail due to the large values of instantaneous twist under resonance condition. The failure in the latter case is termed as dynamic failure.

(ii) Shaft may experience 'fatigue' due to the variations in the values of twist. The failure due to fatigue depends upon the magnitude and frequency of alternating components of twist.

For the case under consideration, Figs. 4.6,4.7 show the variations of twist during a chopper cycle for a uniform load torque and pulsating load torque respectively. The variations of average values of twist (average over a chopper cycle) at steady state are shown in Fig.4.12. Since the value of twist depends on angular positions θ_1 and θ_2, the twist also varies with time

and has two alternating components, one at load torque frequency and the other at chopper frequency [eqns.(4.20 - 4.23)].These components of twist may cause failure of shaft in manners described above.

For the case under study, shear stress under normal operating condition is 20.6 Kg/cm^2 (twist = 16.16 x 10^{-4} rad) while under resonance condition its value is 8172 Kg/cm^2 (twist = 0.641 rad). The shear stress under this condition is much higher than the ultimate stress which is 3700-4500 Kg/cm^2 (Indian Standards Code:1570-1961 for C-14 steel). As such the shaft may fail under resonance condition.

4.15 CONCLUSIONS

The performance of a chopper controlled separately excited d.c. motor driving a mechanical load with a periodically varying load torque and elastic mechanical link is obtained using a non-iterative technique of analysis. Closed-form solutions for armature current and speed are obtained which give a good insight into the transient as well as steady state performance. Such analyses are useful for proper design of system elements. Study of a typical performance, as obtained by the above analysis leads to the following inferences:

(a) The steady-state armature current and speed contain alternating components superposed on a non-varying component. The frequencies of these components depend upon (i) the frequency of the alternating components of the load torque (ii) the chopper frequency, and (iii) β_1 and β_2

which depend upon system parameters like armature resistance and inductance, moment of inertia, damping and torsional stiffness of shaft.

The amplitude of these alternating components depends upon, amongst other parameters, the amplitude of the pulsating component of the load torque and the chopper duty factor. The pulsations of current and speed of frequency ω_1 can be reduced by increasing the moment of inertia of the rotating parts of the system.

(b) The system experiences torsional oscillations of frequency ω_{n2} which depends upon torsional stiffness and moment of inertia of the system. The amplitude of these oscillations under normal system conditions is small.

(c) The system experiences resonance characterized by large pulsations in current and speed when the frequency of any of the components of load torque, or that of chopper, or both approach the natural frequency of torsional oscillations of the system. Under such conditions the amplitudes of pulsation of current and speed as also their instantaneous values may become abnormally large. It is observed that even at the usual values of chopper frequencies, resonance may be experienced. Under resonance condition, the twist in the shaft will be quite large and the mechanical failure of shaft may occur due to excessive shear stress.

While designing a system, the load torque must be analysed to ensure that natural frequency of the system does not match any of the component frequencies. Resonance can be avoided by properly choosing the value of torsional stiffness and system moment of inertia.

CHAPTER-5

ANALYSIS AND DESIGN OF PULSEWIDTH-MODULATED CLOSED-LOOP D.C. MOTOR DRIVE WITH ELASTIC COUPLING

5.1 INTRODUCTION

In a variety of industrial applications using a d.c. motor drive, a desirable performance feature is to obtain a regulated speed of drive during its operation. Automatic regulating schemes with closed-loop d.c. motor drives are being frequently employed for obtaining the desired control of speed. Such schemes comprise of a d.c. motor, a controller with a comparator, and a feedback system. By introducing a feedback path from the output to the controller, any deviations in output from the desired level can be included in the decision making process by the controller. The controller may be as simple as a linear amplifier or as complicated as a full size computer. The use of a linear amplifier in closed-loop drives is not preferred as it involves excessive dissipation of power and results in an inefficient operation.

In order to avoid the power dissipation in the linear amplifiers, they have been replaced by the 'Switching Amplifiers'. Such amplifiers can be operated in a switched mode where the thyristors are turned on and off like a switch. When the amplifier is turned on, voltage across its thyristor is negligible; and when it is turned off, this voltage is large, but the current is zero. In either case, the resulting power dissipation in the amplifier is small. Amplifiers operated in this mode are called

switching amplifiers. The switching can be performed in various ways. One simple method is to switch the amplifier at a constant frequency and vary the 'on' or 'off' periods of thyristor according to need. Such amplifiers are called 'Pulsewidth-Modulated Amplifiers'.

The method of pulsewidth-modulation (PWM) controls the average value of the amplitude of the modulated pulse wave signal by changing the width of the pulse. This method is essentially similar to the time ratio control (TRC) method of chopper control discussed for open loop drives in Chapters 3 and 4. For a given amplitude of the pulse given to the motor input, the width of the pulse is a function of the desired value of motor speed. In case of open loop drives, the pulsewidth is kept constant at a value determined by the desired speed of motor operation.

For closed loop d.c. drives, the method of pulsewidth modulation provides a pulsed input to the motor and controls the average voltage across the armature to maintain its speed at the desired level. This is achieved by a suitable control of the pulsewidth (or duty factor) with regard to the desired change in drive speed. As soon as the motor speed deviates from the set speed, the controller suitably changes the pulsewidth of the modulated wave to maintain the speed at the set level. Thus, unlike open loop drives, the pulsewidth in the case of closed loop drives is not constant but changes continuously with regard to the change in speed from the desired level.

The application of PWM technique for controlling the speed of closed loop d.c. drives has attracted the attention of

researchers in recent past. Maisel [36] has given the model of such a control scheme. Jacob Tal [54] has proposed the use of switching amplifiers for d.c. servo systems in order to reduce the power dissipation and has analysed the operation of PWM amplifiers for different modes of operation. Taft et al. [53] have analysed the operation of a d.c. position control system using PWM techniques and have discussed the advantages of employing a current loop around the amplifier. Unnikrishnan [58,59] has given a technique for maintaining constant average value of the output of a dc-dc chopper controlled converter and has studied the stability of such a system.

The work available in literature deals with the analysis of PWM controlled d.c. drives assuming the mechanical coupling between motor and the load to be perfectly rigid. In all practical systems, this link is always elastic. The degree of elasticity depends upon the size and material of the shaft. The load torque, in many applications, may not be constant but may have a periodic variation. This nature of load torque may be a characteristic of the driven mechanism or a consequence of some mechanical factors of drive system [section 1.1]. The influence of elasticity of shaft and periodic variation of load torque, on the performance of an open loop d.c. drive fed by a PWM power supply has been presented in Chapter-4. However no work appears to be available in literature wherein the effect of elasticity of shaft on the performance of a closed loop d.c. motor drive fed by a PWM power supply is investigated.

5.2 WORK PRESENTED

In this chapter, the analysis and design considerations of a closed-loop d.c. drive employing a separately excited d.c. motor coupled to the load through an elastic coupling and fed by a PWM power supply are presented. A mathematical model of the system is given and the transfer function is obtained. The influence of system parameters, like amplifier gain, torsional stiffness of shaft and armature time constant, on the stability of the system is studied using the D-partition technique. The effect of value of amplifier gain on speed and current pulsations, and steady state error in speed are discussed. The dependence of the value of amplifier gain required to give minimum settling time, on torsional stiffness is investigated. Conditions leading to abnormal operation like resonance are identified. The analysis includes the cases of constant load torque as well as a periodically varying load torque.

The system analysed, as shown in Fig.5.1, consists of three basic components: (i) the comparator (ii) the controller and (iii) the motor coupled to load. These are discussed below:

(i) The Comparator

The comparator has two input signals, one is the reference signal v_r which is proportional to the desired drive speed ω_d and the other is a feedback signal v_o obtained as tachogenerator output proportional to the actual speed of motor $\dot{\theta}_1$. The comparator compares these two signals and the difference, which is the error signal $(v_r - v_o)$, is obtained as its output.
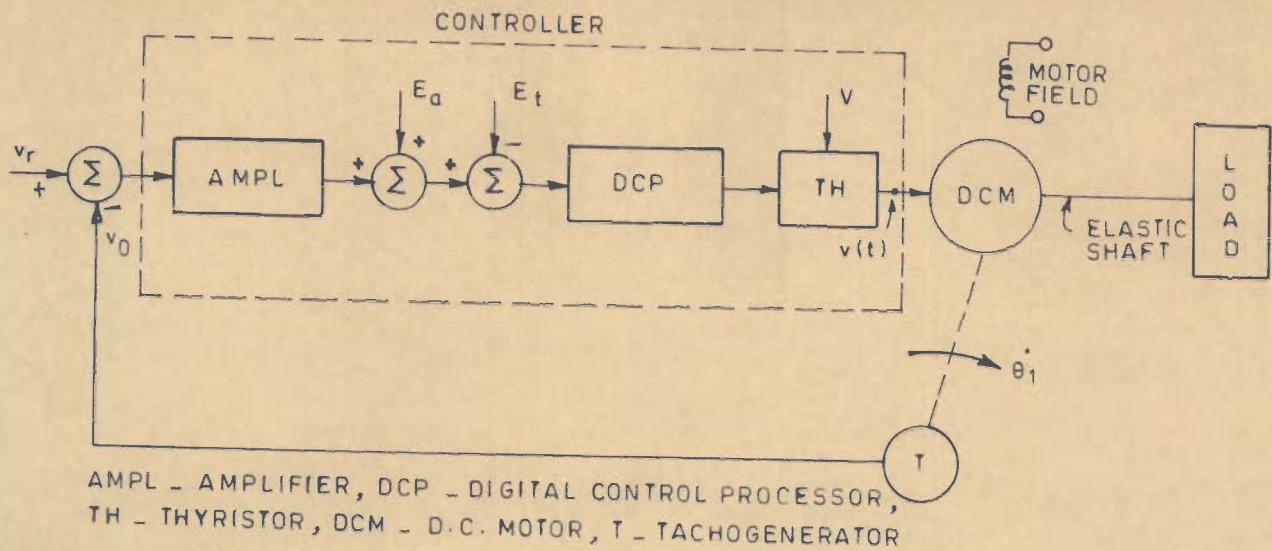
FIG. 5.1 _ SCHEMATIC DIAGRAM OF PWM D.C. MOTOR
DRIVE WITH AN ELASTIC COUPLING

(a) MIXING ERROR AND RAMP SIGNALS AND
COMPARING WITH THRESHOLD SIGNAL

(b) PULSE-WIDTH MODULATED OUTPUT OF
CONTROLLER
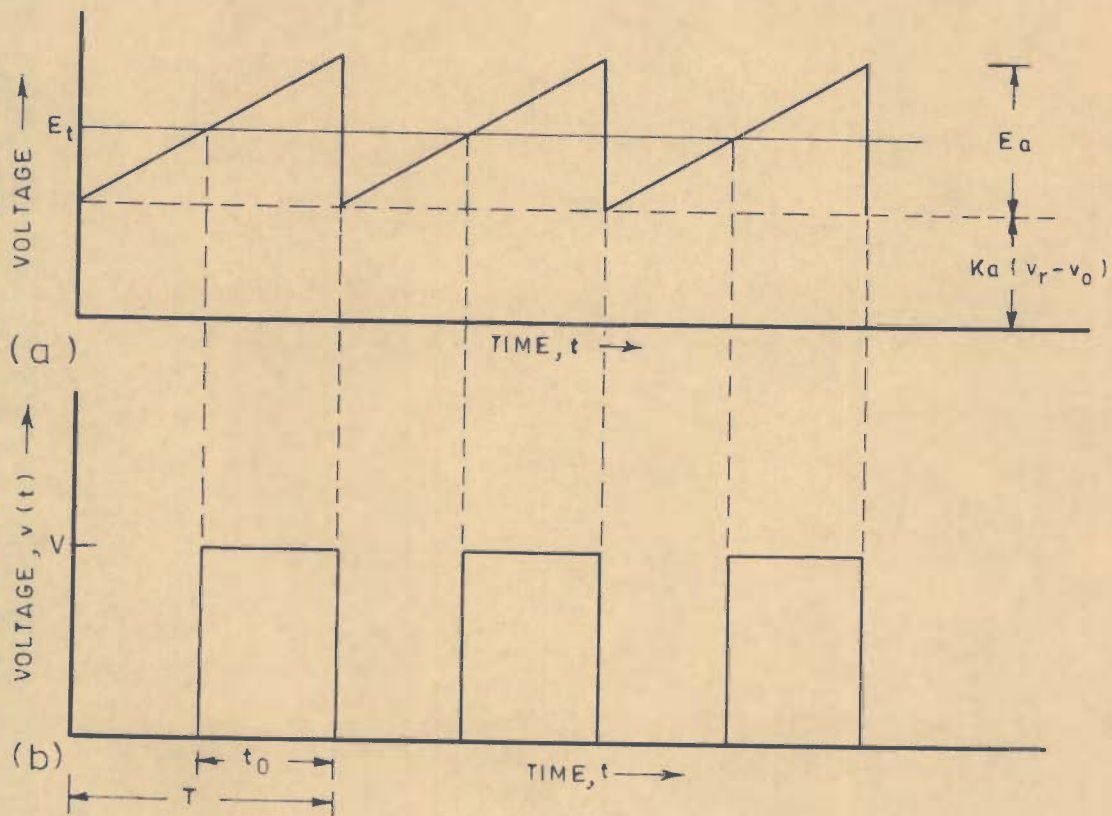
FIG. 5.2

(ii) The Controller

The error signal obtained from comparator is the input to the controller. Here the error signal is amplified through an amplifier of gain K_a and a ramp signal of amplitude E_a is added to it, as shown in Fig. 5.2(a). The combined signal is compared with a threshold level E_t and the resultant signal activitates the thyristor through a digital control processor to give a pulsed output. Thus the controller modulates a d.c. power source voltage V to give a pulsed output voltage as shown in Fig. 5.2(b), the duty factor of which is a function of error signal given to its input. Any departure of speed from the required level changes the error signal which controls the duty factor α and hence the average voltage (αV) applied to motor. Thus, the desired speed level is maintained.

The duty factor $\alpha(t)$ which is a function of error signal can be expressed as:

$$\alpha(t) = 1 - \frac{E_t}{E_a} + \frac{K_a}{E_a}(v_r - v_o) \qquad (5.1)$$

(iii) The Motor and the Load

The drive system analysed consists of a separately excited d.c. motor with an elastic shaft connecting the motor to the load. The analysis takes into account a periodic variation of load torque which consists of a constant component T_{Lo} superposed by a pulsating component T_{L1} as shown in Fig.2.2(b). The frequency of pulsating component of load torque ω_1 is taken equal to the set speed (expressed in rad/s) implying that one cycle of load torque

is completed in one revolution of motor shaft. Other frequencies
of load torque pulsations in multiples of motor shaft speed can
also be easily accounted for in a similar manner.

For the analysis of the above system, a mathematical
model is given. In this model the moments of inertia of the motor
and the load as also the damping factors are considered separately.
A block diagram of the system is obtained and its transfer func-
tion derived. The 'D-composition technique' has been used to
obtain regions in parameter plane which give sets of values of
system parameters (torsional stiffness, amplifier gain and arma-
ture time constant) for stable operation. In many drive appli-
cations, a desirable performance feature may be to bring back
the drive speed to its required level as fast as possible, after
a transient disturbance or change. The measure of the recovery
time is known as 'settling time'. The analysis includes the
consideration of settling time and the value of amplifier gain
that gives minimum settling time is determined. This value of
amplifier gain is observed to be significantly dependent upon
the degree of elasticity of shaft. The system equations are
expressed in state model form and solved using numerical techni-
que to obtain the response, of a system so designed, in transient
as well as steady state conditions. The analysis is illustrated
by an example and some inferences have been drawn.

5.3 PERFORMANCE EQUATIONS AND TRANSFER FUNCTION

The equations governing the performance of system shown
in Fig.5.1 can be written as:

$$V_\alpha(t) = L \frac{di}{dt} + R\,i + K_m\,\dot{\theta}_1 \tag{5.2}$$

$$K_e\,i = J_1\,\ddot{\theta}_1 + B_1\,\dot{\theta}_1 + C(\theta_1 - \theta_2) \tag{5.3}$$

$$-T_L = J_2\,\ddot{\theta}_2 + B_2\,\dot{\theta}_2 + C(\theta_2 - \theta_1) \tag{5.4}$$

$$T_L = T_{Lo} + T_{L1}\,\sin(\omega_1 t - \emptyset) \tag{5.5}$$

$$v_r - v_o = V_\alpha(t)/K_c \tag{5.6}$$

where $\quad v_o = K_t\,\dot{\theta}_1$

The eqns. (5.2)-(5.5) are same as eqns. (2.1)-(2.4). Taking the Laplace transform of above equations and solving,

$$I(s)/[V_\alpha(s) - K_m\,\dot{\theta}_1(s)] = 1/R(1 + s\,\tau_a) \tag{5.7}$$

$$\theta_1(s)/[K_e\,I(s)/C + \theta_2(s)] = 1/[1 + sB_1(1 + s\,\tau_{m1})/C] \tag{5.8}$$

$$\theta_2(s)/[C\,\theta_1(s) - T_L(s)] = 1/C[1 + s\,B_2(1 + s\,\tau_{m2})/C] \tag{5.9}$$

$$V_o(s) = K_t\,\dot{\theta}_1(s) \tag{5.10}$$

$$V_r(s) - V_o(s) = V_\alpha(s)/K_c \tag{5.11}$$

Using equations (5.7 - 5.11), the block diagram of the system can be obtained as shown in Fig. 5.3. The open loop transfer function G(s) can be obtained as:

$$G(s) = \frac{\dot{\theta}_1(s)}{V_r(s)} = \frac{(a_3 s^2 + a_4 s + a_5)K_e\,K_c}{A_1 s^4 + A_2 s^3 + A_3 s^2 + A_4 s + A_5} \tag{5.12}$$

The closed loop transfer function is

$$\frac{G(s)}{1 + K_t\,G(s)} = \frac{(a_3 s^2 + a_4 s + a_5)K_e\,K_c}{A_1 s^4 + A_2 s^3 + A_3 s^2 + A_4 s + A_5 + K(a_3 s^2 + a_4 s + a_5)} \tag{5.13}$$
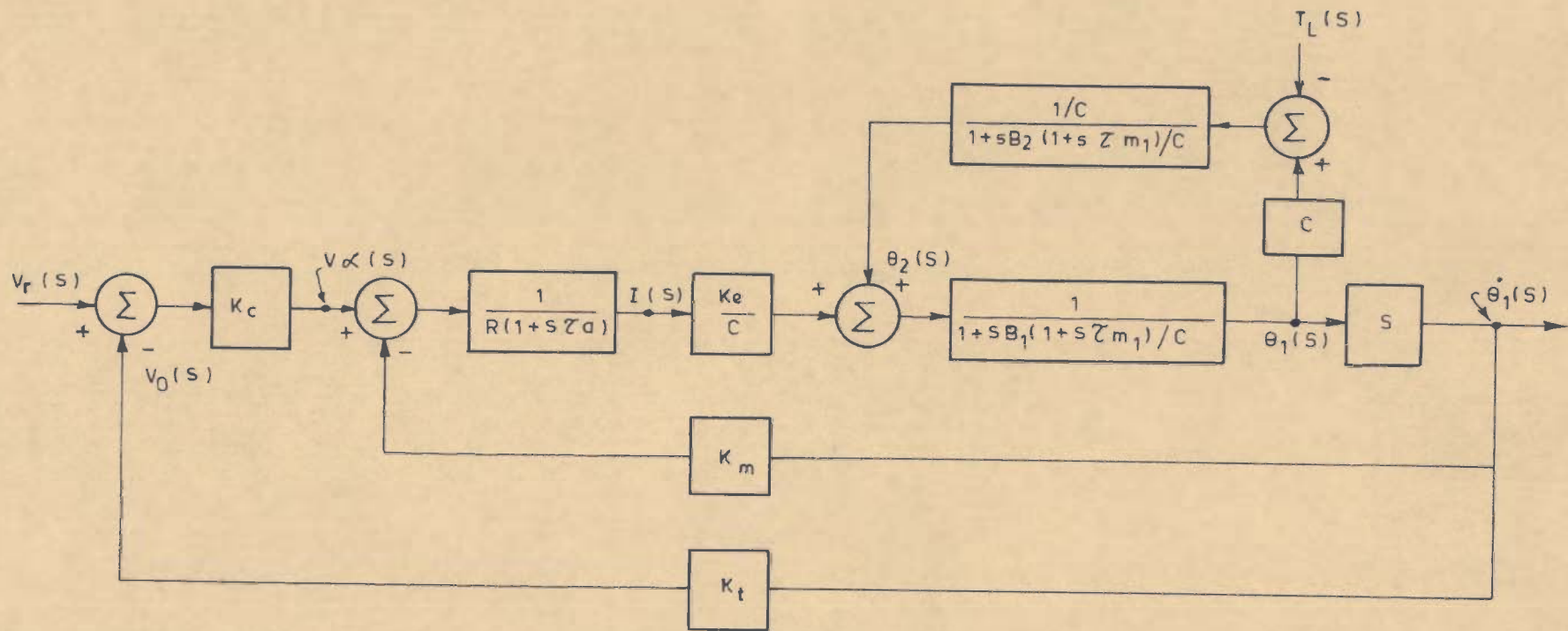
FIG. 5.3 _ BLOCK DIAGRAM OF THE CLOSED - LOOP DRIVE
SHOWN IN FIG. 5.1

From eqn. (5.13), the characteristic equation of the closed loop system can be obtained as:

$$A_1 \, s^4 + A_2 \, s^3 + A_3 \, s^2 + A_4 \, s + A_5 + K(a_3 \, s^2 + a_4 \, s^- + a_5) = 0$$

(5.14)

where

$$A_1 = \tau_a \, B_1 \, B_2 \, \tau_{m1} \, \tau_{m2}$$

$$A_2 = B_1 \, B_2 \, \tau_{m1} \, \tau_{m2} + \tau_a \, B_1 \, B_2(\tau_{m1} + \tau_{m2})$$

$$A_3 = \tau_a \, B_1 \, B_2 + B_1 \, B_2(\tau_{m1} + \tau_{m2}) + C \, \tau_a(B_1 \, \tau_{m1} + B_2 \, \tau_{m2})$$
$$\qquad + K_e \, K_m \, B_2 \, \tau_{m2}/R$$

$$A_4 = B_1 \, B_2 + C \, \tau_a(B_1 + B_2) + C(B_1 \, \tau_{m1} + B_2 \, \tau_{m2})$$
$$\qquad + K_e \, K_m \, B_2/R$$

$$A_5 = C(B_1 + B_2 + K_e \, K_m/R)$$

$$a_3 = B_2 \, \tau_{m2}/R \, , \quad a_4 = B_2/R \, , \quad a_5 = C/R \, , \quad \tau_{m1} = J_1/B_1 \, ,$$

$$\tau_{m2} = J_2/B_2 \, , \quad K = K_e \, K_c \, K_t \, , \quad K_c = K_a \, V/E_a$$

5.4 THE D-COMPOSITION TECHNIQUE

The effect of variation of system parameters on dynamic stability of system can be studied using the D-composition technique [40,50]. The procedure is briefly explained below:

5.4.1 Linear Case

If α and β are chosen as the parameters of interest appearing linearly in the characteristic equation whose effect on dynamic stability of system is to be studied, eqn. (5.14) can be expressed in terms of α and β as:

$$\alpha \, f_1(s) + \beta \, f_2(s) + f_3(s) = 0 \qquad\qquad (5.15)$$

where $f_1(s)$, $f_2(s)$ and $f_3(s)$ are polynomials in s with constant coefficients. Substituting $s = j\omega$ in eqn. (5.15), and equating the real and imaginary parts on the left hand side to zero, two equations are obtained as:

$$\left.\begin{array}{l} \alpha \, f_{11}(\omega) + \beta \, f_{21}(\omega) + f_{31}(\omega) = 0 \\[2mm] \alpha \, f_{12}(\omega) + \beta \, f_{22}(\omega) + f_{32}(\omega) = 0 \end{array}\right\} \qquad (5.16)$$

where $f_{11}(\omega),\ldots,f_{32}(\omega)$ are polynomials in ω with constant coefficients.

Solving eqns. (5.16), the values of α and β in terms of ω can be obtained as:

$$\left.\begin{array}{l} \alpha = [\, f_{32}(\omega) \, f_{21}(\omega) - f_{31}(\omega) \, f_{22}(\omega)\,]/\Delta_1 \\[2mm] \text{and } \beta = [\, f_{12}(\omega) \, f_{31}(\omega) - f_{11}(\omega) \, f_{32}(\omega)\,]/\Delta_1 \end{array}\right\} \qquad (5.17)$$

where $\Delta_1 = f_{11}(\omega) \, f_{22}(\omega) - f_{12}(\omega) \, f_{21}(\omega)$

The values of α and β are functions of ω as shown in eqn. (5.17). Varying the value of ω from zero to infinity, a pair of values of α and β can be obtained for each value of ω. These values of α and β, varying ω from zero to infinity, can be plotted in $(\alpha-\beta)$ plane. A number of points thus plotted can be joined by a smooth curve. A boundary obtained from such a curve is known as the D-partition boundary. Usually eqns. (5.16) cease to be linearly independent for $\omega = 0$ and $\omega = \infty$. Hence the D-partition boundary as plotted above, is supplemented by 'Special Lines' whose equations are obtained by substituting

$\omega = 0$ and $\omega = \infty$ in eqn.(5.15). The D-partition boundary and the special lines are hatched to determine the values of α and β which give most stable operation of the system. The hatching rule, as suggested by Neimark [40], is followed in the work presented in this chapter. The hatching procedure is as below:

For positive values of Δ_1, the left hand side of the D-partition boundary is hatched; and when Δ_1 is negative, the right hand side of the boundary is hatched. To cover the entire region of s plane, the D-partition boundary should actually be plotted for values of ω varying from minus infinity to plus infinity. To take this into account, the D-partition boundary is plotted varying ω from zero to infinity and hatched twice on the same side. The special lines are hatched in a manner such that, near the point of intersection of the special line and the D-partition curve, the hatched side of the special line faces the hatched side of the D-partition curve. Further on, the hatching of the special line remains unchanged.

Determination of the most stable region in $(\alpha - \beta)$ plane:

The D-partition curve and the special lines divide the entire $(\alpha - \beta)$ plane into a number of regions. To determine the most stable region; the number of roots of the system characteristics equation located on the left hand side of s plane, for each region in $\alpha - \beta$ plane, is determined in the following manner:

The number of roots on the left hand side of s plane corresponding to any one of the regions of $(\alpha - \beta)$ plane is assumed an arbitrary number, say n. Now, on moving from a

hatched to an unhatched side of the D-partition boundary in
(α- β) plane, one root is lost on the left hand side of s plane.
Similarly for the boundary hatched twice, two roots are lost on
the left hand side of s plane on moving from a hatched to an
unhatched side. Following this procedure, the number of roots
present on the left hand side of s plane for each region of
(α- β) plane is determined. The region having maximum number of
roots is marked as the most stable region. However, this method
determines the relative stability and the most stable region
obtained indicates the probable region of stability of the system.
As such the selected values of α and β, obtained from the most
stable region, are substituted in the system characteristics
equation and the system stability is verified by known methods
of determining the stability.

5.4.2 Non-Linear Case

In some cases, the parameters of interest, α and β may
not occur linearly in the characteristic equation. In such cases,
eqn. (5.15) may modify to:

$$\alpha \, f_1(s) + \beta \, f_2(s) + f_3(s) + \alpha \, \beta \, f_4(s) = 0$$

The D-partition boundary, for this case, can also be
obtained following the above procedure. In this case two
D-partition boundaries, instead of one boundary as for linear
case, will be obtained. The two boundaries are properly hatched
and the most stable region is determined in a way similar to
that for the linear case.

5.5 TYPICAL CASE STUDY

The specifications of the system studied, as an example, are:

inductance of armature including choke = 0.16 H

threshold signal voltage, E_a = 2.0 V

amplitude of ramp signal, E_t = 5.0 V

The values of other system parameters are same as given in section 2.7. The data for numerical technique [11] used to obtain system response in time domain are as below:

initial step size = 0.1

maximum absolute allowable single step error = 10^{-4}

minimum absolute allowable single step error = 10^{-7}

maximum allowable step size = 0.1

minimum allowable step size = 10^{-6}

reduction factor for step size = 0.5

starting values of dependent variables = zero

starting value of time = zero s

printing time interval = 0.005 s

5.6 EFFECT OF VARIATION OF SYSTEM PARAMETERS ON DYNAMIC STABILITY

The D-partition technique can be used for studying the effect of variation of system parameters, taken only two at a time. In the present case there are three important parameters of interest; C, τ_a and K. The study aims at determining suitable values of gain K and armature time constant τ_a for a known value of torsional stiffness C. Therefore, the dynamic stability of

the system specified in section 5.5 has been studied for variations in these parameters in the following two combinations:

(i) τ_a, K varied ; C kept constant.

(ii) C , K varied ; τ_a kept constant.

5.6.1 Variation of Armature time constant τ_a and gain K

In this case the parameters of interest α,β selected for excursion are armature time constant and gain K. Eqn.(5.14) can be written as:

$$\tau_a(K_1\ s^4 + K_2\ s^3 + K_3\ s^2 + K_4\ s) + K(a_3\ s^2 + a_4\ s + a_5)$$
$$+ (K_1\ s^3 + K_5\ s^2 + K_6\ s + A_5) = 0 \qquad\qquad (5.18)$$

where

$$K_1 = B_1\ B_2\ \tau_{m1}\ \tau_{m2}$$

$$K_2 = B_1\ B_2(\tau_{m1} + \tau_{m2})$$

$$K_3 = B_1\ B_2 + C(B_1\ \tau_{m1} + B_2\ \tau_{m2})$$

$$K_4 = C(B_1 + B_2)$$

$$K_5 = B_1\ B_2(\tau_{m1} + \tau_{m2}) + K_e\ K_m\ B_2\ \tau_{m2}/R$$

$$K_6 = B_1\ B_2 + C(B_1\ \tau_{m1} + B_2\ \tau_{m2}) + K_e\ K_m\ B_2/R$$

Substituting s = jω in eqn.(5.18) and solving for τ_a and K,

$$\tau_a = (P_1\ Q_2 - P_2\ Q_1)/\Delta_1$$

and K $= (Q_1\ S_2 - Q_2\ S_1)/\Delta_1$

where $P_1 = a_5 - a_3\ \omega^2$, $P_2 = a_4\ \omega$

$\qquad\qquad Q_1 = A_5 - K_5\ \omega^2$, $Q_2 = K_6\ \omega - K_1\ \omega^3$

$$S_1 = K_1 \omega^4 - K_3 \omega^2 \quad , \quad S_2 = K_4 \omega - K_2 \omega^3$$

and $\Delta_1 = S_1 P_2 - S_2 P_1$

The D-partition boundary in the $(\tau_a - K)$ plane is shown in Fig.5.4(a). Following the hatching rules discussed in section 5.4, the region of stability is determined. The entire $(\tau_a - K)$ plane is divided into regions marked $R_1 \ldots R_8$ and the number within parenthesis denotes the relative number of roots present in left half of s-plane. The most stable regions are R_1 and R_3 which correspond to the maximum number of roots (n). As the region R_3 pertains to negative values of armature time constant, it is not a feasible region. The most stable region, therefore, is region R_1. This reveals that any combination of positive values of time constant τ_a and gain K will lead to stable operation. From the consideration of desirability of continuous mode of conduction, a large value of τ_a can be selected. However, a large value of inductance makes the system response sluggish. As such, a suitable value of τ_a should be chosen which gives a continuous conduction of armature current without making the system response much sluggish. For the case under study, a value of armature time constant equal to 0.04 s is selected.

5.6.2 Variation of Torsional Stiffness C and gain K

In this case the parameters of interest α and β are the torsional stiffness C and gain K. Eqn.(5.14) can be written as:

$$C(K_7 s^2 + K_8 s + K_9) + K(a_3 s^2 + a_4 s) + CK(K_{10}) + (A_1 s^4 + A_2 s^3 + K_{11} s^2 + K_{12} s) = 0 \tag{5.19}$$
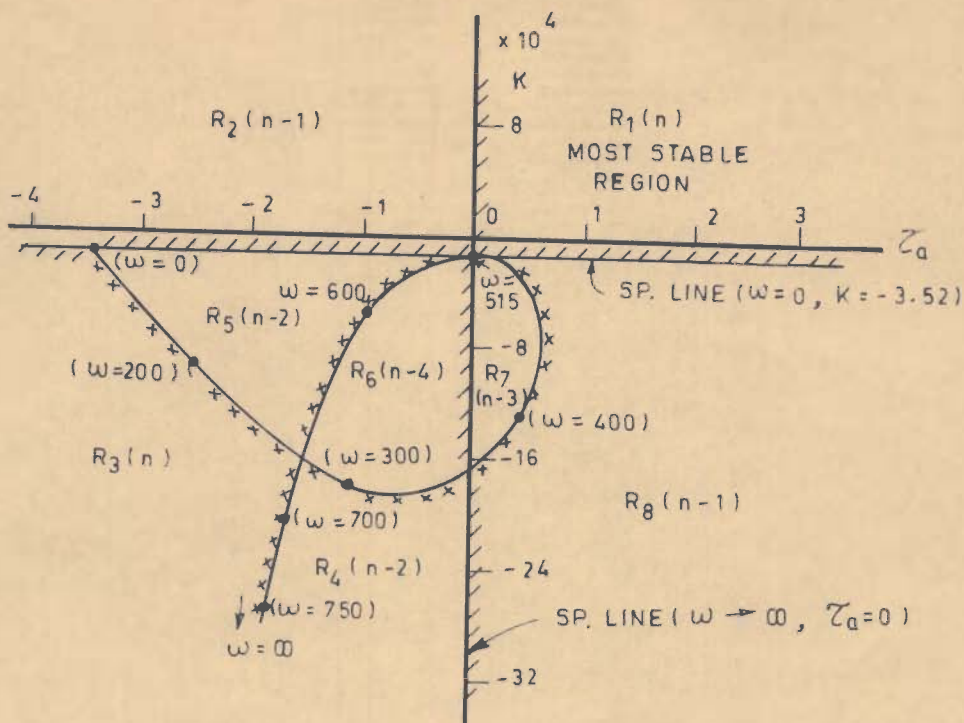
FIG. 5.4(a) – D–PARTITION BOUNDARY WITH RESPECT
TO ARMATURE TIME CONSTANT AND GAIN
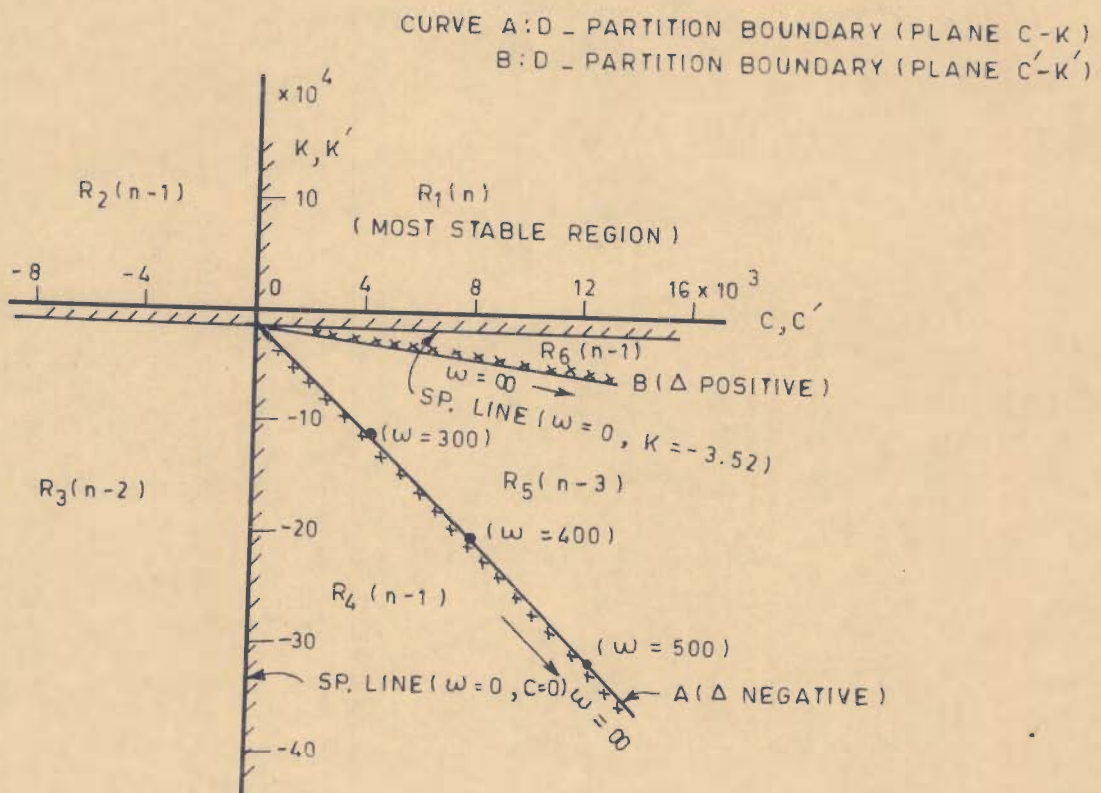
FIG. 5.4(b) – D–PARTITION BOUNDARIES WITH RESPECT
TO TORSIONAL STIFFNESS AND GAIN

where $K_7 = \tau_a(B_1 \tau_{m1} + B_2 \tau_{m2})$

$K_8 = \tau_a(B_1 + B_2) + B_1 \tau_{m1} + B_2 \tau_{m2}$

$K_9 = B_1 + B_2 + K_e K_m/R$

$K_{10} = 1/R$

$K_{11} = \tau_a B_1 B_2 + B_1 B_2(\tau_{m1} + \tau_{m2}) + K_e K_m B_2 \tau_{m2}/R$

$K_{12} = B_1 B_2 + K_e K_m B_2/R$

It may be noted that the parameters of interest, in this case, do not occur linearly in the characteristic equation (5.19). Substituting $s = j\omega$ and solving, two independent sets of values of C and K are obtained [50] as:

$C = \{-e + (e^2 - 4ad)\}/2a$, $K = (D_1 - G_1 C)/(D_2 + H_1 C)$

$C' = \{-e - (e^2 - 4ad)\}/2a$, $K' = (D_1 - G_1 C')/(D_2 + H_1 C')$

where $H_1 = K_{10}$

$G_1 = K_9 - K_7 \omega^2$, $G_2 = K_8 \omega$

$D_1 = A_1 \omega^4 - K_{11} \omega^2$, $D_2 = K_{12} \omega - A_2 \omega^3$

$a = G_2 H_1$, $b = H_1 a_4 \omega$

$d = -(D_2 a_3 \omega^2 + D_1 a_4 \omega)$, $e = H_1 D_2 - G_2 a_3 \omega^2 - G_1 a_4 \omega$

$\Delta_1 = -a C + b K + G_1 a_4 \omega + G_2 a_3 \omega^2$

$\Delta_2 = -a C' + b K' + G_1 a_4 \omega + G_2 a_3 \omega^2$

Plotting each set of values of C and K, i.e. C- K and C'- K', two D-partition boundaries are obtained as shown in Fig. 5.4(b). In this case also the entire region of C-K plane is divided into different regions $R_1 \ldots R_6$ and the most stable

region is R_1 containing a maximum of (n) roots in the left half of s plane. It is again observed that any set of positive values of stiffness C and gain K can be selected to give a stable operation.

5.6.3 Determination of Amplifier Gain For Minimum Settling Time

From the stable region R_1 of Fig. 5.4(b), a number of values of gain K can be selected for a given value of torsional stiffness C. Out of all these values of K, a particular value which gives minimum settling time and hence the fastest transient response may be determined. This value of K has been determined as explained below:

Substituting $s = -\sigma \pm j\omega$ in characteristic equation (5.19), a set of different pairs of D-partition boundaries can be obtained for different and increasing positive values of σ. In each case, the most stable region can be determined as before. Larger the value of σ, narrower is the most stable region and there exists a maximum value of σ beyond which this region disappears. This critical value of σ may be represented as σ_c. The D-partition boundaries for $\sigma = \sigma_c$ can be plotted and most stable region marked. A value of gain K corresponding to a given value of torsional stiffness C selected from this region will give a minimum settling time. It can, therefore, be inferred that the value of gain K is directly influenced by torsional stiffness C, if the system is designed for a minimum settling time.

For the case under study, value of σ_c is obtained as 6.3. For this value of σ, the D-partition boundaries are plotted as shown in Fig. 5.5 and the most stable region is R_1 containing
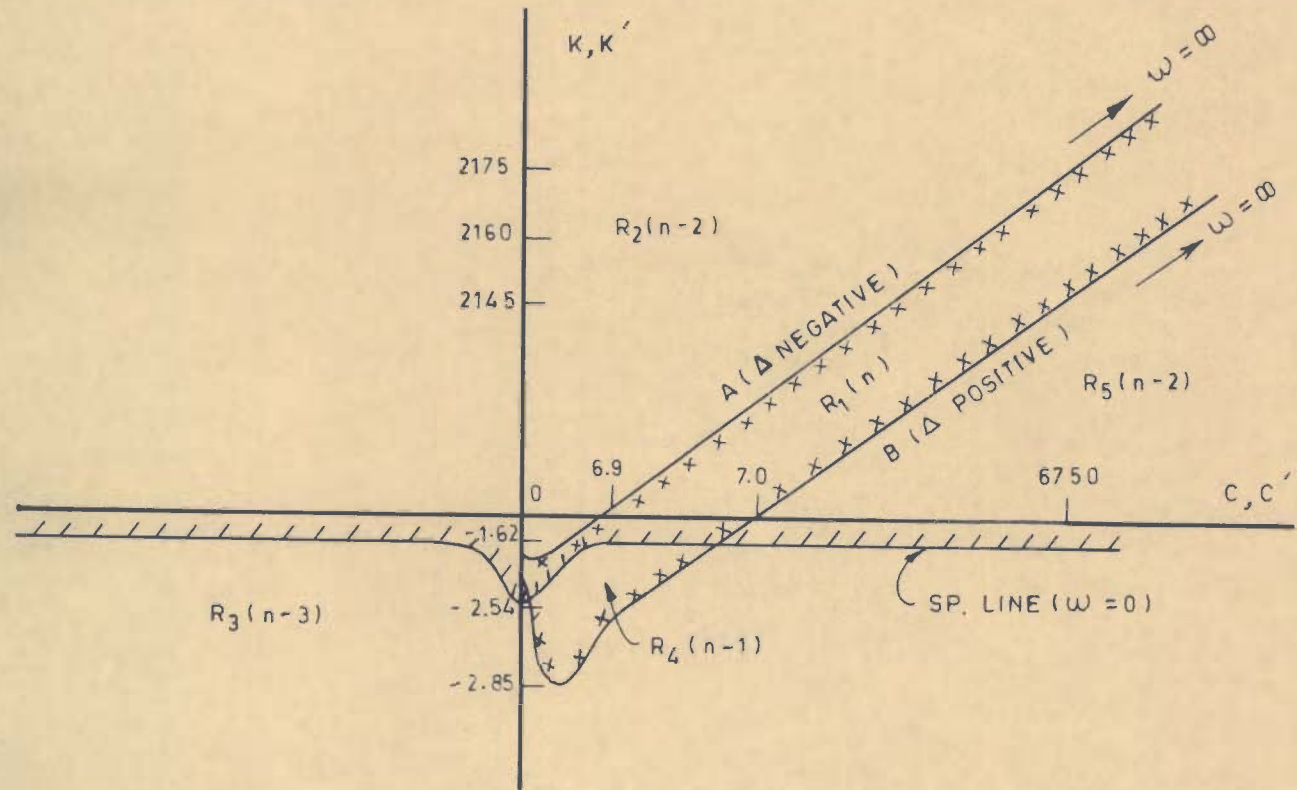
FIG. 5.5 _ D-PARTITION BOUNDARIES WITH RESPECT TO
TORSIONAL STIFFNESS AND GAIN FOR $\sigma = 6.3$
(Not to scale)

a maximum number of (n) roots in the left half of s plane. The value of gain K selected from this region is 2160 corresponding to a given value of C equal to 6750. The corresponding value of amplifier gain K_a can be calculated as:

$$K_a = K E_a / K_e K_t V$$

For the case under study, the value of amplifier gain K_a is obtained as 76. As the D-partition technique indicates only the probable region of stability, the system stability (for $K_a = 76$) has been verified by using Routh criterion.

5.7   SYSTEM PERFORMANCE

The response of the system thus designed, in time domain, can be obtained by expressing eqns. (5.1 - 5.6) in state model form:

$$\dot{x} = A x + D u \tag{5.20}$$

where [A] and [D] are given by eqns. (2.7) and (2.8),

$$u = \begin{bmatrix} V_\alpha(t) \\ T_L \end{bmatrix} \text{ and } x = [\theta_1 \quad \dot{\theta}_1 \quad \theta_2 \quad \dot{\theta}_2 \quad i]^T$$

The duty factor $\alpha(t)$ can be expressed as:

$$\alpha(t) = 1 - \frac{E_t}{E_a} + \frac{K_a K_t}{F_a}(\omega_d - \dot{\theta}_1)$$

Eqn. (5.20) is solved using numerical technique [11] to obtain the system response discussed below:

5.7.1 Transient State Performance

For the system under study, with C, τ_a and K_a chosen as parameters of interest and their values determined in order to give a stable operation with minimum settling time, the switching-in transients in motor speed and armature current are as shown in Figs. 5.6 and 5.7 respectively. It is observed that the motor initially accelerates to a speed slightly higher than the set speed and thereafter attains a speed which is very nearly equal to set speed. The difference between the actual speed and set speed is the steady state error. For a short interval of time, in the transient condition, when the motor accelerates to a speed higher than the set speed, the error between the set speed and the actual speed becomes negative and for this duration the duty factor $\alpha(t)$ remains zero and no voltage is applied to motor. During part of this period, the current tends to go in the negative direction (shown dotted) but remains at zero value as it can not flow in reverse direction due to the inherent characteristics of thyristor switch employed for modulation. Both the speed and the current fluctuate during the transient period. The amplitudes of fluctuation gradually decrease as steady state conditions are approached.

5.7.2 Steady State Performance

(i) Constant Load Torque:

The steady state variations of motor speed and armature current for the system designed with a constant load torque are shown in Figs. 5.8 and 5.9 respectively. It is observed that the
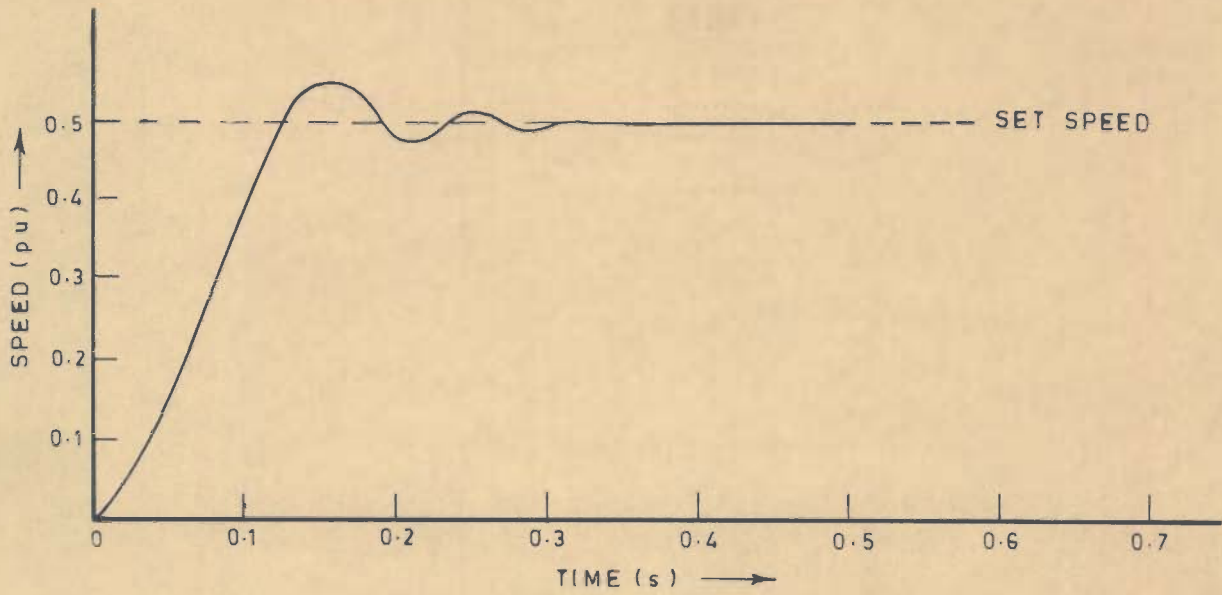
FIG. 5·6 _ TRANSIENT RESPONSE OF MOTOR SPEED
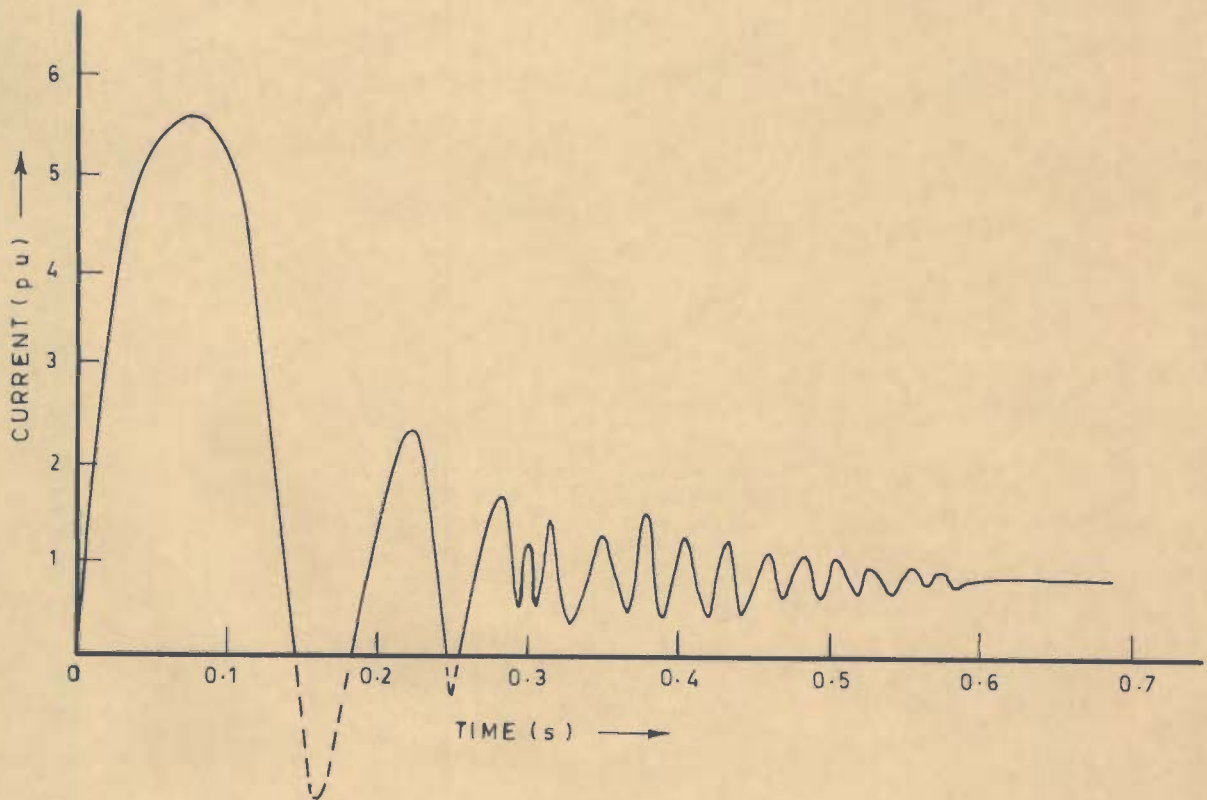

FIG. 5·7 _ SWITCHING-IN TRANSIENT ARMATURE
CURRENT
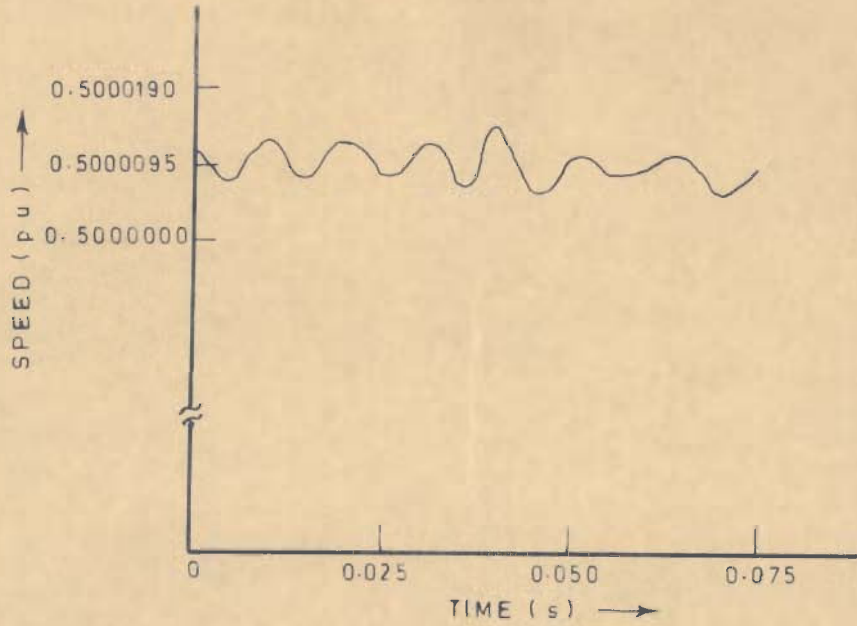
FIG. 5.8 _ STEADY STATE PULSATIONS IN SPEED
FOR CONSTANT LOAD TORQUE (Ka = 76)
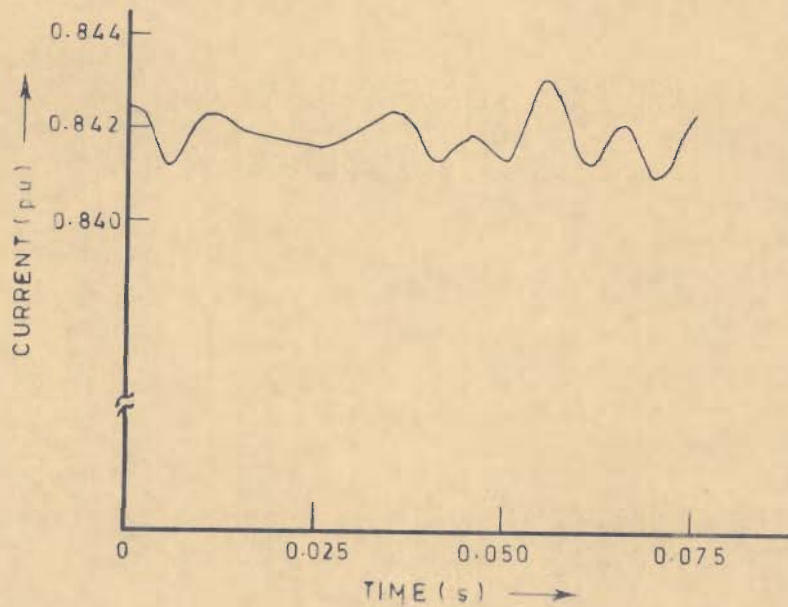
FIG. 5.9 _ STEADY STATE PULSATIONS IN ARMATURE
CURRENT FOR CONSTANT LOAD TORQUE
(Ka = 76)

armature speed and current pulsate under the steady state condi-
tion. The amplitudes of these pulsations are very small. For
the case under study, with K_a = 76, the pulsations in speed and
current are 0.00048 % and 0.055 % respectively [Table 5.1]. The
steady state error in speed is also negligibly small (0.001 % for
the case considered). The settling time to give 0.2 % regulation
of speed is 0.575 sec.

(ii) Pulsating Load Torque:

With a pulsating load torque, as shown in Fig. 5.10,the
pulsations in speed and current for one cycle of load torque are
shown in Figs. 5.11 and 5.12. It is observed that the speed and
current pulsate at a frequency equal to the frequency of load
torque pulsation ω_1. The amplitudes of these pulsations for
K_a = 76 are 0.013 % and 26.81 % for speed and current respective-
ly [Table 5.2]. It is noted that the amplitudes of these pulsa-
tions for pulsating load torque are also small but large compared
with those for constant load torque.

TABLE 5.1 : Effect of Amplifier Gain on System
Performance For Constant Load Torque.

| S. N.	gain K_a	pulsations		steady state error in speed %	settling time sec
		speed %	current %		
1	5.0	0.16634	2.508	0.0134	*
2	10.0	0.02596	0.746	0.0077	1.135
3	25.0	0.00865	0.375	0.0029	0.865
4	50.0	0.00051	0.079	0.0012	0.695
5	76.0	0.00048	0.055	0.0010	0.575
6	100.0	0.00033	0.032	0.0008	0.640
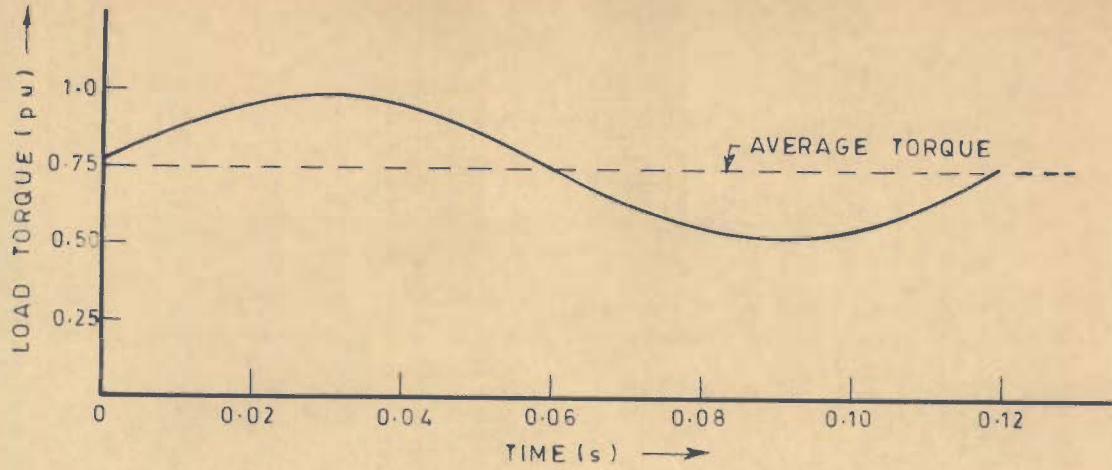
FIG. 5.10 _ VARIATION OF LOAD TORQUE
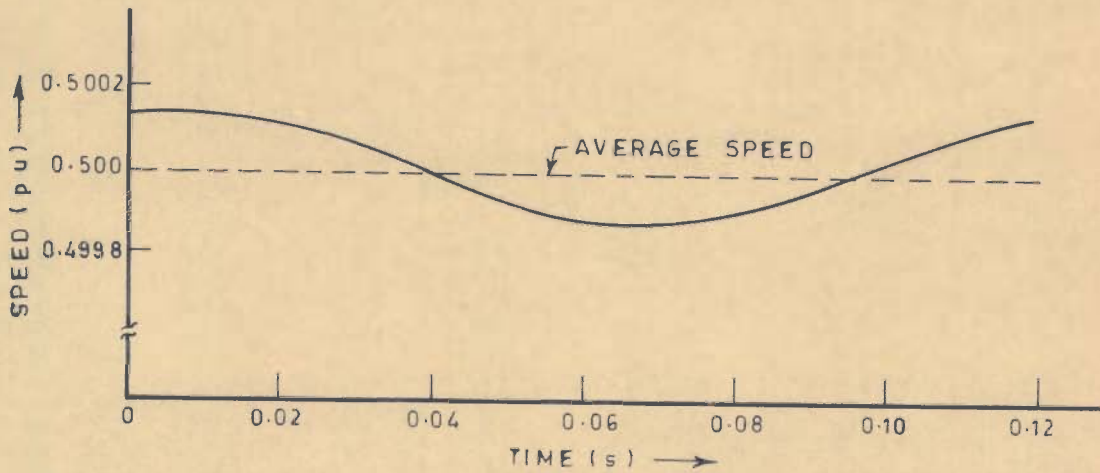
FIG. 5.11_ STEADY STATE PULSATIONS IN SPEED
FOR PULSATING LOAD TORQUE (Ka = 76)
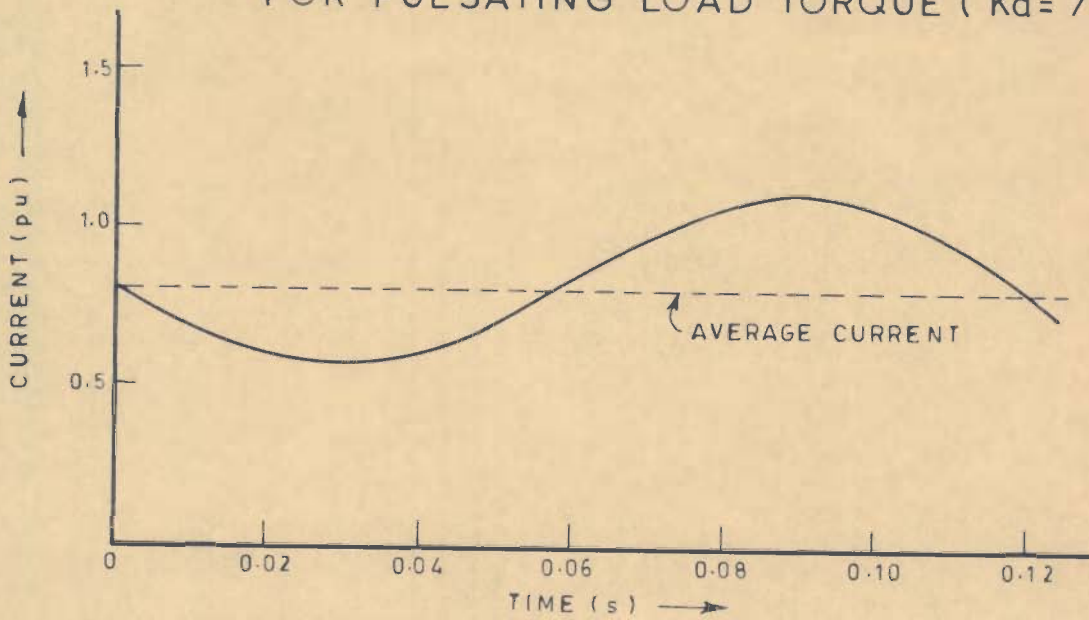
FIG. 5.12 _ STEADY STATE PULSATIONS IN ARMATURE
CURRENT FOR PULSATING LOAD TORQUE
(Ka = 76)

TABLE 5.2 : Effect of Amplifier Gain on System Performance
For Pulsating Load Torque

S.N.	gain K_a	system eigenvalues rad/s	pulsations		settling time,sec
			speed %	current %	
1	0.1	$-12.561 \pm j \quad 15.475$ $- 0.098 \pm j \quad 519.994$	0.932	3.921	*
2	0.5	$-12.528 \pm j \quad 30.771$ $- 0.131 \pm j \quad 520.678$	1.005	13.603	*
3	1.0	$-12.487 \pm j \quad 42.730$ $- 0.173 \pm j \quad 521.538$	1.279	34.175	*
4	1.52	$-12.444 \pm j \quad 52.286$ $- 0.216 \pm j \quad 522.437$	1.371	47.444	*
5	5.0	$-12.146 \pm j \quad 92.997$ $- 0.513 \pm j \quad 528.566$	0.382	39.222	*
6	10.0	$-11.702 \pm j \quad 129.060$ $- 0.958 \pm j \quad 537.705$	0.162	29.762	*
7	25.0	$-10.306 \pm j \quad 193.259$ $- 2.353 \pm j \quad 567.184$	0.044	27.666	*
8	50.0	$- 8.110 \pm j \quad 249.562$ $- 4.549 \pm j \quad 620.931$	0.021	27.016	0.745
9	76.0	$- 6.325 \pm j \quad 281.316$ $- 6.334 \pm j \quad 679.013$	0.013	26.809	0.635
10	100.0	$- 5.132 \pm j \quad 299.284$ $- 7.527 \pm j \quad 732.046$	0.010	26.603	0.680

5.7.3 Effects of Amplifier Gain on System Performance

(a) Effect of Gain K_a on Pulsations in Speed and Current

(i) Constant load torque:

For the case of constant load torque ($T_{L1} = 0$), the variation in pulsations of speed and current for different values of amplifier gain is shown in Fig. 5.13. It is observed that an increase in the value of gain K_a decreases the amplitudes of pulsations of speed and current. The effect of variation of amplifier gain on settling time and steady state error in speed is shown in Fig. 5.14. It is observed that an increase in amplifier gain decreases the steady state error [Table 5.1]. However an optimum value of gain may be selected which gives minimum settling time and an acceptable level of pulsations in speed and current.

(ii) Pulsating Load Torque:

With a pulsating load torque, the pulsations of speed and current for different values of amplifier gain are shown in Figs. 5.15 and 5.16 [Table 5.2]. It is observed that up to a particular value of gain at which resonance occurs, an increase in the value of gain increases the pulsations in speed and current [Fig. 5.15]. An increase of gain beyond this value reduces the pulsations in speed as well as current [Fig. 5.16]. Unlike the case of constant load torque, for a pulsating load torque the pulsations in current are much larger compared to those for speed.

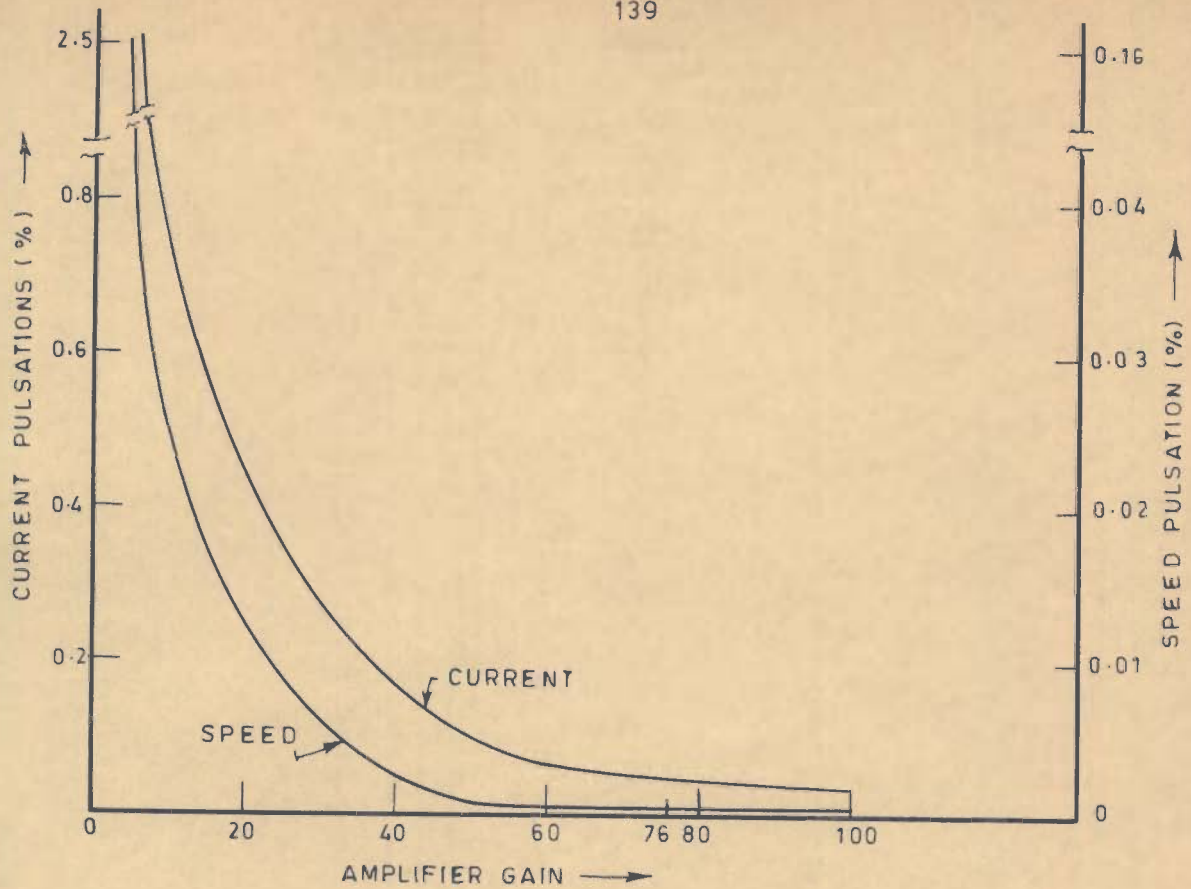FIG. 5.13 _ EFFECT OF AMPLIFIER GAIN ON STEADY STATE
PULSATIONS OF SPEED AND CURRENT FOR
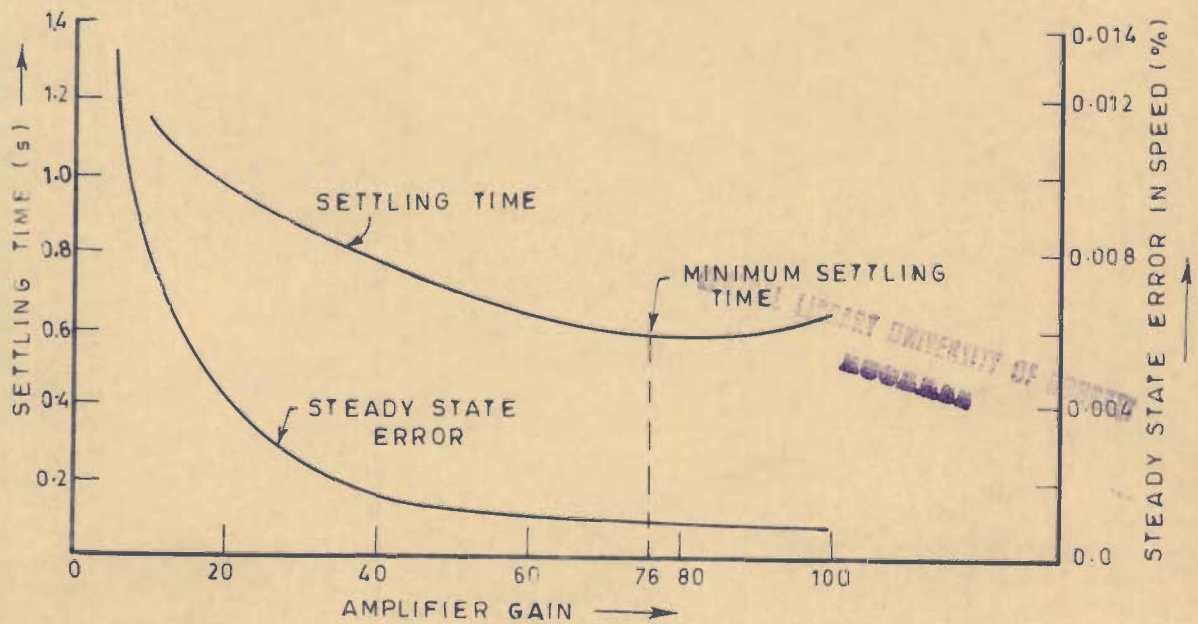CONSTANT LOAD TORQUE

FIG. 5.14 _ EFFECT OF AMPLIFIER GAIN ON SETTLING
TIME AND STEADY STATE ERROR IN SPEED
FOR CONSTANT LOAD TORQUE
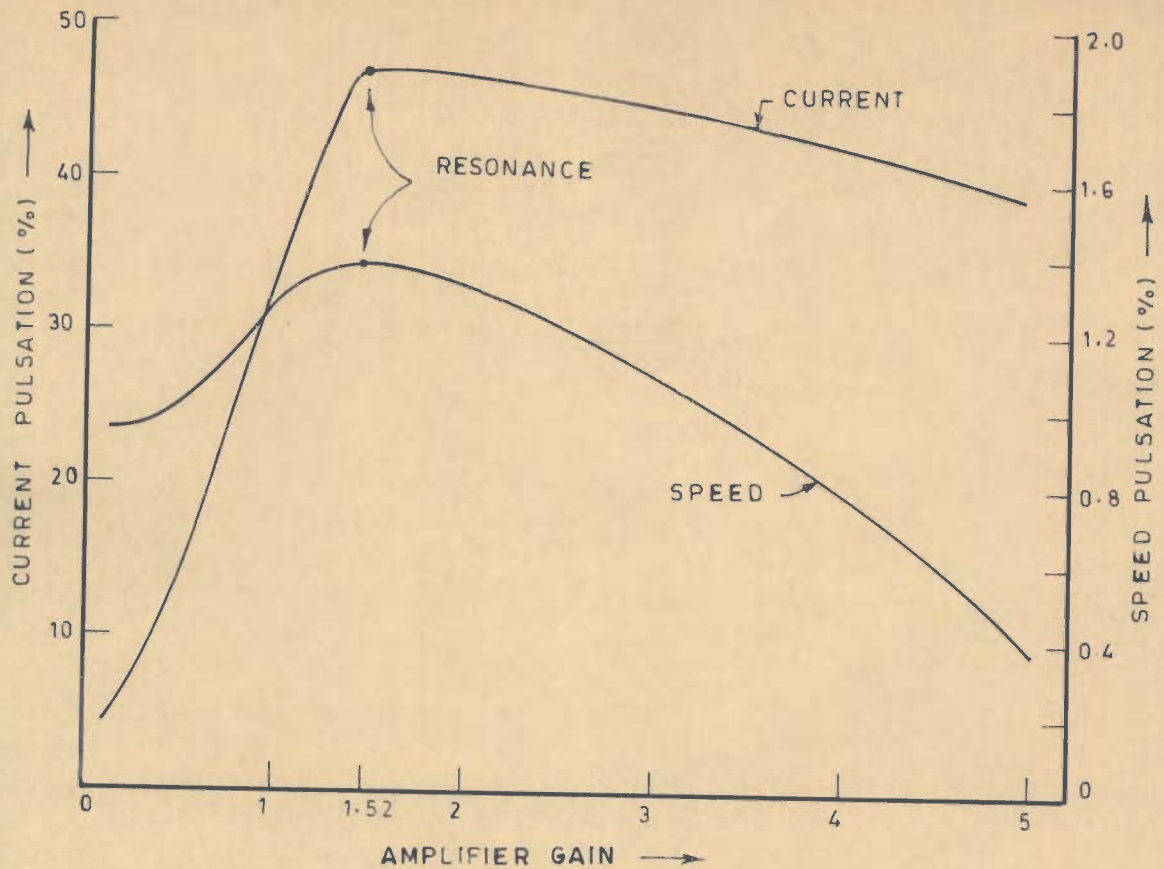
FIG. 5.15 _ VALUE OF AMPLIFIER GAIN CAUSING
RESONANCE FOR PULSATING LOAD TORQUE
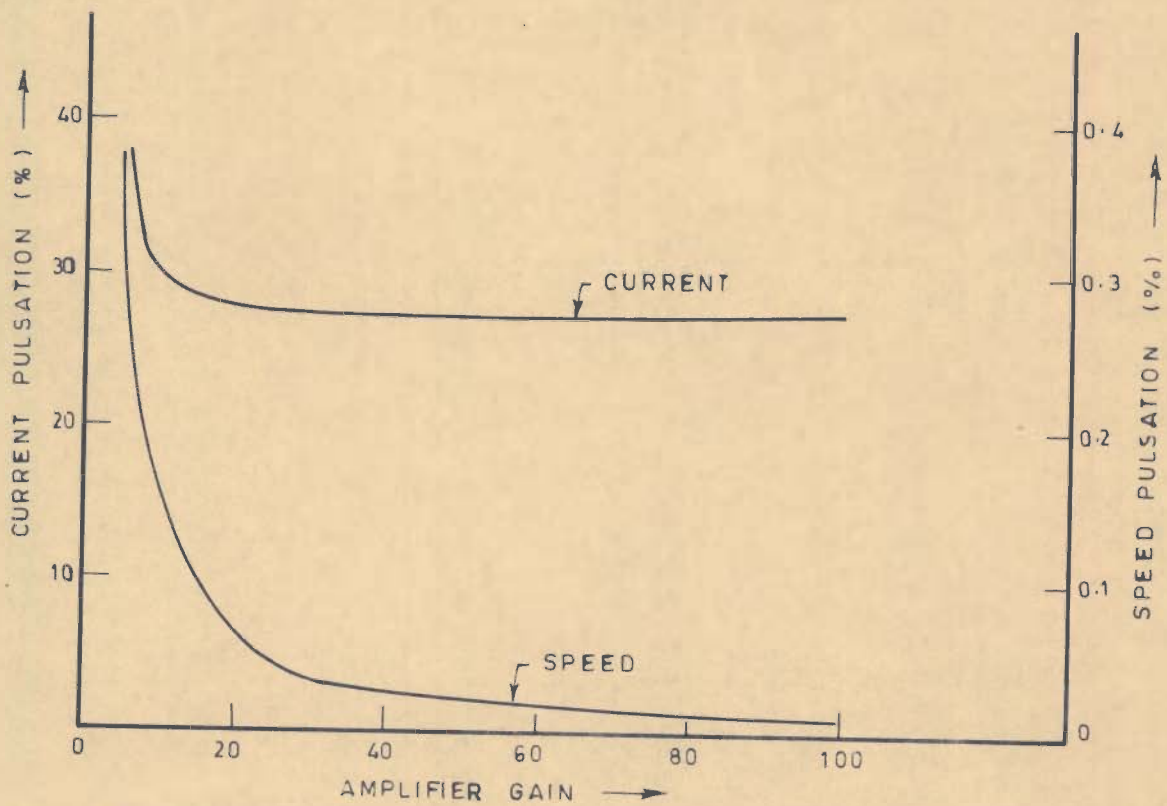
FIG. 5.16 _ EFFECT OF AMPLIFIER GAIN ON STEADY
STATE PULSATIONS OF SPEED AND CURRENT
FOR PULSATING LOAD TORQUE

It is observed that using the value of gain (K_a = 76) corresponding to minimum settling time, the pulsations in speed for a closed loop system are considerably lower (0.013 % - Table 5.2) as compared to the pulsations occurring in an open loop system (1.15 % - Table 4.1). However, the pulsations in current for a closed loop system are much larger (26.8 % - Table 5.2) as compared to the value obtained for open loop system (2.24 % - Table 4.1). Thus using a closed loop system, the speed regulation improves compared to that with an open loop system. But this is achieved only at the cost of larger pulsations in current.

(b) Effect of Gain K_a on Frequency of Resonance

The system analysed is of fourth order and its characteristic equation gives two pairs of complex conjugate roots. Each pair of roots represents a sinusoidal variation of system variables, the frequencies of variation being given by the imaginary parts of the roots. These two frequencies say β_1 and β_2 depend, among other system parameters, on the value of the amplifier gain K_a. The variation in the values of β_1 and β_2 for different values of amplifier gain K_a is shown in Fig. 5.17 [Table 5.2]. When the value of at least one of these two frequencies β_1 or β_2 becomes equal to the frequency of load torque pulsation ω_1, a considerable increase in the amplitude of pulsations of speed and current is obtained. This phenomenon may be termed as resonance. The frequency at which resonance occurs, depends on the value of β_1 or β_2 while these value themselves depend among other system parameters, on the value of amplifier gain K_a. Thus indirectly
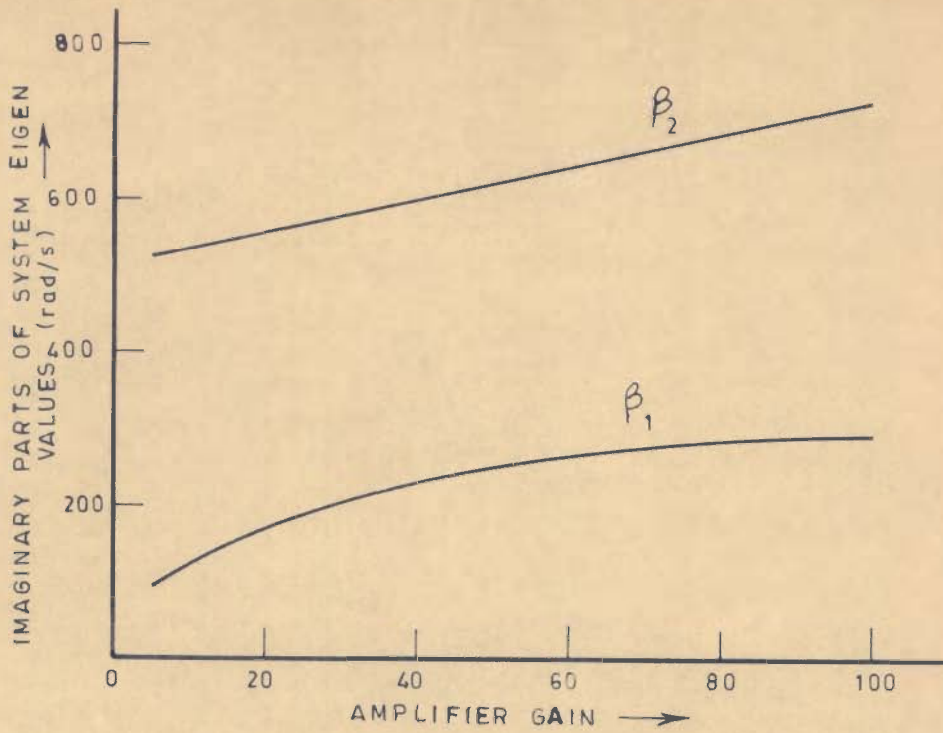
FIG. 5.17 _ EFFECT OF AMPLIFIER GAIN ON
FREQUENCY OF SINUSOIDALLY VARYING
COMPONENTS OF SYSTEM VARIABLES
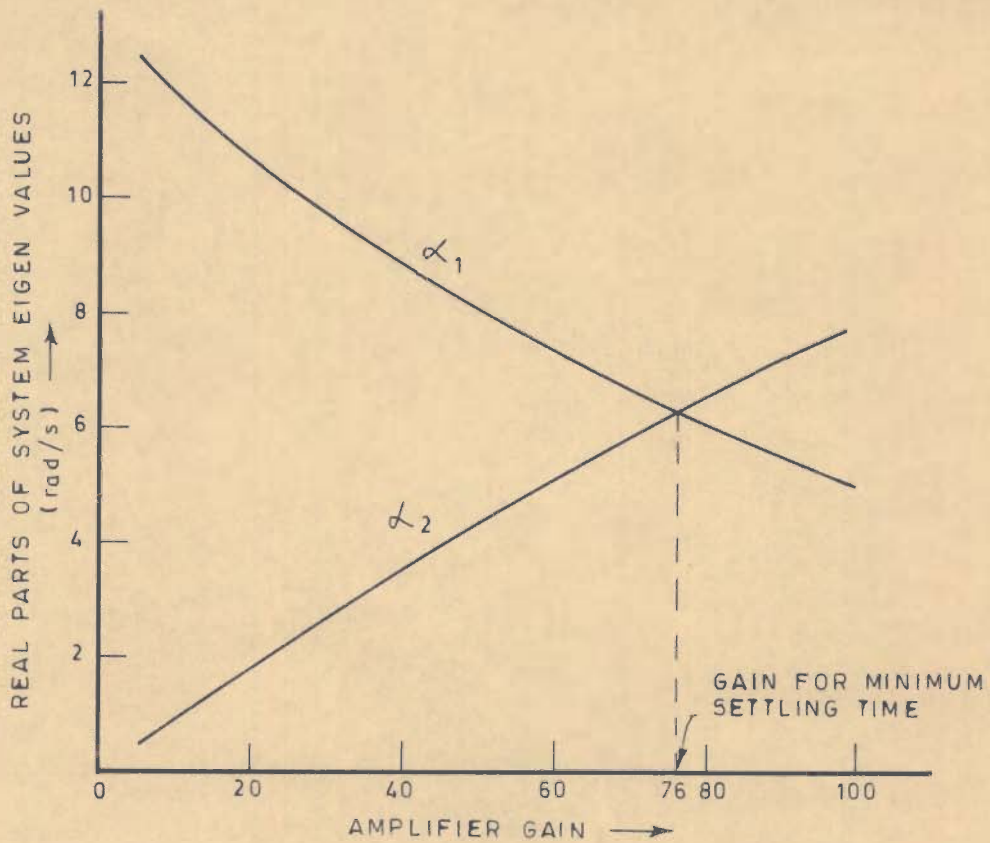
FIG. 5.18 _ EFFECT OF AMPLIFIER GAIN ON RATE OF
DECAY OF SINUSOIDALLY VARYING
COMPONENTS OF SYSTEM VARIABLES

the resonance frequency depends on the value of amplifier gain.

For the system considered, the value of β_1 becomes equal to the frequency of load torque pulsation ω_1 at a particular value of gain $K_a = 1.52$ as shown in Fig. 5.15. For this value of K_a, resonance occurs as the amplitudes of pulsations in speed and current are large compared to those obtained for other values of K_a. As such the value of gain K_a which leads to resonance must be identified and this value should be avoided while designing the system, as large pulsations in speed and current are not desirable for a better performance of the system.

(c) Effect of Gain K_a on Settling Time

The system characteristic equation has two pairs of complex conjugate roots with negative real parts. This indicates that the transient parts of each of the system variables consist of two sinusoidally decaying components. The frequency of these components is determined by the imaginary parts of the complex roots. The negative real parts of the roots are a measure of decay rate of the system variables and hence determine the settling time of the oscillation of these variables. For a practical system, the real parts of the two roots are different. The variation of real parts of the roots with amplifier gain is shown in Fig. 5.18. It is observed that the root with a higher value of imaginary part has a lower value of real part and vice-versa as shown in Figs. 5.17 and 5.18 [Table 5.2]. As such the settling time of the two sinusoidally decaying components are different. The component with a high frequency of oscillation has a lower value of settling time and vice-versa. However, the overall

settling time of the system will depend on the settling time of
the sinusoidal component which is of higher frequency and has a
slower rate of decay.   In order to obtain minimum overall sett-
ling time, it is necessary that both the sinusoidal components
decay at the same rate.

An increase in the value of gain K_a increases the value
of real part of the root of lesser value and decreases that of
other [Fig. 5.18].   As the value of K_a is increased, there occurs
a critical value of K_a for which the real parts of both the roots
become equal.   For this value of K_a, both the sinusoidal compo-
nents of system variables decay at the same rate.   This critical
value of gain K_a gives minimum settling time.   Any further increa-
se in the value of gain beyond this critical value, will not
decrease the settling time.   For the system under study, the
critical value of gain is obtained as K_a = 76.   For this value of
K_a the real parts of the two pairs of roots are equal as shown in
Fig. 5.18 [Table 5.2].   For very low values of gain K_a, the
settling time to give the desired accuracy of speed regulation is
very large and this is indicated by an * mark in Tables 5.1,5.2 .

5.7.4 Effect of Frequency of Load Torque Pulsation ω_1

The steady state pulsations in speed and current (for
K_a = 76) are determined for three different values of frequency
of load torque pulsation viz.; $\omega_1 = \beta_1$, $\omega_1 = \beta_2$ and $\omega_1 = \omega_n$,
where β_1 and β_2 are the frequencies of system oscillation
(which are equal to imaginary parts of roots) and ω_n is the
natural frequency of torsional oscillation of the system given by

$\omega_n = [C(J_1 + J_2)/J_1 J_2]^{1/2}$. The pulsations in speed and current for these three values of ω_1 are shown in Table 5.3. A study of these values reveals that the resonance occurs for all the above three values of ω_1, but the resonance for the case $\omega_1 = \omega_n$ is most severe. Therefore, it is suggested that a combination of system parameters C, J_1 and J_2 should be selected in such a way that the above conditions of resonance are avoided.

TABLE 5.3 : Effect of Variation of Frequency of Load Torque on Speed and Current Pulsations

S. No.	ω_1 rad/s	gain	pulsations	
			speed %	current %
1	β_1	76	0.260	38.269
2	β_2	76	0.156	18.286
3	ω_n	76	9.600	40.600

$\beta_1 = 218.316$, $\beta_2 = 679.013$, $\omega_n = 519.823$

5.8 CONCLUSIONS

The analysis and design of a closed-loop d.c. motor drive fed from a PWM supply is presented. The effects of elasticity of coupling and periodic nature of load torque have been considered. The interaction of the torsional stiffness of shaft, amplifier gain and armature time constant on the system stability and settling time are studied. Using the procedure given, a system can be designed to give satisfactory performance with regard to steady state error, variations in speed and current and settling time. The analysis reveals the following:

(a) An increase in amplifier gain up to a certain critical value decreases the settling time. Any increase in gain beyond this critical value increases the settling time. The value of amplifier gain, required to give the minimum settling time, is affected by the value of torsional stiffness. An increase in the value of torsional stiffness, increases the value of gain to give the minimum settling time.

(b) For a constant load torque, an increase in amplifier gain decreases the pulsations in speed and current, as also the steady state error in speed.

To summarize, from the consideration of current and speed pulsations, a high value of gain K_a is desirable. However, in systems where the settling time has to be kept low, the system gain should be kept equal to critical gain. For systems in which a fast transient response is not a primary consideration, a value of gain higher than the critical value may be selected in order to minimise the pulsations in speed and current.

(c) With a pulsating load torque, the speed and current pulsate at a frequency equal to frequency of load torque pulsation. The amplitudes of these pulsations are large compared with those for constant load torque. A high value of amplifier gain decreases the pulsations in speed and current.

(d) For some specific values of amplifier gain and frequency of load torque pulsation ω_1, the system experiences

resonance characterized by comparatively large pulsations in speed and current.

For a fixed value of ω_1, the resonance occurs when the value of amplifier gain is such that atleast one frequency of oscillation β_1 or β_2 (imaginary parts of roots of characteristic equation) becomes equal to ω_1 [Fig. 5.15]. The value of amplifier gain which leads to resonance will depend on the value of ω_1. Thus for a given value of ω_1, the value of amplifier gain should be selected such that the resonance is avoided.

(e) Some systems may require a particular value of gain K_a for the consideration of minimum settling time. For this fixed value of K_a, resonance occurs when ω_1 becomes equal to either β_1 or β_2. Resonance also occurs when ω_1 becomes equal to the natural frequency of torsional oscillation of system ω_n. The resonance for the condition $\omega_1 = \omega_n$ is observed to be more severe than that for other two cases when $\omega_1 = \beta_1$ or β_2 [Table 5.3]. It is suggested that above three values of ω_1 should be avoided in order to avoid resonance.

In many cases, the value of ω_1 is a system requirement, and not the designers' choice. The amplifier gain K_a may also be fixed to give a minimum settling time. In such cases where ω_1 and K_a are both fixed, resonance may be avoided by changing the value of β_1, β_2 and ω_n which are also functions of torsional stiffness and moment of inertia of the system. Thus a suitable combination of values of torsional stiffness and moment of inertia may be selected to avoid resonance.

CHAPTER-6

NON-LINEAR ANALYSIS OF D.C. MOTOR DRIVE WITH ELASTIC COUPLING AND PULSATING LOAD TORQUE

6.1   INTRODUCTION

In the analysis of a separately excited d.c. motor, fed from a constant d.c. voltage with an elastic coupling and pulsating load torque presented in Chapter-2, the frequency of load torque pulsations was assumed as constant and equal (or proportional) to the average steady state motor speed. This assumption led to linear system equations, simplified the analysis and closed-form solutions for system variables could be obtained.

In a variety of industrial applications, the load torque is a function of path travelled by the driven mechanisms. Examples of such applications include the piston pumps, crank press, mechanisms with crank drives, metal cutting shears, etc. The load torque for some of such type of loads have a periodic variation, the time period depending upon the speed of rotation. The frequency of load torque pulsations is, therefore, a function of motor speed to which the load is coupled. As such the assumption of a fixed frequency of load torque pulsations may lead to some error in the results of the analysis. Therefore, it is worthwhile to investigate the effect of variation of frequency of load torque with speed on the performance of the system. This will also verify the validity of above assumption made in the analysis given in Chapter-2.

6.2 WORK PRESENTED

In this chapter, the analysis of a separately excited d.c. motor fed from a constant d.c. voltage with an elastic coupling and pulsating load torque is presented to determine the effect of speed dependent variations in frequency of load torque pulsations. For two different cases, the system performance is determined in terms of armature current and motor speed for transient as well as steady state conditions. In the first case, the frequency of load torque pulsations is considered as a function of motor speed. This leads to non-linear system equations which are solved using a numerical technique [11] to give the system performance in time domain. In the second case, the system performance is determined using the same numerical technique but assuming the frequency of load torque as constant and equal to average steady state motor speed. This assumption leads to linear system equations. The performance of system for the two cases, in transient and steady state conditions, is compared to determine the effect of frequency of load torque variation with speed.

The system analysed, shown in Fig. 2.1, comprises of a separately excited d.c. motor coupled to a periodically varying load through an elastic shaft. The moments of inertia and damping for motor and the load are considered separately [Fig. 2.2(a)]. A mathematical model for the system in non-linear as well as linear case is given. The equations are expressed in State model form and solved using a numerical technique. For the non-linear case, the frequency of load torque ω_1 is expressed as a function

of speed $\dot{\theta}_2$ and can be written as:

$$\omega_1 = k \, \dot{\theta}_2$$

For linear case, ω_1 is assumed proportional to average value of steady state speed n_1 [eqn.(2.23)] and can be expressed as:

$$\omega_1 = k \, n_1 \quad ; \quad \text{where k is an integer.}$$

The value of k depends upon the type of driven mechanism. For example, k = 1, implies that the load torque completes one cycle in one rotation of motor shaft, and so on.

6.3 PERFORMANCE EQUATIONS

The equations governing system performance for the non-linear and the linear cases can be written as:

(i) NON-LINEAR CASE:

The equations describing the system are:

$$\left.\begin{aligned}
V &= L \frac{di}{dt} + R\,i + K_m \, \dot{\theta}_1 \\
T_e &= J_1 \, \ddot{\theta}_1 + B_1 \, \dot{\theta}_1 + C(\theta_1 - \theta_2) \\
-T_L' &= J_2 \, \ddot{\theta}_2 + B_2 \, \dot{\theta}_2 + C(\theta_2 - \theta_1)
\end{aligned}\right\} \tag{6.1}$$

where $T_e = K_e \, i$

and T_L' is a non-linear function of time given by:

$$T_L' = T_{Lo} + T_{L1} \, \sin (k \, \dot{\theta}_2 \, t - \emptyset) \tag{6.2}$$

Equations (6.1), (6.2) can be expressed in State model form as:

$$\dot{x} = Ax + Du' \tag{6.3}$$

where $[A]$ and $[D]$ are as given in eqns. (2.7) and (2.8),

state variable vector $x = [\theta_1 \quad \dot{\theta}_1 \quad \theta_2 \quad \dot{\theta}_2 \quad i]^T$,

and forcing function vector $u' = \begin{bmatrix} V \\ T_L' \end{bmatrix}$

(ii) LINEAR CASE:

The equations describing the system are:

$$\left.\begin{array}{l} V = L \dfrac{di}{dt} + R\,i + K_m\,\dot{\theta}_1 \\[2mm] T_e = J_1\,\ddot{\theta}_1 + B_1\,\dot{\theta}_1 + C(\theta_1 - \theta_2) \\[2mm] -T_L = J_2\,\ddot{\theta}_2 + B_2\,\dot{\theta}_2 + C(\theta_2 - \theta_1) \end{array}\right\} \qquad (6.4)$$

where $T_e = K_e\,i$

and T_L is a linear function of time given by:

$$T_L = T_{Lo} + T_{L1} \sin(k\,n_1\,t - \emptyset) \qquad (6.5)$$

Equations (6.4), (6.5) can be expressed in State model form as:

$$\dot{x} = Ax + Du \qquad (6.6)$$

where $[A], [D]$ and $[x]$ are same as for the non-linear case,

and forcing function vector $u = \begin{bmatrix} V \\ T_L \end{bmatrix}$

Equations (6.3) and (6.6) are solved using a numerical technique to determine the system performance for non-linear and linear cases respectively.

6.4 SYSTEM PERFORMANCE

The system performance using the values of system para-
meters given in section 2.7 , for non-linear as well as linear
cases is determined in transient as well as steady state condi-
tions. The value of k in eqns.(6.2) and (6.5) is taken as 1.
The performance determined is depicted by Figs. 6.1 - 6.9 .

6.4.1 Transient State Performance

The switching-in transients in armature current for non-
linear and linear cases are shown in Fig.6.1. In both the cases,
the armature current initially rises rapidly and attains a peak
value. Thereafter, it decays slowly till it becomes constant
when steady state is reached. The acceleration characteristics
of motor speed during transient period for non-linear and linear
cases are shown in Fig.6.2. It is clear from Figs. 6.1 and 6.2
that the nature of variation of current and speed for the linear
and non-linear cases is identical.

The error in the values of armature current and motor
speed caused due to the assumption leading to linear case are
expressed as Δi and Δn respectively, and are calculated as
below taking the values for non-linear case as reference:

Δi = (value of current for non-linear case) - (value of current
for linear case)

Δn = (value of speed for non-linear case) - (value of speed for
linear case)

For transient condition, the variation of error Δi and Δn is
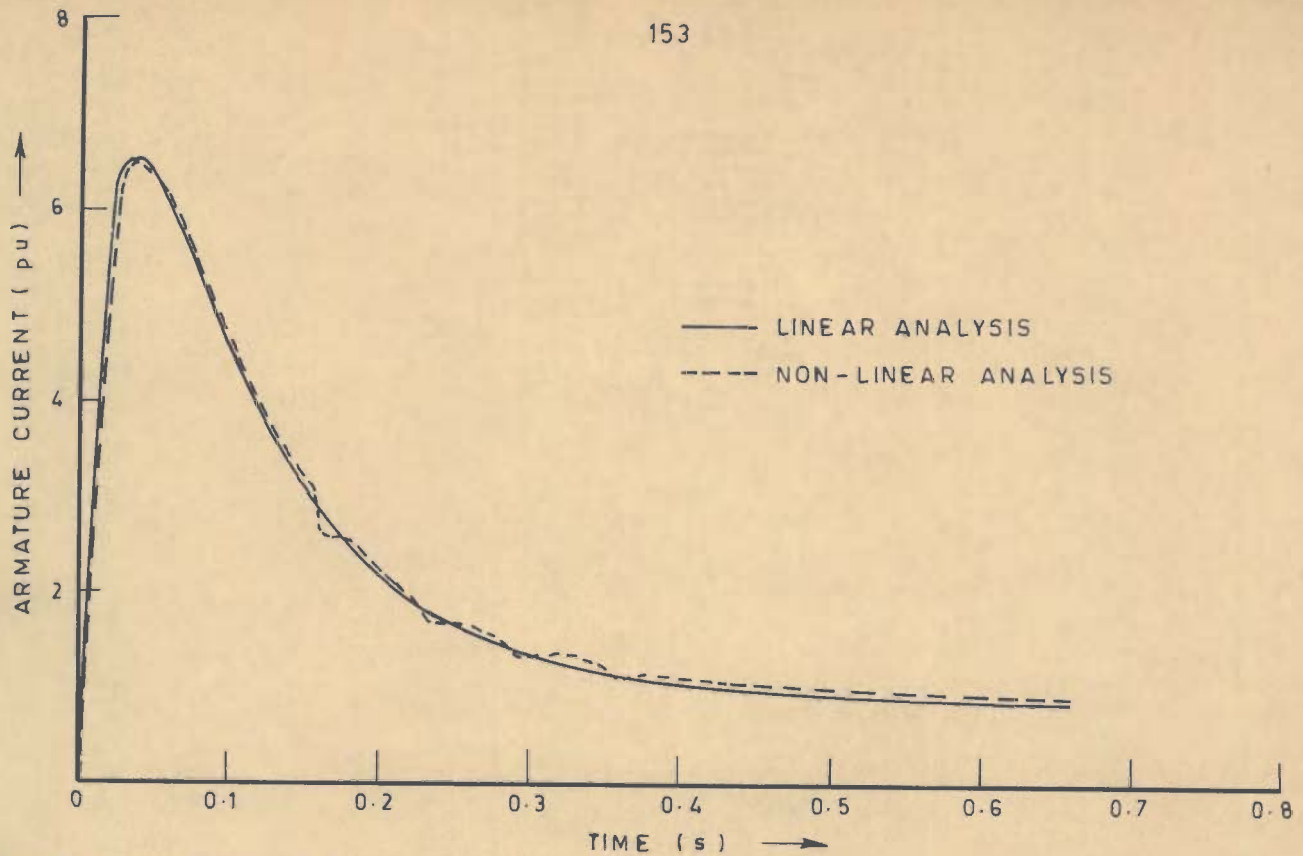shown in Figs. 6.3 and 6.4 . A study of this reveals the

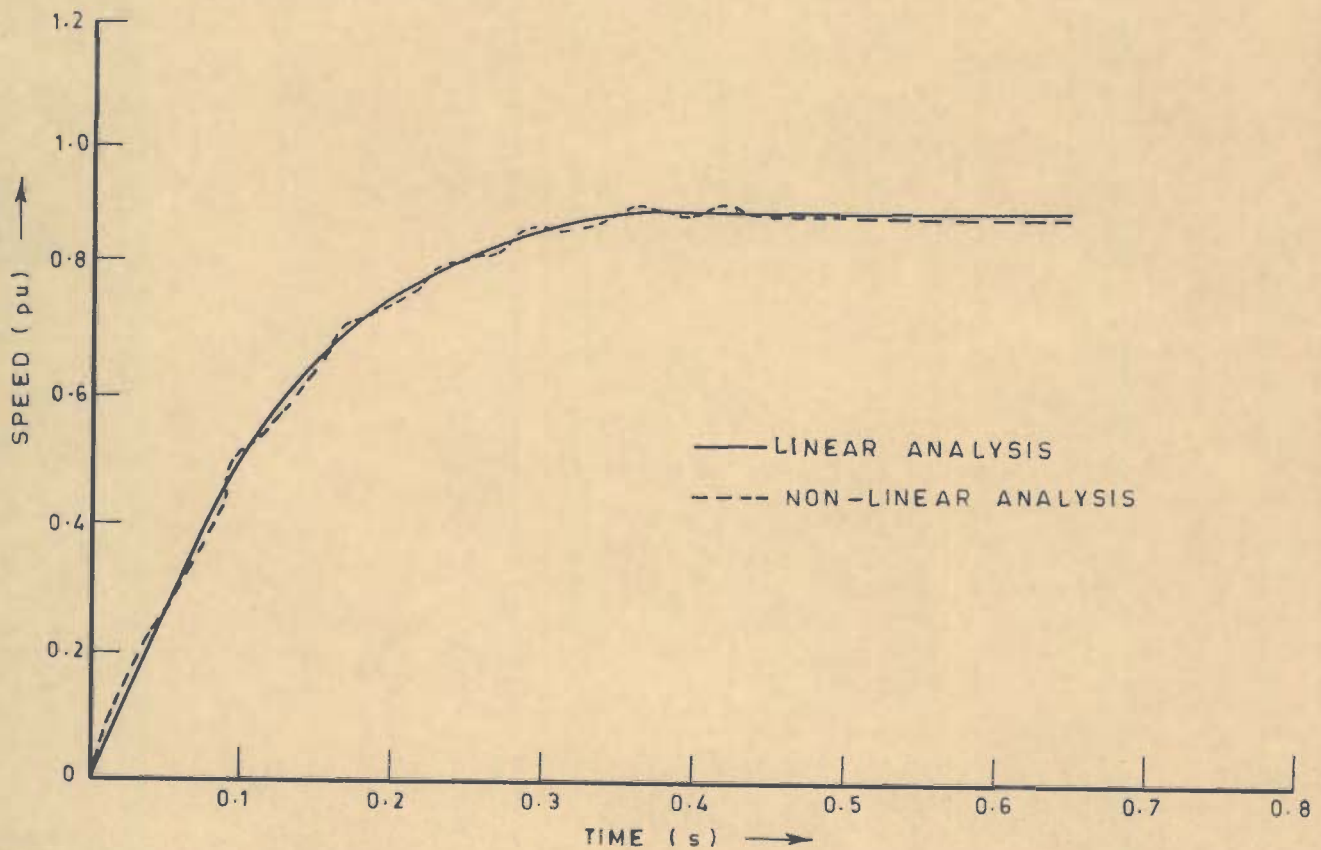.FIG. 6.1 _ SWITCHING-IN TRANSIENT ARMATURE CURRENT
FOR NON-LINEAR AND LINEAR CASES

FIG. 6.2 _ VARIATION OF MOTOR SPEED IN TRANSIENT
CONDITION FOR NON-LINEAR AND LINEAR CASES

following:

(a) the variation of errors Δi and Δn with time is alternating in nature. The instantaneous values of error may be positive or negative depending upon whether the current or speed for the non-linear case is more or less than that for linear case.

(b) the magnitude of errors Δi and Δn during transient condition is low, which further decreases with time and attains still lower values as steady state is reached. The values of maximum and minimum errors in armature current for transient condition are 0.0571 and -0.0269 pu , while for steady state these values are 0.0206 and 0.0079 pu. Similarly the values of maximum and minimum error in motor speed for transient condition are -0.0101 and 0.0048 pu, while for steady state, these values are -0.0034 and -0.0003 pu [Table 6.1].

TABLE 6.1 : Comparison of Error in Transient and Steady State Conditions.

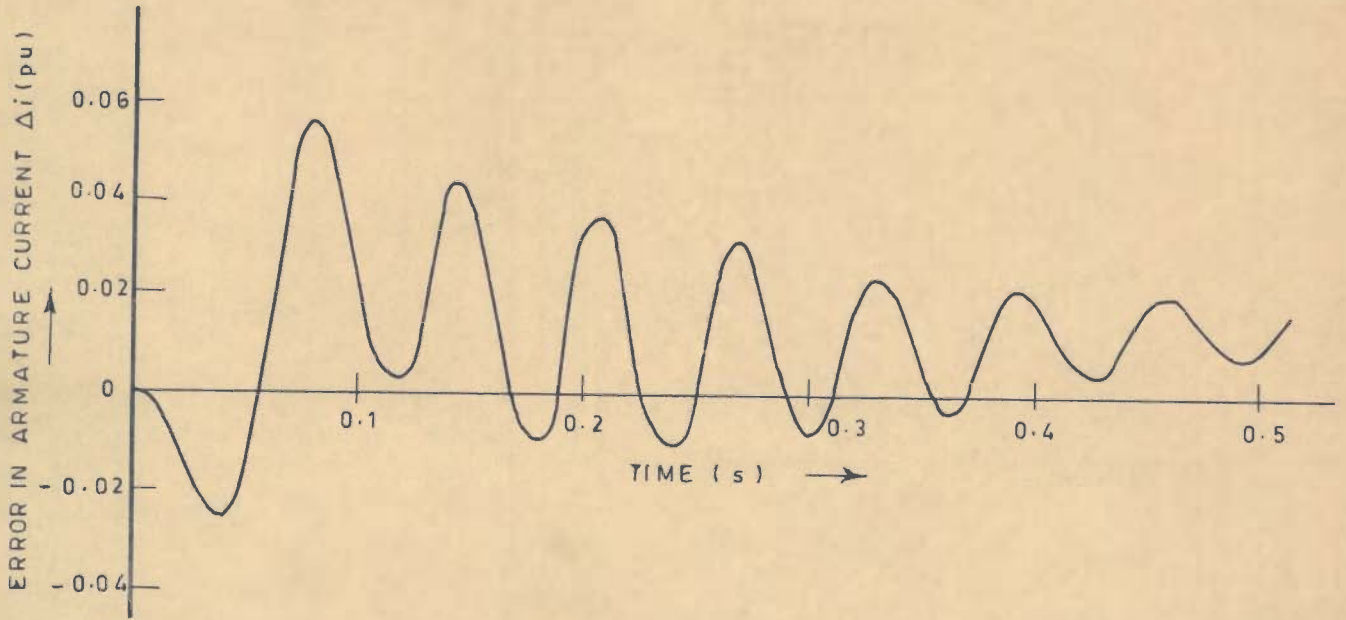| performance variable	transient condition		steady state condition	
	maximum error pu	minimum error pu	maximum error pu	minimum error pu
armature current	0.0571	-0.0269	0.0206	0.0079
motor speed	-0.0101	0.0048	-0.0034	-0.0003

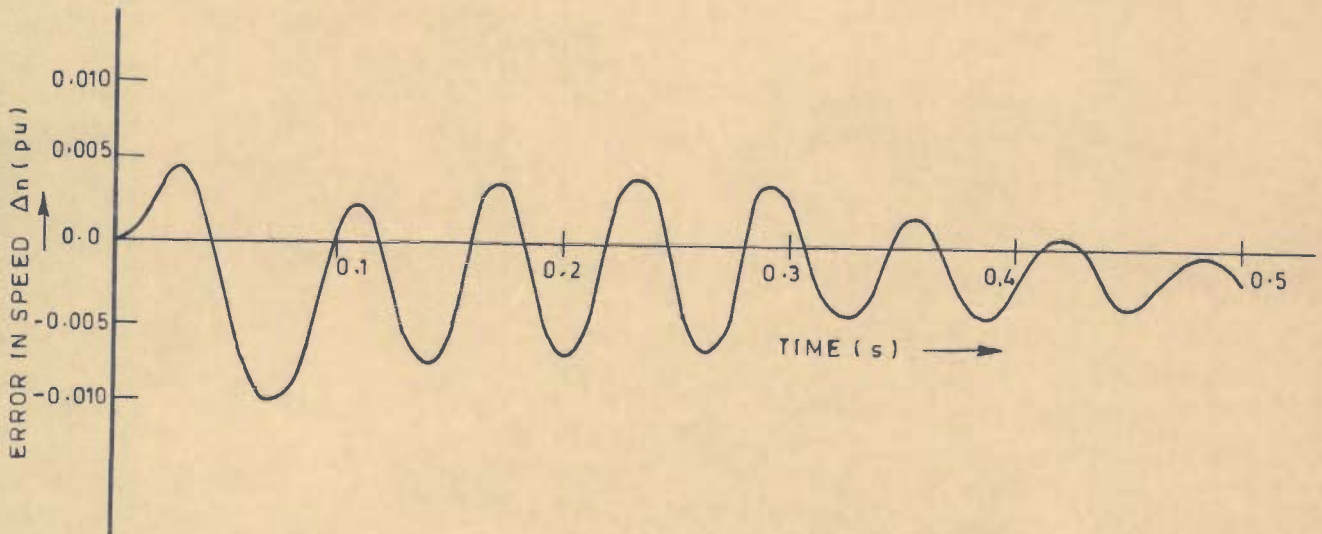FIG. 6.3 _ VARIATION OF ERROR IN ARMATURE CURRENT

FIG. 6.4 _ VARIATION OF ERROR IN MOTOR SPEED

TABLE 6.2 : Comparison of Steady State Performance for Non-Linear and Linear Cases.

analysis	armature current in a cycle			motor speed in a cycle		
	maximum value pu	minimum value pu	amplitude of pulsation pu	maximum value pu	minimum value pu	amplitude of pulsation pu
non-linear	0.9455	0.9153	0.0151	0.9113	0.9019	0.0047
linear	0.9182	0.8895	0.0143	0.9147	0.9050	0.0049

6.4.2 Steady State Performance

For a pulsating load torque as shown in Fig.6.5, the steady state variations in armature current and motor speed determined for the non-linear case are shown in Figs.6.6 and 6.7 respectively. These variations for the linear case are shown in Figs. 6.8 and 6.9 respectively. It is observed that for a pulsating load torque, the armature current and speed for the non-linear case pulsate at the frequency of pulsating component of load torque [Figs. 6.6,6.7], as also for the linear case [Figs. 6.8,6.9]. A study of these variations reveals that there is no appreciable change in the values of amplitude of pulsations in current and speed for the non-linear case as compared to the corresponding values for the linear case. The values of amplitudes of pulsations in current and speed for the non-linear case are 0.0151 and 0.0047 pu respectively, while these values for the linear case are 0.0143 and 0.0049 pu respectively [Table 6.2].
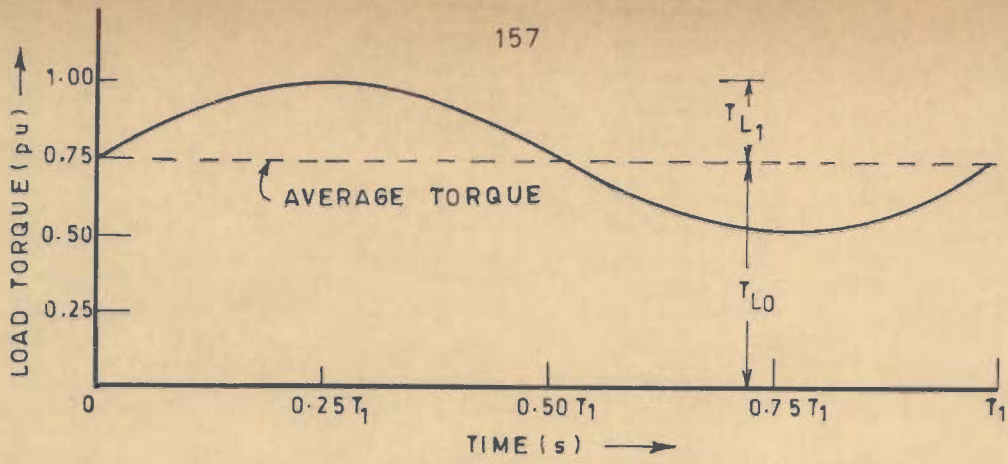
FIG. 6.5 _ VARIATION OF LOAD TORQUE
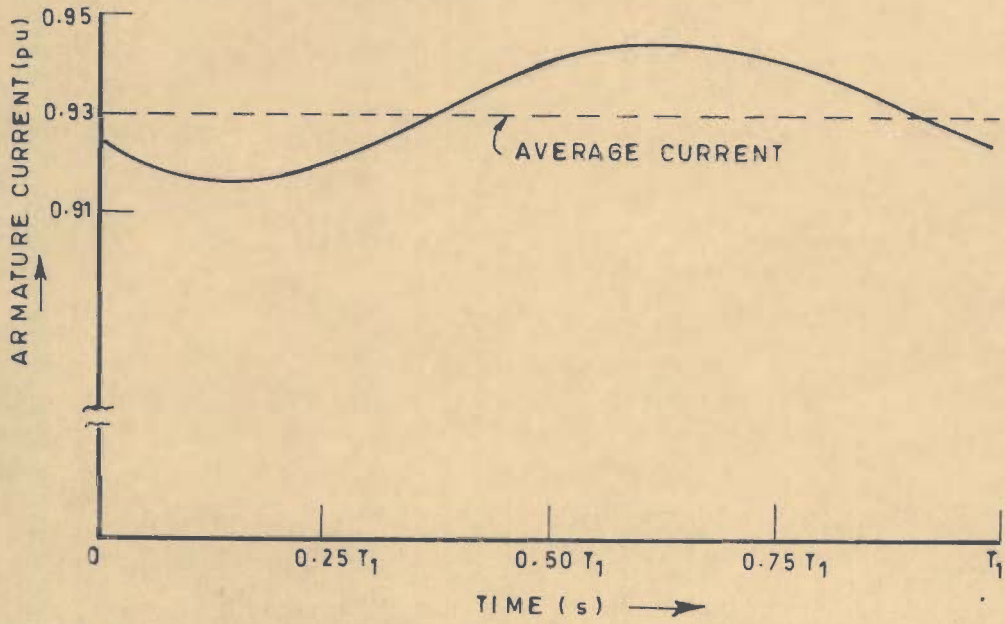
FIG. 6.6 _ VARIATION OF STEADY STATE ARMATURE
CURRENT FOR NON-LINEAR CASE
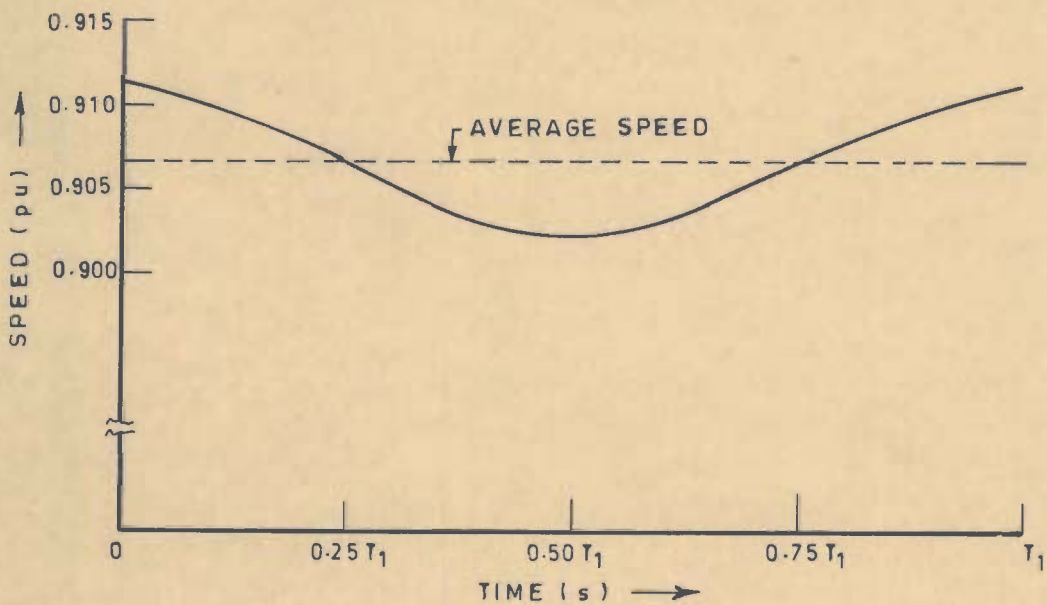
FIG. 6.7 _ VARIATION OF STEADY STATE MOTOR
SPEED FOR NON-LINEAR CASE
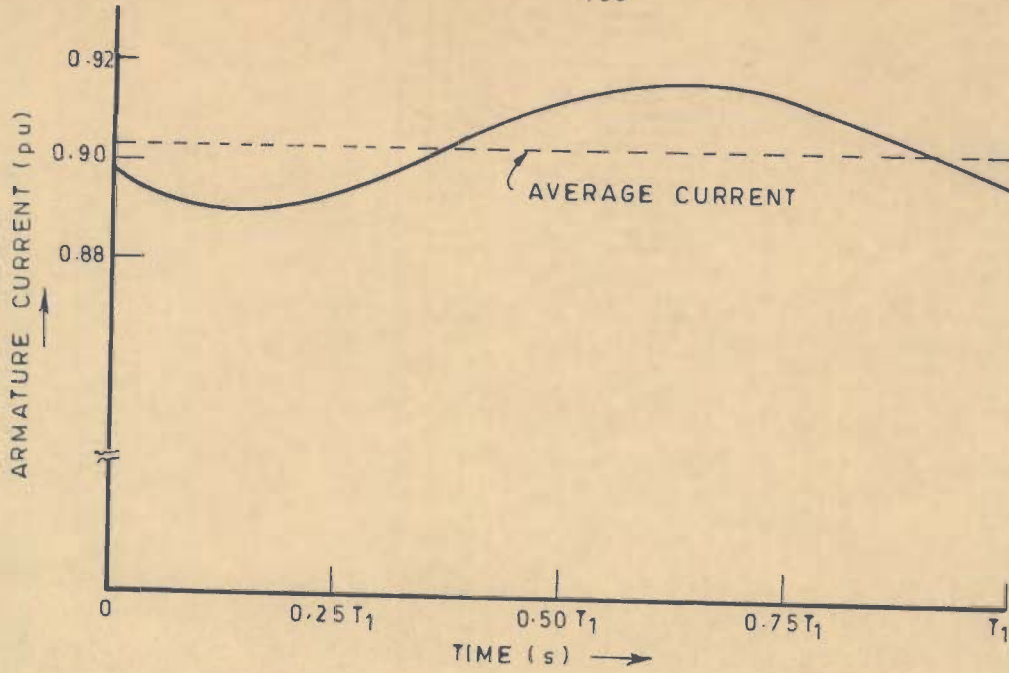
FIG. 6·8 _ VARIATION OF STEADY STATE ARMATURE
CURRENT FOR LINEAR CASE
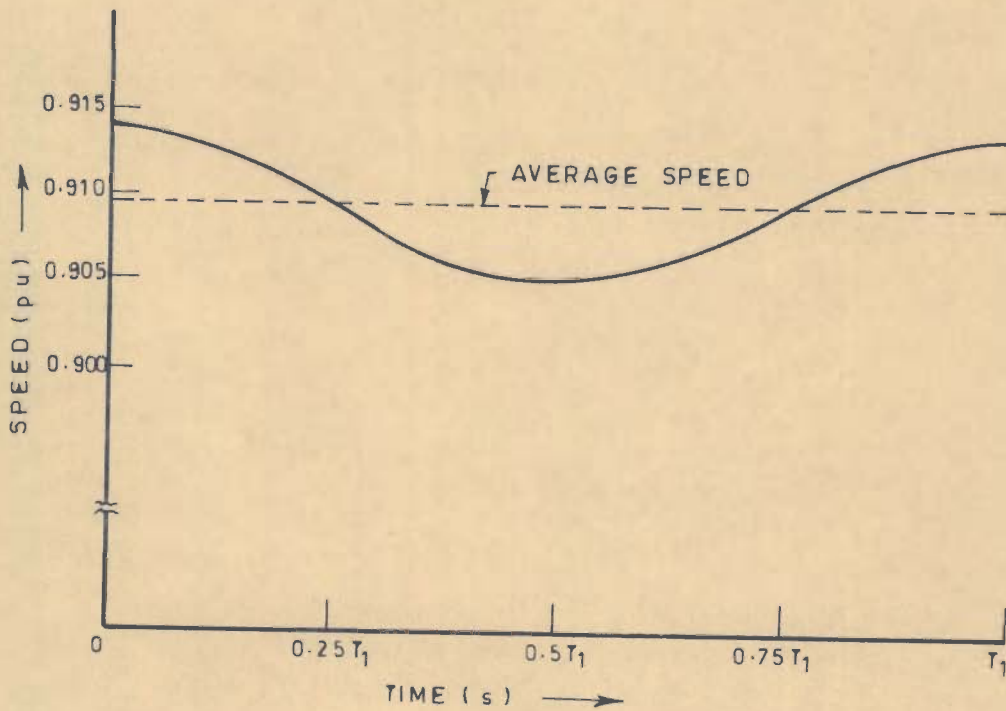
FIG. 6·9 _ VARIATION OF STEADY STATE MOTOR SPEED
FOR LINEAR CASE

6.5 CONCLUSIONS

In this chapter, the performance of a separately excited d.c. motor fed from a constant d.c. voltage with an elastic coupling and pulsating load torque is determined from a rigorous (non-linear) and a simplified (linear) model. In the non-linear case, the frequency of load torque pulsations ω_1 is taken equal to the instantaneous value of motor speed, while for the linear case ω_1 is assumed as constant and equal to the average steady state motor speed. The analysis presented reveals that the results obtained in the two representations are essentially identical with minor variations observed in the values of armature current and motor speed. The error caused, due to the assumption, in the values of armature current and motor speed under transient condition is very low. For steady state, the error is still lower. It can, therefore, be concluded that the assumption of frequency of load torque pulsations being proportional to average steady state motor speed made in the analysis of linear case [Chapter-2] is valid. Moreover, this assumption simplifies the analysis as the system equations in this case are linear and enable to obtain a closed-form solution for system variables determining its performance.

CHAPTER-7

EFFECTS OF ELASTICITY OF COUPLING AND PERIODIC VARIATION
OF LOAD TORQUE ON PERFORMANCE OF D.C. SERIES MOTOR DRIVE

7.1 INTRODUCTION

The analyses dealing with the effects of two important mechanical factors, elasticity of coupling and periodic variation of load torque, on the performance of separately excited d.c. motor open-loop drives fed by a constant d.c. voltage and chopper controlled supply have been presented in Chapters 2 and 4 respectively. D.C. series motors are also used in a variety of industrial drives and in traction, mainly due to better inherent torque-speed characteristics, but hardly any work dealing with the effects of these mechanical factors on the performance of d.c. series motor drives has been reported in literature. It is, therefore, worthwhile to investigate the effects of above mechanical factors on the performance of d.c. series motor drives. A comparison of the effects of mechanical factors on the performance of series and separately excited motors may provide a criterion for the selection of a suitable type of motor for a given application.

7.2 WORK PRESENTED

In this chapter, the analysis of an open-loop d.c. series motor drive with an elastic coupling is presented for (i) a motor fed by a constant d.c. voltage, and (ii) a motor fed by a chopper

controlled supply. The drive performance is determined for cons-
tant load torque as well as for pulsating load torque. The system
equations for series motor drives are invariably non-linear due to
the non-linearity of the magnetisation characteristic of the motor.
Closed-form solutions of such system equations are, therefore, not
possible.

In order to investigate the difference in behaviour of
drives using series motor and separately excited motor, the per-
formance of two drives with elastic coupling, having similar
motors, but in one case the field winding connected to give series
excitation, and in the other case the same field winding separate-
ly excited, is determined. The system equations expressed in
State model form are solved using a numerical technique [11]. For
a typical set of drive system data, the performance in terms of
armature current, motor speed and twist in the shaft for the two
drives is determined in transient as well as steady state condi-
tions. The effects of elasticity of coupling and periodic varia-
tion of load torque on the performance of the two drives are
investigated and compared.

The systems analysed with d.c. series motor fed by a cons-
tant d.c. voltage and by a chopper controlled supply are shown in
Figs.7.1 and 7.2 respectively. The electromechanical system is
represented as a two rotor system and the moments of inertia and
damping for the motor and the load are considered separately
[Fig.2.2(a)]. The periodic variation of load torque is assumed
to comprise of a sinusoidally varying component superposed on a
uniform component [Fig.2.2(b)]. The frequency of load torque
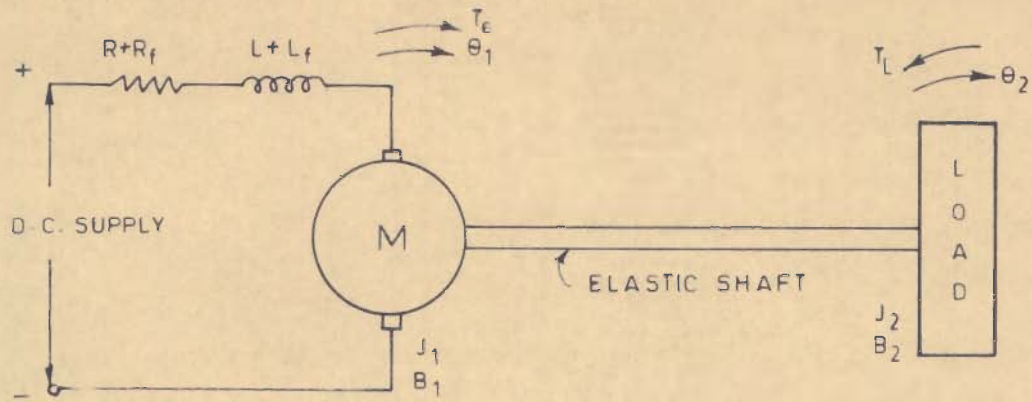
FIG.7.1 _ SCHEMATIC DIAGRAM OF D·C. SERIES MOTOR
COUPLED TO LOAD THROUGH AN ELASTIC SHAFT
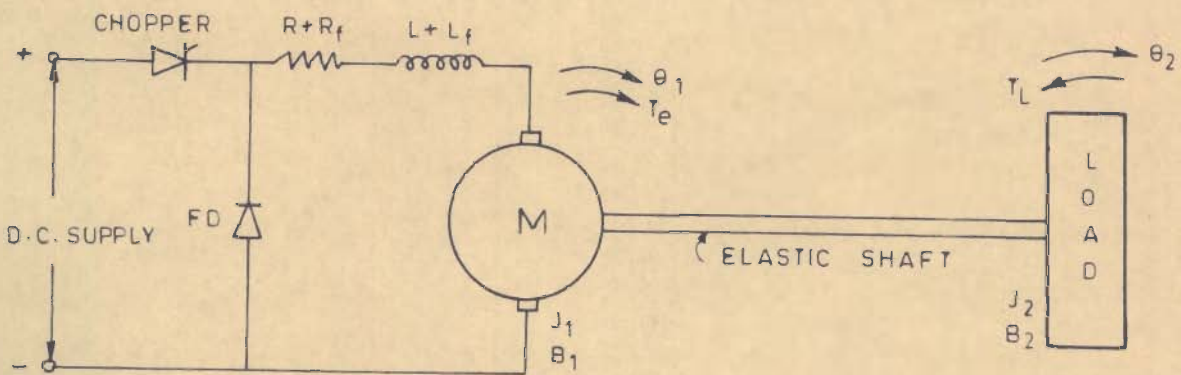
FIG.7.2 _ SCHEMATIC DIAGRAM OF CHOPPER FED D·C.
SERIES MOTOR COUPLED TO LOAD THROUGH
AN ELASTIC SHAFT
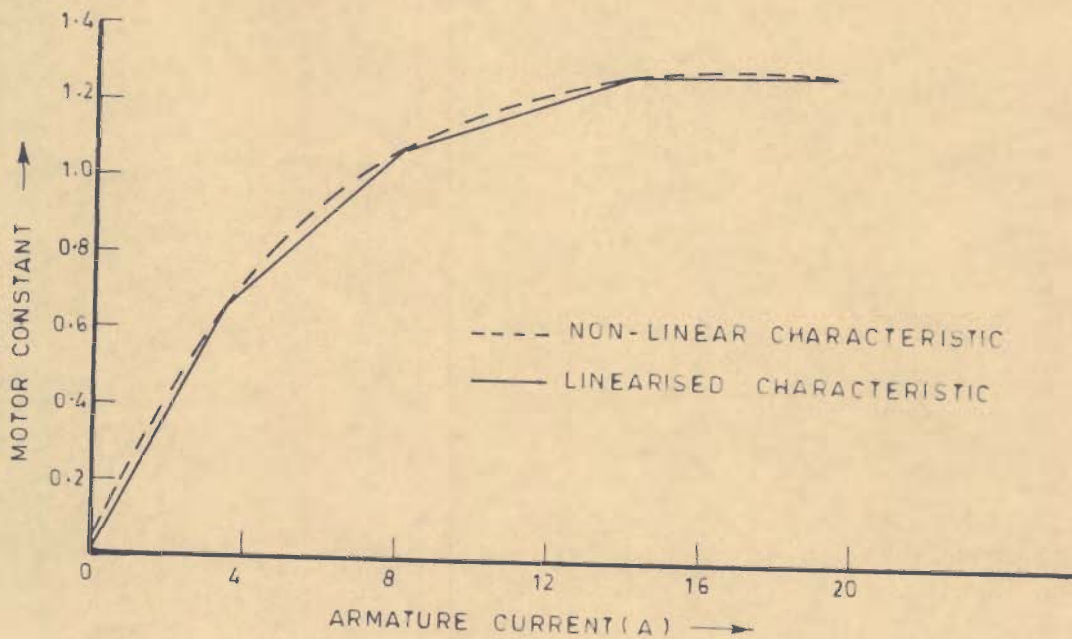
FIG.7.3 _ LINEARISATION OF MAGNETISATION
CHARACTERISTIC OF D·C. SERIES MOTOR

variations, ω_1, is assumed equal to the average steady state speed of motor.

For the drive system with chopper control [Fig.7.2], the 'time ratio control' method with constant chopper frequency is employed to control the drive speed. A freewheeling diode FD is connected in parallel with armature to allow flow of current in the armature circuit during the freewheeling interval of chopper. Separate sets of equations applicable to duty and freewheeling intervals of chopper operation are written. The commutation interval is neglected. These equations are expressed in State model form and solved by step-by-step method using a numerical technique [11], starting from switching-in instant. The values of performance variables at the end of first duty interval are used as initial values for first freewheeling interval, and so on.

The non-linear magnetisation characteristic of series motor is linearised by 'piece-wise linearisation method' as shown in Fig.7.3.

7.3 PERFORMANCE EQUATIONS OF D.C. MOTOR DRIVE WITH CONSTANT VOLTAGE SUPPLY

(a) D.C. Series Motor Drive

The system shown in Fig.7.1 · with a pulsating load torque can be described by the following equations:

$$V = (L + L_f) \frac{di}{dt} + (R + R_f)i + K_m(i)\dot{\theta}_1 \tag{7.1}$$

$$K_e(i)i = J_1 \ddot{\theta}_1 + B_1 \dot{\theta}_1 + C(\theta_1 - \theta_2) \tag{7.2}$$

$$- T_L = J_2 \ddot{\theta}_2 + B_2 \dot{\theta}_2 + C(\theta_2 - \theta_1) \tag{7.3}$$

where

$$T_L = T_{Lo} + T_{L1} \sin (\omega_1 t - \emptyset) \tag{7.4}$$

and $K_m(i)$, $K_e(i)$ are motor back e.m.f. constant and torque constant respectively, which are functions of armature current. Equations (7.1)-(7.4) can be expressed in State model form as:

$$\dot{x} = A'x + D'u \tag{7.5}$$

where

$$A' = \begin{bmatrix} 0 & 1 & 0 & 0 & 0 \\ -\dfrac{C}{J_1} & -\dfrac{B_1}{J_1} & \dfrac{C}{J_1} & 0 & \dfrac{K_e(i)}{J_1} \\ 0 & 0 & 0 & 1 & 0 \\ \dfrac{C}{J_2} & 0 & -\dfrac{C}{J_2} & -\dfrac{B_2}{J_2} & 0 \\ 0 & -\dfrac{K_m(i)}{(L+L_f)} & 0 & 0 & -\dfrac{(R+R_f)}{(L+L_f)} \end{bmatrix}, \tag{7.6}$$

$$D' = \begin{bmatrix} 0 & 0 & 0 & 0 & \dfrac{1}{(L+L_f)} \\ 0 & 0 & 0 & -\dfrac{1}{J_2} & 0 \end{bmatrix}^T, \tag{7.7}$$

$$x = [\theta_1 \quad \dot{\theta}_1 \quad \theta_2 \quad \dot{\theta}_2 \quad i]^T \tag{7.8}$$

and $u = \begin{bmatrix} V \\ T_L \end{bmatrix}$ \hfill (7.9)

(b) D.C. Separately Excited Motor Drive

The d.c. drive system [Fig.7.1] with a pulsating load torque, when the motor field winding is separately excited as show

in Fig. 2.1 , can be described by eqns.(2.1)-(2.5). These
equations can be expressed in State model form as:

$$\dot{x} = Ax + Du \qquad (7.10)$$

where A, D, u and x are given by eqns.(2.7)-(2.10).

With a constant load torque, the system performance
equations given in sections 7.3(a) and 7.3(b) still hold, but in
this case T_{L1} is substituted equal to zero, i.e. $T_L = T_{Lo}$.

7.4 PERFORMANCE EQUATIONS OF D.C. MOTOR DRIVE WITH CHOPPER CONTROLLED SUPPLY

(a) D.C. Series Motor Drive

For the chopper fed d.c. motor drive shown in Fig.7.2
with a pulsating load torque, equations (7.1)-(7.4) are applicable
for duty interval of chopper operation, whereas for freewheeling
interval, the same set of equations hold substituting V equal to
zero.

(b) D.C. Separately Excited Motor Drive

For the chopper fed d.c. drive system [Fig.7.2] with a
pulsating load torque, when the motor field winding is separately
excited as shown in Fig.4.1, equations (2.1)-(2.5) are applicable
for duty interval of chopper operation. The same set of equations
hold for freewheeling interval substituting V equal to zero.

With a constant load torque, the system performance
equations given in sections 7.4(a) and 7.4(b) are applicable, but
in this case T_{L1} is substituted equal to zero, i.e. $T_L = T_{Lo}$.

7.5 TYPICAL PERFORMANCE STUDIES

The performance of a d.c. motor, with a constant voltage input as well as with a chopper controlled supply, is computed using the system parameters and operating data given below. As explained earlier, to facilitate comparison, the same motor is used for series excitation and separate excitation. The parameters chosen are those which correspond to a d.c. series motor. If such a machine is connected as a separately excited motor with a constant field current (which gives rated speed at rated supply voltage), the performance as evaluated in this analysis is not affected. The parameters of the field winding connected in series (R_f and L_f) are, however, crucial in determining the performance. These values, if they do not correspond to the values of a series motor and instead correspond to a shunt motor, will give results which will have no practical significance.

Motor data:

voltage of d.c. supply, V = 220 V (1 pu)

full load current, I_{fl} = 12.8 A (1 pu)

rated speed = 1450 rpm (1 pu)

armature resistance, R = 2.1 ohm

armature inductance, L = 0.06 H

field resistance, R_f = 0.5 ohm

field inductance, L_f = 0.0387 H

motor torque or back emf constant

for separately excited motor, K_e or K_m = 1.27

moment of intertia, J_1 = 0.05 Kg m^2

damping coefficient, B_1 = 0.005 Nm/rad/s

Mechanical system data:

torsional stiffness of shaft, $C = 6750$ Nm/rad

moment of inertia of load, $J_2 = 0.05$ Kg m^2

damping coefficient for load, $B_2 = 0.005$ Nm/rad/s

constant component of load torque, $T_{Lo} = 0.75$ pu

pulsating component of load torque, $T_{L1} = 0.25$ pu

phase difference of pulsating component of load torque, $\emptyset = 0$

frequency of load torque pulsation, ω_1 = average steady state motor speed rad/s

Magnetisation characteristics:

For the analysis of series motor drive, the magnetisation characteristics is non-linear. This characteristic is linearised [Fig.7.3] and expressed as below:

$K_e(i) = 0.1885$ i , $0 \leq i \leq 3.5$

$K_e(i) = 0.0933$ i $+ 0.334$, $3.5 \leq i \leq 8.0$

$K_e(i) = 0.0343$ i $+ 0.806$, $8.0 \leq i \leq 14.0$

$K_e(i) = 1.2862$, $i \geq 14.0$

Chopper data:

chopper frequency = 200 Hz

chopper duty factor = 0.6

7.5.1 Transient State Performance

(a) Transient Performance of D.C. Series Motor Drive With Constant Voltage Supply

For the case under study, the variations in armature current, motor speed and twist in the shaft in transient condition for a constant load torque are plotted as shown in Figs.7.4-7.6.
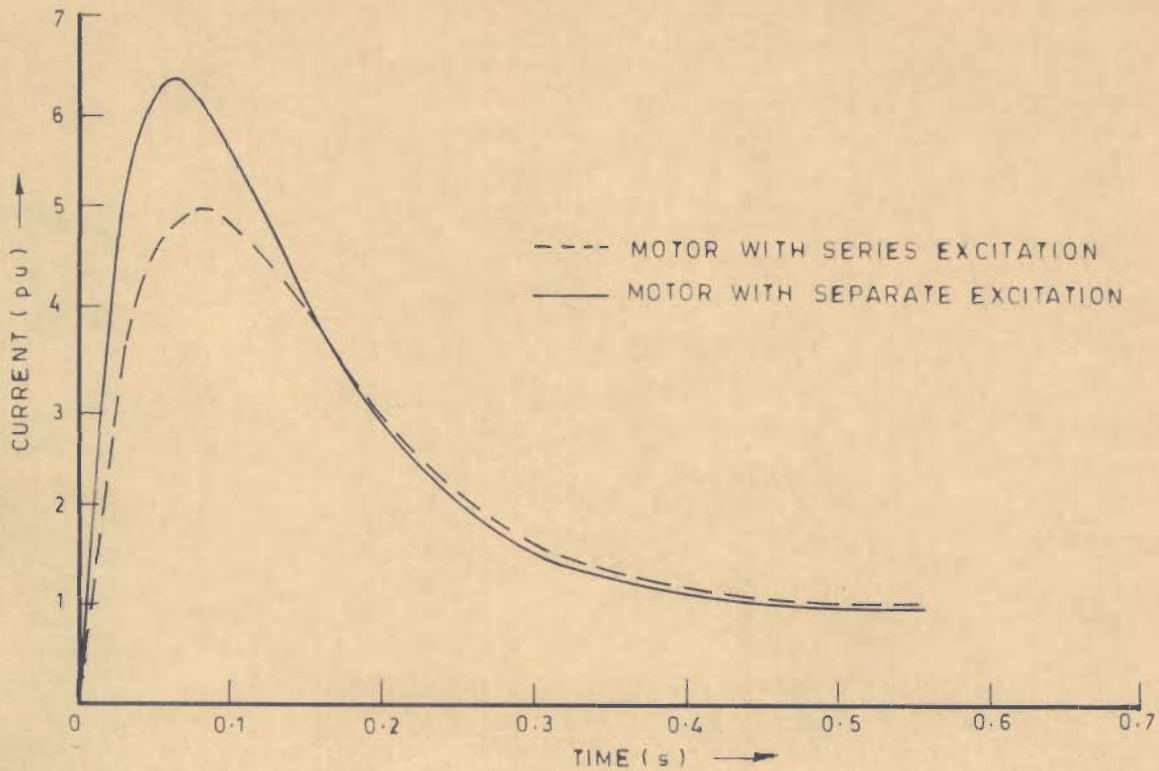
FIG. 7.4 _ SWITCHING-IN TRANSIENT ARMATURE CURRENT
OF D.C. MOTOR FED BY CONSTANT D.C. VOLTAGE
WITH CONSTANT LOAD TORQUE
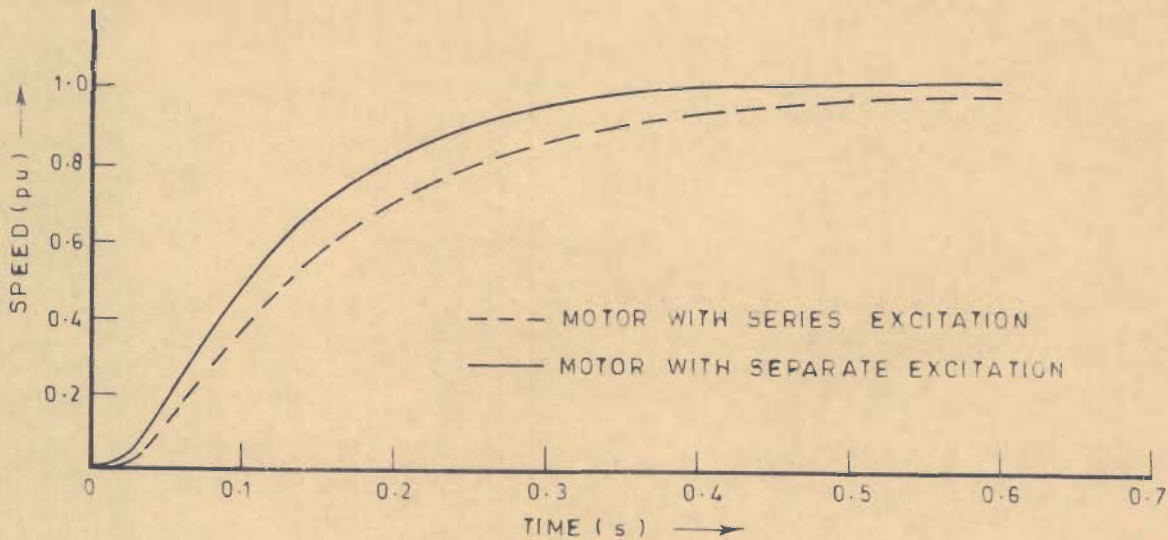
FIG. 7. 5 _ SWITCHING-IN TRANSIENT SPEED RESPONSE OF
D.C. MOTOR FED BY CONSTANT D.C. VOLTAGE
WITH CONSTANT LOAD TORQUE
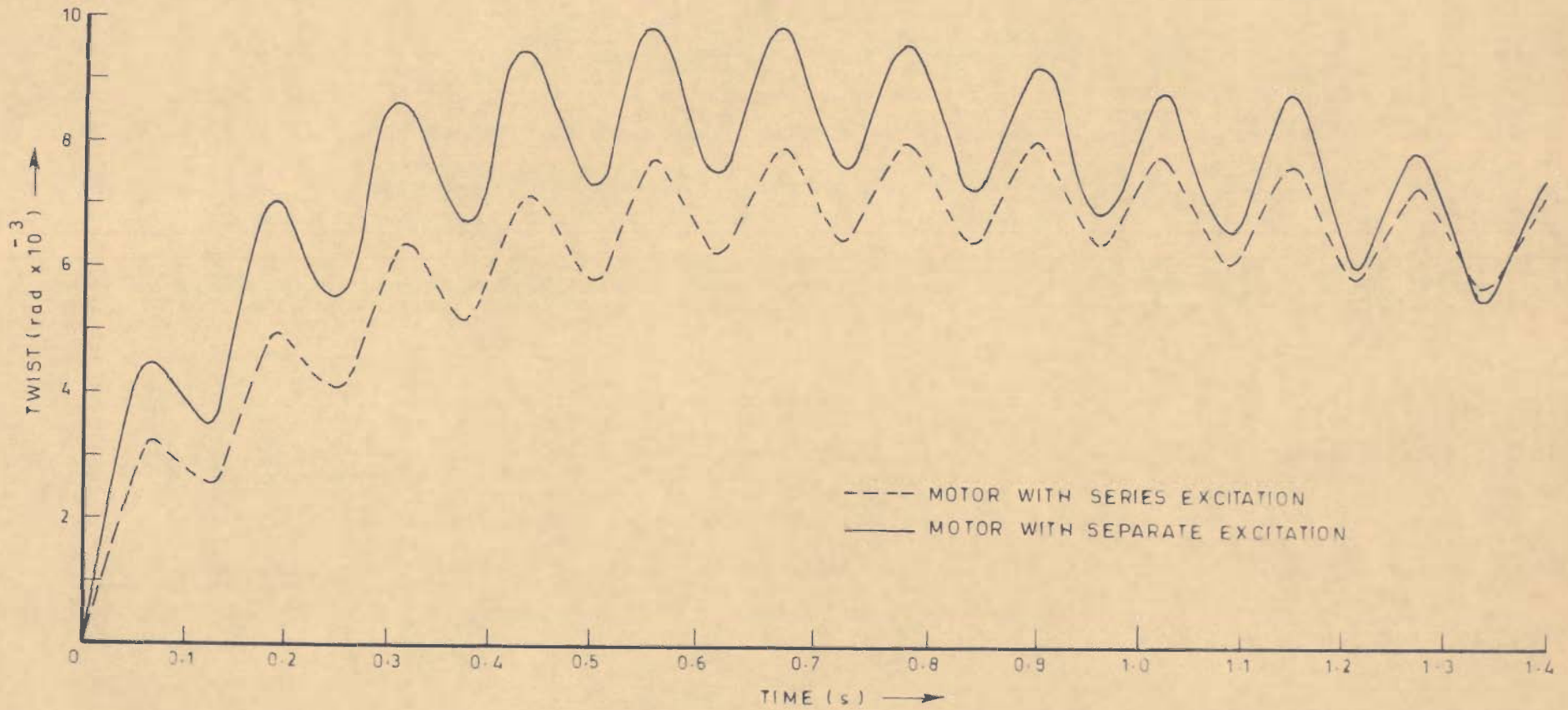
FIG. 7. 6 _ VARIATION OF TWIST IN TRANSIENT CONDITION FOR D.C. MOTOR FED
BY CONSTANT D.C. VOLTAGE WITH CONSTANT LOAD TORQUE

It is observed that the armature current in transient condition initially rises and attains a peak value, and thereafter decays till it attains a constant value as the steady state is reached [Fig.7.4]. The acceleration characteristic of the series motor is plotted as shown in Fig.7.5. The variation of twist in the shaft in transient condition is shown in Fig.7.6. The resultant twist in the shaft comprises of two components. The first component increases till it reaches a peak value and then decreases gradually till it becomes constant as steady state is reached. The second component varies sinusoidally at a frequency equal to the damped natural frequency of torsional oscillations of the system. This component is present only in transient condition and decays with time. Thus in steady state only the first component is present. It is observed that in the transient condition, the twist attains a peak value at the same instant at which the armature current attains its peak value.

(b) Transient Performance of D.C. Series Motor Drive With Chopper Controlled Supply

For the example considered, the transient responses of armature current and speed for chopper fed d.c. series motor with constant load torque are shown in Figs.7.7-7.9.

It is observed that the armature current, in transient condition, rises in duty interval and decays in freewheeling interval of a chopper cycle [Fig.7.7]. These variations are exponential in nature but appear to be linear due to small values of duty and freewheeling intervals of the chopper. The magnitude of variation of current in successive chopper cycles goes on
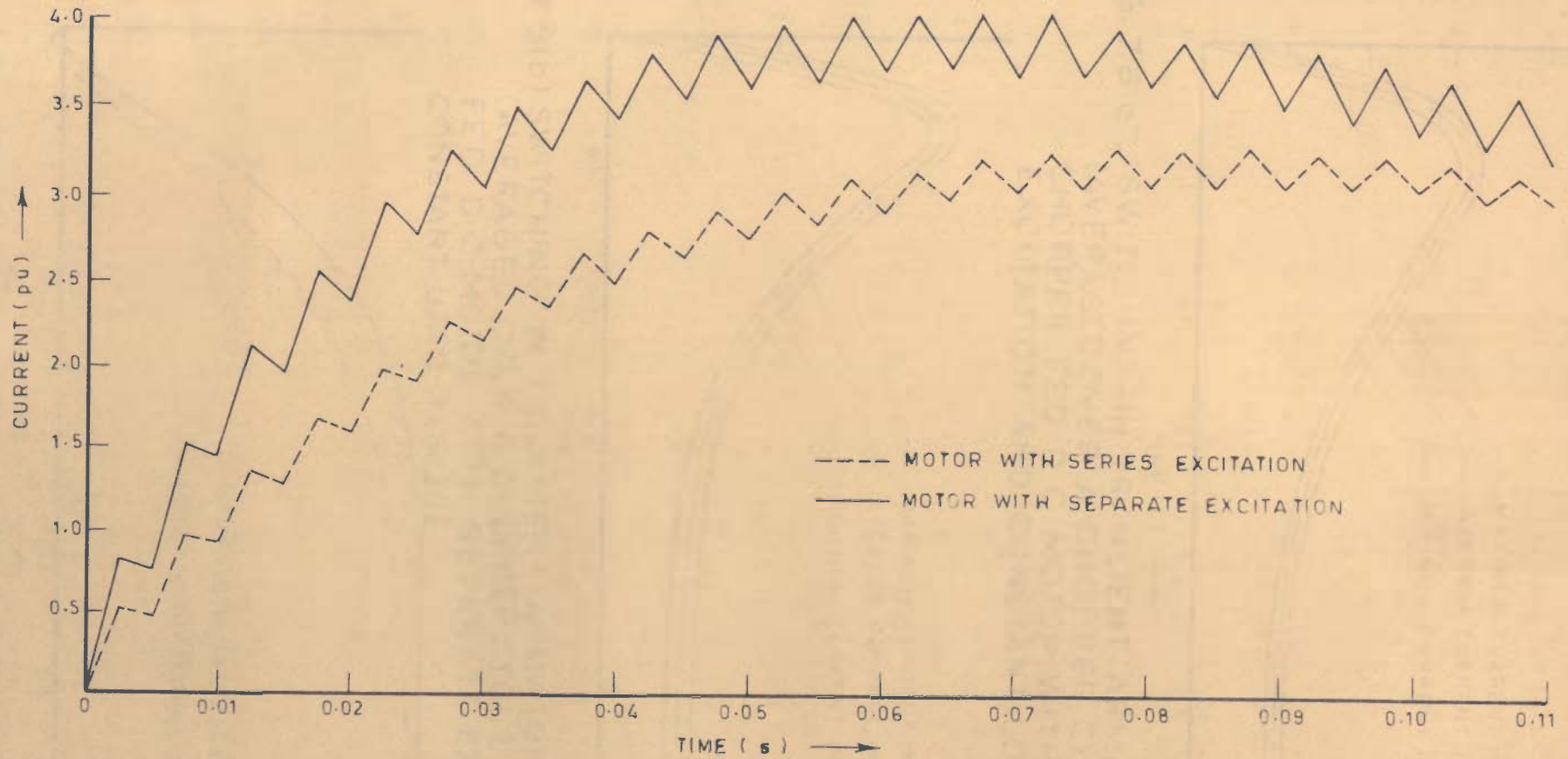
FIG. 7.7 _ SWITCHING - IN   TRANSIENT ARMATURE CURRENT FOR CHOPPER
FED D·C. MOTOR WITH CONSTANT LOAD TORQUE
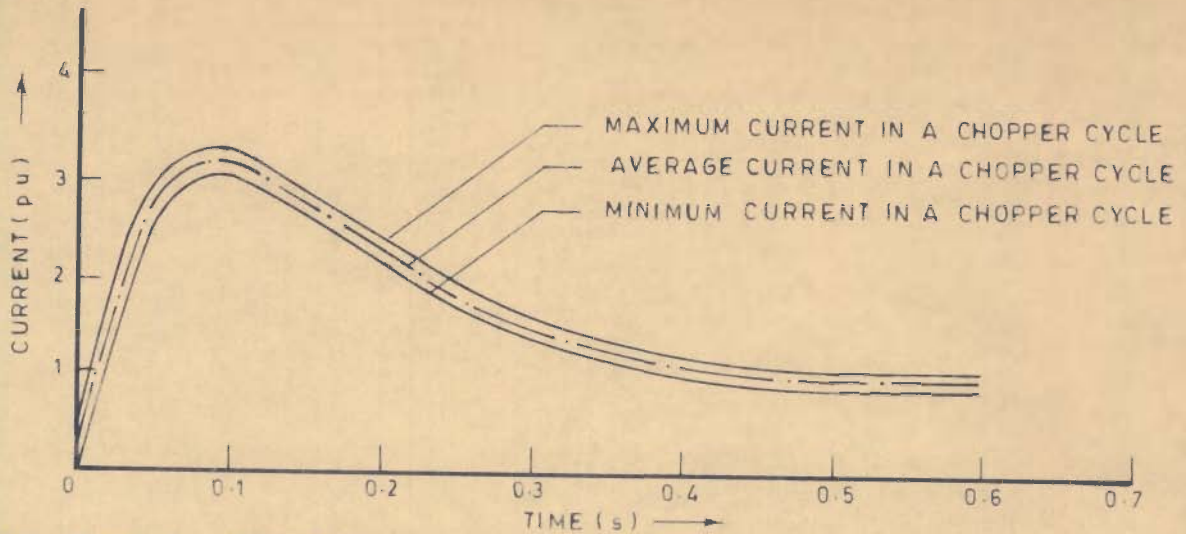
FIG. 7.8(a) _ SWITCHING-IN TRANSIENT ARMATURE CURRENT
(AVERAGED OVER A CHOPPER CYCLE) FOR
CHOPPER FED D.C. MOTOR WITH SERIES
EXCITATION AND CONSTANT LOAD TORQUE
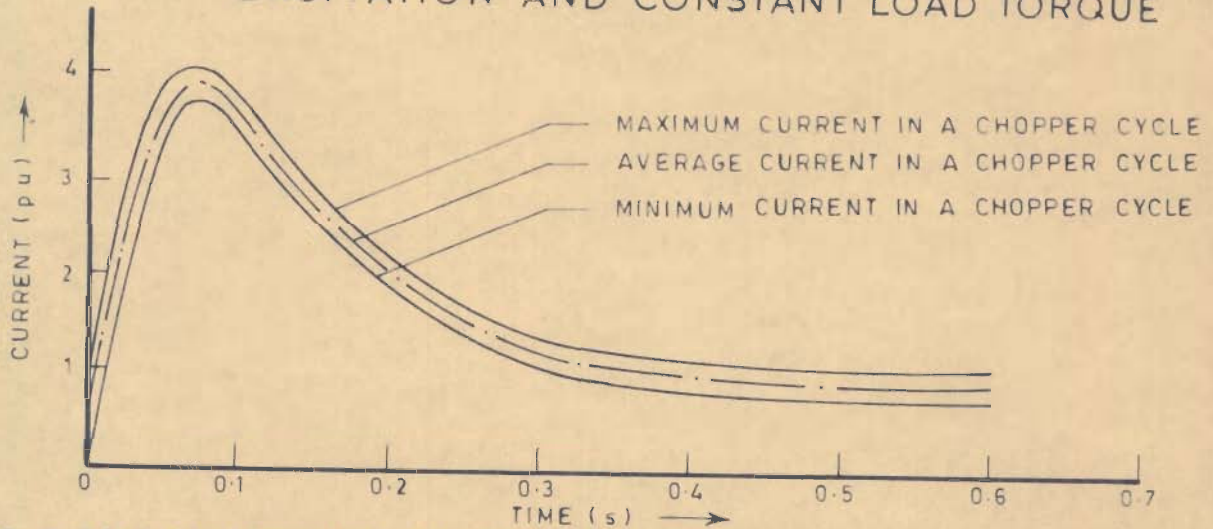
FIG. 7.8(b) SWITCHING-IN TRANSIENT ARMATURE CURRENT
(AVERAGED OVER A CHOPPER CYCLE) FOR CHOPPER
FED D.C. MOTOR WITH SEPARATE EXCITATION AND
CONSTANT LOAD TORQUE
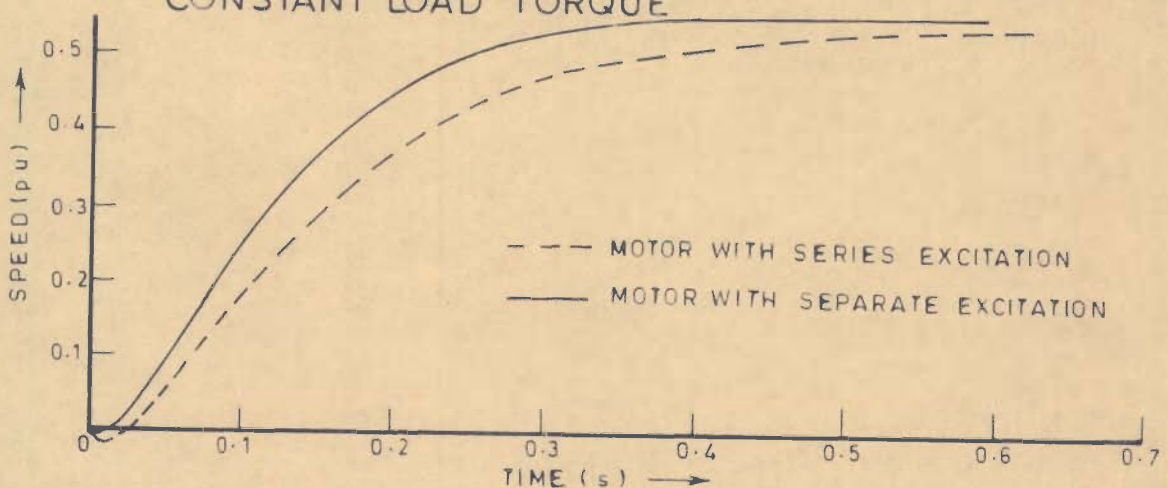
FIG. 7.9 _ TRANSIENT SPEED RESPONSE FOR CHOPPER FED
D.C. MOTOR WITH CONSTANT LOAD TORQUE

changing till steady state is reached when the current varies
between a fixed maximum and minimum limits. The envelope of
variation of maximum and minimum values of current in a chopper
cycle is shown in Fig.7.8(a). The mid-point of the envelope
indicates the average current in a chopper cycle. The nature of
variation of current, averaged over a chopper cycle, is identical
to that of variation with constant voltage input [Figs.7.4 and
7.8(a)]. As expected, the magnitude of current with chopper
input is lower due to the reason that average voltage input with
chopper is lower compared to that with constant voltage input.
The transient response of motor speed is also plotted as shown in
Fig.7.9. The values of speed with chopper input are lower com-
pared to the case of constant voltage input [Figs.7.5 and 7.9].

7.5.2 Steady State Performance

(a) Steady State Performance of D.C. Series Motor Drive
     With Constant Voltage Supply

For the case under study, the steady state variations of
armature current and motor speed of d.c. series motor with a
pulsating load torque are shown in Figs.7.11 and 7.12 respec-
tively. It is observed that if the load torque is pulsating in
nature [Fig.7.10], the armature current and speed also pulsate
at a frequency equal to the frequency of load torque pulsations
[Figs.7.11,7.12]. The amplitude of these pulsations depends
upon the amplitude of pulsating component of load torque T_{L1}, and
other electrical and mechanical parameters of the system.
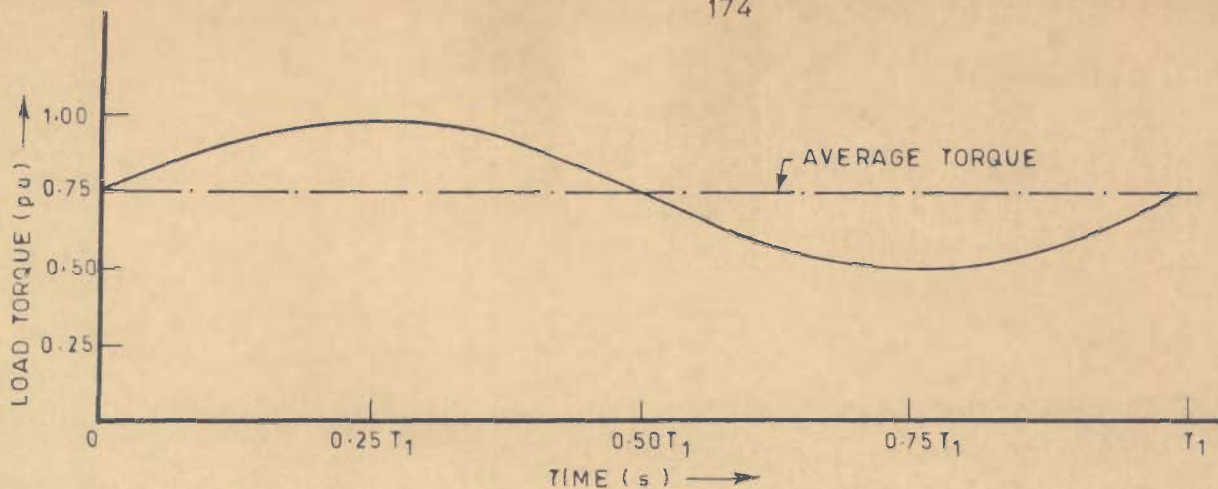
FIG. 7.10 _ VARIATION OF LOAD TORQUE
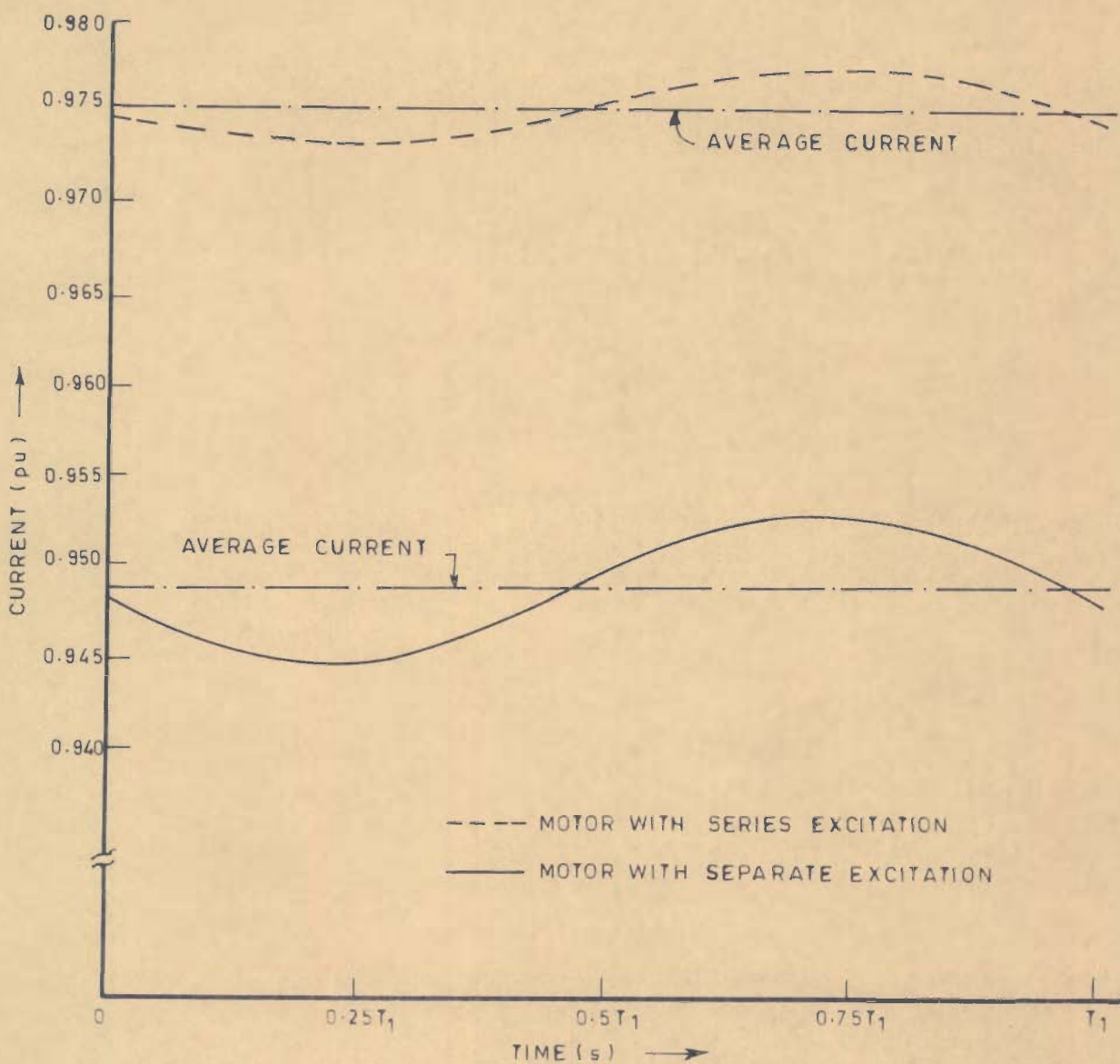
FIG. 7.11 _ STEADY STATE PULSATIONS IN ARMATURE
CURRENT FOR D·C· MOTOR FED BY CONSTANT
VOLTAGE WITH PULSATING LOAD TORQUE
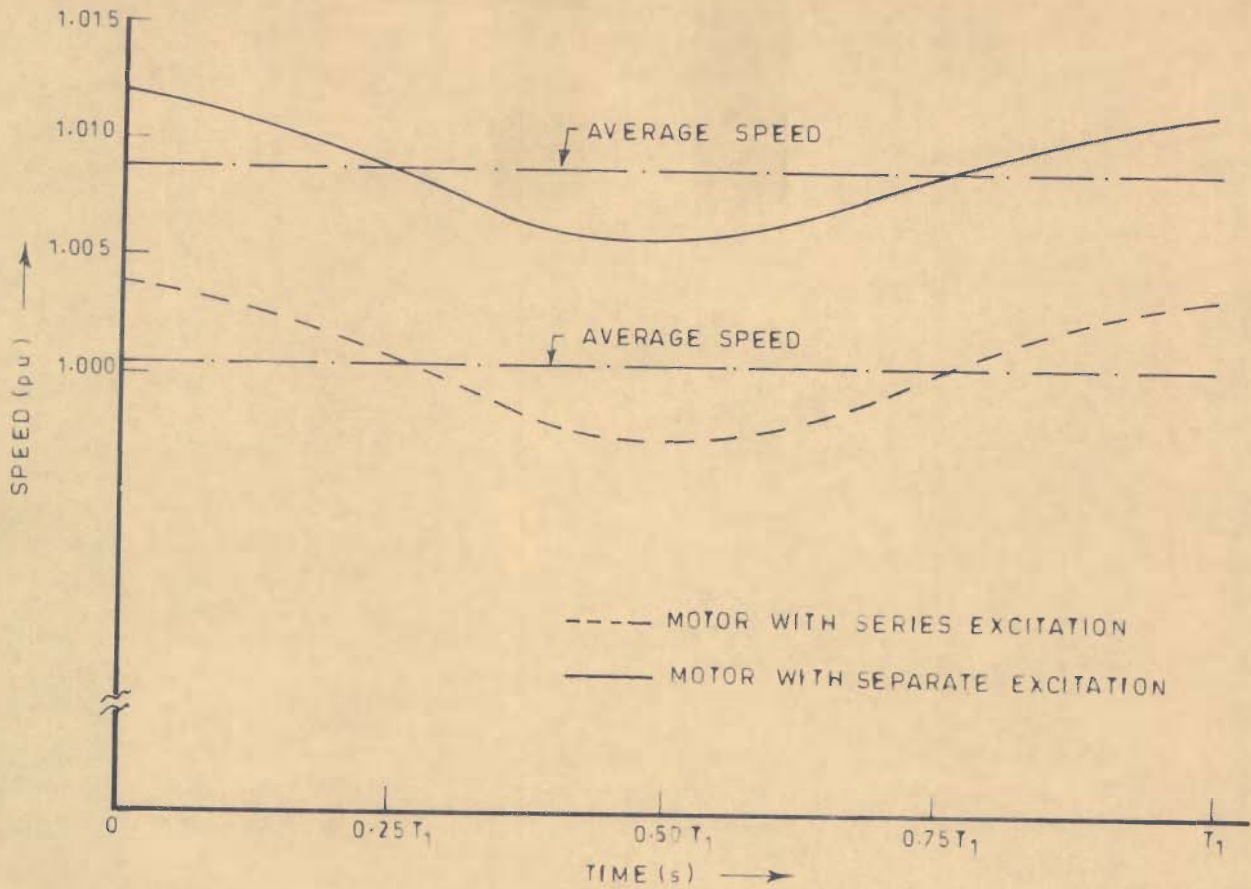
FIG. 7.12 _ STEADY STATE PULSATIONS IN SPEED FOR D.C.
MOTOR FED BY CONSTANT D.C. VOLTAGE
WITH PULSATING LOAD TORQUE
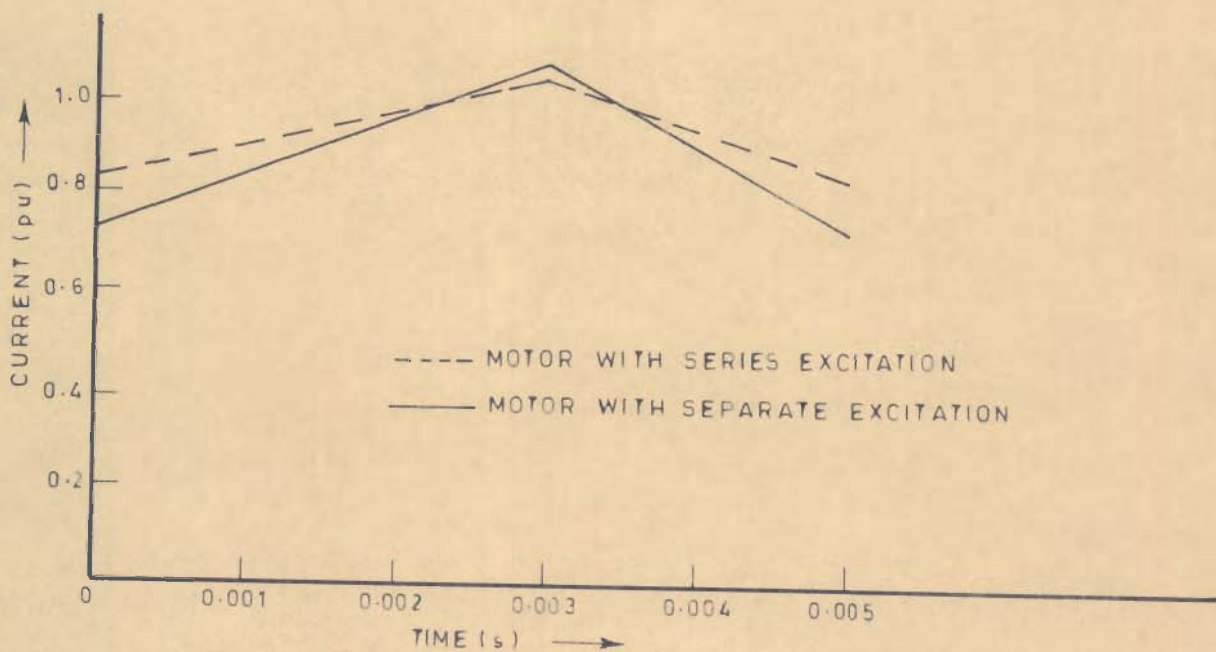
FIG. 7.13 _ VARIATION OF STEADY STATE ARMATURE CURRENT
FOR CHOPPER FED D.C. MOTOR WITH CONSTANT
LOAD TORQUE

(b)   Steady State Performance of D.C. Series Motor Drive
      With Chopper Controlled Supply

The variation of steady state armature current of d.c. series motor with a constant load torque over a chopper cycle is shown in Fig.7.13. It is observed that the current rises in duty interval and decays in freewheeling interval of a chopper cycle. These variations are exponential but appear to be linear due to high value of frequency of chopper operation. The armature current in a chopper cycle varies between a fixed range of maximum and minimum values.

With a pulsating load torque, the armature current rises in duty interval and decays in freewheeling interval as for the case of constant load torque. As the load torque varies with time, the range of variation of current in successive chopper cycles also varies and the whole pattern repeats after an interval of time when the load torque completes its one cycle of pulsation (as discussed in section 4.11, Figs.4.7,4.10). The armature current and speed averaged over a chopper cycle also pulsate at a frequency equal to the frequency of load torque pulsations. The nature of these variations is similar to those for motor with constant voltage input shown in Figs.7.11,7.12, however, the quantitative values are different.

7.6   COMPARISON OF PERFORMANCE OF A D.C. MOTOR DRIVE WITH
      SERIES AND SEPARATE EXCITATIONS

The performance of a d.c. motor with series excitation is discussed in section 7.5. For the sake of comparison,in order to identify any differences in behaviour, the performance of the

same drive but with separate excitation is also determined. The
performance of the drive for the following two cases is compared
as below:

Case A: D.C. motor with series excitation

Case B: D.C. motor with separate excitation.

7.6.1 Transient State Performance

(a) Performance With Constant Voltage Supply

The variation of armature current, motor speed and twist
in the shaft of a d.c. motor for the above two cases is shown in
Figs.7.4-7.6. The nature of these variations for the two cases
are similar. It is observed that the peak value of current for
case A is lower than that for case B. It is due to a higher value
of inductance of armature circuit in case A. The motor in case A
attains a peak current of 5.125 pu in 0.083 s while these values
for case B are 6.367 pu in 0.062 s. Thus the transient response
of motor in case A is sluggish as compared to the case B. The
motor in case A attains 95 % of rated speed in 0.499 s compared
to 0.315 s for case B. The magnitude of peak value of twist in
transient condition for case A is observed to be lower than that
for case B. The peak value of twist for motor in case A is
8.12 x 10^{-3} rad. compared to 9.90 x 10^{-3} rad. for motor in case B.

(b) Performance With Chopper Controlled Supply

With a chopper input, the variation of armature current in
transient condition for cases A and B is shown in Fig.7.7. It is
observed that the nature of this variation for the two cases is
similar, however, the numerical values are different. The

armature current, averaged over a chopper cycle, for the two cases
is shown in Figs.7.8(a),(b). The value of peak current averaged
over a chopper cycle and the time at which this value is attained
are 3.168 pu and 0.083 s for case A and 3.902 pu and 0.062 s for
case B. This is also due to a higher value of inductance in arma-
ture circuit in case A. The acceleration characteristic of the
motor for the two cases is shown in Fig.7.9. In this case also,
similar to the case of drive with constant voltage input [Fig.7.5],
the response of motor for case A is sluggish compared to that for
case B.

7.6.2 Steady State Performance

(a) Performance With Constant Voltage Supply

The steady state variations in armature current and speed
of the d.c. motor with pulsating load torque for the two cases is
shown in Figs.7.11 and 7.12. It is observed that the nature of
these variations for the two cases is similar. The amplitude of
pulsations of current for case A is lower compared to that for
case B, while no appreciable change in pulsations of speed is
noticed for the two cases. The amplitude of pulsations in current
for cases A and B are 0.0021 pu and 0.0041 pu respectively, while
the pulsations in speed for these cases are 0.0033 pu and 0.0031 pu
respectively.

With a constant load torque, the steady state values of
twist for cases A and B are 2.18×10^{-3} rad. and 2.17×10^{-3} rad.
respectively. This shows that there is no appreciable change in
the values of twist for the two cases.

(b)   Performance With Chopper Controlled Supply

The steady state variations of armature current for d.c. motor with chopper controlled supply and constant load torque for the two cases is shown in Fig.7.13. The nature of variation of current for the two cases is observed to be similar. The range of variation of current for case A is smaller compared to that for case B. This is as expected due to a higher value of inductance in armature circuit for case A. The range of variation of current is between 1.045 and 0.837 pu for case A and between 1.078 and 0.735 pu for case B.

With a pulsating load torque, the armature current and speed averaged over a chopper cycle for case B also pulsate similar to that in case A. The uniform component of current and speed for case A are 0.948 and 0.541 pu respectively, while for case B, these values are 0.906 and 0.558 pu respectively.

7.7   CONCLUSIONS

The analysis of a d.c. series motor drive with elastic coupling and fed by a constant d.c. voltage as well as chopper controlled supply is presented for constant and pulsating load torque conditions. The performance of the drive in transient as well as steady state conditions is determined. The performance of the same motor but with separate excitation is also determined. A comparison of the performance of the motor for the two modes of excitations is given. It is observed that, in general, the performance of a d.c. motor with series excitation is qualitatively similar in nature to that of the motor with separate excitation. Some differences in the quantitative aspect of the performance

characteristics are, however, clearly noticeable.

On the basis of the results of the analysis presented, the following conclusions are drawn:

(a) The instantaneous values of twist in transient condition are lower for motor with series excitation compared to that for motor with separate excitation [Fig.7.6]. The twist in transient condition attains a peak value at the same instant when the current reaches its peak. However, no appreciable change in the values of twist in steady state is noted for the motor with two cases of excitation.

(b) For a periodically varying load torque, the armature current and motor speed in steady state pulsate at a frequency equal to the frequency of load torque pulsations. The amplitude of pulsation of current for motor with series excitation is lower compared to that of motor with separate excitation [Fig.7.11]. The amplitude of pulsation of speed for the two cases are not much different [Fig.7.12]. The effect of pulsation of load torque on transient performance is not significant.

(c) The instantaneous values of current, in transient condition, for a chopper fed d.c. motor with series excitation are lower compared to those with separate excitation [Figs.7.7, 7.8]. Under steady state also, the range of variation of current for motor with series excitation is lower than that for motor with separate excitation [Fig.7.13].

(d) The transient performance of a d.c. motor with series excitation is sluggish compared to that of motor with separate excitation.

CHAPTER-8

CONCLUSIONS

This thesis presents the analysis of d.c. drives-fed by
d.c. chopper supply as well as constant d.c. supply-with elastic
mechanical link connecting the motor to the load having periodic
variations in load torque. The interaction of mechanical factors,
chopper supply and drive parameters, and the design factors are
investigated. The importance of including mechanical factors in
the analysis has been brought out. Based on the results of the
investigations, the following conclusions are drawn:

8.1 CONCLUSIONS

The analysis of d.c. drive electro-mechanical system
presented in Chapter-2 can be used to determine the effects of
mechanical factors, viz., elasticity of shaft and periodic varia-
tion of load torque, on the performance of d.c. motor drives fed
by a constant d.c. supply. The analysis reveals that if the load
torque is pulsating in nature, the armature current and motor
speed also pulsate at a frequency equal to the frequency of load
torque pulsations. A decrease in the amplitude of pulsating
component of load torque and an increase in its frequency, reduce
the pulsations in current and speed. These pulsations are mini-
mum when frequency of load torque pulsations is equal to $1/\sqrt{2}$
times the natural frequency of torsional oscillations of system.
The pulsations attain large values as system goes under resonance

when the frequency of load torque pulsations is equal to natural frequency of torsional oscillations of system. The pulsations of current and speed can in general be reduced by increasing the moment of inertia of the system. Under condition of resonance, these pulsations can be reduced by increasing the damping of the system. However, this increases the average value of current and decreases the average value of speed. For proper design of the system, it is therefore suggested that the load torque should be analysed and it must be ensured that natural frequency of oscillation of system is not equal to the frequency of any of the harmonic components of load torque. Further, in order to minimise the pulsations in current and speed, the values of torsional stiffness of shaft and the moment of inertia of the system should be so chosen that the natural frequency of oscillation of the system is $\sqrt{2}$ times the frequency of load torque pulsations. Such a value of moment of inertia may not be the best from the point of view of the transient response of the system.

The methods available for analysis of chopper controlled d.c. drives are cumbersome, less accurate, need large computation time and do not provide closed-form solutions for system performance variables. To overcome the limitations of existing methods, a new technique for analysis of such drives is presented in Chapter-3. The proposed technique is simple and can be used to obtain closed-form solutions for system performance variables. The transient performance at any point in time can be obtained without starting the solutions from the instant of switching. The steady state performance can also be directly obtained and the

solutions do not have to be started from known initial conditions and continued till steady state conditions are reached. These features make the technique presented more efficient as the computational efforts are greatly reduced. Moreover, the technique is more accurate as motor speed over a chopper cycle need not be assumed constant.

The analysis presented in Chapter-4, is useful for determining the performance of chopper controlled d.c. drives with elastic coupling and pulsating load torque and to investigate as to how the performance is affected by these mechanical factors. Study of a typical performance as obtained by this analysis, reveals that the steady state armature current and motor speed contain alternating components superposed on a non-varying component. These components are of frequencies which are equal to the chopper frequency, the frequency of load torque pulsations and the natural frequencies of oscillations of system. It is observed that such systems experience resonance when the frequency of any of the components of load torque, or that of the chopper, or both approach the natural frequency of torsional oscillations of the system. Under such a condition, current and speed attain large peak values and the twist in the shaft may be so high that mechanical failure of shaft may occur due to excessive shear stress. It is suggested that the system should be designed in such a way that any alignment between the value of frequency of torsional oscillations of system and the spectrum of frequencies of chopper and load torque pulsations be avoided in order to avoid resonance. This can be achieved by suitably modifying the value of frequency

of torsional oscillations of system which depends upon the values of elasticity of shaft and moment of inertia of system.

Pulse-width modulation control is commonly employed in closed-loop regulating schemes for obtaining a desired control of speed of the drives. An analysis is presented in Chapter-5, and the influence of elasticity of shaft and periodic variations of load torque on performance of closed-loop d.c. motor drives fed by a PWM power supply is investigated. The analysis is used to determine the values of system parameters in order to obtain stable operation of system with minimum settling time. Study of performance of a typical system, based on this analysis, reveals that for a given value of elasticity of shaft, an increase in the value of amplifier gain upto a certain critical value decreases the settling time. An increase in gain beyond this value increases the settling time. The value of amplifier gain which gives minimum settling time is shown to be affected by value of elasticity of shaft. For a periodic variation in load torque, similar to the case of open loop drives, the current and speed also pulsate at a frequency equal to the frequency of load torque pulsations. A high value of amplifier gain, decreases the pulsations in speed and current as also the steady state error in speed. It is observed that using a closed-loop system, the speed regulation improves but this is achieved only at the cost of larger pulsations in current. The system with a closed-loop drive, similar to that for open-loop drives, experiences resonance when the frequency of pulsations of load torque matches the natural frequency of oscillations of system. In this case also, resonance

can be avoided by a proper selection of values of elasticity of shaft and moment of inertia of the system.

In the analysis presented in Chapters 2,4 and 5, the frequency of load torque pulsations is assumed equal to average value of steady state speed (neglecting pulsating component of speed). The frequency of load torque pulsations in certain types of driven mechanisms, is a function of shaft speed. To take this factor into account, a non-linear analysis of d.c. drives with elastic coupling and taking the frequency of load torque pulsations equal to instantaneous value of shaft speed, is presented (Chapter-6). The results of this analysis show that the assumption of frequency of load torque pulsations equal to the average value of steady state speed is valid as the error caused due to this assumption is negligibly small.

The effects of elasticity of coupling and periodic variations of load torque on the performance of d.c. series motor drives, fed by a chopper as well as a constant d.c. voltage supply, are investigated in the analysis presented in Chapter-7. The performance of a similar drive but using a separately excited motor is also determined and compared with that of a series motor drive in order to study any differences in behaviour of drives using the two types of motors. It is observed that, in general, the performance of a d.c. motor with series excitation is qualitatively similar in nature to that of the motor with separate excitation. However, some differences in quantitative aspects of the performance have been noticed.

It is expected that the above work will be useful for a better design and more precise evaluation of performance of d.c. drives and will open certain new areas of research in the field of electric drives.

8.2 SUGGESTIONS FOR FURTHER WORK

The work presented covers various aspects of analysis of d.c. motor drives taking into account the effects of mechanical factors associated with drives. However, there are still some problems on which further work is suggested.

(i) Backlash is an important mechanical factor caused by loose tolerances in gear meshes, chain drives and couplings [10]. The effect of backlash may be to disconnect a major part of the inertia from the drive system resulting in large variations in developed torque and current. It is, therefore, important that a detailed study of effects of backlash on the performance of chopper controlled d.c. drives be made and necessary changes in design to improve the performance in presence of this mechanical feature be suggested.

(ii) Phase controlled d.c. drives are also commonly used in a number of industrial applications. It may be interesting to investigate the effects of mechanical factors on the performance of phase controlled d.c. motor drives.

(iii) In certain cases, though rather rarely, the chopper may operate in discontinuous mode of conduction. The technique of analysis of Chapter-3, when extended to such cases

becomes involved loosing its main advantages. A corresponding method of analysis for the case of discontinuous conduction, if developed, will be useful.

APPENDICES

APPENDIX : A-1

EXPRESSIONS OF SYMBOLS:

Expressions of different symbols used in the analysis of a separately excited d.c. motor drive with elastic coupling and pulsating load torque, discussed in Chapter-2, are as below:

$$\emptyset_{42}(s) = a_1 s^2 + a_2 s \quad , \quad \emptyset_{45}(s) = a_3 s$$

$$\emptyset_{52}(s) = b_1 s^3 + b_2 s^2 + b_3 s$$

$$\emptyset_{55}(s) = s^4 + b_4 s^3 + b_5 s^2 + b_6 s$$

where

$$a_1 = C/J_1 \ , \ a_2 = C/J_1 \tau_a \ , \ a_3 = C K_m / L J_1$$

$$b_1 = K_e / J_1 \ , \ b_2 = B_2 K_e / J_1 J_2 \ , \ b_3 = K_e C/J_1 J_2$$

$$b_4 = B_1 / J_1 + B_2 / J_2$$

$$b_5 = C/J_1 + C/J_2 + B_1 B_2 / J_1 J_2$$

$$b_6 = C(B_1 + B_2)/J_1 J_2$$

$$C_1 = \alpha_1 \alpha_2(\alpha_3^2 + \beta_3^2)$$

$$C_2 = - \alpha_1(\alpha_2 - \alpha_1)\{(\alpha_3 - \alpha_1)^2 + \beta_3^2\}$$

$$C_3 = - \alpha_2(\alpha_1 - \alpha_2)\{(\alpha_3 - \alpha_2)^2 + \beta_3^2\}$$

$$C_4 = \omega_1 \cos \emptyset + \alpha_1 \sin \emptyset$$

$$C_5 = \omega_1 \cos \emptyset + \alpha_2 \sin \emptyset$$

$$C_6 = (\alpha_2 - \alpha_1)(\alpha_1^2 + \omega_1^2)\{(\alpha_3 - \alpha_1)^2 + \beta_3^2\}$$

$$C_7 = (\alpha_1 - \alpha_2)(\alpha_2^2 + \omega_1^2)\{(\alpha_3 - \alpha_2)^2 + \beta_3^2\}$$

$$P_1 = a_2 - a_1 \, \alpha_3$$

$$P_2 = a_2 \, \omega_1 \cos \emptyset + a_1 \, \omega_1^2 \sin \emptyset$$

$$P_3 = a_1 \, \beta_3^2 \sin \emptyset + (a_2 - a_1 \, \alpha_3)(\omega_1 \cos \emptyset + \alpha_3 \sin \emptyset)$$

$$P_4 = b_1(\alpha_3^2 - \beta_3^2) - b_2 \, \alpha_3 + b_3$$

$$P_5 = a_3(\omega_1 \cos \emptyset + \alpha_3 \sin \emptyset)$$

$$P_6 = a_3 \, \omega_1 \cos \emptyset$$

$$P_7 = b_6 - \alpha_3(\alpha_3^2 - \beta_3^2 - b_4 \, \alpha_3 + b_5) - \beta_3^2(b_4 - 2 \, \alpha_3)$$

$$Q_1 = a_1 \, \beta_3$$

$$Q_2 = a_2 \, \omega_1 \sin \emptyset - a_1 \, \omega_1^2 \cos \emptyset$$

$$Q_3 = a_1 \, \beta_3(\omega_1 \cos \emptyset + \alpha_3 \sin \emptyset) - \beta_3 \sin \emptyset(a_2 - a_1 \, \alpha_3)$$

$$Q_4 = b_2 \, \beta_3 - 2 \, \alpha_3 \, \beta_3 \, b_1 \, , \quad Q_5 = - a_3 \, \beta_3 \sin \emptyset$$

$$Q_6 = a_3 \, \omega_1 \sin \emptyset$$

$$Q_7 = \beta_3(\alpha_3^2 - \beta_3^2 - b_4 \, \alpha_3 + b_5) - \alpha_3 \, \beta_3(b_4 - 2 \, \alpha_3)$$

$$M_1 = 2 \, \beta_3^2\{\alpha_3(\alpha_1 + \alpha_2 - 2 \, \alpha_3) - (\alpha_1 - \alpha_3)(\alpha_2 - \alpha_3) + \beta_3^2\}$$

$$M_2 = - 4 \, \alpha_3 \, \omega_1^2(\alpha_1 \, \alpha_2 - \omega_1^2) - 2 \, \omega_1^2(\alpha_1 + \alpha_2)(\alpha_3^2 + \beta_3^2 - \omega_1^2)$$

$$M_3 = 4 \, \alpha_3 \, \beta_3^2\{(\alpha_1 - \alpha_3)(\alpha_2 - \alpha_3) - \beta_3^2\}$$
$$- 2 \, \beta_3^2(\alpha_1 + \alpha_2 - 2 \, \alpha_3)(\alpha_3^2 - \beta_3^2 + \omega_1^2)$$

$$N_1 = 2 \, \beta_3[\alpha_3\{(\alpha_1 - \alpha_3)(\alpha_2 - \alpha_3) - \beta_3^2\} + \beta_3^2(\alpha_1 + \alpha_2 - 2 \, \alpha_3)]$$

$$N_2 = 2 \, \omega_1(\alpha_3^2 + \beta_3^2 - \omega_1^2)(\alpha_1 \, \alpha_2 - \omega_1^2) - 4 \, \omega_1^3 \, \alpha_3(\alpha_1 + \alpha_2)$$

$$N_3 = - 2 \, \beta_3\{(\alpha_1 - \alpha_3)(\alpha_2 - \alpha_3) - \beta_3^2\}(\alpha_3^2 - \beta_3^2 + \omega_1^2)$$
$$- 4 \, \alpha_3 \, \beta_3^2(\alpha_1 + \alpha_2 - 2 \, \alpha_3)$$

$$K_1 = a_2 / C_1 \, , \, K_2 = (a_2 - a_1 \, \alpha_1)/C_2 \, , \, K_3 = (a_2 - a_1 \, \alpha_2)/C_3$$

$$K_{4r} = (P_1 \, M_1 - Q_1 \, N_1)/(M_1^2 + N_1^2)$$

$$K_{4i} = (P_1 \, N_1 + Q_1 \, M_1)/(M_1^2 + N_1^2)$$

$$K_5 = 2(K_{4r}^2 + K_{4i}^2)^{1/2} \, , \, K_6 = (a_2 - a_1 \, \alpha_1)C_4 / C_6$$

$$K_7 = (a_2 - a_1 \, \alpha_2)C_5 / C_7$$

$$K_{8r} = (P_2 \, M_2 - Q_2 \, N_2)/(M_2^2 + N_2^2)$$

$$K_{8i} = (P_2 \, N_2 + Q_2 \, M_2)/(M_2^2 + N_2^2)$$

$$K_{9r} = (P_3 \, M_3 - Q_3 \, N_3)/(M_3^2 + N_3^2)$$

$$K_{9i} = (P_3 \, N_3 + Q_3 \, M_3)/(M_3^2 + N_3^2)$$

$$K_{10} = 2(K_{8r}^2 + K_{8i}^2)^{1/2}$$

$$K_{11} = 2(K_{9r}^2 + K_{9i}^2)^{1/2} \, , \, K_{12} = b_3 / C_1$$

$$K_{13} = (b_1 \, \alpha_1^2 - b_2 \, \alpha_1 + b_3)/C_2$$

$$K_{14} = (b_1 \, \alpha_2^2 - b_2 \, \alpha_2 + b_3)/C_3$$

$$K_{15r} = (P_4 \, M_1 - Q_4 \, N_1)/(M_1^2 + N_1^2)$$

$$K_{15i} = (P_4 \, N_1 + Q_4 \, M_1)/(M_1^2 + N_1^2)$$

$$K_{16} = 2(K_{15r}^2 + K_{15i}^2)^{1/2} \, , \, K_{17} = a_3 / C_1$$

$$K_{18} = a_3 / C_2 \, , \, K_{19} = a_3 / C_3$$

$$K_{20r} = a_3 \, M_1 /(M_1^2 + N_1^2)$$

$$K_{20i} = a_3 \, N_1 /(M_1^2 + N_1^2)$$

$$K_{21} = 2(K_{20r}^2 + K_{20i}^2)^{1/2}$$

$$K_{22} = a_3 \, C_4 / C_6$$

$$K_{23} = a_3 \, C_5/C_7$$

$$K_{24r} = (P_5 \, M_3 - Q_5 \, N_3)/(M_3^2 + N_3^2)$$

$$K_{24i} = (P_5 \, N_3 + Q_5 \, M_3)/(M_3^2 + N_3^2)$$

$$K_{25r} = (P_6 \, M_2 - Q_6 \, N_2)/(M_2^2 + N_2^2)$$

$$K_{25i} = (P_6 \, N_2 + Q_6 \, M_2)/(M_2^2 + N_2^2)$$

$$K_{26} = 2(K_{24r}^2 + K_{24i}^2)^{1/2}$$

$$K_{27} = 2(K_{25r}^2 + K_{25i}^2)^{1/2}$$

$$K_{28} = b_6/C_1$$

$$K_{29} = (b_6 - b_5 \, a_1 + b_4 \, a_1^2 - a_1^3)/C_2$$

$$K_{30} = (b_6 - b_5 \, a_2 + b_4 \, a_2^2 - a_2^3)/C_3$$

$$K_{31r} = (P_7 \, M_1 - Q_7 \, N_1)/(M_1^2 + N_1^2)$$

$$K_{31i} = (P_7 \, N_1 + Q_7 \, M_1)/(M_1^2 + N_1^2)$$

$$K_{32} = 2(K_{31r}^2 + K_{31i}^2)^{1/2}$$

$$\emptyset_1 = \tan^{-1}(K_{4r}/K_{4i})$$

$$\emptyset_2 = \tan^{-1}(K_{9r}/K_{9i})$$

$$\emptyset_3 = \tan^{-1}(K_{15r}/K_{15i})$$

$$\emptyset_4 = \tan^{-1}(K_{20r}/K_{20i})$$

$$\emptyset_5 = \tan^{-1}(K_{24r}/K_{24i})$$

$$\emptyset_6 = \tan^{-1}(K_{31r}/K_{31i})$$

$$\psi_1 = \tan^{-1}(-K_{8r}/K_{8i})$$

$$\psi_2 = \tan^{-1}(-K_{25r}/K_{25i})$$

APPENDIX : A-2

A-2.1 PROOF OF THEOREM:

The proof of theorem used for determining the Laplace inverse transform of functions containing terms $\{1-\exp(-s\,t_o)\}/\{1-\exp(-s\,T)\}$ in Chapter-3 is as below:

$$\mathcal{L}^{-1}\left[\emptyset(s)\left\{\frac{1-\exp(-st_o)}{1-\exp(-sT)}\right\}\right]$$

$$= \mathcal{L}^{-1}\ \emptyset(s)\left[\{1-\exp(-st_o)\}\{1+\exp(-sT)+\exp(-2sT)+\ldots\}\right]$$

$$= \mathcal{L}^{-1}\ \emptyset(s)\left[\{1+\exp(-sT)+\exp(-2sT)+\ldots\}\right.$$

$$\left. - \{\exp(-st_o)+\exp(-s\,\overline{t_o+T})+\exp(-s\,\overline{t_o+2T})\}\right]$$

$$= [\emptyset(t)U(T)+\emptyset(t-T)U(t-T)+\ldots]$$

$$- [\emptyset(t-t_o)U(t-t_o)+\emptyset(t-t_o-T)U(t-t_o-T)+\ldots]$$

(i) For Duty Interval

$$\mathcal{L}^{-1}\left[\emptyset(s)\left\{\frac{1-\exp(-st_o)}{1-\exp(-sT)}\right\}\right]$$

$$= [\emptyset(t)+\emptyset(t-T)+\ldots+\emptyset(t-\overline{n-1}\,T)]$$

$$- [\emptyset(t-t_o)+\emptyset(t-t_o-T)+\ldots+\emptyset(t-t_o-\overline{n-2}\,T)]$$

$$= \sum_{r=1}^{n}\emptyset(t-\overline{r-1}\,T)-\sum_{r=1}^{n-1}\emptyset(t-t_o-\overline{r-1}\,T) \qquad (A.2.1)$$

(ii) For Freewheeling interval

$$\mathcal{L}^{-1}\left[\emptyset(s)\left\{\frac{1-\exp(-st_o)}{1-\exp(-sT)}\right\}\right]=[\emptyset(t)+\emptyset(t-T)+\ldots+\emptyset(t-\overline{n-1}\,T)]$$

$$- [\emptyset(t-t_o)+\emptyset(t-t_o-T)+\ldots+\emptyset(t-t_o-\overline{n-1}\,T)]$$

$$= \sum_{r=1}^{n}[\emptyset(t-\overline{r-1}\,T)-\emptyset(t-t_o-\overline{r-1}\,T)] \qquad (A.2.2)$$

A-2.2 EXPRESSION FOR ARMATURE CURRENT:

The expression for armature current of a chopper control-
led d.c. motor, in duty and freewheeling intervals is obtained as:
From eqn.(3.9):

$$i(t) = \mathcal{L}^{-1}\left\{\frac{1}{(s+\alpha_1)(s+\alpha_2)}\left[\frac{V}{sL}(s + \frac{1}{\tau_m})\{\frac{1-\exp(-st_o)}{1-\exp(-sT)}\} + \frac{K_m}{sJ}\frac{T_L}{L}\right]\right\}$$

$$= \mathcal{L}^{-1}\left[\frac{K_m}{J}\frac{T_L}{L}\{\frac{K_1}{s} + \frac{K_2}{(s+\alpha_1)} + \frac{K_3}{(s+\alpha_2)}\} + \right.$$

$$\left. \frac{V}{L}\{\frac{K_4}{s} + \frac{K_5}{(s+\alpha_1)} + \frac{K_6}{(s+\alpha_2)}\}\{\frac{1-\exp(-st_o)}{1-\exp(-sT)}\}\right] \qquad (A.2.3)$$

where

$$K_1 = 1/\alpha_1\alpha_2 \ , \ K_2 = -1/\alpha_1(\alpha_2-\alpha_1)$$

$$K_3 = 1/\alpha_2(\alpha_2-\alpha_1) \ , \ K_4 = 1/\tau_m\alpha_1\alpha_2$$

$$K_5 = (\tau_m\alpha_1-1)/\tau_m\alpha_1(\alpha_2-\alpha_1) \ , \ K_6 = (1-\tau_m\alpha_2)/\tau_m\alpha_2(\alpha_2-\alpha_1)$$

(i) Duty Interval:

From eqns.(A.2.1) and (A.2.3),

$$i_{d_n}(t) = \frac{K_m}{J}\frac{T_L}{L}\{K_1 + K_2\exp(-\alpha_1 t) + K_3\exp(-\alpha_2 t)\}$$

$$+ \frac{V}{R\,\tau_a}\left[\sum_{r=1}^{n}\{K_4 + K_5\exp\{(t-\overline{r-1}\,T)(-\alpha_1)\} + K_6\exp\{(t-\overline{r-1}\,T)(-\alpha_2)\}\}\right.$$

$$\left. - \sum_{r=1}^{n-1}\{K_4 + K_5\exp\{(t-t_o-\overline{r-1}\,T)(-\alpha_1)\} + K_6\exp\{(t-t_o-\overline{r-1}\,T)(-\alpha_2)\}\}\right]$$

$$= \frac{K_m}{J}\frac{T_L}{L}\{K_1 + K_2\exp(-\alpha_1 t) + K_3\exp(-\alpha_2 t)\}$$

$$+ \frac{V}{R\,\tau_a}\left[K_4 + K_5\exp(-\alpha_1 t)\{\frac{\exp(nT\alpha_1)-1}{\exp(T\alpha_1)-1}\} + K_6\exp(-\alpha_2 t)\{\frac{\exp(nT\alpha_2)-1}{\exp(T\alpha_2)-1}\}\right.$$

$$-K_5 \exp(-\overline{t-t_o}\ \alpha_1)\{\frac{\exp(\overline{n-1}\ T\alpha_1)-1}{\exp(T\alpha_1)-1}\}-K_6 \exp(-\overline{t-t_o}\alpha_2)\{\frac{\exp(\overline{n-1}\ T\alpha_2)-1}{\exp(T\alpha_2)-1}\}]$$

(ii) Freewheeling Interval:

From eqns. (A.2.2) and (A.2.3),

$$i_{f_n}(t) = \frac{K_m T_L}{JL}\{K_1 + K_2 \exp(-\alpha_1 t) + K_3 \exp(-\alpha_2 t)\}$$

$$+ \frac{V}{R\tau_a}\left[\sum_{r=1}^{n}\{K_4 + K_5 \exp\{(t-\overline{r-1}\ T)(-\alpha_1)\} + K_6 \exp\{(t-\overline{r-1}\ T)(-\alpha_2)\}\}\right.$$

$$\left. -\sum_{r=1}^{n}\{K_4 + K_5 \exp\{(t-t_o-\overline{r-1}\ T)(-\alpha_1)\} + K_6 \exp\{(t-t_o-\overline{r-1}\ T)(-\alpha_2)\}\}\right]$$

$$= \frac{K_m T_L}{JL}\{K_1 + K_2 \exp(-\alpha_1 t) + K_3 \exp(-\alpha_2 t)\}$$

$$+ \frac{V}{R\tau_a}\left[K_5 \exp(-\alpha_1 t)\{\frac{\exp(nT\alpha_1)-1}{\exp(T\alpha_1)-1}\}\{1-\exp(\alpha_1 t_o)\}\right.$$

$$\left. + K_6 \exp(-\alpha_2 t)\{\frac{\exp(nT\alpha_2)-1}{\exp(T\alpha_2)-1}\}\{1-\exp(\alpha_2 t_o)\}\right]$$

A-2.3 EXPRESSION FOR MOTOR SPEED

The expression for motor speed of a chopper controlled d.c. motor, in duty and freewheeling intervals is obtained as:

From eqn. (3.9):

$$\dot{\theta}(t) = \mathcal{L}^{-1}\{\frac{1}{(s+\alpha_1)(s+\alpha_2)}[\frac{VK_e}{sJL}\{\frac{1-\exp(-st_o)}{1-\exp(-sT)}\} - \frac{T_L}{sJ}(s+\frac{1}{\tau_a})]\}$$

$$= \mathcal{L}^{-1}\left[\frac{-T_L}{J}\{\frac{K_7}{s} + \frac{K_8}{(s+\alpha_1)} + \frac{K_9}{(s+\alpha_2)}\} + \frac{VK_e}{JL}\{\frac{K_1}{s} + \frac{K_2}{(s+\alpha_1)}\right.$$

$$\left. + \frac{K_3}{(s+\alpha_2)}\}\{\frac{1-\exp(-st_o)}{1-\exp(-sT)}\}\right] \qquad (A.2.4)$$

where, $K_7 = 1/\tau_a \alpha_1 \alpha_2$; $K_8 = (\tau_a \alpha_2 - 1)/\tau_a \alpha_1 (\alpha_2 - \alpha_1)$,

$K_9 = (1-\tau_a \alpha_2)/\tau_a \alpha_2 (\alpha_2 - \alpha_1)$

(i) Duty Interval:

From eqns. (A.2.1) and (A.2.4),

$$\dot{\Theta}_{d_n}(t) = -\frac{T_L}{J}\{K_7 + K_8 \exp(-\alpha_1 t) + K_9 \exp(-\alpha_2 t)\}$$

$$+ \frac{VK_e}{JL}\left[\sum_{r=1}^{n}\{K_1 + K_2 \exp\{(t-\overline{r-1}\ T)(-\alpha_1)\}+K_3 \exp\{(t-\overline{r-1}\ T)(-\alpha_2)\}\}\right.$$

$$\left. - \sum_{r=1}^{n-1}\{K_1+K_2 \exp\{(t-t_o-\overline{r-1}\ T)(-\alpha_1)\}+K_3 \exp\{(t-t_o-\overline{r-1}\ T)(-\alpha_2)\}\}\right]$$

$$= -\frac{T_L}{J}\{K_7 + K_8 \exp(-\alpha_1 t) + K_9 \exp(-\alpha_2 t)\}$$

$$+ \frac{VK_e}{JL}\left[K_1 + K_2 \exp(-\alpha_1 t)\{\frac{\exp(nT\alpha_1)-1}{\exp(T\alpha_1)-1}\} + K_3 \exp(-\alpha_2 t)\{\frac{\exp(nT\alpha_2)-1}{\exp(T\alpha_2)-1}\}\right.$$

$$\left. - K_2 \exp(-\overline{t-t_o}\alpha_1)\{\frac{\exp(\overline{n-1}\ T\alpha_1)-1}{\exp(T\alpha_1)-1}\} - K_3 \exp(-\overline{t-t_o}\alpha_1)\{\frac{\exp(\overline{n-1}\ T\alpha_2)-1}{\exp(T\alpha_2)-1}\}\right]$$

(ii) Freewheeling Interval:

From eqns. (A.2.2) and (A.2.4),

$$\dot{\Theta}_{f_n}(t) = -\frac{T_L}{J}\{K_7 + K_8 \exp(-\alpha_1 t) + K_9 \exp(-\alpha_2 t)\}$$

$$+ \frac{VK_e}{JL}\left[\sum_{r=1}^{n}\{K_1+K_2 \exp\{(t-\overline{r-1}\ T)(-\alpha_1)\}+K_3 \exp\{(t-\overline{r-1}\ T)(-\alpha_2)\}\}\right.$$

$$\left. - \sum_{r=1}^{n}\{K_1+K_2 \exp\{(t-t_o-\overline{r-1}\ T)(-\alpha_1)\}+K_3 \exp\{(t-t_o-\overline{r-1}\ T)(-\alpha_2)\}\}\right]$$

$$= -\frac{T_L}{J}\{K_7 + K_8 \exp(-\alpha_1 t) + K_9 \exp(-\alpha_2 t)\}$$

$$+ \frac{VK_e}{JL}\left[K_2 \exp(-\alpha_1 t)\{\frac{\exp(nT\alpha_1)-1}{\exp(T\alpha_1)-1}\}\{1-\exp(\alpha_1 t_o)\}\right.$$

$$\left. + K_3 \exp(-\alpha_2 t)\{\frac{\exp(nT\alpha_2)-1}{\exp(T\alpha_2)-1}\}\{1-\exp(\alpha_2 t_o)\}\right]$$

APPENDIX : A-3

A-3.1 EXPRESSIONS OF SYMBOLS

Expressions of different symbols used in the analysis of a chopper fed d.c. motor drive with elastic coupling and pulsating load torque, discussed in Chapter-4, are as below:

$$f_{41}(s) = a_1 s + a_2 \quad , \quad f_{51}(s) = b_1 s^2 + b_2 s + b_3$$

$$f_{43}(s) = s^3 + a_3 s^2 + a_4 s + a_5$$

$$f_{53}(s) = b_3 \quad , \quad f_{45}(s) = -a_6 s$$

$$f_{55}(s) = s^4 + b_4 s^3 + b_5 s^2 + b_6 s$$

where

$$a_1 = C/J_1 \; , \; a_2 = C/J_1 \tau_a \; , \; a_3 = 1/\tau_a + B_1/J_1$$

$$a_4 = B_1/J_1\tau_a + K_e K_m/LJ_1 + C/J_1 \; , \; a_5 = C/\tau_a J_1 \; , \; a_6 = CK_m/LJ_1$$

$$b_1 = K_e/J_1 \; , \; b_2 = K_e B_2/J_1 J_2 \; , \; b_3 = CK_e/J_1 J_2$$

$$b_4 = B_1/J_1 + B_2/J_2 \; , \; b_5 = C/J_1 + C/J_2 + B_1 B_2/J_1 J_2$$

$$b_6 = C(B_1+B_2)/J_1 J_2 \; , \; d_1 = \alpha_1^2 + \beta_1^2 \; , \; d_2 = \alpha_2^2 + \beta_2^2$$

$$M_1 = 4a_1\beta_1^2(\alpha_2-\alpha_1) - 2\beta_1^2\{(\alpha_2-\alpha_1)^2 + \beta_2^2 - \beta_1^2\}$$

$$M_2 = 4a_2\beta_2^2(\alpha_1-\alpha_2) - 2\beta_2^2\{(\alpha_1-\alpha_2)^2 + \beta_1^2 - \beta_2^2\}$$

$$M_3 = 4a_1\beta_1^2\{(\alpha_2-\alpha_1)^2 + \beta_2^2 - \beta_1^2\} - 4\beta_1^2(\alpha_1^2-\beta_1^2+\omega_1^2)(\alpha_2-\alpha_1)$$

$$M_4 = 4a_2\beta_2^2\{(\alpha_1-\alpha_2)^2 + \beta_1^2 - \beta_2^2\} - 4\beta_2^2(\alpha_2^2-\beta_2^2+\omega_1^2)(\alpha_1-\alpha_2)$$

$$M_5 = -4\omega_1^2 a_1(d_2-\omega_1^2) - 4\omega_1^2 a_2(d_1-\omega_1^2)$$

$$M_6 = -4\beta_1^2[(\alpha_2-\alpha_1)(\alpha_1^2-\beta_1^2) - a_1\{(\alpha_2-\alpha_1)^2 + \beta_2^2 - \beta_1^2\}]$$

$$M_7 = -4\beta_2^2[(\alpha_1-\alpha_2)(\alpha_2^2-\beta_2^2) - a_2\{(\alpha_1-\alpha_2)^2 + \beta_1^2 - \beta_2^2\}]$$

$$M_8 = 4\alpha_1\beta_1^2[(\alpha_2-\alpha_1)(\omega_1^2+\alpha_1^2-\beta_1^2)-\alpha_1\{(\alpha_2-\alpha_1)^2+\beta_2^2-\beta_1^2\}$$
$$- 2\beta_1^2[(\omega_1^2+\alpha_1^2-\beta_1^2)\{(\alpha_2-\alpha_1)^2+\beta_2^2-\beta_1^2\}+4\alpha_1\beta_1^2(\alpha_2-\alpha_1)]$$

$$M_9 = 4\alpha_2\beta_2^2[(\alpha_1-\alpha_2)(\omega_1^2+\alpha_2^2-\beta_2^2)-\alpha_2\{(\alpha_1-\alpha_2)^2+\beta_1^2-\beta_2^2\}]$$
$$- 2\beta_2^2[(\omega_1^2+\alpha_2^2-\beta_2^2)\{(\alpha_1-\alpha_2)^2+\beta_1^2-\beta_2^2\}+4\alpha_2\beta_2^2(\alpha_1-\alpha_2)]$$

$$M_{10} = -2\omega_1^2[(d_1-\omega_1^2)(d_2-\omega_1^2) - 4\omega_1^2\alpha_1\alpha_2]$$

$$N_1 = 2\alpha_1\beta_1\{(\alpha_2-\alpha_1)^2+\beta_2^2-\beta_1^2\} + 4\beta_1^3(\alpha_2-\alpha_1)$$

$$N_2 = 2\alpha_2\beta_2\{(\alpha_1-\alpha_2)^2+\beta_1^2-\beta_2^2\} + 4\beta_2^3(\alpha_1-\alpha_2)$$

$$N_3 = -2\beta_1(\alpha_1^2-\beta_1^2+\omega_1^2)\{(\alpha_2-\alpha_1)^2+\beta_2^2-\beta_1^2\} - 8\alpha_1\beta_1^3(\alpha_2-\alpha_1)$$

$$N_4 = -2\beta_2(\alpha_2^2-\beta_2^2+\omega_1^2)\{(\alpha_1-\alpha_2)^2+\beta_1^2-\beta_2^2\} - 8\alpha_2\beta_2^3(\alpha_1-\alpha_2)$$

$$N_5 = 8\omega_1^3\alpha_1\alpha_2 - 2\omega_1(d_1-\omega_1^2)(d_2-\omega_1^2)$$

$$N_6 = 8\alpha_1\beta_1^3(\alpha_2-\alpha_1)-[2\beta_1(\alpha_1^2-\beta_1^2)\{(\alpha_2-\alpha_1)^2+\beta_2^2-\beta_1^2\}]$$

$$N_7 = 8\alpha_2\beta_2^3(\alpha_1-\alpha_2)-[2\beta_2(\alpha_2^2-\beta_2^2)\{(\alpha_1-\alpha_2)^2+\beta_1^2-\beta_2^2\}]$$

$$N_8 = 2\alpha_1\beta_1[(\omega_1^2+\alpha_1^2-\beta_1^2)\{(\alpha_2-\alpha_1)^2+\beta_2^2-\beta_1^2\}+4\alpha_1\beta_1^2(\alpha_2-\alpha_1)]$$
$$+ 4\beta_1^3[(\alpha_2-\alpha_1)(\omega_1^2+\alpha_1^2-\beta_1^2) - \alpha_1\{(\alpha_2-\alpha_1)^2+\beta_2^2-\beta_1^2\}]$$

$$N_9 = 2\alpha_2\beta_2[(\omega_1^2+\alpha_2^2-\beta_2^2)\{(\alpha_1-\alpha_2)^2+\beta_1^2-\beta_2^2\}+4\alpha_2\beta_2^2(\alpha_1-\alpha_2)]$$
$$+ 4\beta_2^3[(\alpha_1-\alpha_2)(\omega_1^2+\alpha_2^2-\beta_2^2) - \alpha_2\{(\alpha_1-\alpha_2)^2+\beta_1^2-\beta_2^2\}]$$

$$N_{10} = 4\omega_1^3[\alpha_1(d_2-\omega_1^2) + \alpha_2(d_1-\omega_1^2)]$$

$$P_1^1 = a_6, \quad P_1^2 = a_6, \quad P_1^3 = a_6(\omega_1\cos\emptyset + \alpha_1\sin\emptyset)$$

$$P_1^4 = a_6(\omega_1\cos\emptyset + \alpha_2\sin\emptyset), \quad P_1^5 = a_6\omega_1\cos\emptyset$$

$$P_1^6 = a_2 - a_1 \alpha_1 \ , \ P_1^7 = a_2 \cdot a_1 \alpha_2$$

$$P_1^8 = (a_2 - a_1 \alpha_1)(\omega_1 \cos \emptyset + \alpha_1 \sin \emptyset) + a_1 \beta_1^2 \sin \emptyset$$

$$P_1^9 = (a_2 - a_1 \alpha_2)(\omega_1 \cos \emptyset + \alpha_2 \sin \emptyset) + a_1 \beta_2^2 \sin \emptyset$$

$$P_1^{10} = a_1 \omega_1^2 \sin \emptyset + a_2 \omega_1 \cos \emptyset$$

$$P_2^1 = b_6 - b_5 \alpha_1 + b_4(\alpha_1^2 - \beta_1^2) - \alpha_1^3 + 3\alpha_1 \beta_1^2$$

$$P_2^2 = b_6 - b_5 \alpha_2 + b_4(\alpha_2^2 - \beta_2^2) - \alpha_2^3 + 3\alpha_2 \beta_2^2$$

$$P_2^6 = b_3 - b_2 \alpha_1 + b_1(\alpha_1^2 - \beta_1^2)$$

$$P_2^7 = b_3 - b_2 \alpha_2 + b_1(\alpha_2^2 - \beta_2^2)$$

$$P_2^8 = P_3^6(\omega_1 \cos \emptyset + \alpha_1 \sin \emptyset) + Q_3^6 \beta_1 \sin \emptyset$$

$$P_2^9 = P_3^7(\omega_1 \cos \emptyset + \alpha_2 \sin \emptyset) + Q_3^7 \beta_2 \sin \emptyset$$

$$P_2^{10} = \omega_1 \cos \emptyset(a_5 - a_3 \alpha_1^2) + \omega_1^2 \sin \emptyset(a_4 - \omega_1^2)$$

$$P_3^6 = a_5 - a_4 \alpha_1 + a_3(\alpha_1^2 - \beta_1^2) + 3\alpha_1 \beta_1^2 - \alpha_1^3$$

$$P_3^7 = a_5 - a_4 \alpha_2 + a_3(\alpha_2^2 - \beta_2^2) + 3\alpha_2 \beta_2^2 - \alpha_2^3$$

$$P_4^6 = b_3 \ , \ P_4^7 = b_3$$

$$Q_1^1 = 0 \ , \ Q_1^2 = 0$$

$$Q_1^3 = -a_6 \beta_1 \sin \emptyset \ , \ Q_1^4 = -a_6 \beta_2 \sin \emptyset$$

$$Q_1^5 = -a_6 \omega_1 \sin \emptyset \ , \ Q_1^6 = a_1 \beta_1 \ , \ Q_1^7 = a_1 \beta_2$$

$$Q_1^8 = a_1 \beta_1(\omega_1 \cos \emptyset + \alpha_1 \sin \emptyset) - \beta_1 \sin \emptyset(a_2 - a_1 \alpha_1)$$

$$Q_1^9 = a_1 \, \beta_2 (\omega_1 \cos \emptyset + \alpha_2 \sin \emptyset) - \beta_2 \sin \gamma (a_2 - a_1 \, \alpha_2)$$

$$Q_1^{10} = a_1 \, \omega_1^2 \cos \emptyset - a_2 \, \omega_1 \sin \emptyset$$

$$Q_2^1 = 3 \, \alpha_1^2 \, \beta_1 - \beta_1^3 - 2 \, \alpha_1 \, \beta_1 \, b_4 + b_5 \, \beta_1$$

$$Q_2^2 = 3 \, \alpha_2^2 \, \beta_2 - \beta_2^3 - 2 \, \alpha_2 \, \beta_2 \, b_4 + b_5 \, \beta_2$$

$$Q_2^6 = b_2 \, \beta_1 - 2 \, b_1 \, \alpha_1 \, \beta_1$$

$$Q_2^7 = b_2 \, \beta_2 - 2 \, b_1 \, \alpha_2 \, \beta_2$$

$$Q_2^8 = Q_3^6 (\omega_1 \cos \emptyset + \alpha_1 \sin \emptyset) - P_3^6 \, \beta_1 \sin \emptyset$$

$$Q_2^9 = Q_3^7 (\omega_1 \cos \emptyset + \alpha_2 \sin \emptyset) - P_3^7 \, \beta_2 \sin \emptyset$$

$$Q_2^{10} = \omega_1^2 \cos \emptyset (a_4 - \omega_1^2) - \omega_1 \sin \emptyset (a_5 - a_3 \, \omega_1^2)$$

$$Q_3^6 = 3 \, \alpha_1^2 \, \beta_1 - \beta_1^3 - 2 \, a_3 \, \alpha_1 \, \beta_1 + a_4 \, \beta_1$$

$$Q_3^7 = 3 \, \alpha_2^2 \, \beta_2 - \beta_2^3 - 2 \, a_3 \, \alpha_2 \, \beta_2 + a_4 \, \beta_2$$

$$Q_4^6 = 0 \quad , \quad Q_4^7 = 0$$

$$K_m^p = 2 \left[\frac{(P_m^p)^2 + (Q_m^p)^2}{(M_p)^2 + (N_p)^2} \right]^{1/2}$$

$$\emptyset_m^p = - \tan^{-1} \left[\frac{P_m^p \, M_p - Q_m^p \, N_p}{(M_p)^2 + (N_p)^2} \right]$$

where for different m's, values of p vary as:

m = 1 ; p = 1,2,...,10

m = 2 ; p = 1,2,6,7,8,9,10

$m = 3; \; p = 6,7$

$m = 4; \; p = 6,7$

$K_3^1/K_2^6 = K_4^1/K_1^6 = K_4^3/K_1^8 = [d_1]^{1/2}$

$K_3^2/K_2^7 = K_4^2/K_1^7 = K_4^4/K_1^9 = [d_2]^{1/2}$

$K_5^1 = a_6/d_1 \; d_2 \; , \; K_5^2 = b_6/d_1 \; d_2 \; , \; K_5^3 = a_2/d_1 \; d_2$

$K_5^4 = \{a_1 \; d_1 \; d_2 - 2 \; a_2(\alpha_3 \; d_1 + \alpha_2 \; d_2)\}/(d_1 \; d_2)^2$

$K_5^5 = a_2 \cos \emptyset/\omega_1 \; d_1 \; d_2 \; , \; K_5^6 = b_3/d_1 \; d_2$

$K_5^7 = \{b_2 \; d_1 \; d_2 - 2 \; b_3(\alpha_3 \; d_1 + \alpha_2 \; d_2)\}/(d_1 \; d_2)^2$

$K_5^8 = a_5/d_1 \; d_2 \; , \; K_5^9 = a_4 \; d_1 \; d_2 - 2 \; a_5(d_1 \; \alpha_3 + d_2 \; \alpha_2)\}/(d_1 \; d_2)^2$

$K_6^0 = a_5 \cos \emptyset/\omega_1 \; d_1 \; d_2 \; , \; K_6^1 = b_3/d_1 \; d_2$

$K_6^2 = -2 \; b_3(d_1 \; \alpha_3 + d_2 \; \alpha_2)/(d_1 \; d_2)^2$

$\emptyset_1 = -\tan^{-1}(\beta_1/\alpha_1) \; , \; \emptyset_2 = -\tan^{-1}(\beta_2/\alpha_2)$

$(\emptyset_3^1 - \emptyset_2^6) = (\emptyset_4^1 - \emptyset_1^6) = (\emptyset_4^3 - \emptyset_1^8) = \emptyset_1$

$(\emptyset_3^2 - \emptyset_2^7) = (\emptyset_4^2 - \emptyset_1^7) = (\emptyset_4^4 - \emptyset_1^9) = \emptyset_2$

A-3.2 EXPRESSION FOR ARMATURE CURRENT

The expression for armature current of a chopper fed d.c. motor with elastic coupling and pulsating load torque is obtained as below:

From eqn.(4.11), i(t) is given as:

$$i(t) = i_1(t) + i_2(t) + i_3(t) \qquad (A.3.1)$$

where

$$i_1(t) = \frac{T_{Lo}}{J_2} \mathcal{L}^{-1} \left[\frac{-f_{45}(s)}{\Delta s} \right]$$

$$i_2(t) = \frac{T_{L1}}{J_2} \mathcal{L}^{-1} \left[\frac{-f_{45}(s)(\omega_1 \cos \emptyset - s \sin \emptyset)}{\Delta (s^2 + \omega_1^2)} \right]$$

$$i_3(t) = \frac{V}{L} \mathcal{L}^{-1} \left[\frac{f_{55}(s)}{\Delta s} \left\{ \frac{1-\exp(-st_o)}{1-\exp(-sT)} \right\} \right]$$

A-3.2.1 Solution for $i_1(t)$:

$$i_1(t) = \frac{T_{Lo}}{J_2} \mathcal{L}^{-1} \left[\frac{a_6}{s(s+\alpha_1-j\beta_1)(s+\alpha_1+j\beta_1)(s+\alpha_2-j\beta_2)s+\alpha_2+j\beta_2)} \right]$$

$$= \frac{T_{Lo}}{J_2} \mathcal{L}^{-1} \left[K_5^1 + K_1^1 \exp(-\alpha_1 t) \sin(\beta_1 t-\emptyset_1^1) + K_1^2 \exp(-\alpha_2 t) \sin(\beta_2 t-\emptyset_1^2) \right]$$

$$(A.3.2)$$

A-3.2.2 Solution for $i_2(t)$:

$$i_2(t) = \frac{T_{L1}}{J_2} \mathcal{L}^{-1} \left[\frac{a_6(\omega_1 \cos \emptyset - s \sin \emptyset)}{(s+\alpha_1-j\beta_1)(s+\alpha_1+j\beta_1)(s+\alpha_2-j\beta_2)(s+\alpha_2+j\beta_2)(s-j\omega_1)(s+j\omega_1)} \right]$$

$$= \frac{T_{L1}}{J_2} \left[K_1^3 \exp(-\alpha_1 t) \sin(\beta_1 t-\emptyset_1^3) + K_1^4 \exp(-\alpha_2 t) \sin(\beta_2 t-\emptyset_1^4) + K_1^5 \sin(\omega_1 t-\emptyset_1^5) \right]$$

$$(A.3.3)$$

A-3.2.3 Solution for $i_3(t)$

$$i_3(t) = \frac{V}{L} \mathcal{L}^{-1} \left[\frac{(s^3 + b_4 s^2 + b_5 s + b_6)}{s(s+\alpha_1-j\beta_1)(s+\alpha_1+j\beta_1)(s+\alpha_2-j\beta_2)(s+\alpha_2+j\beta_2)} \left\{ \frac{1-\exp(-s t_o)}{1-\exp(-s T)} \right\} \right]$$

$$= \frac{V}{L} \mathcal{L}^{-1} \left[\left\{ \frac{K_1}{s} + \frac{K_2}{(s+\alpha_1-j\beta_1)} + \frac{K_2^*}{(s+\alpha_1+j\beta_1)} + \frac{K_3}{(s+\alpha_2-j\beta_2)} + \frac{K_3^*}{(s+\alpha_2+j\beta_2)} \right\} \right.$$

$$\left. \left\{ \frac{1-\exp(-s t_o)}{1-\exp(-s T)} \right\} \right] \tag{A.3.4}$$

The value of $i_3(t)$ for duty and freewheeling intervals can be obtained from eqn. (A.3.4) using theorems given in eqns. (4.14) and (4.15) respectively as below:

(a) Solution of $i_3(t)$ in duty interval:

Expression for $i_3(t)$ in duty interval of nth chopper cycle, $i_{3d_n}(t)$, can be obtained from eqn. (A.3.4) using eqn. (4.14) as:

$$i_{3d_n}(t) = i'_{3d_n}(t) - i''_{3d_n}(t) \tag{A.3.5}$$

where

$$i'_{3d_n}(t) = \frac{V}{L} \left[\sum_{r=1}^{n} \{ K_1 + K_2 \exp\{-(\alpha_1-j\beta_1)(t-\overline{r-1}\,T)\} \right.$$

$$+ K_2^* \exp\{-(\alpha_1+j\beta_1)(t-\overline{r-1}\,T)\} + K_3 \exp\{-(\alpha_2-j\beta_2)(t-\overline{r-1}\,T)\}$$

$$\left. + K_3^* \exp\{-(\alpha_2+j\beta_2)(t-\overline{r-1}\,T)\} \right] \tag{A.3.6}$$

and

$$i''_{3d_n}(t) = \frac{V}{L} \left[\sum_{r=1}^{n-1} \{ K_1 + K_2 \exp\{-(\alpha_1-j\beta_1)(t-t_o-\overline{r-1}\,T)\} \right.$$

$$+ K_2^* \exp\{-(\alpha_1+j\beta_1)(t-t_o-\overline{r-1}\,T)\} + K_3 \exp\{-(\alpha_2-j\beta_2)(t-t_o-\overline{r-1}\,T)\}$$

$$\left. + K_3^* \exp\{-(\alpha_2+j\beta_2)(t-t_o-\overline{r-1}\,T)\} \right] \tag{A.3.7}$$

(i) Solution for $i'_{3d_n}(t)$:

From eqn.(A.3.6), substituting $K_2 = K_{2r} + j\,K_{2i}$ and $K_2^* = K_{2r} - j\,K_{2i}$, $i'_{3d_n}(t)$ can be written as:

$$i'_{3d_n}(t) = \frac{V}{L}\left[n\,K_1 + (K_{2r}+j\,K_{2i})\,\exp\{-(\alpha_1-j\,\beta_1)t\}\left\{\frac{\exp\{(\alpha_1-j\,\beta_1)nT\}-1}{\exp\{(\alpha_1-j\,\beta_1)T\}-1}\right\}\right.$$

$$+(K_{2r}-j\,K_{2i})\,\exp\{-(\alpha_1+j\,\beta_1)t\}\left\{\frac{\exp\{(\alpha_1+j\,\beta_1)nT\}-1}{\exp\{(\alpha_1+j\,\beta_1)T\}-1}\right\}$$

$$+(K_{3r}+j\,K_{3i})\,\exp\{-(\alpha_2-j\,\beta_2)t\}\left\{\frac{\exp\{(\alpha_2-j\,\beta_2)nT\}-1}{\exp\{(\alpha_2-j\,\beta_2)T\}-1}\right\}$$

$$\left.+(K_{3r}-j\,K_{3i})\,\exp\{-(\alpha_2+j\,\beta_2)t\}\left\{\frac{\exp\{(\alpha_2+j\,\beta_2)nT\}-1}{\exp\{(\alpha_2+j\,\beta_2)T\}-1}\right\}\right]$$

or

$$i'_{3d_n}(t) = \frac{V}{L}\,n\,K_1 + \frac{V}{LD_1}\left[2\,K_{2r}[\exp\{-\alpha_1(t-nT)\}\{\exp(\alpha_1 T)\,\cos\beta_1(t-nT+T)\right.$$

$$-\cos\beta_1(t-nT)\}+\exp(-\alpha_1 t)\{\cos\beta_1 t - \exp(\alpha_1 T)\,\cos\beta_1(t+T)\}]$$

$$-2\,K_{2i}[\exp\{-\alpha_1(t-nT)\}\{\exp(\alpha_1 T)\,\sin\beta_1(t-nT+T) - \sin\beta_1(t-nT)\}$$

$$\left.+\exp(-\alpha_1 t)\{\sin\beta_1 t - \exp(\alpha_1 T)\,\sin\beta_1(t+T)\}]\right]$$

$$+\frac{V}{LD_2}\left[2\,K_{3r}[\exp\{-\alpha_2(t-nT)\}\,\{\exp(\alpha_2 T)\,\cos\beta_2(t-nT+T) - \cos\beta_2(t-nT)\}\right.$$

$$+\exp(-\alpha_2 t)\{\cos\beta_2 t - \exp(\alpha_2 T)\,\cos\beta_2(t+T)\}]$$

$$-2\,K_{3i}[\exp\{-\alpha_2(t-nT)\}\,\{\exp(\alpha_2 T)\,\sin\beta_2(t-nT+T) - \sin\beta_2(t-nT)\}$$

$$\left.+\exp(-\alpha_2 t)\{\sin\beta_2 t - \exp(\alpha_2 t)\,\sin\beta_2(t+T)\}]\right]$$

where $D_1 = 1 + \exp(\alpha_1 T)\{\exp(\alpha_1 T) - 2\cos\beta_1 T\}$

and $\quad D_2 = 1 + \exp(\alpha_2 T)\{\exp(\alpha_2 T) - 2\cos\beta_2 T\}$

Hence

$$i'_{3d_n}(t) = \frac{V}{L} n \ K_5^2 + \frac{V \ K_2^1}{L \ D_1} \Big[\exp\{-\alpha_1 (t-n \ T)\}\{\exp(\alpha_1 \ T) \ \sin(\beta_1 (t-n T+T)-\emptyset_2^1)$$

$$- \sin(\beta_1 (t-nT) - \emptyset_2^1)\} + \exp(-\alpha_1 t)\{\sin(\beta_1 t-\emptyset_2^1) - \exp(\alpha_1 \ T)$$

$$\sin(\beta_1 (t+ T) - \emptyset_2^1)\}\Big] + \frac{V \ K_2^2}{L \ D_2}\Big[\exp\{-\alpha_2(t-nT)\}\{\exp(\alpha_2 T)$$

$$\sin(\beta_2(t-n T+T)- \emptyset_2^2) - \sin(\beta_2(t-n T)- \emptyset_2^2)\}+ \exp(-\alpha_2 t)\{\sin(\beta_2 t-\emptyset_2^2)$$

$$- \exp(\alpha_2 T) \ \sin(\beta_2(t+ T) - \emptyset_2^2)\}\Big] \qquad (A.3.8)$$

where $\quad K_5^2 = K_1 \ , \ K_2^1 = 2[(K_{2r})^2 + (K_{2i})^2]^{1/2}$

$$K_2^2 = 2[(K_{3r})^2 + (K_{3i})^2]^{1/2}$$

$$\emptyset_2^1 = \tan^{-1}(K_{2r} / K_{2i})$$

$$\emptyset_2^2 = \tan^{-1}(K_{3r} / K_{3i})$$

(ii) Solution for $i''_{3d_n}(t)$:

From eqn.(A.3.7), the expression for $i''_{3d_n}(t)$ can be obtained as:

$$i''_{3d_n}(t) = \frac{V}{L}\Big[(n-1)K_1 + (K_{2r}+ j \ K_{2i}) \ \exp\{-(\alpha_1-j\beta_1)(t-t_o)\}.$$

$$\{\frac{\exp\{ (\alpha_1- j \ \beta_1)(n-1)T\}-1}{\exp\{ (\alpha_1- j \ \beta_1)T\} - 1}\} + (K_{2r}-j \ K_{2i}) \ \exp\{-(\alpha_1 + j\beta_1)(t- t_o)\}.$$

$$\{\frac{\exp\{ (\alpha_1+ j \ \beta_1)(n-1)T\}-1}{\exp\{ (\alpha_1+ j \ \beta_1) T\} - 1}\} + (K_{3r}+ jK_{3i}).$$

$$\exp\{-(\alpha_2- j\beta_2)(t-t_o)\}\{\frac{\exp\{ (\alpha_2- j\beta_2)(n-1)T\}-1}{\exp\{ (\alpha_2- j\beta_2)T\} - 1}\}$$

$$+(K_{3r}-j\,K_{3i})\,\exp\{-(\alpha_2+j\,\beta_2)(t-t_o)\}\{\frac{\exp\{(\alpha_2+j\,\beta_2)(n-1)T\}-1}{\exp\{(\alpha_2+j\,\beta_2)T\}-1}\}]$$

or $i''_{3d_n}(t) = \frac{V}{L}(n-1)K_1 + \frac{V}{LD_1}\Big[2\,K_{2r}[\exp\{-\alpha_1(t-nT)\}\,\exp\{-\alpha_1(T-t_o)\}$

$\{\exp(\alpha_1 T)\,\cos\beta_1(t-nT+2\,T-t_o) - \cos\beta_1(t-nT+T-t_o)\}$

$+\exp(-\alpha_1 t)\,\exp(\alpha_1 t_o)\{\cos\beta_1(t-t_o) - \exp(\alpha_1 T)\,\cos\beta_1(t+T-t_o)\}]$

$-2\,K_{2i}[\exp\{-\alpha_1(t-nT)\}\,\exp\{-\alpha_1(T-t_o)\}\{\exp(\alpha_1 T)\,\sin\beta_1(t-nT+2T-t_o)$

$-\sin\beta_1(t-nT+T-t_o)\}+\exp(-\alpha_1 t)\,\exp(\alpha_1 t_o)\{\sin\beta_1(t-t_o)-$

$\exp(\alpha_1 T)\,\sin\beta_1(t+T-t_o)\}]\Big]$

$+\frac{V}{LD_2}\Big[2\,K_{3r}[\exp\{-\alpha_2(t-nT)\}\,\exp\{-\alpha_2(T-t_o)\}\{\exp(\alpha_2 T)\,\cos\beta_2(t-nT$

$+2T-t_o) - \cos\beta_2(t-nT+T-t_o)\} + \exp(-\alpha_2 t)\,\exp(\alpha_2 t_o)\{\cos\beta_2(t-t_o)$

$- \exp(\alpha_2 T)\,\cos\beta_2(t+T-t_o)\}]- 2\,K_{3i}[\exp\{-\alpha_2(t-nT)\}\,\exp\{-\alpha_2(T-t_o)\}$

$\{\exp(\alpha_2 T)\,\sin\beta_2(t-nT+2\,T-t_o) - \sin\beta_2(t-nT+T-t_o)\}+ \exp(-\alpha_2 t)$

$\exp(\alpha_2 t_o)\{\sin\beta_2(t-t_o) - \exp(\alpha_2 T)\,\sin\beta_2(t+T-t_o)\}]\Big]$

or $i''_{3d_n}(t)= \frac{V}{L}(n-1)K_5^2 + \frac{V\,K_2^1}{LD_1}\Big[\exp\{-\alpha_1(t-nT)\}\,\exp\{-\alpha_1(T-t_o)\}$

$\{\exp(\alpha_1 T)\,\sin(\beta_1(t-nT+2\,T-t_o)-\emptyset_2^1) - \sin(\beta_1(t-nT+T-t_o) - \emptyset_2^1)\}$

$+\exp(-\alpha_1 t)\,\exp(\alpha_1 t_o)\{\sin(\beta_1(t-t_o)-\emptyset_2^1) - \exp(\alpha_1 T)\,\sin(\beta_1(t+T-t_o)-\emptyset_2^1)\}\Big]$

$+ \frac{V\,K_2^2}{LD_2}\Big[\exp\{-\alpha_2(t-nT)\}\,\exp\{-\alpha_2(T-t_o)\}\{\exp(\alpha_2 T)\,\sin(\beta_2(t-nT+2T-t_o)$

$- \emptyset_2^2) - \sin(\beta_2(t-nT+T-t_o)-\emptyset_2^2)\}+\exp(-\alpha_2 t)\,\exp(\alpha_2 t_o)\{\sin(\beta_2(t-t_o)-\emptyset_2^2)$

$- \exp(\alpha_2 T)\,\sin(\beta_2(t+T-t_o) - \emptyset_2^2)\}\Big]$ (A.3.9)

From eqn.(A.3.5),

$i_{3d_n}(t) = (A.3.8)-(A.3.9)$

Total current in duty interval:

Hence, total current in duty interval of nth chopper cycle, $i_{d_n}(t)$, is given by:

$$i_{d_n}(t) = i_1 + i_2 + i_{3d_n}(t)$$

$$= (A.3.2) + (A.3.3) + (A.3.8) - (A.3.9) \qquad (A.3.10)$$

From eqn.(A.3.10), the expression of $i_{d_n}(t)$ can be written as

$$i_{d_n}(t) = \sum_{m=1}^{2} \left[i_{ds_m} + i_{t_m} + i_{t_{m+2}} \right] + i_{ds_3} + i_{ds_4} \qquad (A.3.11)$$

The expressions for different terms used in eqn.(A.3.11) are given in eqn.(4.16)

(b) Solution of $i_3(t)$ in freewheeling interval:

Expression for $i_3(t)$ in freewheeling interval of nth chopper cycle, $i_{3f_n}(t)$, can be obtained from eqn.(A.3.4) using eqn.(4.15) as:

$$i_{3f_n}(t) = i'_{3f_n}(t) - i''_{3f_n}(t) \qquad (A.3.12)$$

where $\quad i'_{3f_n}(t) = i_{3d_n}(t)$

and

$$i''_{3f_n}(t) = \frac{V}{L} \left[\sum_{r=1}^{n} \{ K_1 + K_2 \exp\{-(\alpha_1 - j\beta_1)(t-t_o-\overline{r-1}\,T)\} \right.$$

$$+ K_2^* \exp\{-(\alpha_1 + j\beta_1)(t-t_o-\overline{r-1}\,t)\} + K_3 \exp\{-(\alpha_2 - j\beta_2)(t-t_o-\overline{r-1}\,T)\}$$

$$\left. + K_3^* \exp\{-(\alpha_2 + j\beta_2)(t-t_o-\overline{r-1}\,T)\} \right] \qquad (A.3.13)$$

(i) Solution for $i''_{3f_n}(t)$:

The expression for $i''_{3f_n}(t)$ can be obtained solving eqn.(A.3.8) as below:

$$i''_{3f_n}(t) = \frac{V}{L}\left[n\,K_1 + (K_{2r}+j\,K_{2i})\,\exp\{-(\alpha_1-j\,\beta_1)(t-t_o)\}\right.$$

$$\left\{\frac{\exp\{\alpha_1-j\,\beta_1)nT\}-1}{\exp\{(\alpha_1-j\beta_1)T\}-1}\right\}+(K_{2r}-j\,K_{2i})\,\exp\{-(\alpha_1+j\,\beta_1)(t-t_o)\}$$

$$\left\{\frac{\exp\{(\alpha_1+j\,\beta_1)nT\}-1}{\exp\{(\alpha_1+j\,\beta_1)T\}-1}\right\}+(K_{3r}+j\,K_{3i})\,\exp\{-(\alpha_2-j\,\beta_2)(t-t_o)\}$$

$$\left\{\frac{\exp\{(\alpha_2-j\,\beta_2)nT\}-1}{\exp\{(\alpha_2-j\,\beta_2)T\}-1}\right\}+(K_{3r}-j\,K_{3i})\,\exp\{-(\alpha_2+j\,\beta_2)(t-t_o)\}$$

$$\left.\left\{\frac{\exp\{(\alpha_2+j\,\beta_2)nT\}-1}{\exp\{(\alpha_2+j\,\beta_2)T\}-1}\right\}\right]$$

or

$$i''_{3f_n}(t) = \frac{V}{L}\,n\,K_1 + \frac{V}{LD_1}\left[2\,K_{2r}[\exp\{-\alpha_1(t-nT)\}\exp(\alpha_1 t_o)\right.$$

$$\{\exp(\alpha_1 T)\,\cos\beta_1(t-nT+T-t_o)-\cos\beta_1(t-nT-t_o)\}$$

$$+\exp(-\alpha_1 t)\,\exp(\alpha_1 t_o)\{\cos\beta_1(t-t_o)-\exp(\alpha_1 T)\,\cos\beta_1(t+T-t_o)\}]$$

$$-2\,K_{2i}[\exp\{-\alpha_1(t-nT)\}\,\exp(\alpha_1 t_o)\{\exp(\alpha_1 T)\,\sin\beta_1(t-nT+T-t_o)$$

$$-\sin\beta_1(t-nT-t_o)\}+\exp(-\alpha_1 t)\,\exp(\alpha_1 t_o)\{\sin\beta_1(t-t_o)$$

$$\left.-\exp(\alpha_1 T)\,\sin\beta_1(t+T-t_o)\}]\right]$$

$$+\frac{V}{LD_2}\left[2\,K_{3r}[\exp\{-\alpha_2(t-nT)\}\exp(\alpha_2 t_o)\{\exp(\alpha_2 T)\,\cos\beta_2(t-nT+T-t_o)\right.$$

$$-\cos\beta_2(t-nT-t_o)\}+\exp(-\alpha_2 t)\,\exp(\alpha_2 t_o)\{\cos\beta_2(t-t_o)$$

$$-\exp(\alpha_2 T)\,\cos\beta_2(t+T-t_o)\}]-2\,K_{3i}[\exp\{-\alpha_2(t-nT)\}\exp(\alpha_2 t_o)$$

$$\{\exp(\alpha_2 T)\,\sin\beta_2(t-nT+T-t_o)-\sin\beta_2(t-nT-t_o)\}$$

$$+ \exp(-\alpha_2 t) \exp(\alpha_2 t_o)\{\sin \beta_2(t-t_o) - \exp(\alpha_2 T) \sin \beta_2(t+T-t_o)\}]$$

Hence,

$$i''_{3f_n}(t) = \frac{V}{L} n K_5^2 + \frac{V K_2^1}{L D_1}\Big[\exp\{-\alpha_1(t-nT) \exp(\alpha_1 t_o)\{\exp(\alpha_1 T)$$

$$\sin(\beta_1(t-nT+T-t_o)-\emptyset_2^1) - \sin(\beta_1(t-nT-t_o)-\emptyset_2^1)\}$$

$$+\exp(-\alpha_1 t) \exp(\alpha_1 t_o)\{\sin(\beta_1(t-t_o)-\emptyset_2^1)-\exp(\alpha_1 T)\sin(\beta_1(t+T-t_o)-\emptyset_2^1)\}]$$

$$+ \frac{V K_2^2}{L D_2}\Big[\exp\{-\alpha_2(t-nT) \exp(\alpha_2 t_o)\{\exp(\alpha_2 T) \sin(\beta_2(t-nT+T-t_o)-\emptyset_2^2)$$

$$- \sin(\beta_2(t-nT-t_o)-\emptyset_2^2)\}+ \exp(-\alpha_2 t) \exp(\alpha_2 t_o)\{\sin(\beta_2(t-t_o)-\emptyset_2^2)$$

$$- \exp(\alpha_2 T) \sin(\beta_2(t+T-t_o)-\emptyset_2^2)\}] \tag{A.3.14}$$

Hence from eqn. (A.3.12),

$$i_{3f_n}(t) = (A.3.18)-(A.3.14)$$

Total current in freewheeling interval:

Therefore, total current in freewheeling interval of nth chopper cycle, $i_{f_n}(t)$, is given by:

$$i_{f_n}(t) = i_1 + i_2 + i_{3f_n}(t)$$

$$= (A.3.2) + (A.3.3) + (A.3.8) - (A.3.14) \tag{A.3.15}$$

Simplifying eqn. (A.3.15), the expression for $i_{f_n}(t)$ can be written as:

$$i_{f_n}(t) = \sum_{m=1}^{2}\Big[i_{fs_m} + i_{t_m} + i_{t_{m+2}}\Big] + i_{fs_3} + i_{fs_4} \tag{A.3.16}$$

The expressions for different terms used in eqn. (A.3.16) are given in eqn. (4.17).

REFERENCES

[1] Barton, T.H.,'The Transfer Characteristics of Chopper Drive', IEEE Trans. Ind. Appl., vol. IA-16, no.4, pp. 489-495, July 1980.

[2] Bhadra, S.N.,'Transient Response of Thyristor Controlled D.C. Series Motor under Small Disturbances', J.I.E.(India), vol.56, pp. 192-197, Feb. 1976.

[3] Bishop, J.A. and Mayer, C.B.,'A Case for High-Fidelity Analysis of Non-linear Electromechanical Torsional Dynamics', IEEE Trans. Ind. Appl., vol. IA-15, no.2, pp. 201-209, Mar. 1979.

[4] Borst, D.W. et.al.,'Voltage Control by Means of Power Thyristors', IEEE Trans. Ind. Gen. Appl., vol.IGA-2, no.2, pp. 102-123, Mar. 1966.

[5] Buckley, G.W.,'The Effects of Torsional Elements on the Transient Performance of Large Induction Motor Drives', J. Elect. Mach. Electromech., vol.5, no.1, pp. 53-64, Jan.1980.

[6] Burger, P.,'Analysis of a Class of Pulse Modulated DC-to-DC Power Converters', IEEE Trans. Ind. Electr. Contr. Instr., vol. IECI-22, no.2, pp. 104-106, May 1975.

[7] Burgin, B.S.,'Study of Absolute Stability of a Non-linear System of Electric Drive Having an Elastic Link', Electrichestvo, no.1, pp. 59-62, 1975.

[8] Burgin, B.S.,'Transient Functions of D.C. Electric Drive With Elastic Coupling', Electrichestvo, no.1, pp. 49-52, 1971.

[9] Burgin, B.S.,'Analysis of Amplitude Frequency Characteristics of Electric Drive Having an Elastic Coupling With Variation of Parameters of Electromechanical System', Electrichestvo, no.10, pp. 33-36, 1968.

[10] Carter, W.C.,'Mechanical Factors Affecting Electrical Drive Performance', IEEE Trans. Ind. Gen. Appl., vol.IGA-5, no.3, pp.282-290, May 1969.

[11] Chan, S.P., et.al.,'Analysis of Linear Networks and Systems', Addison-Wesley Publishing Company, Inc. Philippines.

[12] Cheng, D.K.,'Analysis of Linear Systems', Addison-Wesley Publishing Company, Inc., Tokyo, Japan.

[13] Chilkin, M.,'Electric Drive', Mir Publishers, Moscow.

[14] Church, A.H.,'Mechanical Vibrations', John Wiley and Sons, Inc., N.Y.

[15] Cohen, A.R.,'Outline of Linear Circuits and Systems', Regents Publishing Company, Inc., New York.

[16] Csaki, F., et.al.,'Power Electronics', Akademiai Kiado, Pudapest.

[17] Damle, P.D. and Dubey, G.K.,'Analysis of Chopper Fed D.C. Series Motor', IEEE Trans. Ind. Electr. Contr. Instr., vol.IECI-23, pp. 92-97, Feb.1976.

[18] Damle, P.D. and Dubey, G.K.,'A Digital Computer Program For Chopper Fed D.C. Motors', IEEE Trans. Ind. Electr. Contr. Instr., vol.IECI-22, no.3, pp. 408-412, Aug. 1975.

[19] Dewan, S.B. and Straughen, A.,'Power Semiconductor Circuits', John Wiley and Sons., N.Y.

[20] Dubey, G.K. and Shepherd, W.,'Transient Analysis of Chopper Fed D.C. Series Motor', Trans. IEEE Ind. Electr. Contr. Instr., vol.IECI-28, no.2, pp.146-159, May 1981.

[21] Dubey, G.K.,'Transient Analysis of D.C. Series Motor Fed by a Chopper With Current Limit Control', J.IE(India), vol.59, pp. 115-118, Oct.1979.

[22] Dubey, G.K.,'Calculation of Filter Inductances for a Chopper Fed D.C. Separately Excited Motor', Proc. IEEE, vol.66, no.12, pp. 1671-73, Dec. 1978.

[23] Dubey, G.K. and Shepherd, W.,'Comparative Study of Chopper Control Techniques for D.C. Motor Control', J.IE(India), vol.58, pp. 307-312, June 1978.

[24] Dubey, G.K.,'Analytical Methods for Performance Calculations of Chopper Controlled D.C. Series Motor', J.IE(India), vol.58, pp. 69-74, Oct.1977.

[25] Dubey, G.K. and Shepherd, W.,'Transient Analysis of D.C. Separately Excited Motor Fed by Chopper with Current Limit Control', J.IE(India), vol.58, pp. 108-112, Oct.1977.

[26] Dubey, G.K. and Shepherd, W.,'Transient Analysis of a D.C. Motor Controlled by Power Pulses', Proc.IEE, vol.124, no.3, pp. 229-30, Mar. 1977.

[27] Dubey, G.K. and Shepherd, W.,'Analysis of D.C. Series Motor Controlled by Power Pulses', Proc.IEE, vol.122, no.12, pp. 1397-1398, Dec.1975.

[28] Franklin, P.W.,'Theory of D.C. Motor Controlled by Power
      Pulses', IEEE Trans. Power App. Syst., vol.PAS-91,
      pp.249-255, 1972.

[29] Holbrook,'Laplace Transform for Electronic Engineers',
      Pergamon Press.

[30] Kaminskaya, D.A.,'Vibration of Electromechanical Systems
      under the Effect of Internal Disturbance Forces in Passing
      Through a Resonance', Electromekhanica, no.5, pp.552-555,
      May 1974.

[31] Kluchev, V.I., et.al.,'State of the Art and Prospectives in
      the Development of the Theory of Electromechanical Systems
      With Elastic Couplings', Electrichestvo, no.5, pp. 27-34,
      May 1976.

[32] Kluchev, V.I.,'Analysis of Electromechanical Coupling at
      the Time of Elastic Vibration in the Electric Drive',
      Electrichestvo, no.9, pp. 47-51, Nov. 1971.

[33] Kusko, A.,'Solid State D.C. Motor Drives', M.I.T. Press,
      England.

[34] Lindsay, J.F.,'An Electromechanical Network Model of the
      D.C. Motor', Trans. IEEE, Ind. Appl., vol.IA-14, no.3,
      pp. 227-233, May 1978.

[35] Liou, M.L.,'A Novel Method of Evaluating Transient Response',
      Proc. IEEE, vol.54, no.1, pp.20-23, Jan.1966.

[36] Maisel, J.E.,'Fundamental Concepts of Feedback Control',
      IEEE Trans. Ind. Electr. Contr. Instr., vol.IECI-22, no.2,
      pp. 122-128, May 1975.

[37] Matsui, N. and Miyairi, S.,'Transfer Functions and Estima-
      tion of Dynamic Behaviour of a Separately Excited D.C.
      Motor Controlled by a Thyristor Chopper Circuit', Trans.
      Inst. Electr. Eng. Japan, vol.96, no.2, pp.30-37, Mar. 1976.

[38] Matsuo, H. and Harada,'Dynamic Behaviour of Time Ratio
      Controlled DC-DC Power Converters', Electr. Eng. Japan,
      vol. 93, pp. 116-123, 1973.

[39] Mayer, C.B.,'Torsional Vibration Problems and Analysis of
      Cement Industry Drives', IEEE Trans. Ind. Appl., vol.IA-17,
      no.1, pp.81-89, Jan. 1981.

[40] Meerov, M.V.,'Introduction to the Dynamics of Automatic
      Regulating of Electric Machines', Butterworths, London.

[41] Meirovitch, L.,'Elements of Vibration Analysis', McGraw-Hill
      Book Company, Inc.

[42]   Mellitt, B. and Rashid, M.H., 'Analysis of Chopper Circuits
       by Computer Based Piecewise Linear Technique', Proc. IEE,
       vol.121, no.3, pp.175-178, 1974.

[43]   Nitta, K., et al., 'Dynamic Response of Separately Excited
       D.C. Motor Driven by a Thyristor Pulsating Power Supply',
       Electr. Eng. Japan, vol. 90, no.4, pp. 95-102, 1970.

[44]   Parimelalagan, R. and Rajagopalan, V., 'Steady State Investi-
       gations of a Chopper Fed D.C. Motor with Separate Excitation',
       IEEE Trans. Ind. Gen. Appl., vol.IGA-7, no.1, pp.101-108,
       Jan. 1971.

[45]   Polyakov, L.M., et.al., 'Special Features in the Design of
       Elastic Electromechanical Systems with Thyristor Drives',
       Mach. Tool., vol.47, no.12, pp. 23-25, 1976.

[46]   Ranade, D.B. and Dubey, G.K., 'A Chopper for Control of D.C.
       Traction Motor', J. Elect. Mach. Electromech., vol.4, no.4,
       pp.299-319, 1979.

[47]   Reimers, E., 'Power Transfer in D.C. Chopper Motor Drive',
       IEEE Trans. Ind. Appl., vol. IA-17, no.3, pp.302-314,
       May 1981.

[48]   Schieman, R.G. et.al., 'Solid State Control of Electric
       Drives', Proc. IEEE, pp. 1643-1660, Dec. 1974.

[49]   Sen, P.G. and Doradla, S.R., 'Evaluation of Control Schemes
       for Thyristor Controlled D.C. Motor', IEEE Trans. Ind.
       Electr. Contr. Instr., vol. IECI-25. no.3, pp. 247-254,
       Aug. 1978.

[50]   Siljak, D.D., 'Non-linear Systems-The Parameter Analysis and
       Design', John Wiley and Sons.

[51]   Singh, S.N. and Kohli, D.R., 'Analysis and Performance of a
       Chopper Controlled Separately Excited D.C. Motor', IEEE
       Trans. Ind. Electr., vol.IE-29, no.1, pp. 1-6, Feb. 1982.

[52]   Singh, S.N. and Kohli, D.R., 'Mathematical Foundation of a
       Chopper Controlled Separately Excited D.C. Motor', J.IE
       (India), vol.60, pp. 94-97, Dec. 1979.

[53]   Taft, C.K. and Slate, E.V. 'Pulsewidth Modulated D.C.Control:
       Parameter Variation Study with Current Loop Analysis', IEEE
       Trans. Ind. Electr. Contr. Instr., vol.IECI-26, no.4,
       pp.218-226, Nov. 1979.

[54]   Tal, J., 'Design and Analysis of Pulsewidth Modulated
       Amplifiers for D.C. Servo Systems', IEEE Trans. Ind. Electr.
       Contr. Instr., vol.IECI-23, no.1, pp. 47-55, Feb.1976.

[55] Thornton, D.L.,'Mechanics Applied to Vibrations and Balancing', Chapman and Hall Ltd..

[56] Tse, F.S., et.al.,'Mechanical Vibrations', Prentice Hall of India Pvt. Ltd., New Delhi.

[57] Tsekhovitch, L.I.,'On the Dynamics of D.C. Electric Drive Having an Elastic Coupling', Electrichestvo, no.6,pp.54-57, 1968.

[58] Unnikrishnan, R.,'Stability Analysis of a Thyristor DC-DC Converter', IEEE Trans. Ind. Electr. Contr. Instr., vol.IECI-27, no.3, pp.165-168, Aug. 1980.

[59] Unnikrishnan, R.,'Note on Stability of First Order PWM Systems', Electron. Lett., vol.14, no.24, pp. 774-775, Nov. 1978.

[60] Van Eck, R.A.,'The Separately Excited D.C. Traction Motor Applied to D.C. and Single Phase A.C. Rapid Transit Systems and Electrified Railroads', Parts I,II, IEEE Trans. Ind. Gen. Appl., vol. IGA-7, no.5, pp. 643-657, Sep. 1971.

[61] Verma, V.K., et.al.,'Pulsewidth Modulated Speed Control of D.C. Motors',J. Frank. Inst., vol. 297, no.2, Feb. 1974.

[62] Williams, B.W.,'Complete State Space Digital Computer Simulation of Chopper Fed D.C. Motors', IEEE Trans. Ind. Electr. Contr. Instr., vol.IECI-25, no.3, pp. 255-260, Aug. 1978.

[63] Wilson, W.K.,'Practical Solution of Torsional Vibration Problems', vol.2, Chapman and Hall Ltd..

[64] Yanase. A.,'Starting Characteristics of Chopper Controlled D.C. Series Motor With Non-linear Magnetisation Curve', Elect. Eng. Japan, vol.97, no.1, pp. 94-101, 1977.

[65] Zabar, Z. and Alexandrovitz, A.,'Guidelines on Adaptation of Thyristorized Switch for D.C. Motor Speed Control', IEEE Trans. Ind. Electr. Contr. Instr., vol. IECI-17, no.1, pp. 10-13, Feb. 1970.

PUBLICATIONS FROM THIS THESIS

1. 'Performance of A Chopper Controlled D.C. Drive with Elastic Coupling and Periodically Varying Load Torque', accepted for publication in IEEE Trans. on Ind. Appl.

2. 'Performance Analysis of A D.C. Drive Electromechanical System with Elastic Coupling and Pulsating Load Torque', J. Elect. Mach. Electromech. (U.S.A.), vol.6, pp.541-557, 1981.

3. 'A New Approach to Performance Analysis of Chopper Controlled D.C. Motor Drive', J. Elect. Mach. Electromech.(U.S.A.), vol.6, no.3, pp.239-251, 1981.

4. 'Effects of Some Mechanical Factors on Dynamic Performance of D.C. Motor Drives', accepted for publication, J.IE(India).